

The Characterisation of a Recombinant Cytosolic Shuttle Based on Ricin Toxin

By

Arun Kumar Kotha B.Pharm, MSc.

A thesis submitted in partial fulfilment of the requirements of the University of
Greenwich for the degree of Doctor of Philosophy

School of Science
University of Greenwich at Medway
Chatham Maritime, Kent, ME4 4TB
United Kingdom



December 2011

DECLARATION

“I certify that this work has not been accepted in substance for any degree, and is not concurrently being submitted for any degree other than that of Doctor of Philosophy being studied at the University of Greenwich. I also declare that this work is the result of my own investigations except where otherwise identified by references and that I have not plagiarised the work of others”.

_____ Arun Kumar Kotha (Candidate)

Doctoral Supervisors

_____ Dr. Simon C.W. Richardson (First Supervisor)

_____ Prof. Dr. John Mitchell (Second Supervisor)

ACKNOWLEDGEMENTS

Firstly, I would like to thank my supervisor Dr. Simon Richardson for giving me the opportunity to undertake a PhD and for his excellent scientific guidance. I thank him for his valuable suggestions, discussions in the lab and also for fun filled pub lunches. I would like to thank my second supervisor Prof. John Mitchell for his support and encouragement. I would also like to thank my colleagues Paul Dyer, Dr. Tatiana Christides, Marie Pettit for their help. I thank the technical members of staff Samantha Ingram, Samantha Lewis, Rachel Nice and Atiya Raza for their kind help and they are just wonderful. I would like to thank School of Science, University of Greenwich at Medway for funding my studies.

I would like to thank Dr. Katharina von Gersdorff, Dr. Silvia Murialdo, Santosh Gandham, Balu Ereventi, Dr. Asish Shukla, Nitin Patil, Dr. Florentine Wahl, Ramu Kukunoore, Chitharanjan Bennur and N.V. Bhasker Chary for their friendship and encouragement.

I would also like to thank Dr. Christine Baltus, Dr. Peter John Gunnig, Dr. Aurora Antemir and Dr. Nazanin Zand for their help and friendship.

Finally, I would like to thank my wife, my sister, my brother and my parents for their unconditional love and support.

ABSTRACT

Title: Characterisation of a Recombinant Cytosolic Shuttle Based on Ricin Toxin

Cytosolic access is rate limiting for potential therapeutics such as antisense agents. In nature, several entities deliver macromolecules to the cytosol, one example being ricin toxin (RT). In this thesis, a cytosolic drug delivery system based upon attenuated RT was characterised. The toxicological consequences of mutating RT A chain (RTAC) amino acids: Glu¹⁷⁷, Ala¹⁷⁸, Ala¹⁷⁹, Arg¹⁸⁰, Phe¹⁸¹, Gln¹⁸² to Gly (mut) or deleting (del) them entirely, was evaluated. Epitopes (*i.e.*, 6His, HA) were also incorporated onto either the C- or N-terminus of the RTAC. The resultant plasmid constructs were sequenced, mapped and expressed in *E.coli* BL21*DE3. A plasmid encoding RT B chain (RTBC) was also characterised, mapped and expressed in *E.coli* BL21*DE3. Recombinant proteins were affinity purified from bacterial lysate and were soluble. Proteins were detected at approximately the predicted molecular weight using commercial antibodies specific for RTAC, RTBC or the epitopes incorporated into the constructs (*i.e.* 6His or V5). Optimal culture conditions were obtained by monitoring protein expression in 1.5mL bacterial cultures. Expression levels were established using Western blotting and immuno-detection (using a 6His specific primary antibody). The optimal culture conditions for RTAC with a C-terminal 6His and HA epitope (clone 175) and RTAC with amino acids 177-182 mutated to Gly (and also containing a C-terminal 6His, HA and Lys, Asp, Glu, Leu (KDEL) motif) (clone 189), were found to be 2h pre-induction incubation, induction (with 0.25mM IPTG) and a 4h post-induction incubation, cultured at 37°C. Upon further characterisation, recombinant RTBC (rRTBC) was found not to be lectinic, unlike commercial RTBC (cRTBC). The toxicity of RTAC mutants was characterised *in vitro* (B16 and Vero cells) using the MTT assay. Using the B16 cell model, at concentrations up to 10µg/mL, no IC₅₀ values could be established for rRTAC (clone 189). The published wild type RTAC IC₅₀ was 1.4µg/mL in B16 cells. The aforementioned rRTAC (clone 189) was re-associated with cRTBC to form a preparation containing enriched heterodimers. Heterodimeric rRTAC (clone 189) and cRTBC did not show any cytotoxicity in B16 cells at RTAC concentrations of up to 1µg/mL. The toxicity of heterodimeric rRTAC (clone 189) and cRTBC was measured in Vero cells and the IC₅₀ (0.39µg/mL), although statistically different (P<0.001) from cRTBC associated with cRTAC (at concentrations between 0.01 and 100 ng/mL) may be attributed to cRTBC. It was critical to know if the reduced toxicity of the rRTAC (clone 189) - cRTBC, constructs relative to RT holotoxin, was attributable to the RTAC being unable to access the cytosol. Sub-cellular fractionation was

performed using Vero cells and the majority of the immuno-reactive rRTAC (clone 189) was detected in a crude cytosolic fraction after 4h. Having ascertained that the mutations introduced into RTAC limit the toxicity of this molecule, the RT based drug delivery system was compared with a previously well-characterised polymer based drug delivery system. In order to make this comparison, a recombinant cargo protein was required. As gelonin (Gel) had been previously used as a cargo for poly(amidoamine) (PAA) mediated cytosolic delivery, three recombinant gelonin analogues were produced. The first was designated mature gelonin (mGel), the second was pre-gelonin with an additional C-terminal cysteine residue (Gel+Cys) and the third contained pre-gelonin sequence with no additional cysteine residue (Gel-Cys). The Gel-Cys construct was necessary to control for any toxicity limiting effects being exerted by additional C-terminal sequence (found on pre-gelonin). The three gelonin constructs were successfully cloned, sequenced and expressed in *E.coli* BL21*DE3. All of the recombinant gelonin constructs were detected using commercial antibodies (anti-6His and V5). The cytotoxicity of enriched recombinant gelonin proteins was compared with commercial gelonin (cGel). All of the gelonin preparations were non-toxic up to a concentration of 10µg/mL in B16 cells. Gelonin was then used to evaluate two things: 1) the efficiency of PAA mediated delivery relative to cRTBC and 2) the effect of the inclusion of dithiopyridine monomers upon PAA mediated Gel delivery. The PAA FF103 mediated an increase in cytotoxicity when applied to B16 cells in conjunction with a sub-toxic concentration of either with cGel or rGel (*i.e.* at a Gel concentration of 1.4µg/mL). This indicated that Gel was delivered into the cytosol by PAA FF103. At 10µg/mL of polymer, 93.75% cell viability was recorded and this was reduced to 16% when 1.4µg/mL cGel was added to an equivalent concentration of PAA FF103 (a statistically significant difference ($P<0.001$)). An investigation into the trafficking of the FITC-conjugated PAAs, ISA1-FITC and ISA23-FITC, supported PAA mediated cytosolic delivery. In this experiment, ISA1-FITC and ISA23-FITC polymers were non-toxic up to a concentration of 3mg/mL in both Vero and B16 cells and the accumulation of ISA1-FITC in the nucleus was observed after 5h. No increase in cGel toxicity was documented after it was mixed with cRTBC relative to cGel delivery mediated by PAAs. Further, despite being able to ablate RTAC toxicity, cRTBC toxicity remains a problem. Lack of lectinic activity of rRTBC (clone 204) suggests that this is unlikely to be resolved, which limits the application of this delivery system.

Arun Kumar Kotha B.Pharm, MSc.

CONTENTS

DECLARATION	ii
ACKNOWLEDGEMENTS	iii
ABSTRACT	iv
TABLES	xii
FIGURES	xiv
ABBREVIATIONS	xx
Chapter 1 Introduction	1
1. Introduction	2
1.1 The Molecular basis of disease	2
1.2 Molecular therapeutics	3
1.2.1 Protein replacement therapy	3
1.2.2 Gene replacement therapy	5
1.2.3 Antisense therapies	6
1.2.4 RNA interference (RNAi)	9
1.2.5 Ribozymes	11
1.3 Drug delivery strategies for macromolecular drugs	12
1.3.1 Viral vectors	13
1.3.2 Non-viral vectors	14
1.3.2.1 Liposomes	15
1.3.2.2 Micelles	18
1.3.2.3 Nanoparticles	19
1.3.2.4 Cell-penetrating peptides (CPPs)	21
1.3.2.5 Polyplexes	22
1.3.2.6 Neutral and amphiphilic polymers	23
1.3.2.6.1 Poly(amidoamine)s	23
1.4. Toxins and intracellular membrane trafficking	25
1.4.1 Membrane trafficking, endocytosis and the secretory pathway	26
1.4.1.1 Endocytosis	27
1.4.1.2 Early endosome	28

1.4.1.3 Recycling endosomes	28
1.4.1.4 Late endosomes	29
1.4.1.5 Lysosome	29
1.4.1.6 The secretory pathway	29
1.4.1.7 Golgi complex	30
1.4.1.8 Endoplasmic reticulum	30
1.4.1.9 Rab proteins	31
1.4.1.10 Soluble <i>N</i> -ethylmaleimide-sensitive factor activating protein receptors (SNAREs)	33
1.4.2 Toxins	34
1.4.2.1 Ricin	34
1.4.2.2 Cholera toxin	37
1.4.2.3 Shiga toxin	39
1.4.2.4 Gelonin	41
1.4.3 Toxins as membrane manipulating delivery systems	41
1.5 Applications in medicine and cell biology	42
1.6 Aim of work reported in the thesis	44
Chapter 2 Materials and Methods	47
2.1 Materials	48
2.1.1 Equipment & Chemicals	48
2.1.2 Organisms and Cells	49
2.1.3 Stock solutions	49
2.2. Methods	53
2.2.1 PCR templates, construct preparation and sub-cloning	53
2.2.2. Plasmid DNA purification using the QIAprep Spin Miniprep Kit	54
2.2.3 Measuring the plasmid concentration	55
2.2.4 Agarose gel electrophoresis	56
2.2.5 Protein expression and purification	56
2.2.5.1 Bacterial transformation	56
2.2.5.2 Protein expression	57
2.2.5.3 Bacterial lysis	57
2.2.5.4 Immobilised metal ion affinity chromatography (IMAC)	58
2.2.5.5 Calculation of protein concentration	59

2.2.6 Sodium dodecyl sulphate (SDS)-polyacrylamide gel electrophoresis (PAGE)	59
2.2.7 Western blotting	60
2.2.8 Detection of the protein	62
2.2.9 Optimisation of bacterial culture conditions	63
2.2.10 Mammalian cell culture and viability assay	64
2.2.11 Re-association of ricin A and B chains	66
2.2.12 Sub-cellular fractionation	66
2.2.13 Trichloroacetic acid (TCA) protein precipitation	67
2.2.14 Fluorescence microscopy	68
2.2.15 Live cell imaging	70
Chapter 3 Expression, Purification and Characterisation of Ricin	
Toxin Constructs	71
3.1 Introduction	72
3.2 Materials and methods	73
3.3 Results	75
3.3.1 Characterisation of plasmid constructs	75
3.3.1.1 Plasmid maps	75
3.3.1.2 Maintenance and isolation of plasmids	83
3.3.1.3 Agarose gel electrophoresis of purified plasmid DNA	84
3.3.2 Isolation of protein from 1000mL cultures	85
3.3.2.1 Affinity isolation/enrichment of recombinant proteins	86
3.3.3 Protein detection	89
3.3.4 Optimisation of Western blotting	96
3.3.4.1 Optimisation of anti-6His primary antibody dilutions for rRTBC (clone 204) detection	96
3.3.4.2 Optimisation of anti-RTBC primary and HRP-conjugated anti-rabbit IgG secondary antibody dilutions for rRTBC (clone 204) detection	97
3.3.4.3 Optimisation of anti-6His primary antibody and HRP-conjugated anti-mouse IgG secondary antibody dilutions for, rRTAC (clone 189) detection	98
3.3.4.4 Optimisation of anti-RTAC primary antibody and HRP	

-conjugated anti-rabbit IgG- secondary antibody dilutions for rRTAC (clone 189) detection	99
3.3.5 Production and optimisation of recombinant protein culture conditions using mini-induction experiments	100
3.3.5.1 Growth time (pre-induction) (PrIGT)	100
3.3.5.2 IPTG concentration	105
3.3.5.3 Post induction growth time (PoIGT)	109
3.4 Discussion	113
3.4.1 Characterisation of the plasmid constructs	113
3.4.1.1 Plasmid maps	113
3.4.1.2 Isolating plasmids	115
3.4.1.3 Agarose gel electrophoresis of purified plasmid DNA	115
3.4.2 Isolation of protein from 1000mL cultures	116
3.4.3 Protein detection	117
3.4.3.1 Immuno-detection	118
3.4.3.2 Optimisation of immuno-detection	118
3.4.4 Optimisation of bacterial culture conditions using mini-induction experiments	120
3.4.4.1 Growth time (pre-induction) (PrIGT)	120
3.4.4.2 IPTG concentration	121
3.4.4.3 Post induction growth time (PoIGT)	122
3.5 Conclusions	122
Chapter 4 Biological Evaluation of Ricin Toxin Proteins	124
4.1 Introduction	125
4.2 Materials and methods	128
4.3 Results	131
4.3.1 Assessing B16 and Vero generation time	131
4.3.2 Evaluation of RTBC lectinic activity	132
4.3.3 Re-association of mutant RTAC and commercial RTBC	133
4.3.4 Toxicity studies of recombinant proteins	136
4.3.5 Sub-cellular fractionation	142
4.3.6 Immuno fluorescence microscopy	143

4.4 Discussion	144
4.4.1 Growth curve	144
4.4.2 Lectinic activity of RTBC	145
4.4.3 Re-association of RTAC and RTBC	145
4.4.4 Toxicity studies using MTT assay	146
4.4.5 Sub-cellular distribution preliminary results	147
4.4.6. Immuno fluorescence microscopy	148
4.5 Conclusions	149
Chapter 5 Cloning, Expression, Characterisation and Biological Evaluation of Gelonin Constructs	150
5.1 Introduction	151
5.2 Materials and methods	154
5.3 Results	159
5.3.1 Isolation of gelonin template plasmid from <i>E.coli</i> TOP10	159
5.3.2 PCR using specific oligonucleotide	159
5.3.3 The ligation of PCR products into the expression cassette	160
5.3.4 Characterisation of gelonin constructs	161
5.3.5 Plasmid maps of gelonin constructs	162
5.3.6 Gelonin protein expression and purification	167
5.3.7 Detection of gelonin proteins	168
5.3.8 Cytotoxicity of recombinant gelonin (with and without cysteine), cGel and cRTBC	168
5.4 Discussion	174
5.4.1 Sequencing of gelonin constructs	174
5.4.2 Characterisation of gelonin proteins by SDS-PAGE and Western blotting	175
5.4.3 Evaluation of cytotoxicity of rGel, cGel, cRTBC and polymers	176
5.5 Conclusions	178
Chapter 6 Evaluation of ISA1-FITC and ISA23-FITC Polymer Cytotoxicity and Intracellular Trafficking by Fluorescent Microscopy	180
6.1 Introduction	181
6.2 Materials and methods	183

6.3 Results	185
6.3.1 Evaluation of FITC-conjugated PAA cytotoxicity	185
6.3.2 Evaluation of stability of ISA1-FITC polymer in complete or RP media	188
6.3.3 Investigation of polymer intracellular fate	189
6.3.4 Live cell imaging	191
6.4 Discussion	195
6.5 Conclusions	197
Chapter 7 General Discussion	198
Conclusions	213
Future work	214
References	215
Appendix I	244
Appendix II	248

TABLES

Chapter 1

Table 1.1: Candidate diseases for gene therapy	6
Table 1.2: Commonly used viral vectors in gene delivery	13
Table 1.3: Liposome and lipid based products approved for human use	16
Table 1.4: Physiochemical properties of current polymeric systems	23
Table 1.5: Overview of some plant and bacterial toxins	26
Table 1.6: Immunotoxins used clinically in recent years	43
Table 1.7: Constructs evaluated in the project	45

Chapter 2

Table 2.1: Oligonucleotides used during the sub-cloning of RTAC and RTBC	54
Table 2.2: Dilutions of primary and secondary antibodies used for Western blotting	62
Table 2.3: Cell lines used for cytotoxicity assay (MTT) and sub-cellular trafficking experiments	65

Chapter 3

Table 3.1: Miniprep yields of selected plasmid constructs	83
Table 3.2: Predicted size and M_w of evaluated plasmid constructs	85
Table 3.3: RTAC plasmid constructs without GST-GFP	87
Table 3.4: RTAC plasmid constructs with GST-GFP	87
Table 3.5: Predicted molecular weights and sequences of open reading frames (ORFs) of selected clones	114

Chapter 5

Table 5.1: Molecular weights of FF91, FF103, ISA1 and ISA23 polymers	152
Table 5.2: Oligonucleotide primers used for PCR amplification	155
Table 5.3: Oligonucleotide primers used during the screening of colonies generated after TOPO reaction using PCR	157
Table 5.4: Amino acid sequences of gelonin constructs	175

Chapter 6

Table 6.1: ISA-FITC polymers evaluated in this study	184
Table 6.2: Polymers (PEI, ISA1-FITC and ISA23-FITC) cytotoxicity in B16 and Vero cells	188

Chapter 7

Table 7.1: Protein yields of rRTBC and rRTAC constructs	202
Table 7.2: Cytotoxicity (IC_{50}) of RTAC and RTBC in Vero cells	204
Table 7.3: Cytotoxicity (IC_{50}) of RTAC and RTBC in B16 cells	205
Table 7.4: Cytotoxicity (IC_{50}) of rGel, mGel, cRTBC and cRTBC with cGel	209
Table 7.5: Cytotoxicity (IC_{50}) of FF103 alone or along with cGel, mGel or rGel	212

FIGURES

Chapter 1

Figure 1.1: Triplex formation directed to gene silencing	7
Figure 1.2: Structure of classical back bone modified antisense oligonucleotide	8
Figure 1.3: Mechanism of RNA interference	10
Figure 1.4: Hammerhead Ribozyme and its mechanism of action on target RNA	12
Figure 1.5: Four major types of liposomes	16
Figure 1.6: Different types of Nanoparticles	20
Figure 1.7: Endocytic and secretory pathways	27
Figure 1.8: Localisation and function of Rab proteins	31
Figure 1.9: Mechanism of action of Rab proteins.	32
Figure 1.10: Structure of Ricin toxin	34
Figure 1.11: Binding, internilisation, intracellular trafficking and enzymatic action of Ricin toxin	36
Figure 1.12: Three dimentional structure of Cholera toxin	38
Figure 1.13: Crystallographic structure (left) and schematic (right) structures of Shiga toxin	40
Figure 1.14: Ribbon diagram of Gelonin protein	41

Chapter 3

Figure 3.1: Plasmid map of ricin toxin B chain (clone 204)	76
Figure 3.2: Plasmid map of mutant ricin toxin A chain (clone 216)	77
Figure 3.3: Plasmid map of mutant ricin toxin A chain (clone 217)	78
Figure 3.4: Plasmid map of mutant ricin toxin A chain (clone 192)	79
Figure 3.5: Plasmid map of mutant ricin toxin A chain (clone 224)	80
Figure 3.6: Plasmid map of mutant ricin toxin A chain (clone 189)	81
Figure 3.7: Plasmid map of wild type ricin toxin A chain (clone175)	82
Figure 3.8: Agarose gel electrophoresis of selected RTAC plasmid constructs (wells 3-8) and RTBC (well no. 2)	84
Figure 3.9: Coomassie staining of affinity purified, recombinant RTAC proteins without GST-GFP protein	87
Figure 3.10: Coomassie staining of affinity purified, recombinant RTAC proteins with GST-GFP protein	88

Figure 3.11: Coomassie staining of selected recombinant proteins purified by affinity chromatography	88
Figure 3.12: Coomassie staining of bovine serum albumin (BSA)	90
Figure 3.13: Optimisation of transfer time of BSA	91
Figure 3.14: Transfer of BSA (0.1µg to 50µg) onto the nitrocellulose membrane using optimised transfer time (60minutes) confirmed by Ponceau-S staining	91
Figure 3.15: Coomassie staining of affinity purified wild type RTAC (clone175) protein fractions	92
Figure 3.16: Detection of affinity purified wild type RTAC (clone175) by Western blotting	93
Figure 3.17: Coomassie staining of affinity purified rRTBC (clone 204)	94
Figure 3.18: Detection of affinity purified rRTBC (clone 204) by Western blotting	94
Figure 3.19: Detection of affinity purified rRTAC proteins by Western blotting	95
Figure 3.20: Evaluation of limits of detection of rRTBC (204) by Western blotting, using X-ray films	96
Figure 3.21: Optimisation of anti-6His antibody dilution against rRTBC using Western blotting	97
Figure 3.22: Optimisation of anti-RTBC primary antibody and anti-rabbit IgG-HRP conjugated secondary antibody dilutions against rRTBC (clone 204) using Western blotting	98
Figure 3.23: Optimisation of anti-6His primary antibody and anti-mouse Ig-HRP conjugated secondary antibody dilutions against RTAC (clone 189) using Western blotting	99
Figure 3.24: Optimisation of anti-RTAC primary antibody and anti-rabbit IgG-HRP conjugated secondary antibody dilutions against RTAC (clone 189) using Western blotting	100
Figure 3.25: Optimisation of pre-induction growth time for RTAC (clone 189) at 37°C	102
Figure 3.26: Optimisation of pre-induction growth time for RTAC (clone 189) at 30°C	103
Figure 3.27: Optimisation of pre-induction growth time for wild type RTAC (clone 175) at 30°C and 37°C	104

Figure 3.28: Growth curves of selected plasmids	105
Figure 3.29: Optimisation of IPTG concentration for the expression of RTAC (clone 189) at 37°C	107
Figure 3.30: Optimisation of IPTG concentration for the expression of RTAC (clone 189) at 30°C	108
Figure 3.31: Optimisation of IPTG concentration for the expression of wild type RTAC (clone 175) at 37°C and 30°C	109
Figure 3.32: Optimisation of post-induction growth time (PoIGT) for the expression of RTAC (clone 189) at 37°C	110
Figure 3.33: Optimisation of post-induction growth time (PoIGT) for RTAC (clone 189) at 30°C	111
Figure 3.34: Optimisation of post-induction growth time for expression of wild type RTAC (clone 175) at 37°C and 30°C	112
Chapter 4	
Figure 4.1: Growth curve of B16 cells	131
Figure 4.2: Growth curve of Vero cells	132
Figure 4.3: Evaluation lectinic properties of of recombinant RTBC (clone 204) and commercial RTBC	133
Figure 4.4: Re-association of commercial RTAC and RTBC	135
Figure 4.5: Re-association of mutant RTAC (clone 189) and cRTBC	135
Figure 4.6: Cytotoxicity of imidazole in B16 and Vero cells	136
Figure 4.7: Cytotoxicity of mutant RTAC proteins and cRTAC in Vero cells	137
Figure 4.8: Cytotoxicity of mutant RTAC and rRTBC in Vero cells	138
Figure 4.9: Cytotoxicity of mutant RTAC and rRTBC in B16 cells	138
Figure 4.10: Cytotoxicity of cRTAC and cRTBC in Vero cells	139
Figure 4.11: Cytotoxicity of cRTAC and cRTBC in B16 cells	140
Figure 4.12: Cytotoxicity of re-associated cRTAC-cRTBC and rRTAC (clone 189)-cRTBC in Vero cells	141
Figure 4.13: Cytotoxicity of re-associated cRTAC-cRTBC and rRTAC (clone189)-cRTBC in B16	141
Figure 4.14: Evaluation of intracellular trafficking of rRTAC (clone 189) and rRTBC (clone 204) by sub-cellular fractionation, after 4h incubation in Vero cells	143

Figure 4.15: Immuno-fluorescence imaging of Vero cells after treatment with cRTBC	144
---	-----

Chapter 5

Figure 5.1: Chemical structures of FF91, FF103, ISA1 and ISA23 polymers	153
Figure 5.2: Agarose gel electrophoresis of PCR amplified gelonin products	159
Figure 5.3: Agarose gel electrophoresis of PCR products from the colonies which were obtained after TOPO reaction (gelonin-6His-Cys-HA construct)	160
Figure 5.4: Agarose gel electrophoresis of PCR products from the colonies which were obtained after TOPO reaction. (6His-V5-gelonin construct)	161
Figure 5.5: Agarose gel electrophoresis of gelonin plasmid constructs	162
Figure 5.6: Plasmid map of gelonin with cystiene	163
Figure 5.7: Plasmid map of gelonin without cysteine	164
Figure 5.8: Plasmid map of mature gelonin	165
Figure 5.9: Contigs of recombinant gelonin constructs	166
Figure 5.10: Coomassie stained gel of recombinant gelonin proteins (with and without cysteine), mature gelonin and commercial gelonin	167
Figure 5.11: Detection of recombinant gelonin by Western blotting using either a) 6His or b) V5 antibodies	168
Figure 5.12: Evaluation of cytotoxicity of recombinant, mature and commercial gelonin in B16 cells	169
Figure 5.13: Evaluation of cytotoxicity of cRTBC with cGel in B16 and Vero cells	170
Figure 5.14: Evaluation of cytotoxicity of dextran, FF91 and FF103 with rGel (+Cys) in B16 cells	171
Figure 5.15: Evaluation of cytotoxicity of dextran, FF91 and FF103 with rGel (-Cys) in B16 cells	171
Figure 5.16: Evaluation of cytotoxicity of dextran, FF91 and FF103 with mGel in B16 cells	172
Figure 5.17: Evaluation of cytotoxicity of dextran, FF91 and FF103 with cGel in B16 cells	173
Figure 5.18: Evaluation of cytotoxicity of dextran, FF91 and FF103 with cGel in Vero cells	174

Chapter 6

Figure 6.1: Chemical structures of ISA1-FITC and ISA23-FITC polymers	185
Figure 6.2: Evaluation of effect PEI upon the cell viability of B16 and Vero cells following incubation time of 72h using MTT assay (Mean (\pm S.E.M) of one experiment) (n=8)	186
Figure 6.3: Evaluation of effect of ISA1-FITC, ISA23-FITC and dextran upon the viability of B16 cell lines following an incubation time of 72h using MTT assay (Mean (\pm S.E.M) of 3 experiments) (n=24)	186
Figure 6.4: Evaluation of effect of ISA1-FITC, ISA23-FITC and dextran upon the viability of Vero cell lines following an incubation time of 72h using MTT assay (Mean (\pm S.E.M) of 3 experiments) (n=24)	187
Figure 6.5: Evaluation of effect of ISA1-FITC and ISA23-FITC upon the viability of Vero cell lines following an incubation time of 24h using MTT assay (Mean (\pm S.E.M) of 3 experiments) (n=24)	187
Figure 6.6: Evaluation of stability of ISA1-FITC in cell culture and RP media over 5h	188
Figure 6.7: Intracellular trafficking of ISA1-FITC (2mg/mL) with 4h pulse	189
Figure 6.8: Intracellular trafficking of ISA23-FITC (2mg/mL) with 4h pulse	190
Figure 6.9: Intracellular trafficking of ISA1-FITC (2mg/mL) with 4h pulse and 20h chase	190
Figure 6.10: Intracellular trafficking of ISA23-FITC (2mg/mL) with 4h pulse and 20h chase	191
Figure 6.11: Vero cells at different cell density	192
Figure 6.12: Intracellular localisation of ISA1-FITC (2mg/mL) after 4h incubation	192
Figure 6.13: Intracellular localisation of ISA23-FITC (2mg/mL) after 4h incubation	193
Figure 6.14: Intracellular localisation of ISA1-FITC (2mg/mL) after 24h incubation	193
Figure 6.15: Intracellular localisation of ISA23-FITC (2mg/mL) after 24h incubation	194

Chapter 7

Figure 7.1: Comparative analysis of cell viability in Vero cells dosed at different concentrations with rRTAC (clone 189) (red columns)-cRTBC or cRTBC-cRTAC (blue columns)	206
Figure 7.2: Comparative analysis of cell viability in B16 cells treated with 10µg/mL of either cGel or rGel+Cys	210
Figure 7.3: Comparative analysis of cell viability in B16 cells dosed at different concentrations with either FF103 alone or F103-cGel	210

ABBREVIATIONS

Alanine	Ala
Ammonium persulphate	APS
Arginine	Arg
Aspartic acid	Asp
Base pairs	bp
Bicinchoninic acid	BCA
Bovine serum albumin	BSA
BSA-conjugated Texas red®	BSA-TxR
Commercial gelonin	cGel
Commercial ricin toxin A chain	cRTAC
Commercial ricin toxin B chain	cRTBC
Cysteine	Cys
Deoxyribonucleic acid	DNA
Dimethyl sulphoxide	DMSO
[3-(4,5-Dimethylthiazol-2-yl)-2,5-Diphenyltetrazolium Bromide]	MTT
Dulbecco's-Minimal Essential Medium	D-MEM
Early endosomal antigen 1	EEA1
Enhanced chemiluminescence	ECL
Ethylenediaminetetraacetate	EDTA
Enhanced permeability and retention effect	EPR effect
Ethidium bromide	EtBr
Foetal bovine serum	FBS
Glutamic acid	Glu
Glutamine	Gln
Glutathione-S-transferase	GST
Glycine	Gly
Golgi matrix protein of 130KDa	GM130
Green fluorescent protein	GFP
6Histidine	6His
Horseradish peroxidase	HRP
Interpolyelectrolyte complex	IPEC
Isopropyl β -D-1-thiogalactopyranoside	IPTG

Immobilised metal ion affinity chromatography	IMAC
Kilobase pairs	Kbp
Kilodaltons	kDa
Laemmli sample buffer	LSB
Leucine	Leu
Lysine	Lys
Lysosomal-associated membrane glycoprotein 1	LAMP1
Mature gelonin	mGel
2-Mercaptoethanol	BME
Number average molecular weight	M_n
Optical density	OD
Paraformaldehyde	PAF
Penicillin-streptomycin-glutamine	P/S/G
Phenylalanine	Phe
Phosphate buffered saline	PBS
Poly(ethyleneimine)	PEI
Pounds per square inch	psi
Protease inhibitor	PI
Radius of gyration	R_g
Ras-related in brain	Rab
Recombinant gelonin	rGel
Recombinant ricin toxin A chain	rRTAC
Recombinant ricin toxin B chain	rRTBC
Richardson Piper media	RP media
Revolutions per minute	rpm
Sodium dodecyl sulphate	SDS
Standard deviation	SD
Standard error of the mean	SEM
Super optimal broth with catabolic repressor	SOC
N, N, N' N'-Tetramethylenediamine	TEMED
Texas red®	TxR
Trans-Golgi network protein of 46KDa	TGN46
Trichloroacetic acid	TCA

Tris acetate EDTA	TAE
Trypsin-ethylenediaminetetraacetate	TE
2x Yeast extract and tryptone digest media	2xYT
Volume for volume	v/v
Weight average molecular weight	M_w
Weight for volume	w/v
Weight for weight	w/w
WGA conjugated-Texas red®	WGA-TxR
Wheat germ agglutinin	WGA

Chapter 1
Introduction

1. Introduction

1.1 The Molecular basis of disease

To treat a disease effectively it is vital to understand its pathology at the molecular level, facilitating the treatment of the disease rather than focusing upon the alleviation of its symptoms. Once the molecular interactions (or lack thereof), responsible for a disease's pathology or life cycle are understood, it may be possible to design molecular medicines tailored to replace or inhibit dysfunctional molecules (such as proteins). There are several molecular medicines proposed that have the capacity to act at the molecular level, acting on specific genes and proteins to either ablate (*i.e.* RNA interference (RNAi)) or restore (gene or protein replacement therapy), protein expression and function (Verma and Weitzman, 2005) (section 1.2.1, 1.2.2). Molecular medicines have the capacity to act as very effective anti-viral agents by targeting genes that are critical for viral replication for down-regulation (Leonard and Schaffer, 2006; Haasnoot and Berkhout, 2006). Additionally, the replacement of a specific missing or defective gene has also been attempted clinically (Alexander *et al.*, 2007; Aiuti *et al.*, 2009). However, currently, with the exception of the antisense drug Vitravene® (section 1.2.3), nucleic acid-based drugs are not in routine clinical use. This is due to problems associated with the safety and bioavailability of nucleic acid based drugs and it is possible that these rate limits may be alleviated using advanced drug delivery strategies (Juliano *et al.*, 2008; Patil *et al.*, 2005).

The ultimate goal of drug delivery is to safely deliver a therapeutic agent to the desired target at an optimal therapeutic dose and, where necessary, negating unwanted off target effects. Currently there are two types of nucleic acid delivery system, namely viral and non-viral delivery systems (section 1.3.1 and 1.3.2). Both have advantages and limitations, which also will be discussed herein (section 1.3.1 and 1.3.2).

The aim of this thesis is to explore new technologies capable of delivering macromolecular therapeutics (*i.e.* proteins and nucleic acids or analogues thereof) to a desired compartment within a cell, in a safe, reproducible and efficient fashion. The rationale behind the work undertaken herein has been to identify molecules that in the wild (natural state), access the cytosolic compartment of cells. This information can then be applied to 'drug delivery' through delivering therapeutic macromolecules rather than toxic proteins. (Grimaldi *et al.*, 2007; Johannes and Decaudin, 2005).

Several toxins, such as ricin toxin (section 1.4.2.1), have evolved to escape lysosomal degradation and access the cytosol. Unlike membrane breaching toxins such as diphtheria,

ricin has the potential, once disarmed, to leave cells alive (Smith *et al.*, 2003). The approach adopted herein has been to utilise this ability to deliver therapeutic molecules into the cytosol, without mediating subsequent cellular intoxication or irrevocable membrane damage, leading to cell death.

1.2 Molecular therapeutics

In this thesis potential macromolecular medicines that operate in a gene specific manner will be referred to as molecular therapeutics. In a wider sense, this term covers:

(i) **Protein replacement therapy**, *i.e.* the use of recombinant proteins requiring delivery to an intracellular environment (rather than acting as a ligand in the extracellular environment).

(ii) **Gene replacement therapy** *i.e.* the expression of exogenously produced open reading frames coding for proteins either missing or damaged within the host genome.

(iii) **Antisense therapy**, using agents such as phosphorothioate oligodeoxynucleotides to down regulate messenger ribonucleic acid (mRNA) in a gene specific manner (*i.e.* Virtavene developed by Isis Pharmaceuticals).

(iv) **RNAi therapy**, using RNAi agents to facilitate the gene specific down regulation of mRNA.

(v) **Ribozyme therapy**, using ribozymes (*i.e.* Hammerhead ribozymes) to mediate the sequence specific ablation of protein expression via the gene specific down regulation of mRNA.

1.2.1 Protein replacement therapy

Protein replacement therapy plays an important role in curing genetic as well as acquired diseases. In order to be effective, the cellular compartmentalisation of the target molecule (*i.e.* substrate or receptor) needs to be considered. This is important as the target may not necessarily be presented on the cell's plasma membrane and consequently, may not be accessible to a macromolecule in the interstitium. Examples of molecules that function outside the cell are insulin and growth factors, which activate receptors to initiate a physiological response. Levemir® (Novo Nordisk) is an example of a macromolecular drug that functions outside the cell and is used to treat diabetes. Levemir® contains recombinant insulin which is used to maintain physiological blood glucose levels (*i.e.* 4-7mmol/L before meals, and less than 9mmol/L two hours after meals), by binding to extracellular domains of insulin receptors, distal to the exofacial leaflet of the plasma membrane. By contrast,

potential anti-cancer therapeutic molecules such as the protein p53 need to be delivered to the cytosolic or the nuclear compartments in order to exert a therapeutic effect (*i.e.* monitoring and responding to cell stress so preventing cumulative genetic damage) (Kastan, 2007). This requires the transport of the macromolecule across a biological barrier.

Other less obvious examples of drugs that, from the perspective of topology may still be considered to exert their effect “outside” the cell are seen during the treatment of lysosomal storage diseases. As the internal “lumen” of the lysosome maybe considered topologically equivalent to the interstitium (*i.e.* no biological barriers have been traversed), this compartment (*i.e.* the late endosome or lysosome (section 1.4.1.4 and 1.4.1.5)) is readily accessible via the endocytic internalisation of macromolecules (Luzio *et al.*, 2003).

Lysosomal storage diseases are rare, inherited, metabolic disorders, which result from defects in lysosome function (Winchester *et al.*, 2000; Ballabio and Gieselmann, 2009). Lysosomes are responsible for the storage of enzymes that mediate the digestion of naturally occurring endogenous and exogenous macromolecules and the subsequent transport and recycling of their constituent components into the cytosol (Pastores, 2009). The reduced efficiency of lysosomal catabolism may result in the accumulation of exogenous material in the lysosome. This can result in oxidative stress, further reducing the lysosomes ability to participate in the catabolism of material, eventually resulting in lysosomal storage diseases. Lysosomal storage diseases are manifest in many ways clinically from reduced cognitive function (Sands and Haskins, 2008) to cardiomegaly and macular degeneration (Kopitz *et al.*, 2004). Examples include Pompe’s disease (van der Ploeg and Reuser, 2008), Danon disease (Nishino *et al.*, 2000) and the accumulation of lipofuscin associated with macular degeneration (Terman and Brunk, 2004).

Currently, there are 40 types of lysosomal storage diseases identified and in most instances endocytosis provides a useful mechanism to deliver drugs or exogenous enzymes into the lysosome (Heese, 2008). Cerezyme® (Genzyme) is used to treat Gaucher’s disease, an inherited disorder caused by a deficiency of the lysosomal enzyme glucocerebrosidase (Grabowski, 2008). Cerezyme is recombinant analogue of human β -glucocerebrosidase, which catalyses the hydrolysis of the glycolipid glucocerebroside to glucose and ceramide. Another example of a lysosomal storage disease that is treated with a recombinant protein is Fabry diseases, a rare inherited, X-linked lysosomal storage disorder. Fabrazyme® (Genzyme) is in use for the treatment this disorder.

Enzyme/protein replacement therapy has been effective in the treatment of type 1 diabetes. However, as proteins are immunogenic, susceptible to degradation and may have poor pharmacokinetics, delivery systems are still not useful. Further, protein activity requires the targeting of a topological intracellular compartment *i.e.* the nucleoplasm or the cytoplasm. Therefore advanced drug delivery systems are required.

1.2.2 Gene replacement therapy

Gene replacement therapy requires the delivery of a functional gene into the nucleus (or mitochondrion) of a human cell in order to correct a genetic error (Cotrim and Baum, 2008). This destination is on account of the location of the machinery necessary for transcription, *i.e.* RNAPolymerase II (Sims *et al.*, 2003). Gene replacement therapy differs from pharmacological therapy in that it seeks to correct a disease genotype defect, rather than treating the phenotypic expression of a genotypic defect (Mulligan, 1993). Examples of targets for gene therapy include: (i) disorders that are caused by the lack of an encoded protein (Sauer and Aiuti, 2009) (ii) an abnormal arrangement of one or more chromosomes that may lead to genetic defects (Roizen and Patterson, 2003) or (iii) Mendelian or inherited disorders caused by mutant gene(s) (Walker, 2007).

However, even though the pathologies of many diseases are well characterised at the molecular level, there has been little clinical success documented for the use of gene replacement therapy (*i.e.* examples (i) & (iii) above) (Qasim *et al.*, 2009). This lack of measurable success is not due to a lack of an understanding of the pathology of the disease at the molecular or cellular level, but an inability to successfully deliver the corrective gene to the correct compartment of the target cell type (Verma and Somia, 1997; Cao *et al.*, 2010). Many potential solutions to this problem have been proposed and many have been taken into clinical trials (Alexander *et al.*, 2007; Aiuti *et al.*, 2007; Kohn, 2010). Selected examples of conditions that have been candidates for gene therapy are listed in the table below:

Table 1.1: Candidate diseases for gene therapy

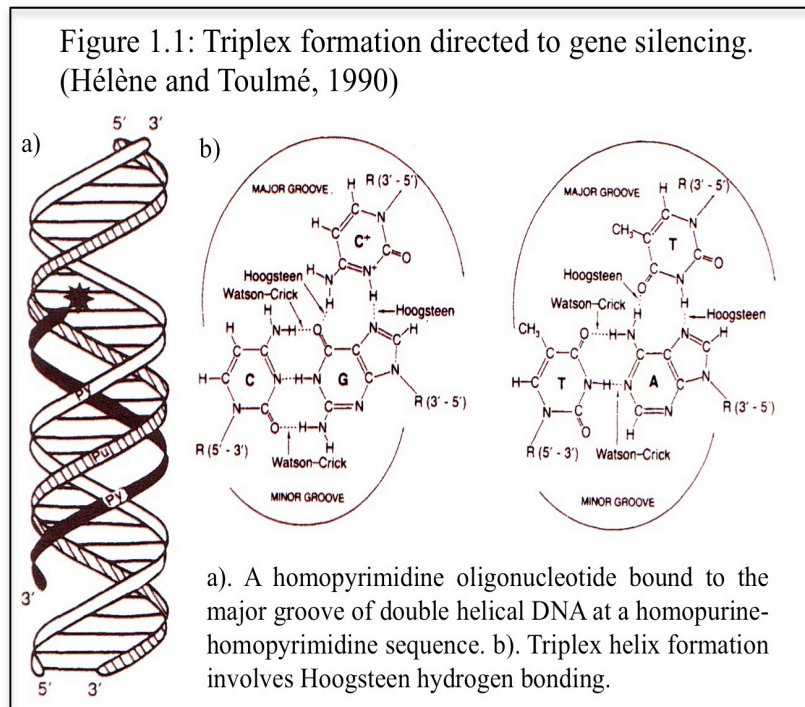
Disease	Cause	Target cells	Market/Clinics	References
Genetic				
Severe combined immunodeficiency (SCID)	Mutation of ADA gene	Bone-marrow cells or T lymphocytes	Adagen [®] , Enzon Pharmaceuticals, Inc	Cavazzanna-Calvo <i>et al.</i> , 2005; Cristalli <i>et al.</i> , 2001
Cystic fibrosis	Mutation of CFTR gene	Airways in the lungs	VX-770, Vertex Pharmaceuticals (Phase III)	Limberis, 2008; Griesenbach <i>et al.</i> , 2006
Muscular Dystrophy	Mutation of genes responsible for dystrophin production	Skeletal muscles and heart	AVI-4658, AVI Biopharma (Phase I, II)	Market <i>et al.</i> , 2009; Duan, 2006
Acquired				
Cancer	Genetic and environmental	Variety of cells: Liver, brain, breast, pancreas and kidney	Gendicine [®] , Oncorine [®] (Only approved in China)	Peng, 2005; Wilson, 2005
Infectious diseases (AIDS)	Infection with HIV virus	T cells, macrophages	VRX496 [™] , VIRxSYS Corporation (Phase II)	Levine <i>et al.</i> , 2006; Lu <i>et al.</i> , 2004

1.2.3 Antisense therapies

Proteins are fundamental components of all living cells, and are involved in both the regulation and execution of many communicatory, metabolic and enzymatic activities, as well as maintaining the structural integrity of supportive material such as fascia (Cho and Stahelin, 2005). The phenomenon of antisense, discovered in bacteria as a means of defence against viral invasion (Stephenson and Zamecnik 1978; Simons and Kleckner, 1988), has been used to prevent the expression of proteins involved in disease process in mammalian cells. This is achieved through the destruction of mRNA, ablating the translation of the target protein.

Duplex Formation: The process of antisense gene-down regulation is mediated via oligonucleotide analogues hybridising to single stranded mRNA via Watson-crick base

pairing. It is this base pairing that provides the transcript specificity, enabling antisense oligonucleotides to be used to down regulate specific genes (Kurreck, 2003). The exact method employed to mediate expression ablation is, from this precept, quite variable, as there are at least seventeen possible oligonucleotide interactions that may inhibit gene expression (Crooke, 1999; Bennett and Swayze, 2010).



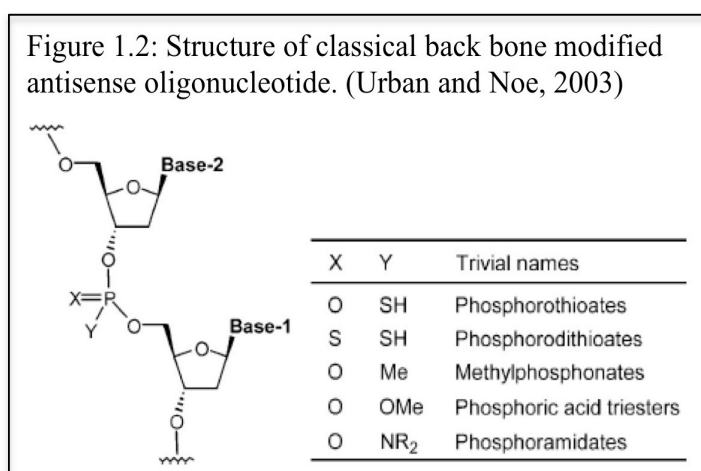
Some of the most commonly cited mechanisms include: (i) the hybridisation of the oligonucleotide over the intron/exon border preventing pre-mRNA maturation (*i.e.* intron splicing) (Crooke, 1999), (ii) the hybridisation of the oligonucleotide preventing the passage of the mature mRNA transcript through the ribosome (Praseuth *et al.*, 1999) and (iii) the oligonucleotide hybridising to the ribosome binding regions associated with the 5' end of the mRNA preventing the initiation of translation (Hélène and Toulmé, 1990). Once the oligonucleotide mRNA hybrid has formed, the mRNA portion of the hybrid is then subject to enzymatic degradation by RNAase H, freeing the oligonucleotide to hybridise to further mRNA transcripts (Ideue *et al.*, 2009).

Triplex formation: Where regions of homo-purine or homo-pyrimidine duplex are present within the target gene, an anti-gene oligonucleotide may bind to the major groove of the DNA duplex forming a triplex. Triplex formation is achieved via Watson-Crick-Hoogsten/reverse Hoogsten bonding (depending upon the orientation of the oligonucleotide) (Hélène

and Toulmé, 1990). The formation of the triplex is then thought to limit the ability of RNA polymerase II to bind to and open a replication bubble, inhibiting pre-mRNA synthesis.

Limitations: Even though antisense has been documented to ablate gene expression *in vitro* (Hassan *et al.*, 2006), *in vivo* (Hadaschik *et al.*, 2008) and in the clinic, there are some fundamental problems that have been reported with this phenomenon (Crooke, 2004a). Phosphodiester oligonucleotides are susceptible to degradation by nucleases, limiting their half-life in biological fluids such as plasma (Akhtar *et al.*, 2000) or within lysosomes (Fischer *et al.*, 1993). In addition, the binding of antisense oligonucleotides to serum proteins has also been documented to limit antisense oligonucleotide bioavailability and hamper the delivery of antisense agents to the desired pharmacokinetic compartment (Akhtar *et al.*, 1991). In addition, similarly to RNAi agents (section 1.2.4) there is also the possibility that polyanions activate an anti-viral interferon response (Schultz *et al.*, 1977). However, there is also the problem of delivering the antisense oligonucleotide to the correct intracellular location *i.e.* into the cytosol or to the nucleus of the cell (Shi and Hoekstra, 2004). Of the rate limits identified above, stability is the one that most work has focused upon, and various strategies centering upon the chemical modification of the oligonucleotide backbone have been documented.

Stability: Oligonucleotide stability in biological fluids has been enhanced by the chemical modification of the nucleotide (Urban and Noe, 2003). All of these strategies require that the position and orientation of the bases relative to one another in space are not altered, so they can still co-ordinate with the target bases located on the mRNA transcript.



The first generation antisense oligonucleotide utilised the substitution of one unbound, non-bridging oxygen atom (of the prochiral phosphorous) with a sulphur, nitrogen or boron atom.

Figure 1.2 documents substitution strategies (figure modified from Urban and Noe, 2003). Second generation antisense oligonucleotides have substitutions within the sugar moiety, at the 2' position (Altmann *et al.*, 1996). Oligonucleotides bearing an alkoxy substituent at position 2' have proven to be stable against DNA or RNA cleaving enzymes (Werner *et al.*, 1998). The third generation of antisense oligonucleotides include the introduction of 6-aminohexyl groups within the sugar moiety (Chan *et al.*, 2006). Peptide nucleic acids (PNA) also demonstrate the replacement of the ribose and phosphodiester backbone with a peptide chain. This peptide chain is very stable with regard to nucleases, and demonstrates increased binding affinity for RNA (Demidov *et al.*, 1993; Demidov *et al.*, 1994).

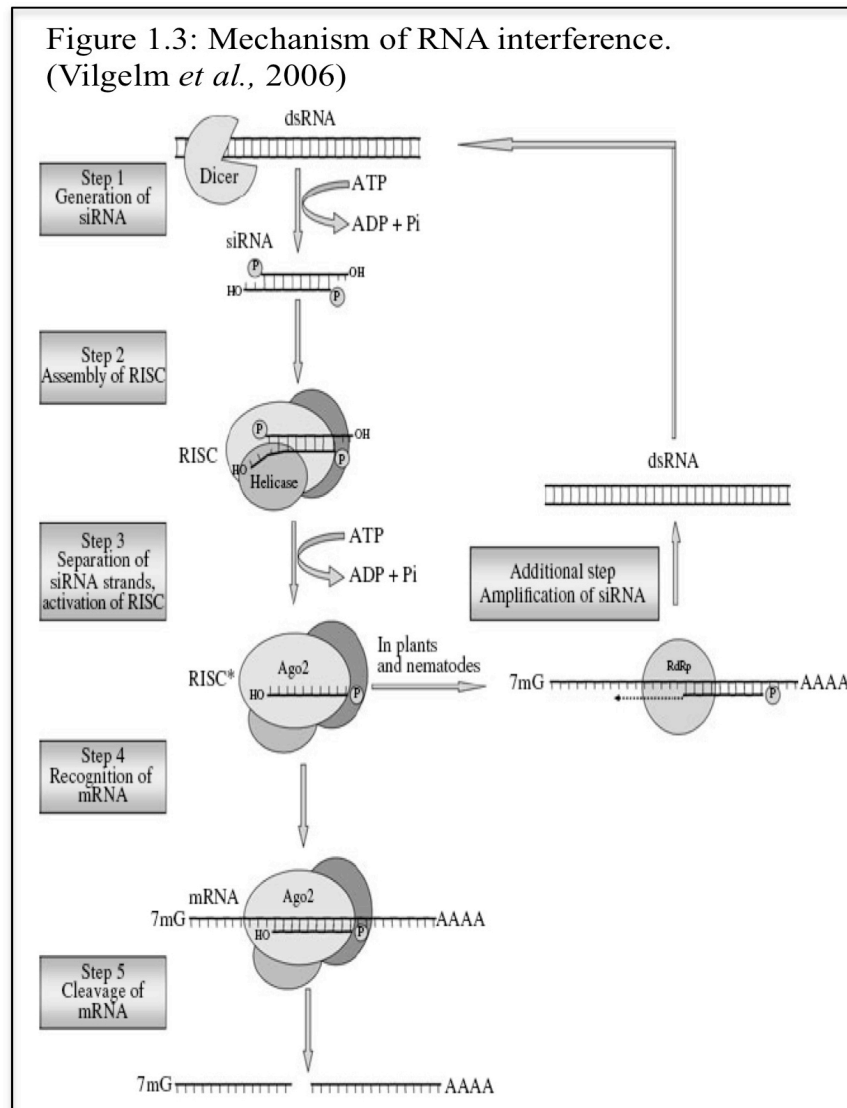
Beyond modulating oligonucleotide stability and hence half-life, increased cellular delivery and decreased serum interactions can be achieved by forming oligonucleotides complexes with delivery vectors such as polymers or liposomes and will be discussed in detail later in this thesis (section 1.3.2.5 and 1.3.2.1).

It is also of note that to date, the only nucleic acid based drug that is routinely used in the clinic is an anti-cytomegalovirus (CMV) antisense phosphorothioate oligonucleotide developed by Isis Pharmaceuticals. This drug is marketed under the name Virtavene[®] and this is administered by intravitreal administration into patients facing CMV mediated blindness during the terminal stages of acquired immunodeficiency syndrome (AIDS) (Crooke, 1998). Virtavene[®] was approved for use in the USA by the FDA in 1989 (Crooke, 2004b).

1.2.4 RNA interference (RNAi)

RNA interference (RNAi) is sequence-specific gene silencing and is induced by small interfering (si) RNA, also known as RNA interference (RNAi). Andrew Z. Fire and Craig C. Mello first documented RNAi in *Caenorhabditis elegans* in 1998 and were awarded the Nobel Prize for Physiology or Medicine in 2006 (Fire *et al.*, 1998). Since its discovery, the phenomenon of RNAi has been demonstrated in organisms ranging from trypanosomes to nematodes and vertebrates (Agarwal *et al.*, 2003). Initial experiments in mammals triggered an interferon response, which resulted in the inhibition of protein translation and finally dramatic alteration in cellular metabolism (Gil and Esteban, 2000). However, as RNA is significantly less stable than DNA in biological fluid (Wang and Kool, 1994) and also shares all of the problems of bioavailability associates with antisense, gene replacement and intracellular protein replacement therapy, it is still not feasible (or safe) for routine clinical use (Juliano *et al.*, 2008).

After the entry of double stranded (ds) RNA into the cells, dsRNA is recognised and cleaved by the Dicer enzyme complex, a member of the type III RNase family, (Scherr *et al.*, 2003). The Dicer complex catalyses the formation of double stranded, siRNAs (20-25bp) (Hannon, 2002). Dicer catalyses the cleavage of siRNAs, containing two protruding non-paired nucleotides with the hydroxyl group at the 3' end and phosphate groups at the 5' end (Chiu and Rana, 2002).



The siRNA produced by the Dicer complex binds to the RNA-induced silencing complex (RISC) of proteins (Leung and Whittaker, 2005). The RISC complex includes the Ago2 protein, an Argonaute family member possessing PAZ domains (P-element induced wimpy testis (PIWI) Argonaut, and Zwiille). The PIWI domain is similar in structure to RNase H, and is responsible for the endonuclease activity associated with the RISC complex (Lingel

and Izaurralde 2004). The PAZ domain is thought to recognise and bind siRNA, having two non-paired nucleotides at the 3' end (Song *et al.*, 2004). Initially RISC binds to double-stranded siRNA and is inactive. This complex is activated by ATP dependent unwinding of the double stranded siRNA molecule through an RNA helicase into single stranded RNA (Nykanen *et al.*, 2001). The now active RISC complex contains only the antisense strand of siRNA which allows RISC to recognise and bind the complementary region of the target mRNA, which is then cleaved by the RISC nuclease Ago2 and rapidly degraded into fragments (Stanislawska and Olszewski 2005). Recently, for the first time in-human phase-I clinical trial was performed using formulated siRNA (using linear cyclodextrin, TfR ligand and PEG) applied systemically to investigate the reduction of expression of RRM2 gene by Mark Davis group (Davis *et al.*, 2010).

RNAi has been reported to be considerably more (several orders of magnitude) active than antisense when down-regulating a specific gene (Bertrand *et al.*, 2002). However, like antisense, RNAi agents suffer from an inability to cross biological barriers (Aagaard and Rossi, 2007) such as cell membranes.

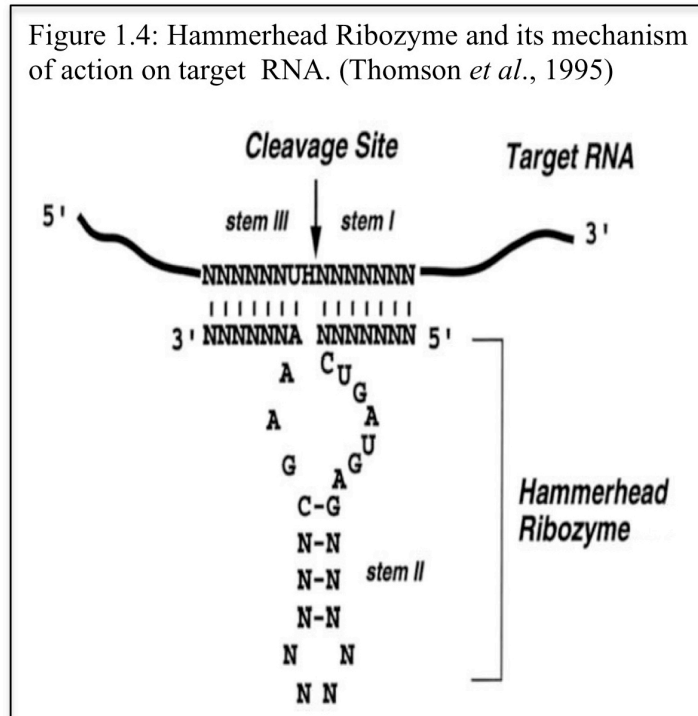
1.2.5 Ribozymes

Ribozymes are sequences of RNA that contain secondary structure, imparting catalytic activity (Lilley, 2005). This catalytic activity may be directed towards the destruction of specific coding sequences of mRNA, thus interrupting gene expression (Grassi *et al.*, 2004). Consequently these molecules have been proposed for the development of therapeutics directed against viral infections and cancer (Schubert and Kurreck, 2004).

Different ribozyme motifs with RNA cleavage activity have been discovered (Symons, 1992) and among these, the hammerhead ribozyme is probably best understood. It has the smallest and has the simplest target sequence requirements (figure 1.4) (Citti and Rainaldi, 2005). The specificity of a ribozyme is determined by the binding arms flanking the cleavage site, forming stem I and stem III (figure 1.4) (Thomson *et al.*, 1995). The sequences of these arms can be varied to direct a hammerhead ribozyme against a specific RNA (Birikh *et al.*, 1997). Such ribozymes can inhibit gene expression by cleaving an mRNA encoding a particular gene product (Citti and Rainaldi, 2005).

The delivery of ribozymes to a cell can be achieved either endogenously by employing a vector based system to promote ribozyme expression (*i.e.* a virus or a plasmid) (Lin *et al.*, 2004) or exogenously (Bramalge *et al.*, 1998) using naked ribozymes or ribozymes in an

ionic complex with a lipid or polymeric delivery vehicle (Aigner *et al.*, 2002; Kashani-Sabet, 2004).



However, as with RNAi agents and antisense agents, cell penetration (Scanlon, 2004) and stability are often rate-limiting (Rossi *et al.*, 1992; Khan, 2006). However, even with the use of plasmid vectors to deliver encoded ribozymes, a delivery strategy for the plasmid is still necessary.

1.3 Drug delivery strategies for macromolecular drugs

There are two principal strategies employed to delivery macromolecular drugs and these are viral based delivery systems and non-viral based delivery systems. Although the latter are sometimes referred to as viral mimetic delivery systems (Verma and Weitzman, 2005) they are usually synthetic in origin and incorporate supramolecular assemblies, such as liposomes, micelles (Pitard, 2002) and hyperbranched synthetic molecules such as dendrimers (Dufès *et al.*, 2005). After many clinical trials, the trends that have emerged show that although the viral systems have higher transfection efficiency, they are less safe than the non-viral delivery systems. Further non-viral systems can also carry larger coding sequences (Schätzlein, 2003; Mastrobattista *et al.*, 2005).

1.3.1 Viral vectors

Viruses have the ability to infect specific populations of cells (Barzon *et al.*, 2005) and in the wild; this is achieved through the intracellular delivery of nucleic acids (Lundstrom, 2003). By suppressing the toxicity of the virus and by regulating the efficiency of gene transfer and expression, replication deficient viruses have been used as vectors to deliver therapeutic genes in the clinic (Walther and Stein, 2000). Several commonly used examples of viral vectors are given below:

Table 1.2: Commonly used viral vectors in gene delivery

Property	Adenovirus	Adeno-associated virus	Lentivirus	Retrovirus
Genome	Double stranded DNA	Single stranded DNA	Single stranded RNA	Single stranded RNA
Coat	Naked	Naked	Enveloped	Enveloped
Virion diameter	70-90nm	18-26nm	80-130nm	80-130nm
Infection	Dividing/non dividing	Dividing/non dividing	Dividing/non dividing	Dividing
Host genome interaction	Non-integrating	Integrating	Integrating	Integrating
Transgene expression	Transient	Long lasting	Long lasting	Long lasting
Packaging capacity	~ 30kb	3.5-4.0kb	7-7.5kb	7-7.5kb
Safety problems	Potentially immunogenic	Inflammatory response	Possibility of insertional mutagenesis	Possibility of insertional mutagenesis
References	Verma and Weitzman, 2005; Russel, 2009	Geoffroy and Salvetti, 2005; Coura and Nardi, 2007	Escors and Breckpot, 2010; Bartosch and Cosset, 2004	Buchsacher, 2001; Lech and Somia, 2008

1.3.2 Non-viral vectors

Non-viral vectors usually require interpolyelectrolyte complex (IPECs) formation (Kabanov *et al.*, 1991). IPECs are ionic complexes formed via the interaction of the negatively charged non-bridging oxygen atoms associated with the phosphate groups of DNA or RNA backbone with the cationic groups associated with the vector (De Smedt *et al.*, 2000). This ionic association between the nucleic acid and the vector will usually cause a dramatic alteration in nucleic acid solution conformation (Kabanov and Kabanov, 1995). This will usually result in the DNA complex behaving as a colloid rather than a solute (Morille *et al.*, 2008). A dramatic change in the nucleic acids radius of gyration (R_g) has been reported following complex formation, which is referred to as condensation (Bloomfeld, 1996) and is a result of DNA coil collapse (Tang and Szoka, 1997). One of the immediate advantages of this alteration in nucleic acid size is that reducing a plasmid's R_g to 100 nm (from that of several microns) makes the plasmid more amenable to endocytic uptake, so facilitating the of the transfection process (Kundu and Sharma, 2008). Further, nuclease stability is conferred via an alteration in solution conformation associated with nucleic acid coil collapse that accompanies nucleic acid condensation (Bielinska *et al.*, 1997).

Typically, non-viral vectors possess low transfection efficiency and are relatively safe when compared to viral vectors (Ogris and Wagner, 2002). However synthetic non-viral vectors also possess several advantages when compared to viral vectors. These include a high capacity to form nucleic acid complexes (*i.e.* there is no limit to the size of the plasmid they can carry) (Wong *et al.*, 2007). These vectors can also be synthesised to be less immunogenic than viral vectors (Schmidt-Wolf and Schmidt-Wolf, 2003) and much effort has been directed towards synthesising biocompatible vectors that show useful body distribution, enhances stability and transfection efficiency (Luten *et al.*, 2008; Massignani *et al.*, 2009).

However a paradox is evident in the literature describing these vectors. In order to mediate transfection and form ionic complexes with (polyanionic) DNA, non-viral vectors are usually highly positively charged (De Smedt *et al.*, 2000; Brown *et al.*, 2001). Conventional thinking states that for a polymeric vector to be able to mediate transfection (requiring the transport of the plasmid across a biological membrane), a net positive charge is required (Ogris and Wagner, 2002). However, imparting a positive charge will impact upon the body distribution of the complex, driving it towards the liver and facilitating sequestration in capillary beds such as those of the lung (Kircheis *et al.*, 1999). Whilst this maybe useful for the transfection of capillary endothelial cells, it limits the usefulness of this approach for systemic tumour targeting. Research into Protective Interactive Non-Condensing polymers (PINC) and

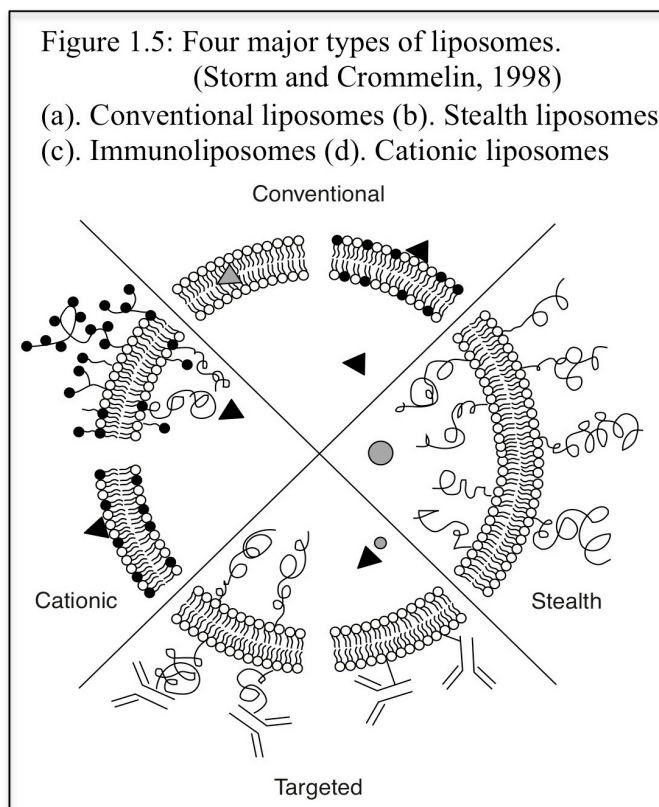
amphoteric polymer systems may provide an answer to this paradox since they do not need to display a net positive charge at pH 7.2-7.4 once they form complex with DNA for cytosolic delivery (Mumpher *et al.*, 1998; Fewell *et al.*, 2001). Detailed below are examples of the more well characterised, non-viral systems documented in the literature, which may be thought of as being either lipid or polymer based.

1.3.2.1 Liposomes

Liposomes are micro-particulate or colloidal carriers which form spontaneously when specific lipids are hydrated in aqueous media (Sharma and Sharma, 1997). Liposomes usually range 0.05-5.0 μ m in diameter and may form mono- or multi-lamella structures (Banerjee, 2001). Drugs with varying lipophilicities can be contained either in the phospholipid bilayer (Fahr *et al.*, 2005) or entrapped within the core of the liposome (Zamboni, 2005). Liposomes can be classified on different parameters. With respect to their interaction, liposomes can be divided into four types: (1) conventional, (2) stealth, (3) targeted and (4) cationic.

Conventional liposomes: Conventional liposomes are typically composed of only phospholipids, which may be neutrally or negatively charged (Storm and Crommelin, 1998). Cholesterol may also be added to relieve curvature strain on either leaflet stabilising the liposome (Sułkowski *et al.*, 2005). Conventional liposomes have relatively short blood circulation time as after intravenous administration, they show a strong tendency to accumulate in the mononuclear phagocytic system (MPS) (Scherphof *et al.*, 1985). Consequently, due to the large abundance of macrophages within the liver and spleen, these organs are major sites for lipoplex accumulation (Agarwal and Gupta, 2000; Basu and Lala 2004).

This property of conventional liposomes can be used to effectively deliver anti-parasitic and antimicrobial drugs to treat infections localised in the MPS and can also be used in delivery of immunomodulators to increase the capacity of macrophages to kill neoplastic cells (Daemen *et al.*, 1995; Killion *et al.* 1994). Liposome based vaccines proved effective against viral, bacterial, parasitic infections and against tumours in experimental models. A liposomal hepatitis-A vaccine has received marketing approval in Switzerland (Glück, 1995). The most serious disadvantage of conventional liposomes is that if the target is beyond macrophages, the payload may not reach the target as they have short blood circulation time.



Sterically stabilised stealth liposomes. MPS uptake can be avoided by coating the surface of the liposome with inert molecules, such as PEG. PEG coating provides a spatial barrier resulting in the inhibition of opsonisation in the blood stream (Immordino *et al.*, 2006). This has the effect of dramatically increasing the plasma residence time of the liposome (Blume and Cevc, 1993; Immordino *et al.*, 2003). Having extended circulation time, stealth liposomes demonstrate extravasation and passive accumulation within tissue with increased vascular permeability *i.e.* solid tumours and sites of infection and inflammation. This process is driven by the aforementioned EPR effect (Maeda *et al.*, 2001).

Table 1.3: Liposome and lipid based products approved for human use.
(Sharma and Sharma, 1997)

Product	drug	Formulation	Company	Indication/target	Country
Doxil™(a)	Doxorubicin	Liposomes (LCL)	Sequus Pharmaceuticals, Inc., CA	Kaposi sarcoma in AIDS	USA and Europe
Ambisome™	Amphotericin B	Liposomes (CL)	NeXstar Pharmaceutical, Inc., CO	Serious fungal infections	Around the world in 24 countries
DaunoX-ome™	Daunorubicin citrate	Liposomes (LCL)	NeXstar Pharmaceutical, Inc., CO	Kaposi sarcoma in AIDS	USA and Europe
Amphocil™	Amphotericin B	Lipid complex	Sequus Pharmaceutical, Inc., CA	Serious fungal infections	Asia and Europe
Abelcet™	Amphotericin B	Lipid complex	The Liposome Company, NJ	Serious fungal infections	USA and Europe

PEG has been extensively studied as a mediator of the “stealth” effect and has been incorporated into several types of liposome (Harrington, 2000) also referred to as sterically stabilised liposomes (Papahadjopoulos, 1991). PEG is a linear polyether diol and has been shown to be highly soluble in aqueous and organic media whilst lacking toxicity and demonstrating low immunogenicity and antigenicity (Dreborg and Akerblom, 1990). In most cases longer-chain PEGs have produced the highest improvement in blood residence time (Allen *et al.*, 1991). Doxil® (Centocor Ortho Biotech) and the DaunoXome® (Gilead Sciences Inc.) are examples of stealth liposomes that are in routine clinical use.

Immunoliposomes: To increase target specificity and to achieve high drug concentrations at the site of action, targeting moieties have been incorporated onto the surface of liposomes. This venture has been undertaken to not only improve the targeting of diseased cells, but also to increase the avidity of cell binding, inducing the internalisation of the liposome (and the encapsulated drugs) (Immordino *et al.*, 2006). Various targeting moieties are available, such as monoclonal antibodies (Park *et al.*, 2002) or antibody fragments (Laginha *et al.*, 2008), peptides (Mastrobattista, 2002), growth factors (Mamot *et al.*, 2005), glycoproteins (Huwyler *et al.*, 2002), carbohydrates (Zhang *et al.*, 2010) or receptor ligands (Yang *et al.*, 2009). Immunoliposomes are liposomes that have had antibody or antibody fragments attached to them to facilitate the targeting of a specific cell type.

Cationic liposomes: Cationic liposomes are attractive candidates for gene delivery as they can condense DNA into a highly organised structure and may protect it from degradation by endonucleases. A proportion of the components of cationic liposomes contain a positively charged head group, which interacts with negatively charged DNA. In addition, a linker group determines the lipids chemical stability, biodegradability and gene transfer efficacy. A hydrophobic region, anchoring the cationic lipid onto the bilayer (Immordino *et al.*, 2006) is also required. The polar head group consist of a single quaternary ammonium group and examples such as (1,2-dioleyloxypropyl-trimethyl ammonium chloride) (DOTMA) or 1,2-dioleyoxy-3-(trimethylammonio) propane chloride (DOTAP), polyamine moieties *i.e.* 2,3 dioleyloxy-*N*-[sperminecarboxaminoethyl]-*N*, *N*-dimethyl-1-propanaminium-trifluoroacetate (DOSPA), guanidinium salts (Vigneron *et al.*, 1996) or bis(guanidinium)-tren-cholesterol (BGTC) are widely cited (Luton *et al.*, 2004). The most commonly used linker groups include ethers (Ghosh *et al.*, 2002), esters (Safinya *et al.*, 2006) and amides (Heinze *et al.*, 2010). The hydrophobic domain contains lipids derived from either simple aliphatic hydrocarbon chains or steroids (Karmali and Chaudhuri, 2006). The majority of the commonly used cationic transfection lipids contain two linear aliphatic chains in their

hydrophobic domains such as DOTMA and DOTAP (Zhi *et al.*, 2010). Lipofectins are internalised by endocytosis (Zabner *et al.*, 1995; Xu and Szoka, 1996) though whether DNA may partition through the plasma membrane to effect transfection is unclear as other mechanisms such as fusion is also indicated (Almofti *et al.*, 2003). Co-lipids such as cholesterol or DOPE facilitate the fusion of liposomes with cellular membranes and enhance their cellular uptake (Farhood *et al.*, 1995). Cationic liposomes are widely using for the transfer of nucleic acids into primary or cultured cells *in vivo* and in the clinic in the form of approved clinical trials (Podesta and Kostarelos, 2009). In treating cystic fibrosis two cationic liposome formulations, involving lipid (Caplen *et al.*, 1995) and connective tissue-activating peptide (CTAP) (Karmali and Chaudhuri, 2007) have shown promising results.

Limitations of liposomes: Liposome transfection efficiency needs to be enhanced. Work has to be done to overcome some of the stability and toxicological problems *in vivo*. PEGylation has contributed to stability and improved pharmacokinetics.

1.3.2.2 Micelles

Micelle formation in either polar or non-polar solvent is driven by the interaction of amphiphilic material (*i.e.* polymers) as a function of pH, salt concentration and polymer concentration, to form supramolecular assemblies (Croy and Kwon, 2006). One of the critical parameters when assembling micelles is the concentration of the amphiphilic units (Riess, 2003). Below a specific concentration threshold, dictated by the physicochemical properties of the amphiphile, assembly will not occur (Jones and Leroux, 1999). Above this specific concentration, assembly of the constituent amphiphiles into a micelle will be observed. This constant concentration is known as the critical micelle concentration (CMC) (Nagarajan and Ruckenstein, 1977).

Polymeric micelles containing A-B di-block polymers, where the A block represents a hydrophilic polymer segment which, in a polar solvent, forms the outer hydrophilic corona. This outer hydrophilic corona acts to stabilise and sequestering the hydrophobic core (the B block) away from the aqueous phase. The B block (hydrophobic polymer segment) forms the inner core and is capable of solubilising lipophilic substances (Kataoka *et al.*, 2001). These structures may then be cross-linked (or not) to offer further stability within a biological environment.

Micelles may take the form of spherical, rod or lamellar structures with a size distribution in nanometer range (10-100nm), have similarities to natural carriers like virus and serum lipoproteins (Lavasanifar *et al.*, 2002a). A small virus like size helps micelles escape capture

by the reticuloendothelial system (RES) and facilitates their extravasation through fenestrated capillary beds and may lead to the passive accumulation in neoplastic (Kwon *et al.*, 1994) or inflammatory (Wu *et al.*, 2009) tissues via the enhanced permeability and retention (EPR) effect (Maeda *et al.*, 2009). Drug delivery may be further augmented by the rational design of the micelles constituents. For example if the hydrophilic shell is designed to contain PEG, it may contribute to a “stealth” effect, enhancing the circulation time of the micelle in the blood (Stolnik *et al.*, 1995).

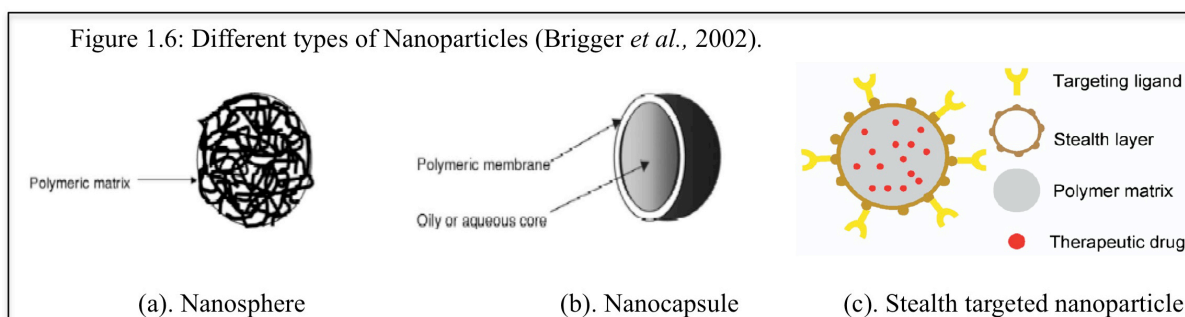
Polymeric micelles may also be used to deliver poorly water-soluble drugs as the drug can be entrapped within the hydrophobic core (Torchilin, 2004), increasing bioavailability and retention, as the drug is protected from possible inactivation (Torchilin, 2005). Release of the drug from the micelles may occur through diffusion or after the dissociation of the micelles into free polymeric chains (Kataoka *et al.*, 2001). Examples of drugs that have been subject to inclusion in micelle formulations include: paclitaxel (Miwa *et al.*, 1998), indomethacin (Zhang *et al.*, 2007), amphotericin B (Lavasaniyar *et al.*, 2002b) and dihydrotestosteran (Allen *et al.*, 2000). An example of the effective targeting of cytotoxic agents to solid tumours has also been reported using doxorubicin conjugated poly(ethylene glycol)-poly(α,β -aspartic acid) block copolymer [PEG-PAsp(DOX)] (Nakanishi *et al.*, 2001). This system showed (relative to free doxorubicin), prolonged retention in blood circulation, high doxorubicin accumulation in solid tumour mass and complete regression of the solid tumour mass in mice (Nishiyama and Kataoka, 2003).

Recently, polyionic complex micelles (PIC) formed from block ionomers by electrostatic interaction have been used to deliver enzymes and DNA to cells. Block copolymer (PEG-poly(L-lysine)) containing hydrophilic segment (PEG) and cationic segment poly(L-lysine) were combined with a hydrophobic block, to form supramolecular assemblies which may incorporate DNA or RNA (Katayose and Kataoka, 1997).

1.3.2.3 Nanoparticles

Nanoparticles are polymeric colloidal particles in the submicron size range (*i.e.* 1-999 nm) with a therapeutic agent entrapped within their polymeric matrix or adsorbed (or conjugated), onto the surface (Mishra *et al.*, 2010). Depending on the process used for the preparation of nanoparticles, nanospheres or nanocapsules can be obtained (Brigger *et al.*, 2002). Nanocapsules are vesicular systems in which a drug is confined to a cavity surrounded by a polymeric wall (Mishra *et al.*, 2010), whereas nanospheres are matrix systems in which the

drug is dispersed (Singh *et al.*, 2009). The advantages of using nanoparticles in drug delivery are due to two crucial properties: (i) the size (and hence surface to volume ratio) and (ii) the choice of (biodegradable) material used in the formulation (Panyam and Labhasetwar, 2003).



The small size of nanoparticles allows extravasation, allowing escape from the endothelium associated with sites of inflammation (Moghimi *et al.*, 2001), as well as across the “leaky” fenestrated epithelium of solid tumour mass via the EPR effect (Maeda *et al.*, 2009). Particle composition, size, charge and size distribution determine the *in vivo* distribution (Singh *et al.*, 2009), biological fate (Lundqvist *et al.*, 2008), toxicity (Ispas *et al.*, 2009), and targeting ability (Xia *et al.*, 2006) of these delivery systems. Particle size also influences the drug loading (Mainardes and Evangelista, 2005), drug release (Redhead *et al.*, 2001) and stability (Dunne *et al.*, 2000) of the nanoparticles. The use of biodegradable material for the formulation of nanoparticles allows sustained drug release within a target site for longer duration and allows for the elimination of the nanoparticles from the body (Rytting, *et al.*, 2008).

Nanoparticles have many advantages when compare to microparticles. They have relatively high cell uptake compared to microparticles (Panyam and Labhasetwar, 2003) and are available to a wider range of cellular and intracellular targets (Kroll *et al.*, 1998). Nanoparticles are also better suited for intravenous application (Jain *et al.*, 2005). Nanoparticles can be used to treat brain tumours, as they have been shown cross the blood-brain barrier following the opening of endothelium tight junctions by hyper-osmotic mannitol (Kroll *et al.*, 1998), though the safety of this system remains to be rigorously tested (Kreuter, 2001).

In the blood stream, conventional nanoparticles are opsonised and rapidly cleared by the mononuclear phagocyte system (MPS). To prolong the circulation time nanoparticles maybe coated with hydrophilic polymers or surfactants and also formulating nanoparticles with biodegradable or hydrophilic (Feng *et al.*, 2004) copolymers. Examples include: PEG

(Yoncheva *et al.*, 2005), poloxomer (Redhead *et al.*, 2001) or polysorbate 80 (Tween 80) (Kreuter *et al.*, 2003). Active targeting can be achieved by conjugating the nanoparticles to the targeting moiety, which allows preferential accumulation of the drug in the target tissue (Panyam and Labhasetwar, 2003), cells (Faraji and Wipf, 2009) or intracellular organelles (Choi *et al.*, 2007). Examples include the galactose-mediated targeting of material to the liver and specifically hepatocytes via the asialoglycoprotein receptor (Kim and Kim, 2003) or the targeting of macrophages via the use mannose receptor (Park *et al.*, 2008). Nanoparticles maybe internalised through a variety of endocytic processes (Sahay *et al.*, 2010). However, toxicity is still a major problem as similar to the cationic polymers, cell membranes are being compromised during this process (De Jong and Borm, 2008).

Like microparticles, nanoparticles have been prepared from polymers such as polylactic acid (PLA) (Jiao *et al.*, 2010), polyglycolic acid (PGA) (Hans and Lowman, 2002), poly (lactic-co-glycolic acid) (PLGA) (Bala *et al.*, 2004), poly(methyl methacrylate) (Rimessi *et al.*, 2009). PLA, PLGA are commonly used as they can be easily hydrolysed into their component monomers (lactic acid or glycolic acid) which are cleared from the body (Kumari *et al.*, 2010). In 2005, Abraxane (ABI-007) was approved by Food and Drug Administration (FDA) in the United States. Abraxane (Abraxis Biosystems) is an albumin-taxol nanoparticle that is used for the treatment of breast cancer (Cortes and Saura, 2010). However, all of these technologies offer a less than optimal intercellular delivery profile, with the plasma membrane or the endomembrane system offering a potential barrier to the delivery of therapeutic macromolecules. Consequently several families of peptide have been characterised that can breach membranes and these have been termed Cell Penetrating Peptides (CPPs).

1.3.2.4 Cell-penetrating peptides (CPPs)

Cell-penetrating peptides (CPPs) enter the cells independent of membrane receptors (Derossi *et al.*, 1996) and possess the ability to enter any cell undergoing endocytosis (Kerkis *et al.*, 2006). CPPs vary in size, amino acid sequence and charge but share the common feature of translocating across the plasma membrane, facilitating the delivery of molecules into the cytoplasm (Lindgren *et al.*, 2000). Several different pathways may be used to facilitate cytosolic delivery depending on the cargo and biophysical properties of the CPP. At a fundamental level, the efficient translocation of CPPs into the cytosol is due to a high proportion of positive residues such as arginine and lysine within in the CPP primary structure (Drin *et al.*, 2001). In an *in vivo* mouse model, a TAT derived CPP was used to

deliver active beta-galactosidase (β -gal) protein (116kDa) to the cytosol in all tissues tested (Schwarze, *et al.*, 1999). CPPs (pAntp and SynB) have also been shown to cross the blood brain barrier, delivering anticancer agent such as doxorubicin to the brain after *i.v.* administration (Scherrmann and Tamsamani, 2005). In addition, many oligonucleotides and their functional analogues have been reported, delivered efficiently by CPPs.

To increase the delivery yield, functional groups can be included in the CPP sequence. Addition of the fusogenic influenza virus hemagglutinin peptide HA2 to the TAT-peptide enhanced protein uptake. However it was also noted that this also resulted in increased CPP mediated cytotoxicity (Wadia *et al.*, 2004).

1.3.2.5 Polyplexes

Cationic polymers form polyelectrolyte complexes with DNA molecules, which results in formation of particles in the nanometre range (Bloomfield, 1996), referred to as polyplexes (Gebhart and Kabanov, 2001). As previously stated this condensation also protects the nucleic acids from nuclease degradation from most mammalian nucleases (Katayose and Kataoka, 1998).

Cationic polymers may contain amino groups, which can be engineered to display pKa's that will result in protonation over a range of physiological pH values (*i.e.* pH 7.4 to 5.5) (Griffiths *et al.*, 2004). At a sufficient nitrogen to phosphate charge ratio (N:P), cationic polymers can condense DNA effectively giving rise to torroidal structures that are suitable for endocytic uptake (*i.e.* 100-200nm in diameter) (Di Gioia and Conese, 2009). Some of the examples of polycations used to condense DNA include poly(ethylenimine) (PEI) (Lungwitz *et al.*, 2005), poly(L-lysine) (PLL) (Lollo *et al.*, 2002), poly(2-(dimethylamino)ethyl methacrylate) (Verbann *et al.*, 2005), diethyl aminoethyl (DEAE) dextran (Onishi *et al.*, 2007), chitosan (Tong *et al.*, 2009) and hyper-branched polymers such as the poly(aminoamine) dendrimers developed by Tomalia and colleagues (Kukowska-Latallo *et al.*, 1996; Hui *et al.*, 2009).

Toxicity is a problem that has hampered the generation of cationic polymer vectors and toxicity is usually proportional to the density of positive charges found within the polymer backbone (De Smedt *et al.*, 2000) as well as polymer molecular weight (Kunath *et al.*, 2003), and salt-form (Per-Olof Wahlund *et al.*, 2003). In an effort to combat these phenomena, several strategies have been attempted, including the generation of cationic and neutral di-block polymer systems (Petersen *et al.*, 2002). These consist of a cationic block (*i.e.*

poly(ethyleneimine)) next to a biocompatible neutral block such as poly(ethylene glycol) (PEG) (Zhang *et al.*, 2008; Namgung *et al.*, 2009).

Table 1.4: Physiochemical characteristics of current cationic polymeric systems (Morille *et al.*, 2008).

Cationic systems	Particles charge (mV)	Particles size (nm)	Degradability	References
PEI/DNA	+30	20-130	No	Breunig <i>et al.</i> , 2005
PLL/DNA	+40	60-140	Yes	Kwoh <i>et al.</i> , 1999; Ward <i>et al.</i> , 2001
Chitosan/DNA	+25 to +37	20-500	Yes	Fang <i>et al.</i> , 2001
PAMAM dendrimer/DNA	+9 to +20	50-100 (generation 6-7)	Yes	Dennig and Duncan, 2002.

1.3.2.6 Neutral and amphiphilic polymers

The literature reports several types of neutral or amphoteric polymer systems that can be used as transfection systems. These include, the PINC systems (Mumper and Rolland, 1998) (section 1.3.2) and the biologically responsive SMART polymer systems such as poly(amidoamine)s (Richardson *et al.*, 2010).

1.3.2.6.1 Poly(amidoamine)s

Poly(amidoamine)s are synthetic, water soluble, biocompatible and biodegradable polymers (Richardson *et al.*, 1999). They are relatively non-toxic (>100) compared to poly(L-lysine) (Richardson *et al.*, 1999) and PEI (Sgouras, 1990). Poly(amidoamine) families ISA1 and ISA23 have been reported to form IPECs when exposed to nucleic acids in a similar way to conventional polycationic polymers (Richardson *et al.*, 2001). However PAA backbone chemistry may be manipulated to behave as polycations below pH 7.4 and like a neutrally charged polymer at pH 7.4 (and above). This imparts some very interesting physicochemical properties to these PAAs, which enable PAAs to be targeted towards solid tumour mass if desired or equivalently the liver (Richardson *et al.*, 1999). These body distribution profiles make PAAs as potential candidates for soluble drug or gene carriers.

In the past PAAs have been used as heparin-complexing agents (Marchisio *et al.*, 1973). PAAs also used as vectors to deliver proteins like ricin A chain and gelonin into the cytosol of the cell (Patrick *et al.*, 2001).

PAAs contain amido and tertiary amino groups along the backbone of the polymer. At low pH, protonation of tertiary amino groups results in a conformational change of the polymer coil. The relatively coiled form is more neutrally charged but at low pH, protonation increases and relaxed open structure, which increased radius of gyration of the polymer, was observed (Griffiths *et al.*, 2004). This was confirmed by a both chromatographic techniques as well as small angle neutron scattering (Griffiths *et al.*, 2004). The increase in size (driven by an increase in net positive charge) also gives PAAs ISA1 and ISA23 the ability to disrupt the biological membranes at low pH whilst not destabilising them at pH 7.2-7.4.

PAAs can be functionalised to provide sites for attaching drug molecules and can also be used to conjugate specific ligands to enhance the targeting efficiency and increasing cell specificity. It can also be possible to synthesise different M_w over a wide range.

Here two families of PAAs, ISA1 and ISA23 were further characterised, their toxicity and ability to deliver proteins (*i.e* gelonin) to the cytosol was evaluated. These two polymers have slightly different physicochemical and toxicological properties.

Despite, at pH 7.4 ISA1 being a more cationic than ISA23, ISA1 did not show higher transfection efficiency than ISA23. This phenomenon was surprisingly not replicated during the delivery of ricin A chain and gelonin to the cytosol (Patrick *et al.*, 2001), ISA1 being documented as more efficient than ISA23. ISA4 contains approximately 1% 2-p-hydroxyphenylethylamine which allows the radiation of the polymer, and is an analogue of ISA1. When administered intravenously, more than 90% of the administered ISA4 was captured by the liver (Richardson *et al.*, 1999). This property maybe used to target liver diseases.

ISA23 was found to be less cationic than ISA1 at pH 7.4 due to a carboxyl group, which was fully ionised at the physiological pH (Ferruti *et al.*, 2002). When administered intravenously to rats, ISA22 (which is the analogue of ISA23), showed less than 10% liver capture after 5h (Richardson *et al.*, 1999).

This polymer also accumulated in tumour tissues, possibly via EPR effect (Maeda *et al.*, 2009). This property of the polymer might be used to deliver therapeutic moieties into cancers tissues.

However, it has been known for some years that, in nature specific bacterial (shiga toxin, cholera toxin and pseudomonas exotoxin etc) and plant toxins (ricin) also access the cytosol in order to mediate intoxication. This property of specific toxins might also be used to deliver therapeutic macromolecules into the cytosol.

1.4. Toxins and intracellular membrane trafficking

A number of proteinaceous virulence factors (toxins), produced by a variety of bacteria and some plants, have cytosolic targets. To enter the cell, these virulence factors bind to specific receptors, use different endocytic pathways and finally translocate to the cytosol, where they exert their intoxicating effects (Sandvig *et al.*, 2004; Sandvig and van Deurs 2005). Generally these proteinaceous virulence factors or toxins have evolved to exploit two methods of intracellular entry.

The first mechanism deployed to mediate cytosolic access requires the rupture of endomembrane (*i.e.* the endosomal limiting membrane) to enter into the cytosol. Diphtheria and botulinum toxins (Collier, 2001; Binz and Rammel, 2009) utilise this pathway. Here the influential factor for the translocation is the low endosomal pH, which induces a conformational change in the toxin molecule, resulting in the exposure of hydrophobic areas able to interact with and insert into endosomal membrane (Falnes and Sandvig, 2000).

Alternatively, retrograde trafficking pathways may be subverted to allow the toxin to evade lysosomal degradation and permit cytosolic access (Lord *et al.*, 2003). Shiga, cholera and ricin toxins are examples of two quite different families of toxin that exploit the retrograde trafficking of material from endosomes to the Golgi, then to the endoplasmic reticulum. Once in the ER, these toxins translocate into cytosol via *Sec61p* translocon (Sandvig and van Deurs 2002). Ricin toxin (RT) and shiga toxin (ST) (belongs to RIPs family proteins) have ribosomal targets whereas cholera toxin (CT) has a non-ribosomal target when mediating intracellular intoxication (Chinnapen *et al.*, 2007). It is of note that none of these families of retrograde translocating proteins breaching endocytic membranes which may release pro-apoptotic lysosomal hydrolyses (Sandvig and van Deurs, 2005; Kagedaal *et al.*, 2001). To understand the intracellular trafficking of toxins, it is vital to know the key organelles involved in endocytic and secretory pathways inside the mammalian cell.

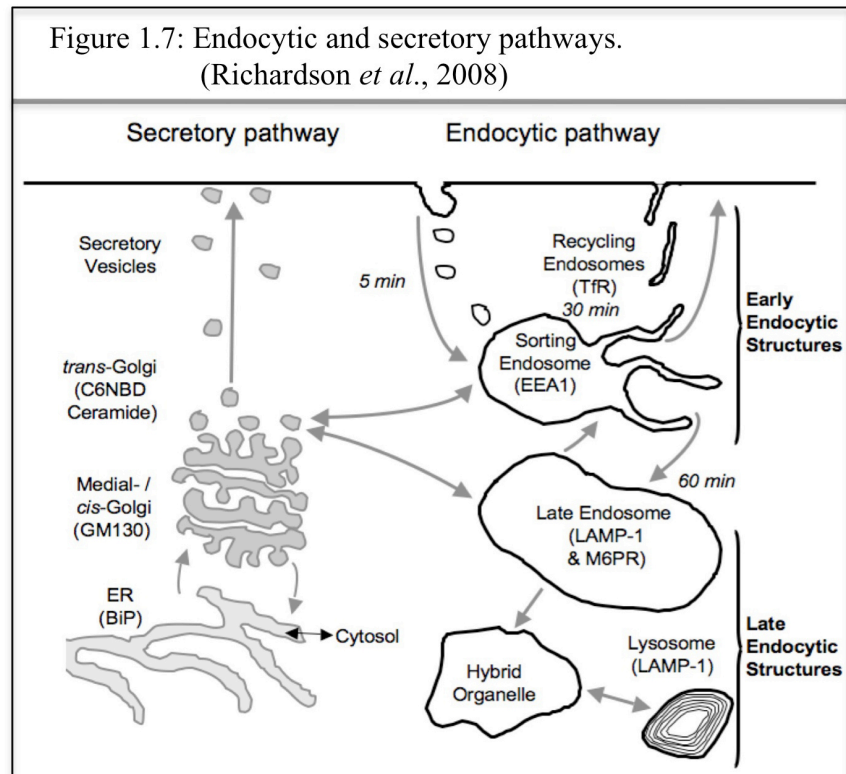
Table 1.5: Overview of some plant and bacterial toxins (modified from Sandvig and van Deurs, 2005).

Toxins	Activity	Intracellular target	References
Plant Toxins Ricin, abrin, modeccin and viscumin	N-glycosidase	28S rRNA	Olsnes, 2004; Pohl, 1998.
Gelonin	N-glycosidase	28S rRNA	Nicolas <i>et al.</i> , 2000
Bacterial Toxins Diphtheria toxin	ADP- ribosyl transferase	EF-2	Pappenheimer, 1977
Pseudomonas exotoxin A	ADP- ribosyl transferase	EF-2	Jackson <i>et al.</i> , 1999
Anthrax toxin Clostridium botulinum C2 toxin	Adenylyl cyclase Zinc endoprotease ADP-ribosyl transferase	cAMP-induced changes of protein MAPKK G actin	Collier, 2009; Aktories and Barth, 2004
Shiga toxin	N-glycosidase	28S rRNA	Johannes and Rower, 2009
Cholera toxin <i>E. coli</i> heat-labile toxin	ADP-ribosyl transferase	Heterotrimeric G-protein	Sánchez and Holmgren, 2008

1.4.1 Membrane trafficking, endocytosis and the secretory pathway

Endocytosis incorporates the regulation of many diverse functions and is used by cells to internalise macromolecules, membrane, membrane components (such as activated receptors) and particles. Small molecules such as amino acids, sugars and ions can cross the plasma membrane via active mechanisms involving pumps and ion channels present throughout the endomembrane system. However cells have evolved to exclude biologically active macromolecules, such as exogenous proteins, DNA or RNA, in order to prevent genomic

plasticity. Consequently macromolecules carried into the cells via endocytosis, will usually be subject to lysosomotropic delivery and catabolism.



Endocytosis may be divided into phagocytosis (cell eating) and pinocytosis (cell drinking). Phagocytosis is typically restricted to specialised mammalian cells (professional phagocytes), however pinocytosis occurs in most cells and may be divided into four categories: macropinocytosis, clathrin-mediated endocytosis, caveolae-mediated endocytosis and clathrin (and caveolae) independent endocytosis (Conner and Schmid, 2003).

The endocytic pathway of mammalian cells consists of distinct membrane delineated compartments. Functionally these intracellular compartments may be thought of as early endosome, recycling endosome, late endosome and lysosomes (Mellman, 1996). Once material is internalised, it is either recycled back to the surface either via the early endosome and recycling endosome, or in some instances directly back to the surface from the early endosome. Equivalently material may be trafficked to the late endosome for degradation.

1.4.1.1 Endocytosis

Endocytosis plays a crucial role in the regulation of nutrient uptake (Miaczynska and Stenmark, 2008), receptor signalling (von Zastrow and Sorkin 2007), neurotransmission (Hirling, 2009), pathogen entry (Gruenberg and van der Goot, 2006), antigen presentation

(Burgdorf and Kurts, 2008), cell adhesion and migration via the sorting of intracellular and extracellular material *i.e.* the differential sorting of endogenous material into a recycling pathway or into a catabolic (lysosomal) pathway (van Vliet *et al.*, 2003). Endocytosis is also responsible for nutrient uptake, well-characterised examples being iron (Subramaniam *et al.*, 2002) and albumin (John *et al.*, 2003). There are also many examples of phagocytosis being used as part of the body's defence systems, engulfing foreign particulate matter such as bacteria and digesting them (Stuart and Ezekowitz, 2008). Recycling may take material from one compartment to several functional pre- or post- trafficking compartments. This operation may require the anterograde (forward) movement of both cargo and intracellular trafficking machinery, as well as the retrograde (reverse) movement of intracellular membrane trafficking machinery. This is necessary to facilitate the participation of mechanical and regulatory molecules (*i.e.* cell-surface ligand receptors and soluble *N*-ethylmaleimide attachment protein receptor (SNARE) proteins), in multiple rounds of fusion to the same compartment (van Vliet *et al.*, 2003).

The different compartments associated with endocytosis in most mammalian cells are described below:

1.4.1.2 Early endosome

The early endosome (EEs) (or early sorting endosome) is the first discrete compartment internalised material is delivered to during its passage through the endocytic pathway (Gruenberg and Maxfield, 1995). EEs have a tubulo-vesicular morphology and a mildly acidic pH (typically 6.5). Internalised material reaches this organelle after 5-10 minutes and is sorted into either the default lysosomal (catabolic) pathway or into a recycling pathway (Gruenberg, 2001; Bishop, 2003). Due to the low pH of the EE, sorting and segregation of receptor and ligand occurs, driven by pH mediated conformational changes in protein structure (Mellman, 1996). EEs are characterised by the presence of the small GTPase Rab5 (Roberts *et al.*, 1999) and the Rab5 effector Early Endosomal Antigen 1 (EEA1), (Mills *et al.*, 2001) which both participate in the regulation of vesicle fusion to this compartment.

1.4.1.3 Recycling endosomes

Recycling Endosomes (REs) have a heterogeneous, tubular, vesicular (reticular) morphology, which suggest intense trafficking activity (van Ijzendoorn, 2006). Typically REs are positive for the Rab GTPase Rab11, which, like Rab5 and Rab7 regulate membrane fusion. Recycled

material, such as the Transferrin receptor (TfR) can be detected in REs 30 minutes after internalisation (Macedo and de Sousa, 2008).

1.4.1.4 Late endosomes

Late endosomes (LEs) receive internalised material from early endosomes and often contain internal membrane in the form of vesicles, as well as membrane proteins characteristic of lysosomes such as the Lysosome Associated Membrane Protein (LAMP) families of integral membrane proteins. The mannose-6-phosphate receptor (M-6-PR) is the exception to this rule as it recycles between the LE and the Golgi body, delivering biosynthetic cargo to the LE, facilitating lysosomal biogenesis. Internalised material can be seen in this organelle 60 minutes after internalisation and it has a pH of approximately 5.5. There is some controversy as to the genesis of LE with some reports suggesting the transit of material from early endosome to LE in vesicles (Gu and Gruenberg, 1999) but there is also evidence that the maturation of early sorting endosome into LE (Rink *et al.*, 2005).

1.4.1.5 Lysosome

The lysosome (Lys) may be considered the terminal compartment of the endocytic system however a more accurate description of Lys maybe that of storage compartment for hydrolytic enzymes (Saftig and Klumperman, 2009). Although Lys are generally considered as the principle hydrolytic compartment of the cell (Luzio *et al.*, 2001), there is robust evidence that catabolism actually takes place in a transient LE/Lys hybrid organelle (Mullock *et al.*, 1988).

After the EL/Lys fusion event, Lys are thought to re-form from this hybrid organelle (Piper *et al.*, 2004). Both heterotypic and homotypic LE fusion events are thought to be regulated by Rab7 (Bucci *et al.*, 2000) which, like Rab5 on EEs and Rab11 on REs acts to define this compartment. Further characterisation of lysosomes (particularly dense core-lysosomes) is possible as unlike LEs they are positive for LAMP proteins (Luzio *et al.*, 2001) and do not contain the M-6-PR as a membrane component (Futter *et al.*, 1996).

1.4.1.6 The secretory pathway

The secretory pathway is intimately linked to the endocytic system, and is normally associated with the trafficking, sorting and quality control of endogenous proteins. The organelles of secretory pathway sort proteins into a variety of intracellular membrane delimited compartments including the cell surface. This process facilitates the biogenesis of

intracellular organelles via cross-communication with the endocytic pathway. Anterograde and retrograde trafficking to and from the Golgi has been documented to occur between REs (Sannerud *et al.*, 2003), EEs (Hinnens and Tooze, 2003) and LEs (Johnston *et al.*, 2005).

1.4.1.7 Golgi complex

The Golgi body sorts material that has been synthesized by the cell, either to another intracellular location or into the secretory pathway (van Vliet *et al.*, 2003). It may be divided into 4 sub-compartments, the *trans*-Golgi network (TGN), the *medial*-Golgi, the *cis*-Golgi and the endoplasmic reticulum (ER) to Golgi Intermediate Compartment (ERGIC). The *cis*-face of the Golgi receives cargo from the ERGIC, which has been subject to “quality control” and helped to fold correctly in the ER (Appenzeller-Herzog and Hauri, 2006; Ellgaard and Helenius, 2003). From ER exit sites, material is transported through the ERGIC, to the *cis*-Golgi, through the Golgi stack to the TGN. Within the TGN, nascent material is sorted and packaged into membrane carriers destined for the plasma membrane, REs, EEs and LEs as well as related secretory organelles (Keller and Simons 1997).

1.4.1.8 Endoplasmic reticulum

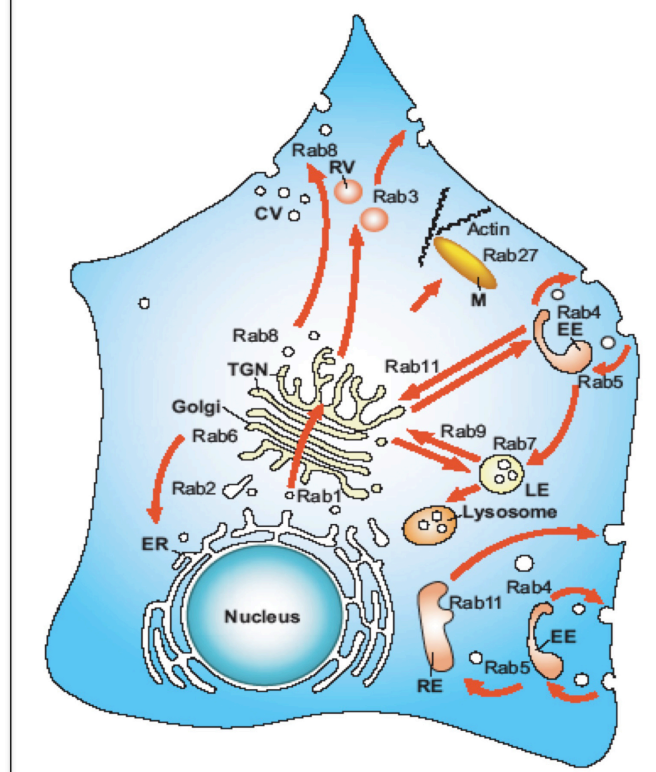
The endoplasmic reticulum (ER) is an extensive membrane network of cisternae held together by the cytoskeleton (Voeltz *et al.*, 2002). Smooth ER is a site of lipid synthesis and the ER in general acts as part of the cell’s quality control system for newly synthesised proteins (Roth *et al.*, 2008). Protein translation begins at the ribosome, which may be either free in the cytosol or bound to the ER (rough ER) (van Vliet *et al.*, 2003). Proteins destined for secretion or require transport through an endomembrane (*i.e.* for luminal lysosomal access required during the biogenesis of lysosomes), are targeted into the ER, where the nascent protein chain is fed through the *Sec61p* translocon (or into the ER membrane in the case of transmembrane proteins). Once in the ER, the cell performs “quality control” checks ensuring that the nascent chain(s) have folded appropriately prior to the proteins transport to the Golgi for distribution around the cell or for secretion (van Vliet *et al.*, 2003). Luminal proteins called chaperons play crucial role in this process and include binding immunoglobulin protein (BiP) (Gething, 1999), lectins calnexin and calreticulin (Williams, 2006) and protein disulphide isomerase (Wilkinson and Gilbert, 2004). Chaperones assist in the folding of the nascent polypeptide chain protein by slowing folding, preventing aggregation and ensuring the correct disulphide bonds are formed (Yu-Jen Chen and Masayori Inouye, 2008). Both the anterograde and retrograde movement of material between

these compartments is highly regulated. However, as previously mentioned, several toxins have evolved to exploit these trafficking events in order to access what would normally be inaccessible cellular components. RIP type toxins are one example of a set of toxins that have evolved to manipulate the aforementioned membrane trafficking events in order to access the cytosol (Sandvig and van Deurs, 2002; Hartley and Lord, 2004). During the intracellular trafficking and transport of exogenous and endogenous proteins, Rab proteins and SNAREs play crucial regulatory role.

1.4.1.9 Rab proteins

Ras-associated binding (Rab) proteins are small GTPases of the Ras superfamily (Wennerberg *et al.*, 2005). Along with Rab-associated proteins, Rab proteins play key role in regulation of vesicular transport, which is essential for delivery of proteins to specific intracellular compartments (Corbeel and Freson, 2008; Zerial and McBride, 2001).

Figure 1.8: Localisation and function of Rab proteins (Stenmark and Olkkonen, 2001)



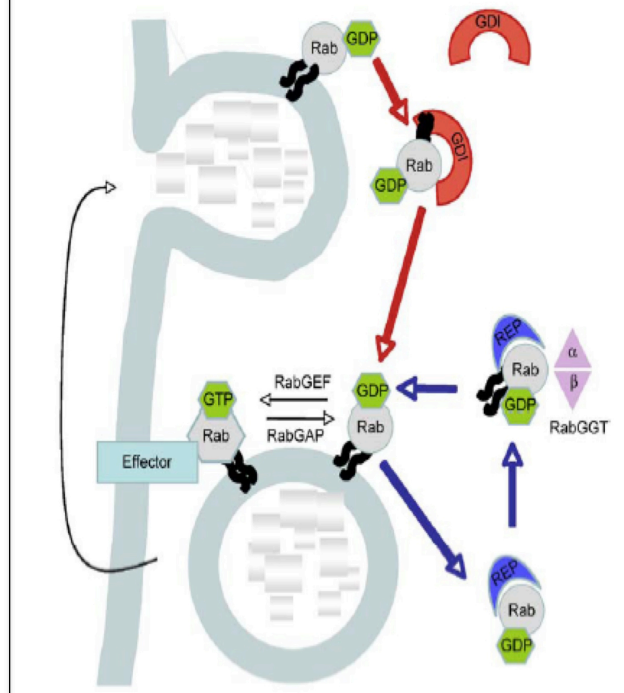
To date more than 60 human Rab proteins have been identified (Pfeffer, 2007). Most of them are ubiquitous in their tissue and cellular distribution, though cellular differentiation may alter the compartmental function of a specific Rab protein (Wade *et al.*, 2001). The level of

expression of these proteins may vary from one cell to another. Some of the Rab proteins are cell type or tissue specific.

Rab proteins are distributed in specific intracellular compartments and they play an important role in regulation of transport between organelles (Deneka *et al.*, 2003; Lee *et al.*, 2009) and function as molecular switches that cycle between the active GTP-bound and non-active GDP-bound forms (Corbeel and Freson, 2008).

The transition between GTP and GDP bound states is assisted by Rab-associated proteins such as guanidine nucleotide-exchange factors (GEF) and GTPase-activating proteins (GAPs) (Pereira-Leal and Seabra, 2000). In the cytosol Rabs were recognised by soluble chaperone like protein called Rab escort protein (REP) (Alexandrov *et al.*, 1994), which brings the Rab to the Rab geranylgeranyl transferase (GGT) for the addition of geranylgeranyl groups (Anant *et al.*, 1998). This post-translational modification of Rabs is needed to attach Rab proteins into the lipid bilayer of the organelle. After exerting their function, Rab proteins are detached from the membrane by Rab GDI (GDP dissociation inhibitor) and they remain in a cytosolic pool until their next cycle (Pereira-Leal and Seabra, 2000; Ullrich *et al.*, 1993).

Figure 1.9: Mechanism of action of Rab proteins. (Corbeel and Freson, 2008)



GTP-bound Rab proteins exert their influence during regulatory events through their recruitment of, and interaction with Rab effector proteins. One Rab protein can interact with

multiple effector proteins that either function in a larger complex or provide the basis for distinct downstream functions (Grosshans *et al.*, 2006). Alteration in Rabs, Rab-associated proteins and effectors results in variety of human diseases (Seabra *et al.*, 2002; Cheng *et al.*, 2006).

1.4.1.10 Soluble *N*-ethylmaleimide-sensitive factor activating protein receptors (SNAREs)

SNAREs play a key role in membrane fusion in biosynthetic, secretory and endocytic pathways (Jahn and Scheller, 2006). Currently 36 SNARE proteins have been identified in humans. In the cell they are specifically associated with a particular organelle and catalyses the membrane fusion reactions in vesicular transport (Duman and Forte, 2003).

SNAREs are divided into two distinct groups on the basis of both structure and function. These groups are (i) v-SNAREs, (which usually found on vesicle membranes) and (ii) t-SNAREs (found on target membranes) according to their vesicle or target membrane localisation (Söllner *et al.*, 1993). This classification is not useful in describing homotypic fusion events and to overcome this problem, SNAREs have been reclassified as R-SNAREs (arginine containing SNAREs) or Q-SNAREs (glutamine containing SNAREs) (Fasshauer *et al.*, 1998).

With few exceptions, SNARE proteins contain a SNARE domain with 60-70 amino acids that are arranged in heptad repeats mediating coiled-coil formation (Brunger, 2005). Most SNAREs have a single transmembrane domain at C-terminal ends that is connected to the SNARE motif by a short linker. Specific SNARE proteins such as Syntaxin7 possess an N-terminal, independently folded domain, which may vary between the subgroups of SNAREs and this domain acts as an inhibitory regulator limiting SNARE-pin *i.e.* trans-SNARE pairing. This domain is the target for Sec1/Munc18 (S/M) like proteins type proteins such as mVPS45, which can, in an ATP dependant fashion interact with and open the R-SNARE N-terminal inhibitory domain (Hong, 2005; Fasshauer, 2003).

Once activated and brought into proximal contact by tethering proteins (*i.e.* HOPS, p115 and GM130), SNARE proteins are in the correct conformation, a monomeric R-SNARE on either the donor or the acceptor membrane can bind to oligomeric Q-SNAREs on the prospective fusion partner, leading to *trans*-SNARE assembly, forming a stable four-helix bundle that promotes fusion (Jahn and Scheller, 2006).

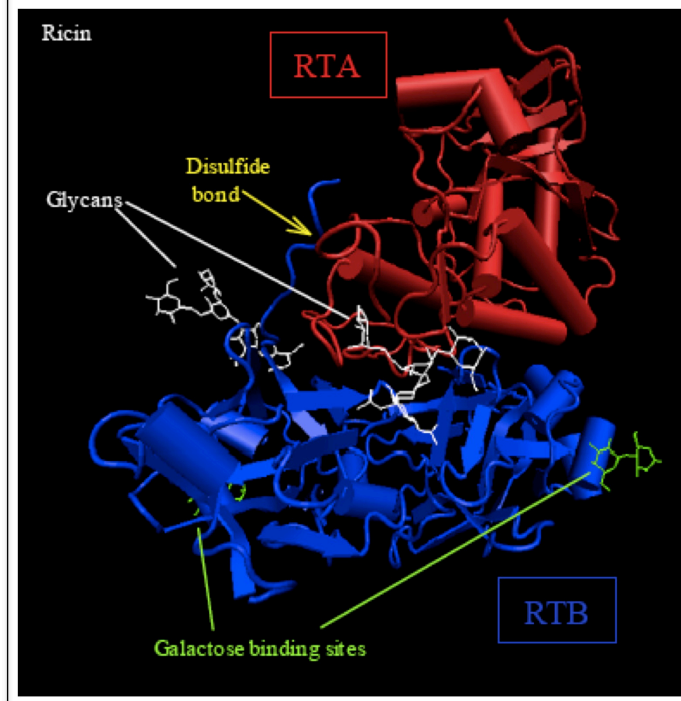
1.4.2 Toxins

Ricin, shiga toxin and cholera toxins have several architectural similarities in that they employ either one or more lectin binding B chains, which binds to the cell surface, and an A chain containing a “lethal” domain to mediate intoxication. After internalisation, from the endosome, ricin, shiga and cholera toxins exhibit retrograde trafficking into Golgi and then to the ER and eventually to the cytosol, where they exert their toxicity (Sandvig and van Deurs, 2002).

1.4.2.1 Ricin

Ricin is a plant toxin, found in the seeds of Castor bean plant *Ricinus communis* (Olsnes and Kozlov, 2001). Ricin Toxin (RT) belongs to the ribosome inactivating protein toxins-II (RIP-II) family (Lord *et al.*, 1994). Generally RIP-II family toxins are heterodimeric proteins, where an enzymatically active A chain is responsible for the toxicity and a lectinic B chain is responsible for endocytosis and trafficking of the toxin inside the cells (Olsnes and Pihl, 1973).

Figure 1.10: Structure of Ricin toxin. A-chain (Red color), B chain (blue color) (Reidy, 2007).



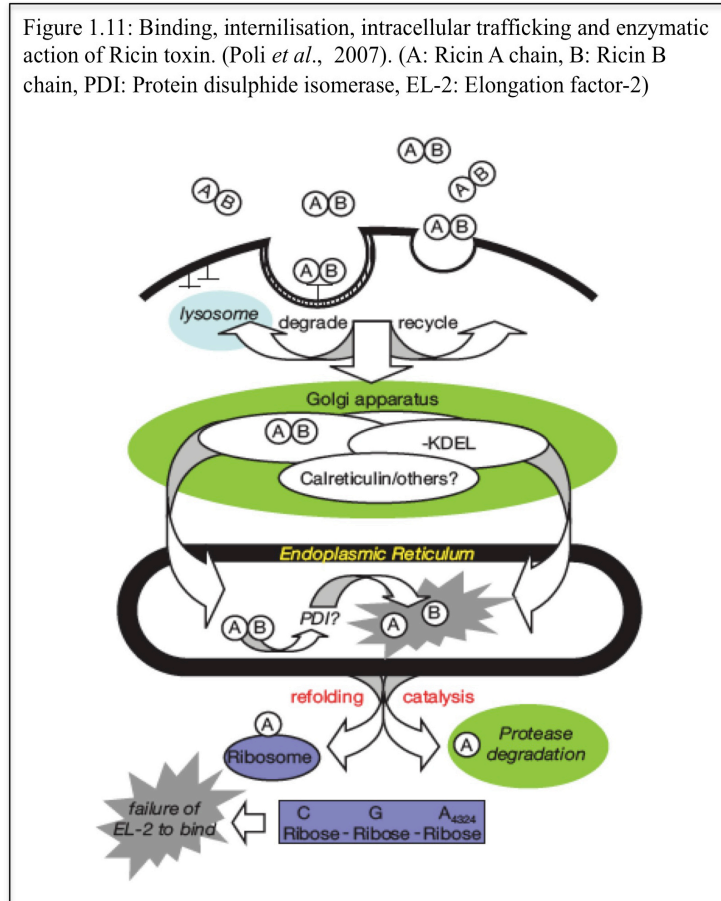
Once inside the lumen of the ER, protein disulphide isomerase (PDI) reduces the disulphide bond between A and B chains (Spooner *et al.*, 2004) liberating the A chain. The A chain is then translocates into the cytosol using *Sec61p* translocon (Lord and Roberts, 1998; Wesche *et al.*, 1999).

RT A chain (RTAC) has molecular weight of 32kDa and it is an *N*-glycosidase protein (Endo and Tsurugi, 1987). RTAC exerts toxicity by removing an adenine residue from an exposed loop of 28S ribosomal RNA, which results in the inhibition of protein synthesis. The sarcin/ricin loop is a highly conserved sequence present in all large ribosomal subunits of RNA (Szewczak *et al.*, 1993) and this loop involved in the binding of elongation factors, which are required for protein synthesis. RTAC contains the residues Glu 177 and Arg 180 located in the active site and these residues are responsible for enzymatic activity (Frankel *et al.*, 1990). Mutations in this regions results in strong reduction in the toxicity of the protein (Day *et al.*, 1996), consequently, in this study, various RTAC constructs, which have deletions and mutations in their active sites were produced. The toxicity and trafficking properties of these recombinant RT mutants was examined (table 1.7; figures 3.1 to 3.7). This is in an attempt to utilise the trafficking properties of ricin toxin to mediate the cytosolic delivery of a high molecular weight therapeutic, whilst negating the toxicity associated with this molecule.

Ricin toxin B chain (RTBC) is a galactose/*N*-acetyl glucosamine specific lectin and it has molecular weight of 32kDa (Falnes, Sandvig, 2000). The protein folds into two globular domains each of which contains a binding site. Ricin binds to both glycoproteins and glycolipids with terminal galactose and therefore binds ubiquitously to the surface of most cell types (Sandvig and van Deurs, 2000). RTAC and RTBC are directly associated through a disulfide bond (Spooner *et al.*, 2004). Without RTBC, RTAC is not as potent as the holotoxin (Cola *et al.*, 2001). But when ricin A chain is modified with endoplasmic reticulum (KDEL) or Golgi (YQRL) retention sequences, its cytotoxicity and translocation from the Golgi to the ER are enhanced (Zhan *et al.*, 1998; Wales *et al.*, 1993).

Ricin is endocytosed by both clathrin dependent and clathrin independent mechanisms, which can operate simultaneously (Sandvig *et al.*, 2004). Since RTBC can bind to both glycoproteins and glycolipids on the cell surface, there is enormous binding capacity for ricin on an average mammalian cell (Sandvig and van Duers, 2000).

Figure 1.11: Binding, internalisation, intracellular trafficking and enzymatic action of Ricin toxin. (Poli *et al.*, 2007). (A: Ricin A chain, B: Ricin B chain, PDI: Protein disulphide isomerase, EL-2: Elongation factor-2)



Once in the endosome, a proportion of the toxin is recycled back to the cell surface via the recycling endosomes whilst the majority of the toxin is transported to the late endocytic compartment (LE) and is degraded. Approximately 5-10% of endocytosed RT traffics to the *trans*-Golgi network and eventually to the cytosol (van Deurs *et al.*, 1988).

From the sorting endosome, the toxin reaches Golgi by different pathways. RT Golgi translocation is independent of Rab9, which regulates fusion of LE derived vesicles to the Golgi (Iversen *et al.*, 2001), Rab7, which regulates fusion between late endosome and lysosome (Feng *et al.*, 1995; Bucci *et al.*, 2000) and Rab11, which regulates fusion to the RE (Ulrich *et al.*, 1996).

Retrograde transport of RT can be observed by monitoring tyrosine sulfation and glycosylation of the ricin holotoxin (Rapak *et al.*, 1997). When the toxin enters into the Golgi, sulfation of tyrosine occurs, which can be observed if the cells are incubated in the presence of radioactive sulfate. Glycosylation can be monitored in the ER by monitoring an increase in molecular weight of the protein (Wesche, 2000) or through the association of a radiolabel (Rapak *et al.*, 1997). If the Golgi is disrupted with brefeldin A, the toxicity is

greatly reduced which also confirms the retrograde traffic of the ricin toxin through the Golgi (Sandvig *et al.*, 1991).

Once in the Golgi, RT has been documented to translocate to the lumen of the ER. Debate with regards to the utilisation of COPI coated vesicles by RT is still on ongoing, as one school of thought has documented the involvement of RT binding to calreticulin which utilises COPI dependant ER transport (Day *et al.*, 2001). It is however well documented that the inclusion of a C-terminal KDEL moiety into RTAC dramatically increases the toxicity of this molecule (Wales *et al.*, 1993).

After entering into the ER, the internal disulfide bond present in the ricin toxin is reduced, which liberates the A chain to undergo a final retrograde transport step through the *Sec61p* translocon into the cytosol (Roberts and Smith, 2004).

It is thought that the “quality control” machinery resident within the ER mediates the final toxin retrograde transport step. This final toxin transport step has been documented to involve the machinery responsible for the phenomena of ER associated degradation (ERAD) (Roberts and Smith, 2004). The ERAD pathway is responsible for the eradication of misfolded proteins resident in the ER. Luminal ER proteins are translocated to the cytosol (another retrograde transport step involving the *Sec61p* translocon) where they are degraded by proteasomes (Matlack *et al.*, 1998; Stolz and Wolf, 2010).

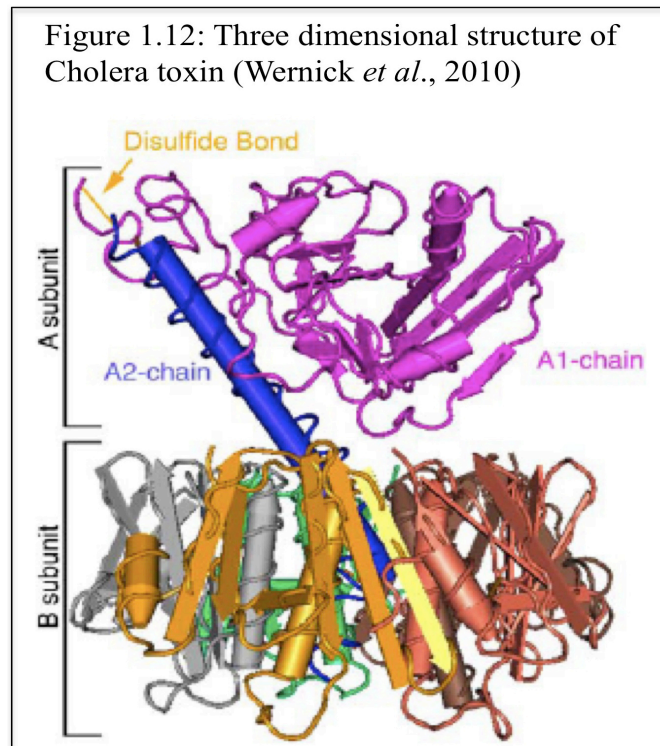
Once in the cytosol, RTAC avoids proteosomal degradation. This could be partly due to the fact that RTAC chain contains few lysine residues, which are necessary for the attachment of polyubiquitin chains. Polyubiquitin serve as an entry motif initiating protein degradation by proteasomes (Deeks *et al.*, 2002). Once in the cytosol, RTAC is refolded (Argent *et al.*, 2000). Once it is in its active form RTAC inhibits protein synthesis by depurination of 28S ribosomal RNA (Olsnes and Kozlov, 2001).

1.4.2.2 Cholera toxin

Cholera toxin (CT) has many similarities with RT, especially in its intracellular trafficking pathway, which it follows inside the cells. CT is secreted by gram-negative bacteria *Vibrio cholerae* (Vanden Broeck *et al.*, 2007).

The toxin belongs to AB₅ family of toxins, where a heterodimeric A-subunit and a homopentameric B-subunit self assemble into holotoxin before secretion from the bacteria (Lencer and Tsai, 2003). The 27kDa A-subunit, which extends well above the pentameric ring, consists of enzymatically active A1- domain and an A2- domain. The A1 and A2 domains are initially synthesised as part of the same protein chain, but following proteolytic

cleavage are linked together by a disulphide bond. The A2 chain acts as a linker, which non-covalently attaches the A1 chain to the B-subunit assembly (Wernick *et al.*, 2010). The B-subunit consists of five 11.5kDa peptides assembled non-covalently into a ring like configuration, with each single binding site for ganglioside GM1 on the plasma membrane (Chinnapen *et al.*, 2007) and carries the A chain subunit into the ER.



Once the CT binds to the cell membrane via the interaction of the B chain with its receptor molecules (GM₁ gangliosides) (Sanchez and Holmgren, 2011) it can be internalized by caveole and clathrin-dependent as well as caveolae- and clathrin independent endocytic mechanism (Torgersen *et al.*, 2001; Sandvig *et al.*, 2004). Once in the endosome a proportion of the toxin avoids late endosome and lysosomes by trafficking to the Golgi. The mechanisms by which CT reaches Golgi is not completely clear, however several mechanisms and regulatory steps have been proposed (Mallard *et al.*, 1998; Iversen *et al.*, 2001). At least two routes have been proposed for the trafficking of CT from TGN to ER. It can either bypass cisterne (Feng *et al.*, 2004) or enter the ER in COPI dependent manner, by utilizing a KDEL, an ER-retrieval motif (Majoul *et al.*, 1998; Richards *et al.*, 2002). The CT A2 chain contains a C-terminal KDEL sequence, which is recognised by KDEL receptors distributed all over the *cis*-Golgi (Wernick *et al.*, 2010). Mutation in this sequence causes the delay in the action of the toxin, but not the complete inhibition of its action, suggesting that

retrograde transport can occur without the KDEL sequence (Lencer *et al.*, 1995). This observation is supported by RT and shiga toxin (ST), which both lack this sequence but are still able to traffic from the Golgi to the ER (Sandvig and van Deurs, 2002).

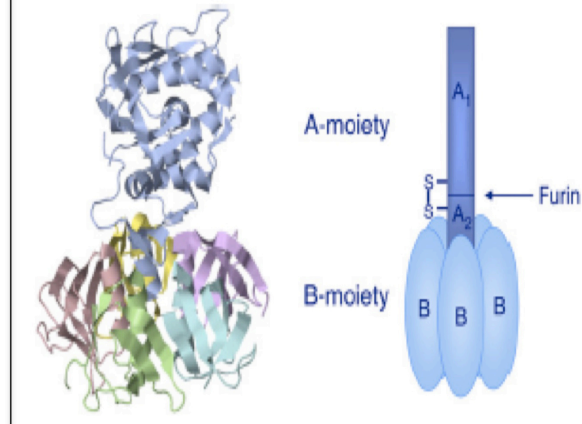
In the lumen of the ER, redox-dependent chaperone, protein disulfide isomerase (PDI) binds and unfolds the A1 chain (Tsai *et al.*, 2001). Membrane associated ER oxidase protein, Ero1, oxidizes PDI to release the unfolded A1 chain (Tsai and Rapoport, 2002). By utilizing the endoplasmic reticulum associated protein degradation (ERAD) pathway CT crosses ER through *Sec61p* translocon (Schmitz *et al.*, 2000). Other ER proteins may also play a role in retrotranslocation of CT, like Derlin 1 and Hrd1 may also play a role in retro translocation of the CT (Dixit *et al.*, 2008; Bernardi *et al.*, 2008).

Once in the cytosol, CT avoids proteolytic degradation in similar way to RT (Rodighiero *et al.*, 2002). In the cytosol, the A1- chain, which is an ADP-ribosyltransferase, modifies the heterotrimeric G protein, G α . This results in constitutive activation of adenylate cyclase and rapid production of cAMP (Wernick *et al.*, 2010). This raise in cAMP levels opens chloride channels and results in the extracellular secretion of water. It is this secretion of water this is responsible for the diarrhea that can lead to dehydration and death (Chinnapen *et al.*, 2007).

1.4.2.3 Shiga toxin

Shiga toxin is secreted by *Shigaella dysenteria*. Shiga like toxins (Stx1 and Stx2), which are identical to shiga toxin, are secreted by certain strains of *E.coli* (shiga-toxin producing *Escherichia coli*) (Sandvig, 2001) and other bacteria. Infection with these bacterial strains results in haemorrhagic colitis and haemolytic uremic syndrome (HUC) (O'Loughlin and Robins-Browne, 2001). They belong to the family of AB₅ protein toxins, and they have structure similar to CT (Sandvig, 2001). In enzymatic A chain, A1 and A2 chains are linked together with a disulphide bond and they also contain furin recognition sequence RXXR between the two domains. In the endosome, furin cleaves the A-moiety in a loop formed by the disulphide bond (Garred *et al.*, 1995). Even after cleavage, the A1 chain is attached to the A2 chain via a disulphide bond. In endoplasmic reticulum disulphide bond is reduced by PDI and releases enzymatically active A1 chain. The B chain is composed of five monomers and each monomer (7.7kDa) binds to three Gb3 molecules on the cell surface (Soltys *et al.*, 2002).

Figure 1.13: Crystallographic structure (left) and schematic (right) structures of Shiga toxin (Sandvig *et al.*, 2010)



Shiga toxins, after binding to the cell surface receptors, enter into the cell via different types of endocytic mechanisms (Sandvig *et al.*, 2010). From the EE, shiga toxin reaches the Golgi via a Rab9 independent pathway (Mallard *et al.*, 1998). Several other Rab- or Rab associated proteins like, Rab11 (Wilcke *et al.*, 2000), Rab6a and Rab6a' (which regulates fusion to the Golgi) (Mallard *et al.*, 2002; Del Nery *et al.*, 2006) involved in regulation of ST transport. Even though ST does not contain KDEL or KDEL-like sequence, toxin move in a retrograde manner from Golgi to ER via a COP-I independent Rab6a'-dependent route (White *et al.*, 1999; Girod *et al.*, 1999).

In the ER lumen, the A1 fragment disassociation is mediated by PDI, which reduces the disulfide bond between the STAC A1 and A2 chains (Sandvig *et al.*, 2010). ST interacts with ER-lumen resident chaperons such as HEDJ/ERdj3 (Yu and Haslam, 2005) and BiP (Falguieres *et al.*, 2006), which is necessary to induce the unfolding of the A1-fragment prior to the transport across the ER membrane. Like other toxins (RT and CT), it has been suggested that ST also uses *Sec61p* translocon to enter into the cytosol (Johannes and Römer, 2010). Once in the cytosol, the enzymatically active A1 chain removes an adenosine residue from the 28S ribosomal subunit (O'Brien *et al.*, 1992), which results in inhibition of protein synthesis.

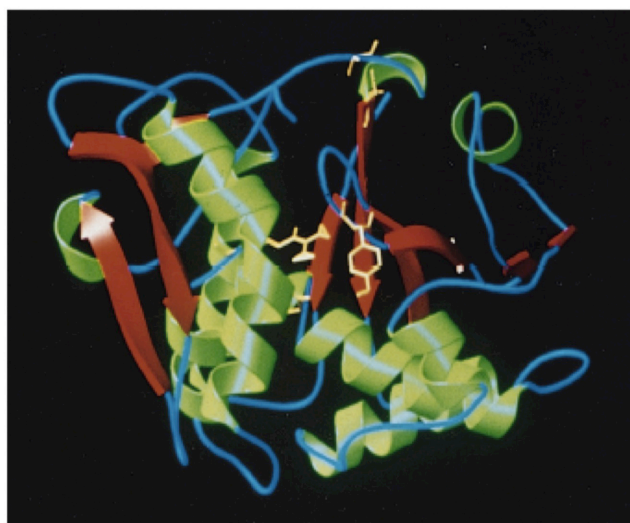
The above-mentioned toxins contain two chains, however RIP-I family proteins contain only one chain and they have been documented to also exert toxicity, if they were deliver into the cytosol. In cell free systems, RIP-I family proteins like gelonin, saponin, pokeweed antiviral protein (PAP) and trichosanthin have demonstrated cytotoxicity. Consequently RIP-I family proteins can be used as markers to evaluate the successful delivery of a macromolecule to the cytosol.

1.4.2.4 Gelonin

Gelonin is extracted from the seeds of the plant *Gelonium Multiforum* (Stirpe *et al.*, 1980). The toxin belongs to ribosome inactivating proteins I (RIP-I) family, containing no obvious lectinic chain (Barbieri *et al.*, 1993).

Devoid of a binding domain, the RIP chain demonstrates little cytotoxicity to intact cells (Lambert *et al.*, 1988) due mainly to the limited cytosolic (and hence target) access. Gelonin shows activity when evaluated in a cell-free system by eukaryotic ribosome deactivation, releasing adenine-4324 from the 28S rRNA (Endo *et al.*, 1988; Stirpe *et al.*, 1988). Gelonin is a glycosylated protein and contains high concentrations of terminal mannose residues (Stirpe *et al.*, 1980). Since, it does not contain binding domain, gelonin is endocytosed via non-specific fluid phase pinocytosis and by mannose receptor mediated endocytosis (Madan and Ghosh, 1992).

Figure 1.14: Ribbon diagram of Gelonin protein (Housr *et al.*, 1995)



1.4.3 Toxins as membrane manipulating delivery systems

Due to their highly evolved and unusual endomembrane trafficking, several types of toxin have been proposed not only as therapeutics but also as drug delivery systems (Watson and Spooner, 2006; Johannes and Decaudin, 2005). In the latter case, the lethality of the toxin can be diminished, making them non-toxic entities, whilst preserving their ability to navigate endomembrane system (Sandvig and van Deurs, 2000; Tarragó-Trani and Storrie, 2007).

These disarmed toxins can be used as vectors to delivery other proteins, antigens into the cytosol (Grimaldi *et al.*, 2007).

Synthetic non-viral delivery systems *i.e.* polyplexes or lipoplexes break the endosomal membranes when delivering material, which can result in the leakage of lysosomal hydrolytic enzymes, damaging the cell and resulting in cell death (Minchin and Yang, 2010). Where as RT, CT and ST may be utilised for the delivery of macromolecules into the cytosol, as they do not need to breach the endomembrane system.

1.5 Applications in medicine and cell biology

Immunotoxins, consisting of a cell-selective antibody chemically linked to a toxin moiety, were designed to specifically bind to target cells *i.e.* cancer cells (Kreitman, 2006). The targeting of cancer cells, over expressing tumour associated antigens, membrane receptors, or carbohydrate antigens by synthesizing specific ligands (or antibodies) has been postulated as a potential delivery platform for toxic proteins and has been rigorously investigated (Reiter, 2001; Potala *et al.*, 2008). Bacteria toxins like *pseudomonas exotoxin A* (Pastan, 2003; Pai *et al.*, 1996), anthrax toxin (Lu *et al.*, 2000), diphtheria toxin (Moolten and Cooperband, 1970; Frankel *et al.*, 2009;) RT (Schnell *et al.*, 2000), saporin (Bergamaschi *et al.*, 1996), gelonin (Delprino *et al.*, 1993) and pokeweed antiviral proteins (Myers *et al.*, 1991) have been used as immunotoxin components.

Immunotoxins have several advantages when treating cancer compared to conventional treatment modalities (*i.e.* chemotherapy, radiotherapy and surgery), as they may be very potent and highly specific in their action (Messmer and Kipps, 2005). One single immunotoxin molecule has been reported to be sufficient to kill the cancer cell (Pastan *et al.*, 2007), whereas 10^5 molecules of a chemotherapeutic drug are needed to show the same effect (Hall and Fodstad, 1992). This may have the effect of reducing the dose size and frequency (Pastan *et al.*, 2007). Since immunotoxins are potentially very specific, systemic toxicity is (potentially) reduced and high local concentrations may be achieved. Immunotoxins show effective penetration of solid tumour tissue relative to whole antibody molecules (Pastan, 2003; Pai-Scherf *et al.*, 1999). To improve the specificity of the toxin, native toxin binding domains are either deleted or blocked to prevent their interaction with normal cells (Kreitman, 2009).

Table 1.6: Immunotoxins used clinically in recent years (Kreitman, 2006)						
Chemical Conjugates						
Agent	Antigen	Ligand	Truncated Toxin	Basic toxin	Disease	References
RFB4-Fab'-dgA	CD22	Fab'	dgA	Ricin	HD	Schnell <i>et al.</i> , 2000
HD37-dgA	CD19	MAb	dgA	Ricin	B-NHL	Stone <i>et al.</i> , 1996
TF-CRM107	TFR	Tf	CRM107	DT	Glioma	Laske <i>et al.</i> , 1997
B43-PAP	CD19	MAb	PAP	PAP	ALL	Uckun, 1993
Ber-H2-Sap6	CD30	MAb	Sap6	Saporin	HD	Winkler <i>et al.</i> , 1997

Many immunotoxins have entered into clinical trials, one most active are those that bind to hematologic tumours. One fusion protein (Denileukin diftitox) was approved by for use in the USA by the FDA in 1999 (Piascik, 1999). Denileukin contains human interleukin-2 and truncated diphtheria toxin and is used to treat cutaneous T-cell lymphoma, although it has also shown activity against leukaemia (Kreitman, 2009). Another immunotoxin that has shown promising results contains truncated *pesudomonas* exotoxin conjugated to an antibody fragment specific for CD22. This conjugate has induced complete remission in a high proportion of cases of hairy cell leukaemia (Kreitman *et al.*, 2001).

Immunotoxins have also been used to deliver specific antigens into the major histocompatibility complex class I (MHC-I) compartment of targeted cells in the lumen of the ER via peptide transporters associated with antigen processing (TAP). This forms part of the cells immuno-surveillance system and detects the presence of non-self proteins such as those encoded by viruses. Peptides loaded into MHC class 1 receptors are transported to the plasma membrane via the Golgi apparatus, where they may interact with cytotoxic CD8⁺ T-cells. Several bacterial toxins have been used in antigen presentation including CT, RT and ST (Smith *et al.*, 2002).

However, several obstacles remain when considering the clinical use of imunotoxins, including a high degree of humoral response in humans (Frankel, 2004) and vascular leak syndrome (Amlot *et al.*, 1993) demonstrating non-specific toxicity.

1.6 Aims of work reported in the thesis

The need for intracellular drug delivery systems suitable for the cytosolic delivery of genes, proteins and RNAi/antisense agents has been identified (sections 1.2.3 and 1.2.4). Further, the delivery system is required to be non-toxic and avoid sequestration in capillary beds and by the reticuloendothelial systems. These requirements may preclude cationic systems (section 1.3.2.5). **Here in, the hypothesis that recombinant, disarmed ricin based toxins can retain the capacity to deliver macromolecular cargo to the cytosol, without mediating toxicity, is to be tested.** This objective is completely novel. Consequently, disarmed, recombinant potential cytosolic shuttles, based on the molecular architecture of RT (section 1.4.2.1) have been characterised. These molecules have been disarmed using recombinant PCR, specifically site-specific mutagenesis. These clones were subject to DNA sequencing prior to the start of this thesis and the proteins the plasmids code for have been expressed and characterised (for the first time) herein. The efficiency of PAA delivery was then compared with toxin based delivery systems using gelonin. This comparison was not direct but gave an indication of relative levels of success (cytosolic delivery). Specifically the following questions were addressed:

1) Can RTBC or mutant RTAC (incorporating “Del” (¹⁷⁷⁻¹⁸²Δ) or “Mut” (¹⁷⁷⁻¹⁸²G) mutations (2.1) be expressed in *E.coli*? This question was addressed by undertaking mini-induction experiments and solubilising the entire culture in detergent. The solubilised lysate was then subjected to electrophoretic separation followed by detection by either Coomassie brilliant blue R-250 staining or immuno-blotting. When the recombinant proteins based on RTAC were expressed, a C-terminal epitope tag (6His residues) served not only to facilitate the enrichment of the protein by affinity chromatography (section 2.2.5.4) but also as an indicator that translation had not ended prematurely (RTAC mutants).

2) Are the recombinant RTAC and rRTBC (clone 204) analogues described above soluble when expressed in *E.coli*? This question was answered by assessing the concentration of the soluble protein eluted from the affinity chromatography column (after the removal of the imidazole by dialysis).

3) Are these proteins recognised by a commercial antibody specific for the template? Commercially available polyclonal antibodies were used to answer this question and were

used as primary antibodies during the immuno-detection of both the RTAC and RTBC analogues by both protein immuno-blotting and during immuno-fluorescent microscopy.

4) What were the optimal culture conditions for expressing the mutant RTAC and RTBC analogues? Coomassie brilliant blue R-250 staining and Western blotting were deployed in order to investigate the optimal culture time for protein production pre- and post-expression induction (*i.e.* adding isopropyl- β -D-thiogalactopyranoside (IPTG)) as well as the optimal concentration of IPTG required to stimulate induction.

5) Were the “Del” or “Mut” mutation more effective at ablating toxicity? Having produced soluble well-characterised RTAC and RTBC analogues, the recombinant proteins were incubated with immortalised mammalian cells grown in culture. A positive control was included to show the sensitivity of the cells to the wild type RTAC. After mixing the A and B chains (not refolded) over a concentration range previously reported to be toxic for wild type RTAC (Ready *et al.*, 1991; Smith *et al.*, 2003), cell viability was assayed after 48h using a well characterised colorimetric assay (Mosmann, 1983).

6) Did the presence or absence of N- or C- terminal epitopes or domains (*i.e.* GFP) fused in frame with RTAC analogues influence any of the above factors? A list describing the proteins tested is given below (table 1.7)

Table 1.7: Constructs evaluated in the project		
Clone Number	Description	Cartoon
204	RTBC	
216	HA-RTAC (Mut)	
217	HA-RTAC (Del)	
192	RTAC(Del)-eGFP-KDEL	
224	eGFP-RTAC (Mut)-KDEL	
189	RTAC (Mut)-HA-KDEL	
175	HA-WT RTAC	

7). Was it possible to produce recombinant gelonin constructs with specific epitope tags and an additional C-terminal cysteine? The question was answered by sub-cloning of gelonin using specific primers.

8). Could the recombinant gelonin constructs be detected using commercial antibodies specific to the epitope tags engineered into the recombinant proteins? This question was answered by expression and production of recombinant gelonin in *E.coli* BL21*DE3 cells and purified proteins were characterised by SDS-PAGE and immuno-blotting.

9). Were the recombinant gelonin proteins toxic? This question was answered by incubating the recombinant gelonin proteins with immortalised mammalian cells. The cell viability was assayed after 72h using MTT assay.

10). Were the ISA PAA polymers or engineered toxins (commercial RTBC) more efficient at delivering gelonin? The question was answered by applying ISA PAAs and gelonin (either commercial or recombinant) or cRTBC and gelonin (either commercial or recombinant) separately onto immortalised mammalian cells. The viability of cells was performed using MTT assay after 72h incubation time.

11). Were ISA-FITC conjugated PAA polymers biocompatible? This question was answered by incubating polymers with immortalised mammalian cells and the viability of cells was assayed after 72h using the MTT assay. Positive (PEI) and negative (dextran) controls were also included to validate the assays.

12). Do ISA-FITC polymers reach cytosol/nucleus after 5h incubation? This question was answered by identifying polymer-conjugated FITC within the cytosol/nucleus by fluorescence microscopy and live cell imaging, using an optimised polymer concentration and exposure time.

Chapter 2

Materials and Methods

2.1 Materials

2.1.1 Equipment & Chemicals

The 6315 UV Spectrophotometer was supplied by JENWAY (Chelmsford, UK). The Sub-Cell[®] GT Agarose Gel Electrophoresis Systems, Mini-PROTEAN[®] Tetra Cell, Mini Trans-Blot[®] Electrophoretic Transfer Cell and PowerPac[™] HC Power Supply were supplied by BioRad (Hemel Hempstead, UK). The French press cell disrupter, centrifuges (Heraeus fresco 21, Sorvall[®] RC6 Plus, Sorvall[®] Discovery M120), Forma orbital shaker and Multiscan EX Microplate photometer were all supplied by Thermo Scientific (Essex, UK). The dry block heater (Talboy) was supplied by Fisher Scientific (Leicestershire, UK). The EpiChemi BioImaging system was supplied by UVP (Cambridge, UK). Nikon ECLIPSE 90i advanced automated research microscope and Nikon ECLIPSE Ti-U inverted microscope systems were supplied by Nikon (Surrey, UK).

Isopropyl β -D-1-thiogalactopyranoside (IPTG), sodium azide, ethidium bromide (EtBr), nitrocellulose membrane (0.2 μ m pore size, 33cm \times 3m), dialysis tubing cellulose membrane (average flat width 25nm), bovine serum albumin (BSA), α -Lactose-agarose saline suspension, deglycosylated commercial ricin A chain were purchased from Sigma (Dorset, UK). Commercial RTBC was supplied by Vector laboratories Ltd (Peterborough, UK). Commercial gelonin was purchased from Enzo Life Sciences (Exeter, UK). Coomassie brilliant blue G-250, acrylamide, bis-acrylamide, ammonium persulphate (APS), β -Mercaptoethanol (BME), sodium dodecyl sulphate (SDS) were purchased from BioRad (Hemel Hempstead, UK). Tris-base, ampicillin sodium salt, glycerol, imidazole, sodium chloride, agar, yeast extract, glycine, paraformaldehyde and agarose were purchased from Fischer Scientific (Leicestershire, UK). Tryptone was supplied by OXOID (Hampshire, UK). Ni Sepharose[™] High performance resin, PD10 desalting columns, ECL Western blotting detection reagents were supplied from GE healthcare (Buckinghamshire, UK) and TALON[®] Metal affinity resin was purchased from CLONTECH (Takara Bio Europe S.A.S, France). KODAK Medical X-ray films were purchased from Scientific Laboratory supplies (Nottingham, UK). ILFORD PQ UNIVERSAL paper developer and Kodak UNIFIX liquid fixer were purchased from Agar Scientific Ltd (Essex, UK). Indicator stop bath was purchased from Kodak (Hemel Hempstead, UK).

2.1.2 Organisms and cells

Chemically competent One Shot BL21*DE3 and TOP10 *E.coli* were supplied by Invitrogen (Paisley, UK). The B16 cells were a kind gift from Prof. Ruth Duncan (Cardiff University). Vero cells were a kind gift from Prof. Robert Piper at the University of Iowa, USA. Dimethyl sulphoxide (DMSO), MTT reagent ([3-(4,5-dimethylthiazol-2-yl)-2,5-diphenyltetrazolium bromide]), poly(ethyleneimine) (PEI) ($M_n \sim 60,000$) and dextran (M_w 35,000-45,000) were from Sigma (Dorset, UK). Dulbecco's-Minimal Essential Medium (D-MEM), RPMI 1640, foetal bovine serum, trypsin-EDTA (TE), penicillin-streptomycin-glutamine (P/S/G) were supplied by Gibco (Paisley, UK).

2.1.3 Stock solutions

2x Yeast extract and Tryptone digest media (2xYT): The bacterial growth medium 2xYT was prepared by mixing bacto tryptone (16g) with bacto yeast extract (10g) and sodium chloride (5g) in 800mL of de-ionised distilled water and the final volume adjusted to 1000mL prior to being autoclaved at 121°C for 30minutes on a liquid cycle. Antibiotic was always added after autoclaving and the media having been allowed to cool below 50°C.

2xYT agar plates: To 800mL of de-ionised water, 16g of bacto tryptone, 10g of bacto yeast extract, 5g of sodium chloride and 15g of agar were added and mixed thoroughly and the final volume was made up to 1000mL. The solution was sterilised by autoclaving, after it was left at room temperature to bring down the temperature to 50°C. 1g of ampicillin was added to the medium and mixed thoroughly. Then the medium was poured into plates up to specified level and they were dried at room temperature. Once dried, plates were stored at room temperature.

Resolving gels (10%): was prepared by adding 4mL of de-ionised water, 3.3mL of acrylamide/bis, 2.5mL of 1.5M Tris-buffer (pH 8.8), 100µL of 10% (w/v) sodium dodecyl sulphate (SDS), 50µL of 10% (w/v) ammonium persulphate (APS) and *N, N, N', N'*-tetramethylethylenediamine (TEMED).

The Stacking gel: was prepared by mixing de-ionised water (3.4mL), acrylamide/bis (0.66 mL), 1.5M Tris-buffer (pH 6.8) (0.83mL), SDS (10% (w/v)) (50µL), 10% (w/v) APS (50µL), TEMED (10µL).

APS (10% (w/v)): was prepared by adding APS (0.1g) to de-ionised water to a final volume of 1mL.

1.5M Tris-HCl (pH 8.8): was prepared by mixing 181.5g of Tris base in 800mL of de-ionised water and pH of the solution was adjusted to 8.8 with 6N HCl and the final volume was made up to 1000mL with de-ionised water.

0.5M Tris-HCl (pH 6.8): was prepared by mixing 60g of Tris base in 800mL of de-ionised water and pH of the solution was adjusted to 6.8 with 6N HCl and the final volume was made up to 1000mL with de-ionised water.

10x PBS: was prepared by adding 80g of sodium chloride, 2g of potassium chloride, 14.4g of disodium hydrogen phosphate, 2.4g of potassium dihydrogen phosphate to 800mL of de-ionised water and mixed thoroughly. The pH of the solution was adjusted to 7.4 and final volume adjusted to 1000mL with de-ionised water.

1M IPTG: was preparing by adding 2.38g of IPTG in 10mL of de-ionised water and it was aliquoted (1mL) into 1.5mL Eppendorf tubes and stored at -20°C.

SDS PAGE running buffer (10x): was prepared by mixing Tris base (30.2g), glycine (188g), sodium dodecyl sulphate (10g) and adjusting the volume to 1000mL with de-ionised water.

Laemmli sample buffer (LSB) (6x): was prepared by mixing 0.5M Tris-HCl (pH 6.8) (1mL), glycerol (0.8mL), sodium dodecyl sulphate (10% (w/v) (1.6mL), β -Mercaptoethanol (BME) (0.4mL), bromophenol blue (1% (w/v) (0.4mL), and de-ionised water (3.8mL).

SDS (10% (w/v)): was prepared by adding SDS (10g) to de-ionised water and adjusting the to volume of 100mL.

Coomassie brilliant blue R-250 staining solution: was prepared by mixing Coomassie brilliant blue R-250 (0.25g) with methanol (40mL), de-ionised water (50mL) and glacial acetic acid (10mL).

Coomassie de-staining solution: Methanol (40mL) was added to de-ionised water (50mL) and to this, glacial acetic acid (10mL) was added.

Towbin electro-blotting buffer: was prepared by adding Tris-base (3g) and glycine-HCl (14.08g) to de-ionised water (800mL) and methanol (200mL). To this solution SDS (5mL 10% (w/v)) was added and the final volume was then adjusted to 1000mL with de-ionised water.

Imidazole (1M): was prepared by adding 0.68g of imidazole in to de-ionised water and final volume was made up to 10mL with de-ionised water.

Ponceau-S stock solution (10x): 2g of Ponceau-S [(3-hydroxy-4-(2-sulfo-4-(4-sulphophenylazo)-phenyl-azo)-2,7-naphthalenedisulfonic acid)], 30g of trichloro acetic acid (TCA) and 30g of sulphosalicylic acid were added to de-ionised water and after gentle mix, the final volume was adjusted to 100mL with de-ionised water. Working solution was prepared by diluting the stock solution in 1:10 ratio with de-ionised water.

Complete EDTA free protease inhibitor cocktail (50x): One complete EDTA free protease inhibitor cocktail tablet was dissolved in 1mL of 1xPBS.

Western blotting blocking solution: was prepared by adding non-fat dried milk (5g) to 1x PBS (100mL final volume) containing Tween 20 (0.01% (v/v)).

Tris Acetate EDTA (TAE) (50x) buffer: was prepared by mixing Tris-base (242g) with glacial acetic acid (57.1mL) and 0.5M EDTA (pH 8.0) (100mL). The final volume was then adjusted to 1000mL with de-ionised water.

Blocking buffer: was prepared by adding 1mL of goat serum to 49mL of 1x PBS.

2% (w/v) Paraformaldehyde: was prepared by adding 5mL of 10xPBS into 30mL of de-ionised water and it was heated to approximately $\sim 100^{\circ}\text{C}$, then 1g of paraformaldehyde was added and it was dissolved by adding 5N NaOH. Then 900 μL of 5M HCl was added into it. The pH of the solution was adjusted to 7.2 by adding 1N HCl drop wise. Final volume of the

solution was made up to 50mL with de-ionised water. This solution was made fresh every time it was used.

Triton extraction buffer: was prepared by taking 5mL of 10xPBS into 50mL Falcon tube. To this 190mg of glycine was added (giving a final concentration of 50mM). After mixing thoroughly, Triton X-100 was added (to a final concentration of 0.2% (v/v)) and the final volume of the solution made up to 50mL with de-ionised water.

Mounting media: was prepared by taking 10mg of *n*-propyl gallate (NPG) (final concentration of 1% (w/v)) into an Eppendorf tube. To this 100 μ L of 10xPBS, 400 μ L of glycerol and 500 μ L of de-ionised water were added. The NPG was dissolved by placing the Eppendorf tube in boiling water for 2-3minutes.

Trichloroacetic acid (TCA) stock solution (100%): To 350 μ L of de-ionised water, 500g of TCA was added and mixed gently by using magnetic flea.

Richardson Piper (RP) media: was prepared by mixing glucose (5mM), FBS (10%), calcium chloride (1mM), magnesium acetate (1mM) in 1xPBS with their stated concentrations and then the media was filter sterilised using 0.2 μ m filter.

2.2 Methods

2.2.1 PCR templates, construct preparation and sub-cloning

Gene synthesis was performed by Bio Basics Inc. (BBI). Sequences obtained from published data, which is accessible via National Centre for Biotechnology Information (NCBI). Sequence was used to order synthetic gene from BBI, which was cloned into pUC57.

pET TOPO vectors contains selectable markers, T7 *lac* promoter, N-or C- terminal specific epitope tags and cleavage sites which all play major role in growth, expression of the gene of interest in the host and also identification of the resultant protein. There are several types of pET TOPO vectors available and they have different selectable markers and epitope tags. For cloning, pET151/D-TOPO vectors were used. They contain an ampicillin selectable marker, T7 *lac* promoter and N-terminal 6His and V5 tags. (Invitrogen, Paisley, UK)

TOPO cloning is used for the direct insertion of *Taq* amplified PCR products into a plasmid vector. It utilises inherent biological activity of DNA topoisomerase I. The cloned plasmids then transfected into suitable bacterial strains such as *E.coli* BL21*DE3 for the expression of the inserted gene.

PCR products for cloning were obtained from synthesized template in pUC57 (Clontech, CA, USA) using appropriate oligonucleotide primers (as detailed in table 2.1). PCR products were characterised by agarose gel electrophoresis to assess apparent molecular weight prior to their ligation into a plasmid vector. For bacterial expression, selected PCR products were cloned into champion pET151/D-TOPO (Invitrogen) using the manufacturers protocol. Resultant colonies were characterised by PCR using mid-ORF and vector oligonucleotide primers selected and designed to ensure the orientation of the PCR insert. Colonies that were positive for both the presence of the desired insert and the orientation of the insert were cultured overnight in 2xYT media containing ampicillin (200µg/mL), and plasmids were prepared using a commercial plasmid Miniprep Kit (Qiagen). Sequencing was carried out on all successful colonies using the DNA Core (University of Iowa, Iowa City USA) and analysed using the DNASTar software suit (LaserGene Inc. Madison Wisconsin, USA).

Table 2.1: Oligonucleotides used during the sub-cloning of RTAC and RTBC

Oligo number	Sequence
1	caccgctgatgtttgatggatcct
2	tcaaaataatggtaacatattg
3	cacctaaaggaggaaaggatccatgtatccttacgacgtaccagattacgcaatgatattcc ccaacaatac
4	caactctggctcgttcctttataatttgcaccaaattgattggaggaggaggaggagacaat atattgaggagaaatgcgacagagaattagg
5	cctaattctcgtgcgcatcttccctcaatatattgtcctcctcctcctcctcaatcatttggatg caaattataaaggaacgagccagagttg
6	tcatcaatgatgatgatgatgaaactgtgacgatggg
7	aactctggctcgttcctttataatttgcaccaaattgattcaatatattg aggagaaatgcgacagagaattaggtaga
8	tgtacctaattctcgtgcgcatcttccctcaatatattgaatcatttggatgcaaattataaagg aacgagccagagtt
9	cacctaaaggaggaaaggatccatggccagcaaaggagaagaa
10	tcatcacaactcgtccttatgatgatgatgatgaaactgtgacg atggg
11	atgatgatgatgatgtgcgtaactctggtagcgtcgtgtaaggataaaac tgtgacgatggagg
12	gaaaggatccatggccagcaaaggagaagaa

2.2.2 Plasmid DNA purification using the QIAprep Spin Miniprep Kit

Preparation of overnight (saturated) bacterial cultures: Sterile wooden applicators were used to transfer a small quantity (~5 μ L) of a frozen stock of *E.coli* containing the specific plasmid, into 10mL of 2xYT medium containing the appropriate antibiotic. The culture was then incubated in an orbital shaker (Thermo Scientific, Essex, UK) overnight at 37°C (200 rpm).

Protocol for isolating low copy number plasmids from TOP10 *E.coli*: This method is adapted from the protocol supplied by the manufacturer of the Miniprep Kit from Qiagen (West Sussex, UK). From the saturated, overnight 10mL *E.coli* cell culture, 1.2mL was transferred into a sterile 1.5mL Eppendorf tube and centrifuged at 13000rpm for 1minute. The supernatant was then discarded. An additional 1.2mL of culture was then added to the

same Eppendorf and the process repeated. This step was repeated until a single pellet was obtained from 9mL of culture.

The pellet was then re-suspended in 500 μ L of buffer P1 (Qiagen). The pellet was then mixed thoroughly by aspiration, until no aggregated cells were visible. To this suspension 500 μ L of buffer P2 (Qiagen) was added and mixed thoroughly by inverting the Eppendorf tube 4-6 times. To the cell lysate 700 μ L of buffer N3 (Qiagen) was added and mixed thoroughly by inverting the tube 4-5 times. The lysate was then cleared by centrifugation (10minutes at 13000rpm at 4°C) and the supernatant applied to a spin column (Qiagen). The spin column was then centrifuged for 60seconds and the flow through discarded. The spin column was then washed by adding 0.5mL of PB buffer (Qiagen) and centrifuged as before. The flow through was discarded and the spin column was washed again with 0.75mL buffer PE (Qiagen) and centrifuged as before. The flow through was again discarded and an additional centrifugation step was performed to remove any residual wash buffer (using the same conditions as before). Plasmid DNA was eluted by placing the spin column in a clean, sterile 1.5mL Eppendorf tube and adding 50 μ L of sterile de-ionised water which was then allowed to stand at room temperature for 1-2 minutes. The eluted plasmid DNA was then collected by centrifugation (1minute at 13000rpm at 4°C) and stored at 4°C for short periods and -20°C for long periods.

Protocol for isolating high copy number plasmids from Top10 *E.coli* and MC1061 (high copy number plasmid): When the host strain of *E.coli* was known to contain a high plasmid copy number, the following adaptations were made to the protocol listed above. Initially only 5mL of the overnight culture was used to isolate the plasmid and as per the manufacturers instructions, 250 mL of P1 (Qiagen), 250mL P2 (Qiagen) and 350mL P3 (Qiagen) were used.

2.2.3 Measuring the plasmid concentration

Plasmid DNA was diluted with de-ionized water at a 1:20 ratio. By measuring the plasmid solution's absorbance at 260nm, the concentration of plasmid DNA could be determined using the Beer-Lambert law. As solution containing 50 μ g/mL of double stranded (DS) DNA has an absorbance of 1 at 260nm, *i.e.* $OD_{260} = 1 = 50\mu\text{g/mL}$ (Sambrook, *et al* 1989). Consequently 1 μ g of DS DNA will have an OD_{260} of $1/50 = 0.02$. Consequently the concentration of the plasmid DNA can be determined by dividing the OD_{260} of the sample by 0.02 and multiplying by the dilution factor.

2.2.4 Agarose gel electrophoresis

Agarose gel electrophoresis was used to separate, characterise and visualize DNA. This was achieved by preparing a 1% (w/v) stock agarose (4g) in Tris acetate EDTA (TAE) (8mL of 50x) buffer and diluted to 400mL with de-ionised water.

The agarose was dissolved by boiling the gel preparation in a microwave oven (Sanyo, Watford, UK) until all the agarose powder was seen to dissolve (~4 minutes at full power (75w)). When the mixture was then left to cooled to approximately 40°C, and 20µL of ethidium bromide (EtBr) stock solution (Sigma, Dorset, UK) (10mg/mL) was added to give a final concentration of 0.5µg/mL, EtBr. The liquid agarose was then poured into a gel casting tank (with a comb placed to form the sample loading wells) and left on a level flat surface to set (approximately 20minutes). Any bubbles were removed using a sterile pipette.

Next, 1µL of loading dye (6x) (Fermentas, Cambridgeshire, UK) (Appendix I) was added to 0.5µg of plasmid sample and the volume adjusted to 6µL total, using sterile DNase free water. Having removed the comb, this preparation was then loaded into a gel well and its location within the gel documented. In order to gauge the apparent molecular weight of any linear DNA, and to act as a positive control, 6µL of 1kb DNA ladder (Fermentas, Cambridgeshire, UK) was loaded into a separate well. The gel was then immersed in 1xTAE and placed in a DC electric field (60V for 1h) and documented using the EpiChem BioImaging systems (UVP) following the manufacturers instructions.

2.2.5 Protein expression and purification

2.2.5.1 Bacterial transformation

Chemically competent *E. coli* BL21*DE3 (Invitrogen, Paisley, UK) were thawed on ice over 15minutes and 10µL transferred into a sterile Eppendorf tube pre-chilled to 4°C containing 5µL of plasmid DNA (5ng). This preparation was then left at 4°C for 30minutes. The cells were then heat shocked by rapidly transferring the Eppendorf tube from 4°C to a dry block heat block set at 42°C where they were left for 30seconds. The cells were then immediately placed back on ice for 2minutes. Next the cells were allowed to recover by adding 100µL of SOC medium (Invitrogen, Paisley, UK) and incubated at 37°C for an hour on an orbital shaker set to 200rpm. If the plasmid was well characterised and being subject to isolation, rather than spreading the transformants on selective agar, the entire culture was transferred into liquid selective media (2xYT containing 200µg/mL ampicillin). Samples were then

transferred into 10mL of 2xYT medium and incubated at 37°C on an orbital shaker (set at 200rpm) and left over-night.

2.2.5.2 Protein expression

Saturated, transformed *E.coli* cultures (10mL) were added to 1000mL of 2xYT medium containing 200µg/mL of ampicillin and incubated at 37°C for three hours on an orbital shaker (Thermo Scientific, Essex, UK). To induce protein expression, 250µL of IPTG (1M) (Isopropyl β-D-1-thiogalactopyranoside) was added and cultured at 37°C for 3h and 30minutes on an orbital shaker. The resulting cell suspension was centrifuged in 500mL aliquots at 6000 x g (rcf). The supernatant was discarded and the remaining pellet was stored at -80°C.

2.2.5.3 Bacterial lysis

The generation of a bacterial lysate was undertaken by using a French press (Thermo Scientific, Essex, UK). This apparatus generates high pressure and relies upon rapid decompression to break the membranes of cells. The bacterial pellet was thawed on ice and re-suspended in 5mL of PBS buffer. To the re-suspended cell suspension Complete[®] EDTA free protease inhibitor cocktail (Roche, Hertfordshire, UK) was added to a final concentration of 5x according to the manufactures instructions. Sodium azide was then added to a final concentration of 0.02% (v/v). The cell suspension was placed into the pressure cell and mounted on to the French press apparatus (Thermo Scientific, Essex, UK). The motor driven piston inside the cylinder was allowed to increase the pressure in the pressure cell to 1500 pounds per square inch (psi), and the pressurised samples were allowed to pass through the bled-through needle (part of the French press) at an approximate rate of 1mL/minute. The cell lysate was collected into fresh sterile 50mL disposable centrifuge tube. The procedure was repeated 2-3 times and the resultant cell lysate was cleared by sedimentation using a centrifuge fitted with an SS34 rota set to generate at 20000 x g (rcf) for 20minutes at 4°C. The resulting supernatant was collected into fresh, sterile 50mL centrifuge tube and was stored at -80°C until required.

2.2.5.4 Immobilised metal ion affinity chromatography (IMAC)

Proteins were purified by immobilised metal ion chromatography. Ni²⁺ sepharose high performance medium (Ni-sepharoseTM) contained highly cross-linked agarose beads to which a chelating group was coupled, which, in this instance was charged with Ni²⁺ ions.

Recombinant proteins containing a six histidine residues (6His epitope) specifically binds to Ni²⁺ ions. Native *E.coli* proteins, (that don't contain a 6His epitope and hence not bound to the solid phase support) were washed away. Recombinant 6His epitope containing proteins were then eluted from the column using high concentrations of imidazole solution (100-500mM). Further, slightly lower concentration of imidazole (10-25mM) was also used in the wash to elute and non-specifically bound *E.coli* proteins that may have weakly adhered to the solid phase support and might be sensitive to imidazole concentrations.

Ni-sepharoseTM slurry was re-suspended and 1.5mL was transferred into a fresh polyprep column (BioRad, Hemel Hempstead, UK). The preservative (20% (w/v) ethanol) was then allowed to drain from the resin under the effect of gravity. The slurry was then washed twice with 5 column volumes of 1xPBS and then with 5 column volumes of wash buffer (PBS containing 25mM imidazole). The slurry was then incubated with protein lysate on ice for 1h under mild shaking conditions. The slurry and protein lysate mix was then poured back into the polyprep column and the lysate allowed to drain through (this flow through was collected). The collected protein lysate was passed through the column one more time and the column washed twice with 5 column volumes of wash buffer (1xPBS containing 25mM imidazole). The protein was then eluted in 0.5mL fractions by adding 0.5mL of elution buffer (1xPBS containing 500mM imidazole). Six to 12 fractions were collected and each protein fraction was collected into fresh, sterile Eppendorf tube and stored at -80°C. All the above steps were performed at 4°C.

From the each eluted protein fractions, 20µL was collected into a 96 well plate and 100µL of Bradford reagent added. The fractions containing the most protein were identified by the change in color associated with a positive result from the Bradford assay (the oxidation of a blue chromophore). Bradford reagent contains the Coomassie brilliant blue pigment G-250, that in its protonated form appears in red. When this pigment binds to proteins it becomes de-protonated and turns blue. The protein fractions containing significant quantities of recombinant protein were pooled into sterile Eppendorf tube(s) and stored at -80°C until further use.

2.2.5.5 Calculation of protein concentration

Bradford assay: In a 96 well plate, in one row different amounts of bovine serum albumin solution (10mg/mL in 1xPBS) was taken (0 μ g, 2 μ g, 4 μ g, 6 μ g, 8 μ g, 10 μ g). To each of these wells, 100 μ L of Bradford reagent (BioRad, Hemel Hempstead, UK) was added. In a separate row, 20 μ L of eluted protein fractions were transferred into three separate wells and 100 μ L of Bradford reagent was applied into each well and the absorbance was measured at OD_{595nm}. A standard curve was drawn using the BSA concentrations and absorbance values, from which the concentrations of protein fractions were calculated so long as the values obtained, were within the linear region of the calibration curve. If this was not the case then the samples were diluted and the experiment repeated.

The bicinchoninic acid (BCA) assay: The BCA reagent was prepared by adding copper sulphate and bicinchoninic acid (Sigma, Dorset, UK) in 1:49 ratio in a 15mL tube. The same procedure was followed as above, except instead of Bradford reagent, BCA reagent was added to the proteins and absorbance was measured at OD_{540nm}. Measurements were only taken once the linear range of the assay had been determined *i.e.* from 1-50mg/mL of protein. For both assays, where the protein concentration was above the linear range, the sample was diluted.

2.2.6 Sodium dodecyl sulphate (SDS)-polyacrylamide gel electrophoresis (PAGE)

SDS-PAGE separates charged proteins in complex mixture on the basis of their size and hence resistance to the passage through a hydrogel matrix in a DC electric field. This system can be calibrated to give information about the molecular weight and subunit composition of a protein or mixture of proteins.

Gel plate assembly was performed according to the protocol provided by the manufacturers (BioRad, Hemel Hempstead, UK). SDS-PAGE system contains a stacking gel and resolving gel (Laemmli *et al.*, 1970). First, the resolving gel was prepared by mixing the all the reagents except APS and TEMED. After gentle shaking, APS and TEMED were added into the reaction and it was poured in between the clean glass plates to the required level. The resolving gel was allowed to polymerise for 45minutes at room temperature. A comb was then inserted into the space above the resolving gel and the un-polymerised stacking gel reaction was poured on the top of the resolving gel. The stacking gel mix was allowed to polymerise for a further 30minutes also at room temperature.

The comb was then removed and the gel was clamped into the Mini-Protean® Tetra cell system. The top electrolyte compartment and the gel tank were filled with running buffer to the required level. The wells in the gels were rinsed with running buffer by using a Hamilton gas syringe (Hamilton Bonaduz AG, Switzerland) fitted with a blunt needle (50 μ L volume). For a 10 well gel, 20 μ L of the protein sample was mixed with 5 μ L of 6x Laemmli sample buffer and, if reducing conditions were required, 3 μ L of BME was added. The samples were then loaded into the wells of the gel using a Hamilton gas syringe. To estimate the size of the protein and also to act as a positive control for the gel run, 10 μ L of Spectra™ Multicolor broad range protein ladder (Fermentas, Cambridgeshire, UK) was loaded into the separate well. DC electric field (100V for 80minutes) was applied. The gels were then taken out and immersed in Coomassie brilliant blue R-250 staining solution (section 2.1) for 2h on orbital shaker at 20rpm and at room temperature. The gel was de-stained by using de-staining solution (section 2.1). The gel was then documented by scanning (CanoScan LiDE 60, Cannon Ltd, Surrey, UK) after drying the gel using a drying kit following the manufactures instruction (PROMEGA, Hampshire, UK).

2.2.7 Western blotting

Western blotting is an analytical technique used to detect a specific protein within a mixture of proteins. To a limited extent, it can also be used to quantify the specific protein of interest in a given sample.

Western blotting and immuno-detection is a two-step procedure. Firstly, proteins were separated using polyacrylamide gel electrophoresis before being transferred into a solid phase support such as a nylon nitrocellulose or polyvinylidene fluoride (PVDF) membrane. In every instance herein nitrocellulose with a pore size of 0.2 μ m (Steinheim, Germany) was used. The second step requires the immuno-detection of the protein using specific antibody, which is in turn was detected using a horse radish peroxidase (HRP)-conjugated secondary antibody binding in a specific manner to the primary antibody. The HRP can then be used to liberate a photon from the enhanced chemiluminescence (ECL) reagent (GE Health care, Buckinghamshire, UK), which exposes to X-ray film (Kodak, Nottingham, UK) placed on top of the nitrocellulose membrane in the dark.

To facilitate the electrophoretic transfer of the protein from an SDS-PAGE gel onto the solid phase support (Western blotting), the gel was assembled between fiber pads (supplied by BioRad) and filter paper (Whatman number 1). The nitrocellulose membrane was placed in

direct contact with the gel whilst taking care to exclude any air bubbles. The assembled cassette was then transferred into the mini-trans blot electrophoretic transfer cell (BioRad, Hemel Hempstead, UK) in a orientation that ensured the migration of the protein onto the membrane (as opposed to “away” from the membrane). A magnetic flea and a bio-ice pack were then placed in the tank and transfer buffer (Towbin buffer) was added as recommended by the manufacturer. DC current was then applied (0.4A) for 1h.

Following the transfer, the membrane was removed from the blotting apparatus and washed with de-ionised water. The effectiveness of the transfer was then observed by placing the nitrocellulose membrane in 2-3mL Ponceau-S and incubated for 2-3minutes. The Ponceau-S was then removed and the membrane was again washed with de-ionised water. The presence of protein bands denoted a successful transfer of proteins from gel onto the nitrocellulose membrane. This step could also be used as a control for the presence of air bubbles between the gel and the transfer membrane.

The immuno-detection of proteins transferred onto the solid phase support, were first required the blocking of the membrane to limit non-specific protein binding by fragments of the primary or secondary antibody (Kurien and Scofield, 2003). This has the effect of limiting background noise during the detection of the secondary antibody. The membrane was first transferred into a plastic wrap with 3mL of 5% (w/v) non-fat dried milk (Marvel, Lincs, UK) solution dissolved in PBS containing 0.01% (v/v) Tween 20 and the plastic assembly sealed using heat sealer (Essex, UK). This was incubated at 37°C in an orbital shaker (200rpm) for 1h (Thermo Scientific, Essex, UK). After the blocking step, the membrane was transferred into a new plastic sheath and the primary antibody solution was added following dilution with fresh blocking solution (dilution determined empirically see table 2.2 for specific dilution factors).

After the protein sheath had been heat sealed, it was incubated at 37°C on orbital shaker (Thermo Scientific, Essex, UK) for 1h (200rpm). After this incubation period, the membrane was washed three times with 10mL of PBS-Tween 20 (0.01% (v/v)) at room temperature, each wash being approximately 5minutes in duration. Following the last wash, the membrane was transferred into clean plastic sheath and was incubated with a secondary-HRP conjugated antibody, diluted 1:000 in fresh 5% (w/v) non-fat dried milk (Marvel) solution. This was then incubated at 37°C on orbital shaker (200rpm) for an hour. The membrane was then washed as before using fresh PBS-Tween 20 (0.01% (v/v)). Finally, after the third wash the membrane was left in PBS for 10minutes.

Table 2.2: Dilutions of primary and secondary antibodies used for Western blotting

Antibody	Catalogue/Clone No.	Supplier	Dilution for Western blotting	Dilution for Immuno fluorescence microscopy
Anti-RTAC (PAb)	ab27169	Abcam	1:1000	
Anti-RTBC (Pab)	ab27170	abcam	1:1000	1:100
Anti-6His (MAb)	631212	Clontech	1:1000	
Anti-V5 (MAb)	R960-25	Invitrogen	1:1000	
Anti-EEA1 (MAb)	610456	BD Biosciences	1:1000	1:100
Anti-LDH (MAb)	L7016/HH-17	SIGMA	1:1000	
Anti-TfR (MAb)	612124	BD Biosciences	1:1000	1:100
GM130 (MAb)	610822	BD Tranduction labs		1:100
Anti-LAMP1 (MAb)	H4A3	Development studies hybridoma bank, University of Iowa	1:100	1:10

2.2.8 Detection of the protein

Finally, the membrane was transferred into a dish containing equal volumes (0.5mL) of ECL detection reagents 1 and 2 and incubated for 2minute at room temperature. ECL detection reagent was drained and membrane was wrapped in plastic cling film (Sainsburys', Holborn, UK) and it was fixed onto the lid of a lightproof autoradiography cassette (SLS, Nottingham, UK). X-ray film was then placed into the cassette, which was sealed for an exposure time of between 1second and 20minutes depending upon the strength of the signal from the secondary antibody. The X-ray film was then developed in a dark room. The specific protein

bands were identified by super-imposing the developed film on to the membrane. The position of pre-stained broad range molecular markers (Fermentas, Cambridgeshire, UK) relative to the exposed bands were recorded in order to be able to estimate the apparent molecular weight of the protein detected.

Development of X-ray film: In dark room, after taking out X-ray film from the autoradiography cassette, it was immersed into developing solution and left for 3minutes. After that, X-ray film was rinsed in water bath, then transferred into stopper solution and immersed for 30seconds. After this period it was again rinsed in water bath and transferred into fixing solutions and immersed for 5minutes. The X-ray film was then washed with tap water and dried. Developed X-ray film was scanned using the scanner (Canon, Surry, UK).

2.2.9 Optimisation of bacterial culture conditions

Chemically competent One Shot *E. coli* BL21*DE3 (Invitrogen, Paisley, UK) were thawed on ice for 15minutes. Then 10 μ L of bacteria was transferred into a sterile Eppendorf tube pre-chilled to 4°C containing 5 μ L of plasmid DNA (5ng). This preparation was then left at 4°C for 30minutes. The cells were then heat shocked by rapidly transferring them from 4°C to a dry heat block set at 42°C where they were left for 30seconds. The cells were then immediately placed back on ice for 2minutes. Next the cells were allowed to recover by adding 100 μ L of super optimal broth with catabolic repressor (SOC) medium (Invitrogen, Paisley, UK) and incubated at 37°C for an hour on an orbital shaker set to 200rpm. After the incubation, the entire culture was transferred into liquid selective media (2xYT containing 200 μ g/mL of ampicillin). Samples were then transferred into 10mL of 2xYT medium and incubated at 37°C on an orbital shaker (set at 200rpm) and left over-night.

To the 5mL over night culture, 45mL of 2xYT medium with the selective antibiotic (ampicillin: 200 μ g/mL) was added and the culture was incubated at 37°C on an orbital shaker (200rpm). At twenty minute intervals, up to 300minutes, 1mL of culture was taken under sterile conditions and its absorbance was measured at 600nm. A graph of absorbance values was then plotted against the time. This procedure was repeated for each clone, which was transformed into fresh competent cells. Growth was measured pre- and post- induction.

Protein mini-induction experiments: Transformation of plasmid DNA was performed as above. From the overnight transformed culture 150mL was added to 1350mL of 2xYT medium with selective antibiotic (ampicillin: 200 μ g/mL) in a sterile Eppendorf tube. Culture was incubated at 37°C on orbital shaker (200rpm) for 75minutes. Protein expression was

induced by adding IPTG, with a final concentration of 0.25mM. Then culture was allowed to grow at 37°C on orbital shaker (200rpm) for 2h. Culture was centrifuged at 6000 x g (rcf) for 20minutes in a centrifuge. Supernatant was discarded and the pellet dissolved in 200µL of LSB with 10% (v/v) BME. The expressed protein was analysed using SDS-PAGE and Western blotting. The cultural conditions like pre and post induction time and IPTG concentration were optimised by mini-induction experiments.

2.2.10 Mammalian cell culture and viability assay

Immortalised mammalian cells were maintained at 37°C and an atmosphere of 5% (v/v) CO₂ in a humidified CO₂ culture incubator. The cells were grown in 75cm² cantered neck flasks and were passage once every three to four days. All materials added to cell culture were sterile, osmotically balanced and heated to 37°C. All manipulations performed aseptically under the tissue culture hood. Animal cells grow either as an adherent monolayer or in suspension. Here cells grew as an adherent monolayer.

Subculture routine: Media was removed by aspiration and cell monolayer washed twice with 10mL of 1xPBS. Then cells were detached from the flask using trypsin-ethylenediaminetetraacetate (TE) (500µL). After 3-5minutes incubation under standard conditions, the monolayer was examined microscopically. Once the majority of cells have been detached from the substrate (and were visible in suspension), 9.5mL of complete media was added (different media compositions were used for B16 and Vero cells, details about the composition of the media were listed in the table 2.3). The cell suspension was then gently aspirated 3-4 times to disaggregate cells using a 10mL serological, sterile pipette. From the cell suspension 0.5mL was put back into the flask and rest of the suspension was discarded. Complete media (9.5mL) was added into the flask and placed the flask back into the incubator.

Table 2.3: Cell lines used for cytotoxicity assay (MTT assay) and sub-cellular trafficking experiments.

Cell line	Name	Adherent	Split ratio	Culture media
B16	Murine malignant melanoma	Yes	1:20	RPMI1640, 10%(v/v) FBS, penicillin (100units/mL), streptomycin (100µg/mL), glutamine 0.292mg/mL.
Vero	African green monkey kidney epithelial cells	Yes	1:20	DMEM, 10%(v/v) FBS, penicillin (100units/mL), streptomycin (100µg/mL), glutamine 0.292mg/mL.

Assessing cell viability using the MTT assay: The MTT assay is a colorimetric assay that was used to measure cell viability and growth. When applied to cells, the water soluble, yellow tetrazolium salt, 3-(4,5-dimethylthiazol-2-yl)-5-(3,4-diphenyl) tetrazolium bromide (MTT) is reduced into a water insoluble formazan salt by mitochondrial reductases (Mosman *et al.*, 1983). The purple formazan crystals can be dissolved in DMSO and the optical density of the resultant purple solution can be measured at 540nm using a Multiscan EX Microplate photometer (Thermo Scientific, Essex, UK).

Suspended cells were used to seed into sterile, flat-bottomed 96 well plates at a density of 1×10^4 cells/well. The culture was incubated at standard conditions for 24h. Before finishing the incubation period, stock solutions of 10µg/mL of recombinant, commercial (RTAC, gelonin) proteins and/or cRTBC chains were added (as either separate A and B chains, re-folded A and B chains or mixed A and B chains as dictated by the experiment) in respective media for both Vero and B16 cells. From the stock solutions, serial dilutions were made to make required concentrations of proteins solutions (1µg to 10ng) in cell culture media with 1mL final volume. Here two protocols were followed depending on the specific requirement of the experiment. In first one, after the incubation period (24h), the media was replaced with 100µL of prepared stock solutions, except in control wells (rows 6 and 7). Then the cells were incubated for defined period (48h). In second protocol, after applying specific concentrations of proteins alone or with polymers in to the wells, they incubated for defined period (24h, 48h and 72h), depending on the experiment requirement. The MTT stock solution was prepared by dissolving 250mg of MTT reagent in 50mL of 1xPBS buffer, which was sterilized by passing it through a 0.22µm filter (Corning®, Germany). After the

incubation period, MTT reagent (10 μ L (50 μ g)) was added to the each well and left under standard incubation conditions for 4h. After the incubation time, the media was removed and 100 μ L of dimethyl sulfoxide (DMSO) was added into each well and cells were incubated at room temperature for 30minutes. The plates were read at 540nm using a microtiter plate reader. The results were expressed as viability (%) (\pm Standard error of the mean (SEM)) against protein (*i.e.* RTAC equivalent) or polymer concentration.

For positive and negative controls PEI and dextran were used. The same protocol was followed as above with 72h incubation time. In analysis of PAA polymer toxicity, the seeding of cells was performed as above. 1st and 12th wells were treated as controls. From the sterile polymer stock solution, required concentrations of polymer solutions were made by serial dilutions (from 2mg/mL to 100ng/mL) in Eppendorf tube with 1mL final volume. After 24h of incubation, media was removed from the wells (2nd to 10th) and suitable concentrations of polymer solutions applied into the wells in 100 μ L volume. Cells were incubated for specified time (48 or 72h). After the incubation, MTT assay was performed as above.

2.2.11 Re-association of ricin A and B chains

To 200 μ L of agarose beads, 10 μ g of cRTBC and 20 μ g of cRTAC (or 50 μ g of rRTAC (clone189)) along with BME (with final concentration of 2%) were added and left at 4°C for 20minutes. After the incubation, the whole sample was transferred into the column and flow through was collected and applied onto the column and the same was repeated two more times. Then beads were washed three times (1mL each time) with 1xPBS. The re-associated, cRTBC-cRTAC was eluted by using 75mM galactose solution (10 x 500 μ L). The Bradford assay was used to identify the fractions containing detectable protein, which were pooled into sterile Eppendorf tube. The re-associated protein was then dialysed using 4000mL of 1xPBS for 4h (with gentle mixing using magnetic flea) and it was repeated one more time. After the dialysis, re-associated RTAC-RTBC was filter sterilized using a 0.22 μ m sterile filter and the protein concentration determined again using by using Western blotting.

2.2.12 Sub-cellular fractionation

Vero cells were seeded into two 150mm² plates at a density of 5x10⁶ cells in 15mL of culture media and culture was incubated using standard conditions for 24h. After the incubation period the media was discarded and the cells were washed three times with PBS (10mL each

time). The RTAC and RTBC protein mix was added to 9mL of media. From this preparation, 5mL was added onto the cells in each plate and the culture was incubated at standard conditions for 1h. After the incubation period 10mL of complete media was added to the cells in each plate and cultures were incubated at standard conditions for 3h. After the incubation, the media was discarded and the cells were washed three times with chilled 1xPBS (10mL each time) and in the last wash PBS was completely removed from the plates. A Complete EDTA-free Protease inhibitor cocktail (PI) tablet (Roche, Burgess Hill, UK) was dissolved into 1mL PBS, giving a stock solution of 50x. To the first plate 250 μ L of PI was added and gently spread all over the cells which were scraped and disrupted using a sterile disposable cell scraper (rubber policeman) (Fisher Scientific, Loughborough, UK). The cell homogenate was then transferred into the second plate. Cells were scraped and the cell homogenate transferred into an Eppendorf tube. This process was then repeated using 200 μ L of above stock solution of PI and the cell homogenates pooled prior to lysed by sheer stress through being passed 10 times through a 21 gauge needle. The lysed cells were centrifuged at 2000 x g (rcf) for 2minutes to remove intact cells and nuclei. The pellet was then re-suspended in 100mL of the supernatant and subject to a second round of lysis again using 10 passes through a 21 gauge needle. The lysate was then centrifuged at 4000 x g (rcf) for 2 minutes at 4°C. The pooled supernatants was transferred into ultracentrifugation vials (Hitachi Koki, Japan) and subject to 200 000 x g (rcf) for 2h at 4°C (Micro-ultra centrifuge, Thermo Scientific, Essex, UK). The resulting supernatant was collected and subject to trichloroacetic acid (TCA) precipitation (section 2.2.13) and dissolved in 100 μ L of LSB and 20 μ L of BME. The pellet from the centrifugation step was dissolved in the same volume of LSB and BME and stored at -20°C prior to analysis by SDS-PAGE and Western blotting.

2.2.13 Trichloroacetic acid (TCA) protein precipitation

In a 1.5mL Eppendorf tube, 1mL of protein solution and 250 μ L of TCA (100% (w/v)) was added (1:4 ratio) and incubated for 10minutes at 4°C. After the incubation, it was centrifuged at 14000rpm for 5minutes. The supernatant was discarded and the resultant pellet was washed with 200 μ L of cold acetone and centrifuged at 14000rpm for 5minutes. The acetone was then removed by careful pipetting. The washing step was repeated 2 more times. Finally, the pellet was dried by keeping it in 95°C heat block for 5-10minutes to drive off acetone. The resultant pellet was dissolved in 80 μ L of LSB and 20 μ L of BME and stored the sample at 20°C, for further use.

2.2.14 Fluorescence microscopy

In Fluorescence microscopy imaging, 3 basic steps were involved: (i) The preparation of cells (ii) Cell treatment and (iii) Fixation.

The preparation of cells: At first, under the class II hood, a coverslip (22mm x 22mm x 0.5mm) was submerged in absolute ethanol and it was taking out of the ethanol with using mico-forceps and was ignited with burner. During the ignition, care was taken not to ignite the ethanol reservoir. Sterile cover slip was placed into a sterile 6 well TC coated plate or a 35mm diameter sterile TC coated dish.

Vero cells were detached (section 2.2.10) and suspended in complete media. In each well, Vero cells were applied at the density of 1×10^5 cells per well and the final volume of the media in each well was then adjusted to 2mL. Then cells left in cell culture incubator for 24h at standard incubation conditions (37°C, 5% (v/v) CO₂)

After the incubation period, media was removed and cells were washed three times with sterile 1xPBS. Fresh media was applied into each well.

Adding protein to the cells: To the first two wells, 50µg of protein (rRTBC and cRTBC in individual wells) was added and 6 well plate was placed back in the incubator. After 20 minutes, 50µg of protein was added into next two wells and it was repeated after 10minutes. Culture was placed back into the incubator and incubated for 10minutes at standard conditions.

Aldehyde fixation: The medium was removed from all the 6 wells. Cells were washed three times with 1xPBS and 2mL of 2% (w/v) paraformaldehyde solution (in 1xPBS) was added into each well. Cultures incubated at room temperature for 20minutes. After the incubation, paraformaldehyde was discarded and cell monolayer was washed three times with 1xPBS. Then Triton extraction buffer was added into each well and incubated with the cells for 5minutes at room temperature. After the incubation, the Triton buffer was discarded and the cell monolayer washed with 1xPBS three times. Blocking non-specific antibody binding was achieved by adding 1mL of blocking buffer to cell monolayer prior to being left at room temperature for 1h.

Primary antibody hybridisation: In a sealable container, a damp paper towel was placed under a strip of Parafilm™. The primary antibody was diluted using 1xPBS containing 1% (v/v) FBS at the required ratio (table 2.2), and 40µL was transferred onto the Parafilm™. The

cover slips from the wells were taken and placed face down on to the primary antibody mix, ensuring the antibody was in contact with the cells. After documenting which cell had received which immuno-stain, the hybridization was left for 1h at room temperature. Cells were washed three times with 1xPBS (approximately 3mL /well) at room temperature.

Secondary antibody hybridisation: Specific dilutions of secondary antibody (typically 1:100) were made in 1xPBS containing 1% (v/v) FBS and cells were hybridised as above, using a hybridisation time of 30-45minutes (in dark). Cells were washed 3 times with 1xPBS as before.

Mounting cover slips: On a glass slide 30 μ L of mounting media was placed. The cover slip was then gently placed on top of mounting media and gentle but firm pressure was applied to remove the excess mounting media. Care was taken to avoid sheer forces and disrupting the cells. Excess media was removed with paper towel and the cover slip was sealed with nail varnish. The slides were stored at -20 $^{\circ}$ C prior to analysis. The cells were imaged using Nikon 90i overhead epifluorescence microscope, attached to a Nikon Digital Camera (DS-Qi1Nc) and a computer running Nikon NIS Elements Advanced Research software. The objective used in imaging was an oil immersion CFI Plan Apochromat VC 60XN2 (NA 1.4 WD 0.13mm).

Aldehyde fixation for polymers: Preparation of cell cultures was performed as above. After the 24h incubation time, the medium was removed from the wells and cells were washed three times with 1xPBS. Then, 0.5mL of bovine serum albumin-Texas Red (BSA-TxR) (10mg/mL) or Texas Red-conjugated Wheat germ agglutinin (WGA-TxR) (10-20 μ g/mL) (Invitrogen, Paisley UK) was added to each of the 6 wells. In the first two wells, two polymers (ISA1-FITC and ISA23-FITC) were added into separate wells (2mg/mL) and left the cells at 37 $^{\circ}$ C for 4h. After the incubation, cells were washed three times with 1xPBS and 2mL of media with leupeptin (final concentration: 200 μ M) was added and incubated cells at standard culture conditions. Next day, after 20h of incubation, in the next two wells, the media was removed and cells were washed three times with 1xPBS. The two polymers (ISA1-FITC and ISA23-FITC) were added separately (2mg/mL) and cells were left at 37 $^{\circ}$ C for incubation. After 3h, the same procedure was repeated for last two wells and left cells at standard culture conditions.

The medium was removed from all the 6 wells and cells were washed three times with 1xPBS. Then 2mL of 2% (w/v) paraformaldehyde solution was added into each well.

Cultures incubated at room temperature for 20minutes. After the incubation, paraformaldehyde was discarded and cells were washed three times with 1xPBS. Blocking solution (2mL) applied into each well and incubated for 2-3minutes. After the incubation, cells were washed thrice with 1xPBS. Mounted the cover slips as described above. Here Triton extraction was not used.

2.2.15 Live cell imaging

Preparation of cells in sterile 35mm² TC treated dishes (at cell density of 1x10⁵ cells/well) was performed as described above (section 2.2.14), except that in this experiment, no cover slip was placed inside the dish. After 24h of incubation at standard incubation conditions, cell monolayer was washed three times with sterile 1xPBS. WGA-TxR (20µg/mL) and polymer (either ISA1-FITC or ISA23-FITC) with final concentration of 2mg/mL along with leupeptin (final concentration: 200µM) in 0.5mL volume, was added into the dish and incubated for 1h at standard incubation conditions. After the incubation, media was removed and the cell monolayer was washed three times with sterile 1xPBS. 2mL of RP media (pre-warmed to 37°C) containing 200µM of leupeptin was added into the dish. Live cell imaging was obtained using Nikon Eclipse Ti inverted microscope with a heated stage (set to 37°C) attached to a Nikon (DS-Fi1) digital camera connected to the Nikon NIS Elements Advanced Research Software. The objective used for imaging was a CFI Super Plan Flour 20X (dry). The temperature was maintained through out the experiment. Once the region of interest in the cell monolayer was selected using phase contrast microscopy (using appropriate fluorescent channels), images were taken every 10minutes over 4h. Alternatively, the time and required fluorophore channels (FITC and TxR) can be set and images were automatically captured at selected time intervals using the software provided by Nikon. After completing the imaging process, the data was exported as an avi file and edited in final cut studio (Apple Computing Ltd. Cupertino, USA).

Chapter 3
**Expression, Purification and Characterisation of Ricin Toxin
Constructs**

3.1 Introduction

Several plants (*Ricinus communis*, *Gelonium multiflorum*) and bacteria (*Shigella dysenteriae*, *Vibrio cholerae*) harbour virulence factors (producing protein toxins) that act on other cells with lethal effects. This helps increase the chance of survival and proliferation of the toxin-producing organism, by providing a competitive advantage favouring the host (Odumosu *et al.*, 2010). One of the distinctive properties of the aforementioned toxins is that they are exquisitely specific in their action and some have evolved to traverse cell membranes in order to reach specific targets inside the cell. Toxins such as ricin toxin (RT) and shiga toxin (ST) reach the cytosol and target ribosomes to disrupt protein synthesis (Sandvig and van Deurs, 2002). When attenuated, such toxins may be used to deliver biological macromolecules to the inside (cytosol) of the cell (Smith *et al.*, 2003). Even though there are currently viral vectors (section 1.3.1) and non-viral vectors (section 1.3.2) in pre-clinical and clinical development (for gene delivery), both systems have their limitations (section 1.3).

Modern cell and molecular biology technologies such as recombinant PCR allow the introduction of specific mutations within the catalytic regions of toxic proteins (Ready *et al.*, 1991; Suvan and Hovde, 1998). This may be used to ablate intoxication whilst leaving the molecular architecture necessary for cytosolic translocation intact.

Ricin is a heterodimeric, ribosome inactivating protein, obtained from seeds of castor oil plant (*Ricinus communis*) (Audi *et al.*, 2005). RTAC demonstrates catalytic activity and is responsible for inhibiting protein synthesis in mammalian cells. RTBC is essentially lectinic, binding to surface carbohydrates, facilitating endocytosis and the intracellular trafficking of the holotoxin (Olsnes and Kozlov, 2001). To render RTAC non-toxic, two residues (Glu¹⁷⁷ and Arg¹⁸⁰) have been identified as being critical to the process of ribosome depurination (Schlossman *et al.*, 1989; Frankel *et al.*, 1990; Ready *et al.*, 1991) and were either altered (to Gly) or deleted, with a significant amount of flanking sequence. Consequently three types of RTAC constructs have been generated. The first contains multiple mutations where amino acids 177-182 have been changed to Gly. The second type of RTAC construct has been subject to a sequence deletion resulting in the absence of amino acids 177-182 and the third construct was unchanged (equivalent to wild type RTAC). Epitopes such as: V5, 6His, HA, GST-GFP and a KDEL motif were also introduced as described (table 1.7).

To produce recombinant proteins, several host systems are available such as bacteria, yeast, insects and mammalian cells. An *E.coli* expression system was chosen in this instance as this bacterium has been well characterised and can grow very quickly to a high cell density using

inexpensive media. Additionally, there is the availability of large number of cloning vectors and mutant host strains (Baneyx, 1999).

Here, the expression of sub-cloned, recombinant genes was performed in *E.coli* BL21*DE3. *E.coli* BL21*DE3 contains the lambda DE3 lysogen, which carries the gene for T7 RNA polymerase under the control of the *lacUV5* promoter (Studier and Moffatt, 1986). Consequently, when isopropyl β -D-1-thiogalactopyranoside (IPTG) is added to a culture of *E.coli* BL21*DE3 containing a pET151/D-TOPO vector (encoding the gene of interest sub-cloned in frame with the *lacUV5* promoter), IPTG will induce the expression of T7 RNA polymerase. This will result in an increase in the intracellular concentration of T7 RNA polymerase, which, when it reaches a sufficient level, will bind to the T7 promoter and initiate the transcription of the gene of interest (Donovan *et al* 1996). Expressed proteins were purified by affinity chromatography (section 2.2.5.4) and they were further characterised by SDS-PAGE (section 2.2.6), Western blotting and immuno-detection (section 2.2.7).

3.2 Materials and methods

Plasmid characterisation

Isolation of plasmids from overnight bacterial cultures (mini-prep)

Here the pET151/D-TOPO vector (low copy number) from Invitrogen (Paisley, UK) was used (Rosenberg *et al.*, 1987; Studier *et al.*, 1990). For plasmid maintenance and storage, the *E.coli* TOP10 strain was used, as it does not contain T7 RNA polymerase encoding gene, limiting the possibility of expressing any potentially toxic genes sub-cloned into the pET151/D-TOPO vector. To isolate 1-5 μ g of plasmid, a saturated, overnight bacterial culture containing the selected plasmid was prepared and the plasmid isolated using a “Miniprep Kit” (Qiagen, West Sussex, UK) as described in methods section (section 2.2.2).

Storage of bacterial cultures harbouring plasmid constructs

Extended long-term storage of bacterial cultures was facilitated by freezing a bacterial culture suspended in 2xYT containing 7% (v/v) DMSO at -80°C.

Agarose gel electrophoresis

Was used to analyse the purity and to estimate the molecular weight of the isolated plasmid DNA. Using this method, it was theoretically possible to separate nucleic acids from 20base

pairs to 20kilo base pairs in size. The preparation of the agarose gel matrix, the gel running conditions (*i.e.* time and voltage) and the visualisation of the DNA were documented in section 2.2.4

Sodium dodecyl sulphate polyacrylamide gel electrophoresis (SDS-PAGE)

The protocol for preparing acrylamide gel and electrophoretic separation of purified proteins was described in section 2.2.6. After electrophoresis, proteins were stained using Coomassie brilliant blue R-250 (section 2.2.6). Coomassie staining was a useful method for the identification of the protein of interest (relative to stained molecular weight markers). Even though Coomassie staining is not specific, this method of detection gave a semi-quantitative estimation of the quantity of a protein concentration in a cell lysate (or affinity enriched fraction).

Western blotting

A complete protocol for Western blotting and immune-detection was described in section 2.2.7. With the exception of a few experiments at the beginning of this investigation, X-ray films were used for immuno-blotting detection. This protocol was adopted in preference to the use of a CCD camera (EpiChemi Bio Imaging system (UVP), Cambridge, UK), which was found to be 3-4 orders of magnitude less sensitive than secondary antibody detection using ECL and X-ray film.

Monitoring protein expression via bacterial mini-induction

Before producing a recombinant protein using litre quantities of culture, the optimal conditions necessary to achieve a high yield of the protein were determined on a millilitre scale (1.5mL) using “mini-induction” experiments. A comparison of protein yield after growth using a variety of culture conditions was conducted using immuno-blotting. The parameters investigated were: pre-induction growth time, IPTG concentration, post-induction growth time and temperature. The procedure for mini-induction was described in section 2.2.9.

Densitometry as a tool to evaluate protein concentration

Densitometry was used to assess the concentration of an unknown protein either in a SDS-PAGE gel or after detection by immuno-blotting by comparing its pixel density with a known

amount of protein (using ImageJ software (NIH) (<http://rsbweb.nih.gov/ij/>)). Known amounts (0.5µg, 1µg and 2µg) of BSA were loaded onto a 10%(w/v) SDS-PAGE gel, as well as 5µL, 10µL and 20µL of protein sample. After separation of protein, the gel was stained with Coomassie brilliant blue R-250 (2h with gentle shaking) and de-stained (section 2.2.6). The gel was dried using gel-drying kit as specified by manufacture instructions (Promega, Hampshire, UK). The gel was then digitised and saved in TIFF (Tagged image file format) format. The calibrants were then checked to ensure they maintained a linear relationship and that the sample was within this range. A summation of pixel density was then performed for each region of interest (*i.e.* band) and protein concentration was calculated relative to the calibrants using a calibration curve.

3.3 Results

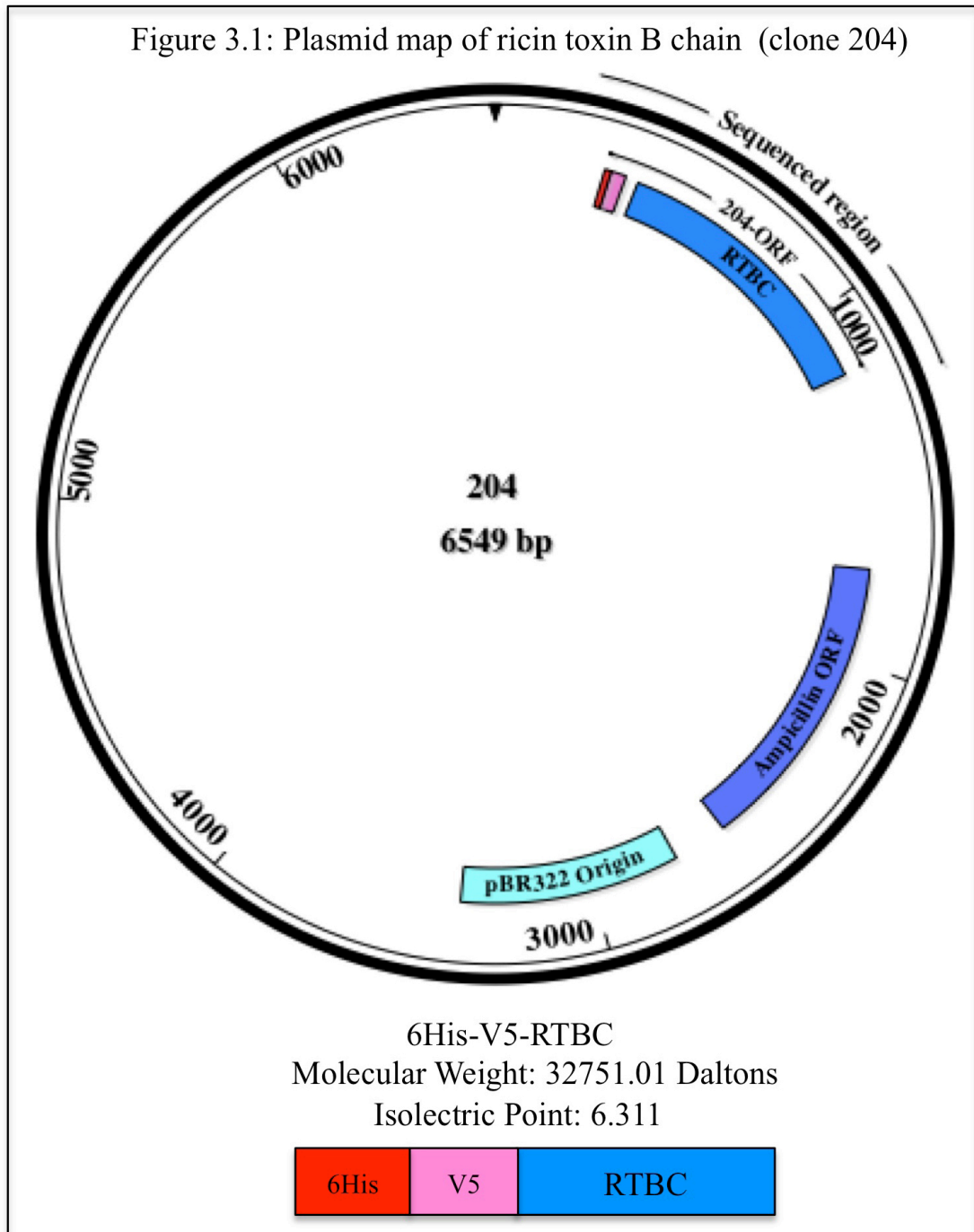
3.3.1 Characterisation of plasmid constructs

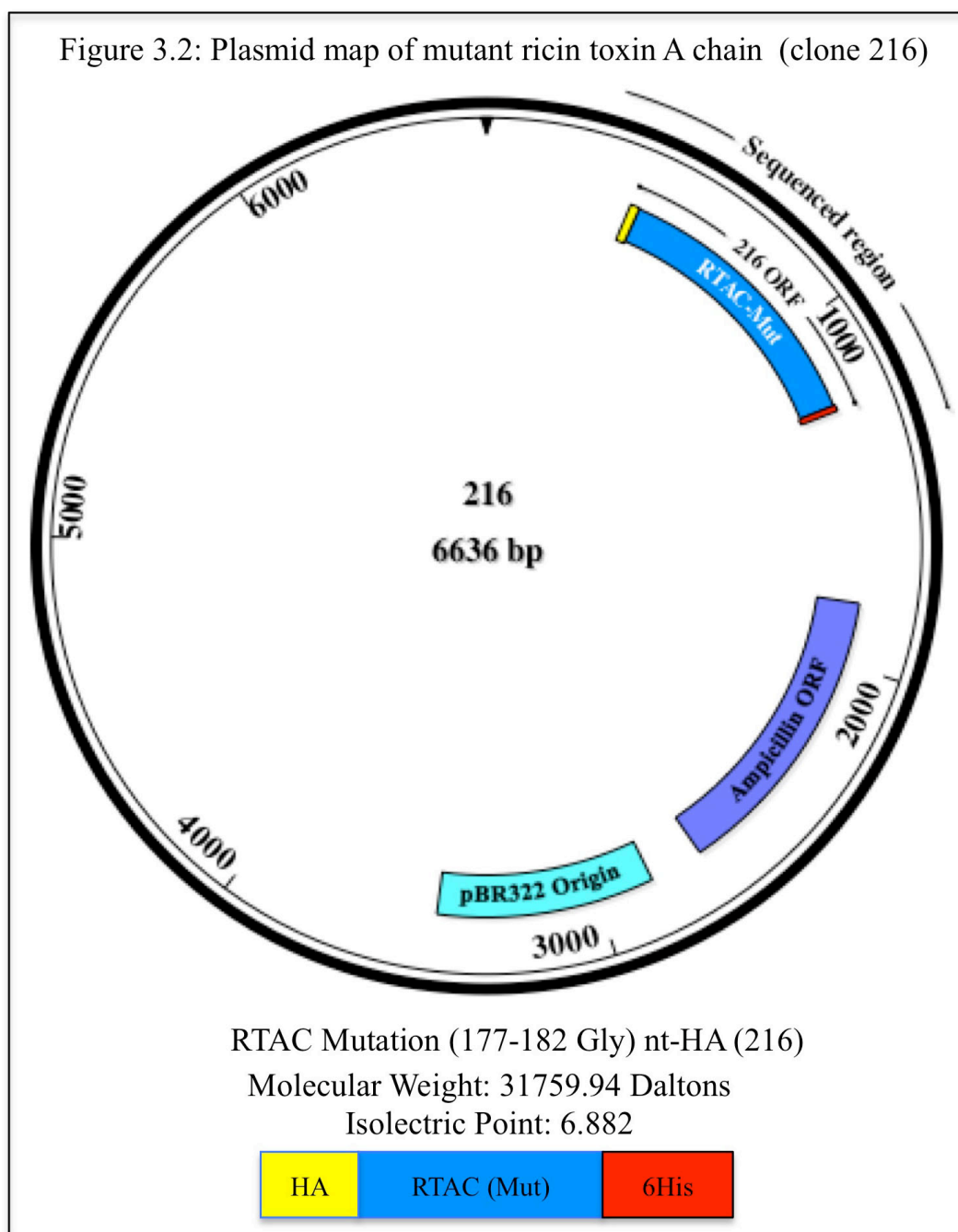
In order to begin to characterise the materials (plasmids) generated at the University of Iowa, the sequence data from The University of Iowa DNA facility (<http://dna-9.int-med.uiowa.edu/>) was first assembled into contiguous fragments, annotated and assembled with the published vector sequence (*i.e.* pET151/D-TOPO) using the SeqMan module, part of the LaserGene DNA analysis suite (DNASar, Madison WI, USA). The consensus sequence exported from SeqMan was then imported into the SeqBuilder module (also part of the LaserGene software suit) where it was manipulated *in silico* and used to draw maps of the plasmids generated (figures 3.1 to 3.7).

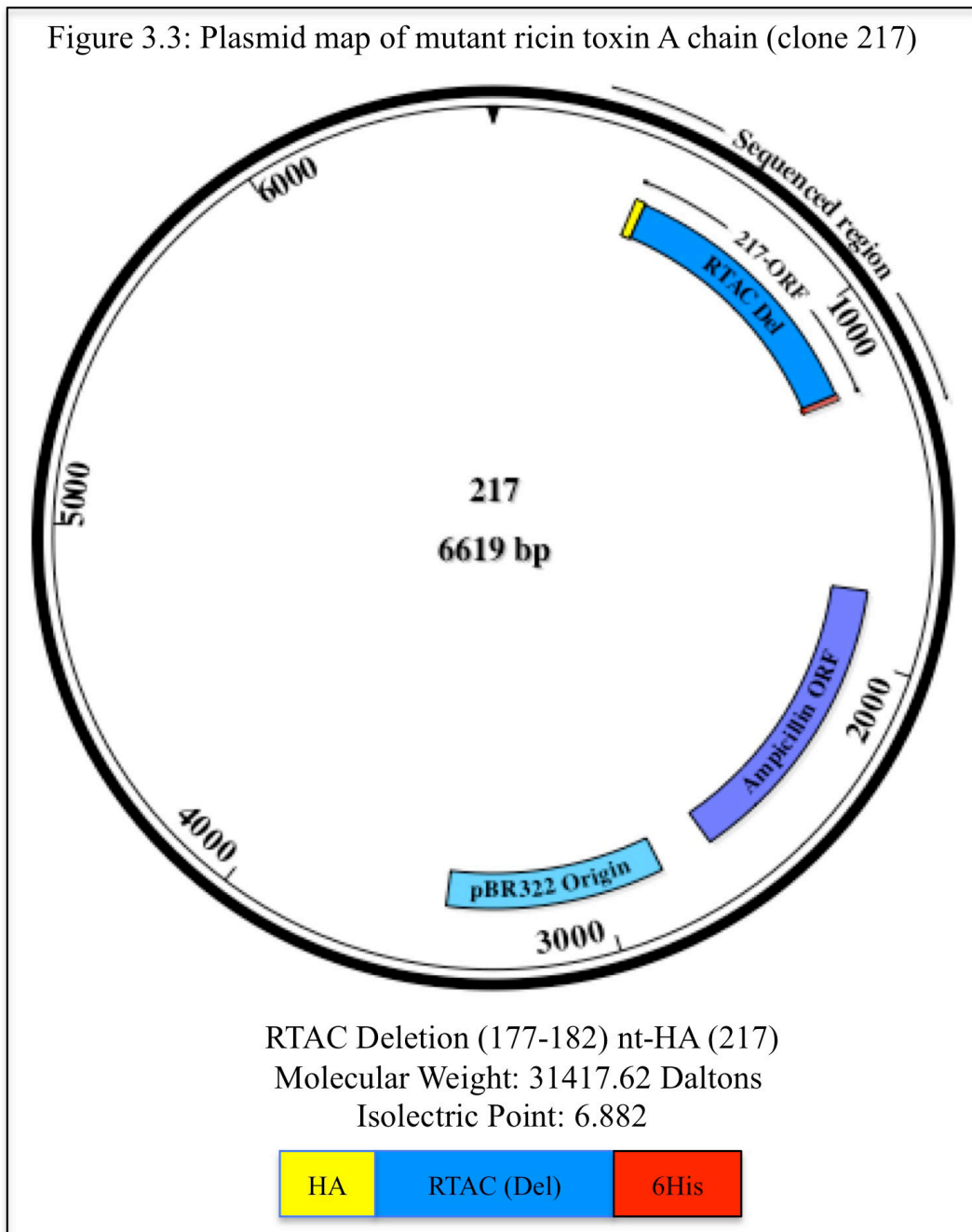
3.3.1.1 Plasmid maps

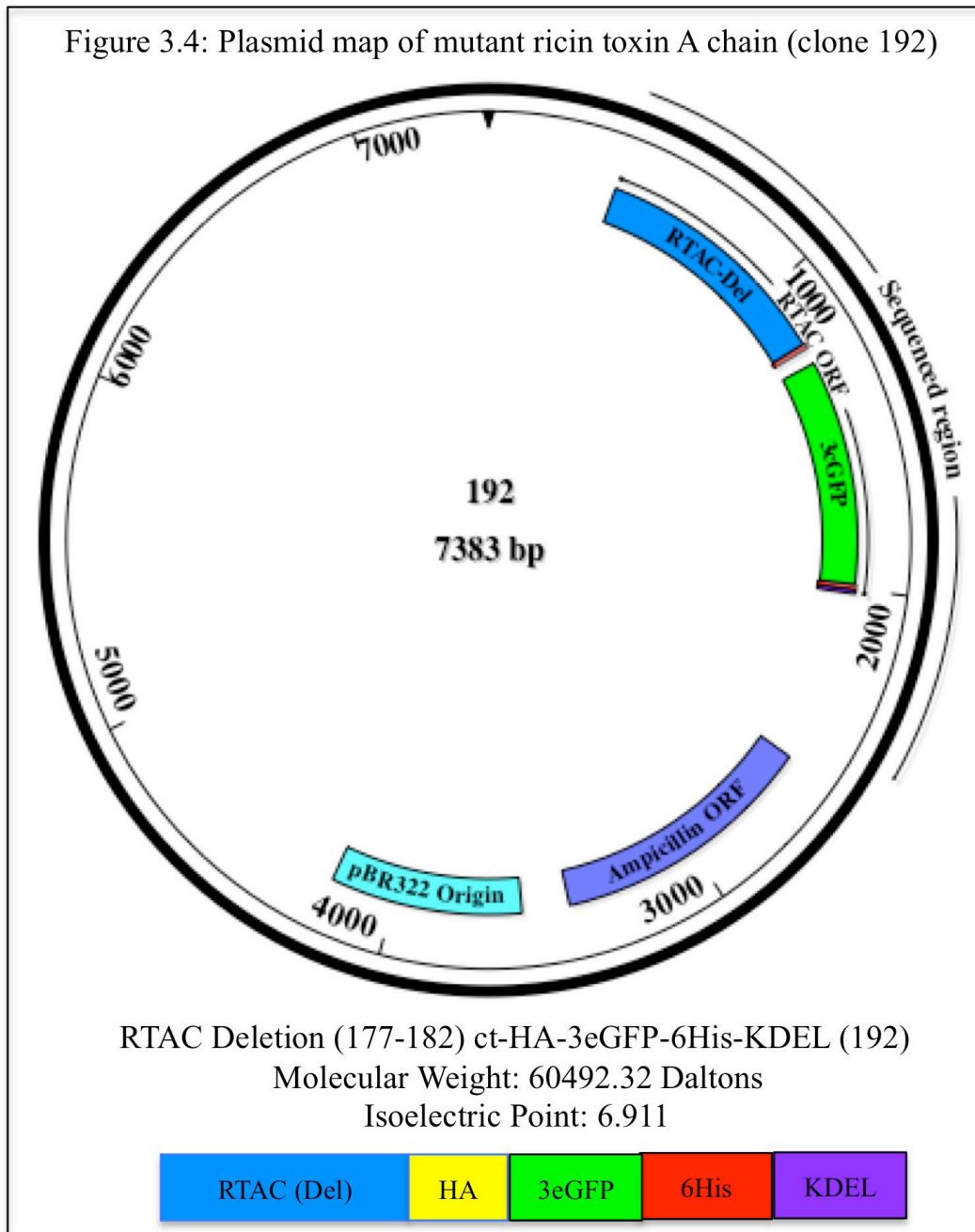
The oligonucleotides used to sequence the plasmids are listed in table 2.2. From the plasmid maps, the domain structure, composition and molecular weight of the predicted, recombinant fusion protein constructs were documented in cartoon format. It was also possible to identify and plot the location of the epitopes incorporated into the amplifying oligonucleotides as well as specific markers within the plasmid constructs. The documentation of the results and efforts to map various plasmids generated in Iowa has been presented in figures 3.1-3.7. This is the first time the sequence data generated in Iowa has been assembled and annotated in this fashion. Having assembled the plasmid maps for all of the constructs under investigation herein, the plasmids were isolated and further characterised empirically. Initially, this was

performed by agarose gel electrophoresis (*N.B.* restriction sites have been omitted from the plasmid maps in the interests of clarity and can be provided as required).









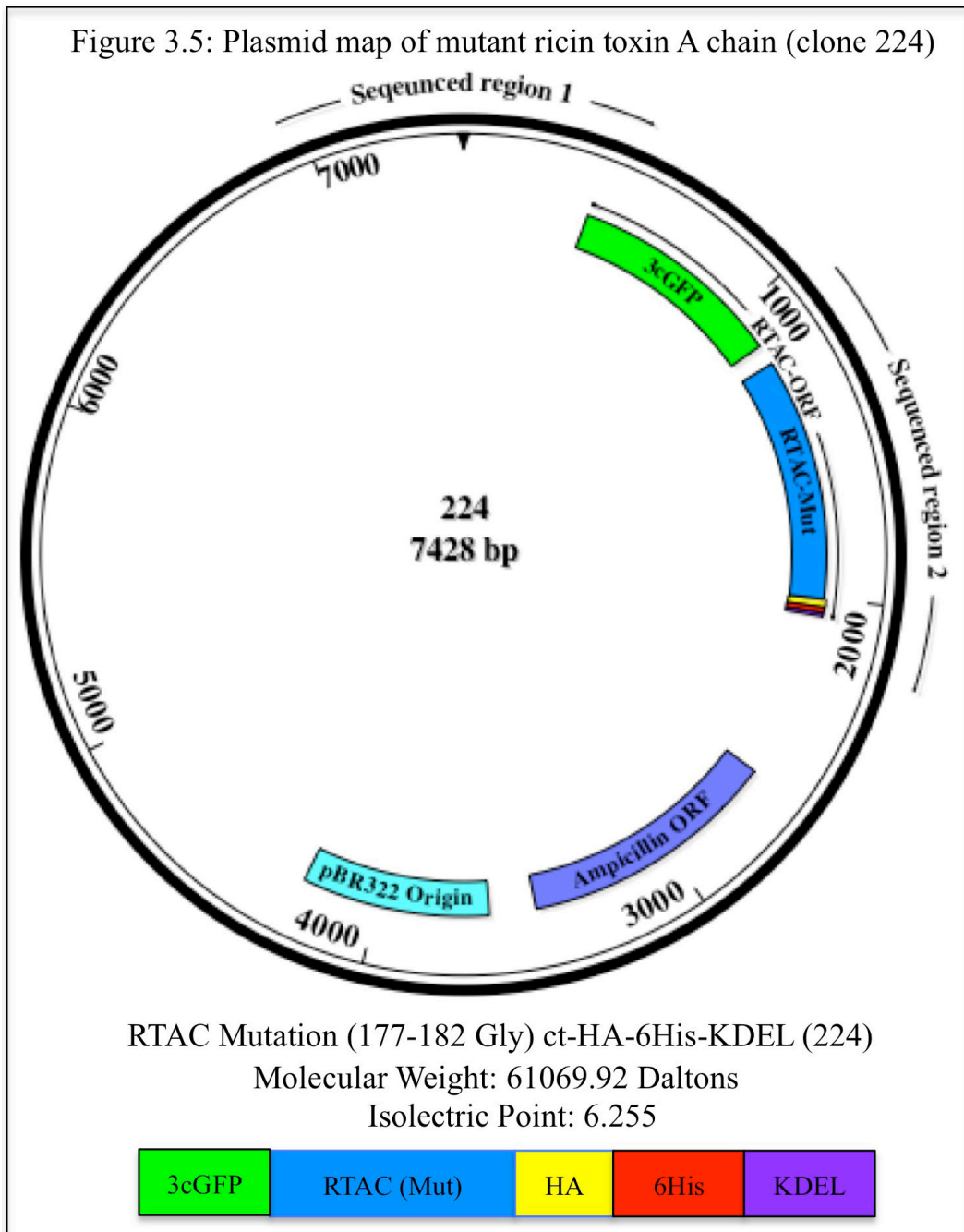
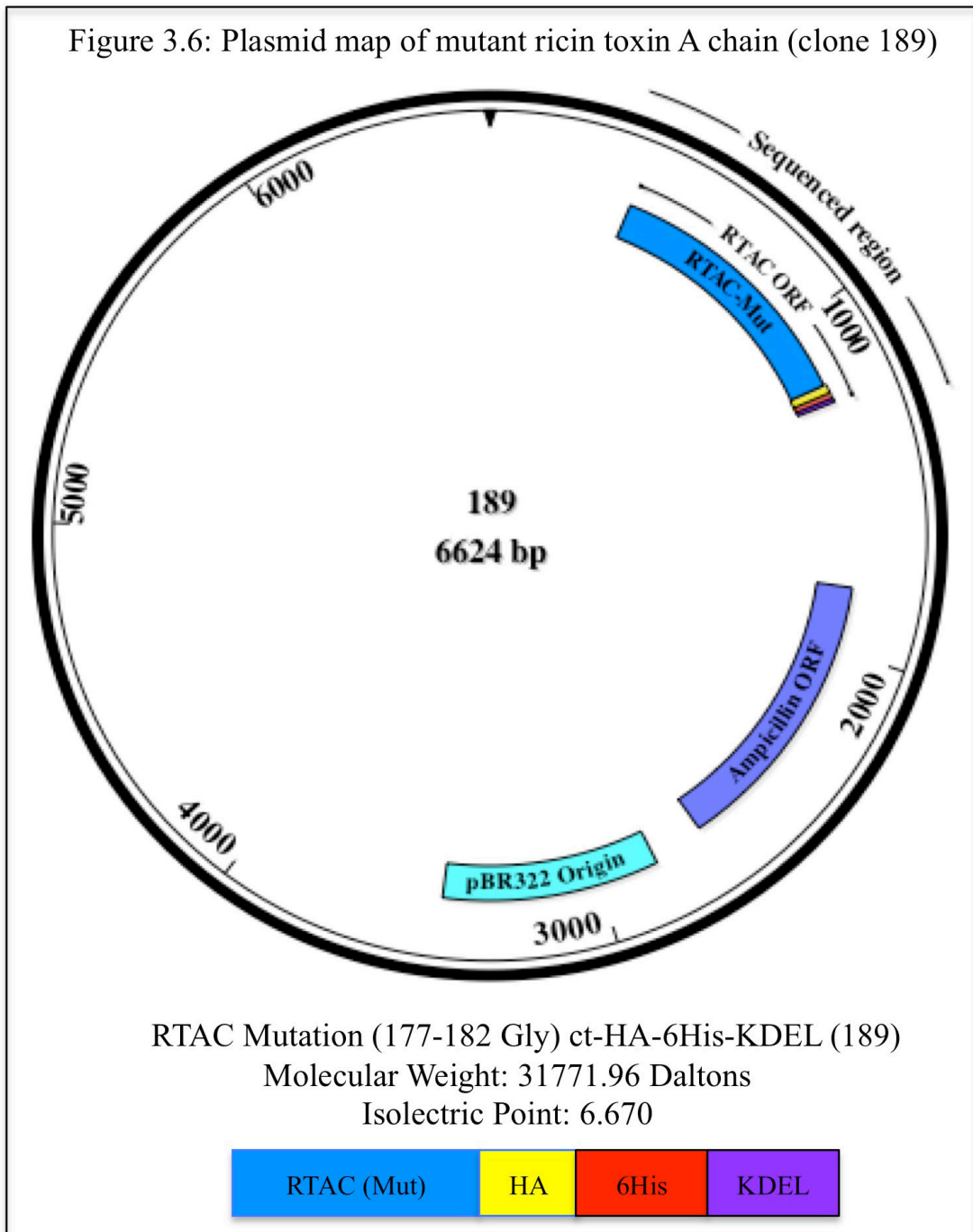
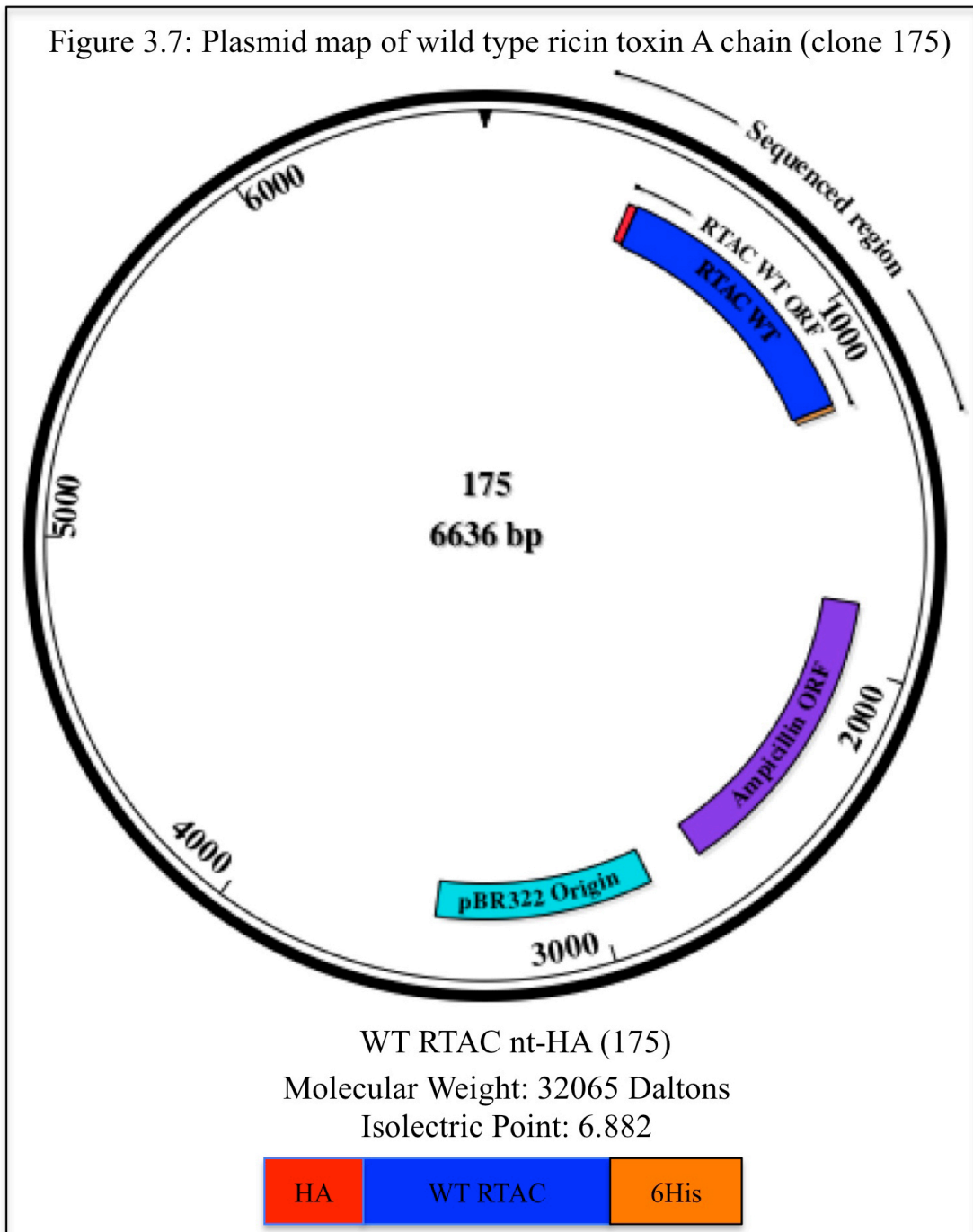


Figure 3.6: Plasmid map of mutant ricin toxin A chain (clone 189)





3.3.1.2 Maintenance and isolation of plasmids

Plasmids were stored and maintained in *E.coli* TOP10 bacteria, which, by design cannot express genes under the regulation of the T7 promoter system within the pET151/D-TOPO plasmid expression system. The *E.coli* BL21*DE3 strain was not suitable for propagation and maintenance of the plasmid, as it contained T7 RNA polymerase which, even at a basal level, may result in gene expression in the absence of the inducer, IPTG (Studier and Moffatt, 1986). This phenomenon is known as promoter leakage (Tegel *et al.*, 2011). In addition, depletion of low abundance tRNAs, critical to protein synthesis necessitates the frequent re-transformation of fresh stocks of *E.coli* BL21*DE3.

Miniprep was performed using the over night incubated, saturated, 10mL, fresh cultures of *E.coli* TOP10 containing the plasmid under investigation (section 2.2.2). The yield of plasmids obtained from bacterial cultures harbouring the plasmids detailed herein, are given in table 3.1 (below).

Table 3.1: Miniprep yields of selected plasmid constructs

Clone number	Description	Yield of plasmid DNA (from 5mL over night culture)	Strain
204	RTBC-V5-6His	5.2 µg	TOP 10 <i>E.coli</i>
216	HA-RTAC (Mut)-6His	4.75 µg	TOP 10 <i>E.coli</i>
217	HA-RTAC (Del)-6His	5.2 µg	TOP 10 <i>E.coli</i>
192	RTAC (Del)-ct-HA-3eGFP-6His-KDEL	5.4 µg	TOP 10 <i>E.coli</i>
224	eGFP-RTAC (Mut)-ct-HA-6His-KDEL	5.7 µg	TOP 10 <i>E.coli</i>
189	RTAC (Mut)-ct-HA-6His-KDEL	4.32µg	TOP 10 <i>E.coli</i>
175	HA-WT RTAC-6His	4µg	TOP 10 <i>E.coli</i>

3.3.1.3 Agarose gel electrophoresis of purified plasmid DNA

The results of the agarose gel electrophoresis of selected plasmids were shown in figure 3.8 and it was noticed that plasmids were running in three forms. In general, plasmid DNA may adopt three conformations after electrophoretic separation, super helical circular form (form I), nicked circular (form II) and linear form (form III) (Sambrook *et al.*, 1989). Despite having the same molecular weight these conformations migrate at different rates through an agarose gel.

Bands were visible at the predicted molecular size (approximately at 7000bp, figure 3.8, table 3.2). It is likely that the observed bands (bands indicated with red arrow) correspond to the linear form of plasmid DNA. Below lighter bands may correspond to the nicked circular form (bands indicated with blue arrow) and bright lower bands may be in super-helical circular form (bands indicated with yellow arrow) of the plasmid. The majority of the DNA examined appears to be in the super-helical circular form indicating that the DNA has not been subject to substantial degradation. Since the super-helical circular form has compact shape, it migrates through the agarose gel faster than the linear form of the plasmid, though ethidium bromide intercalation may effect the rate of form II and form III plasmid migration relative to each other (Sambrook *et al.*, 1989).

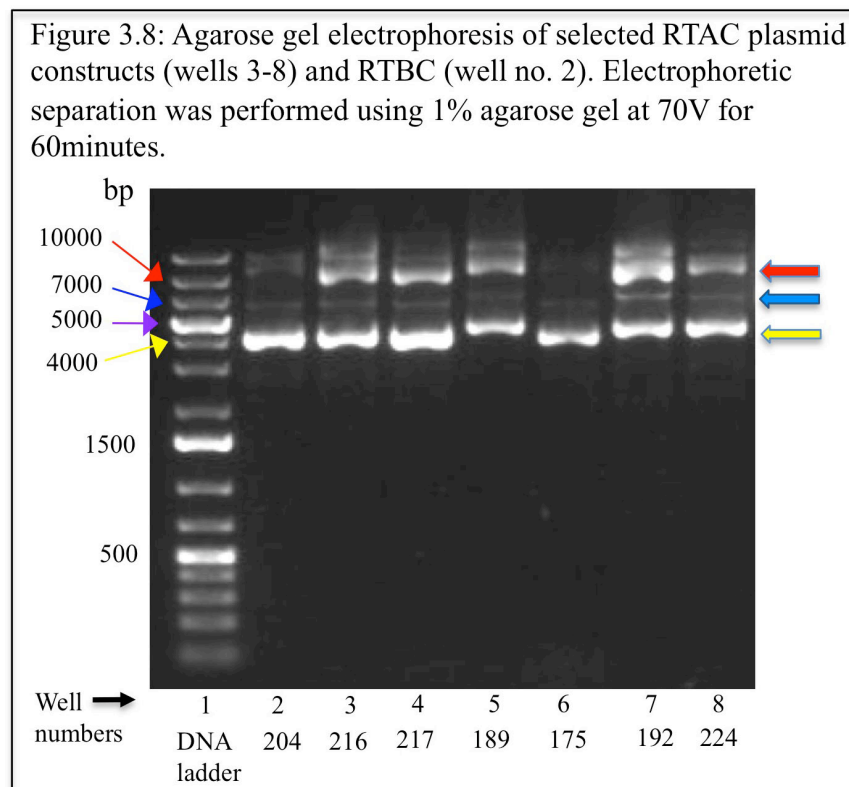


Table 3.2: Predicted size and M_w of evaluated plasmid constructs

Clone number	Description	Predicted size (bp)	M_w (kDa)
204	RTBC-V5-6His	6549	32.75
216	HA-RTAC (Mut)-6His	6636	31.75
217	HA-RTAC (Del)-6His	6619	31.41
192	RTAC (Del)-ct-HA-3eGFP-6His-KDEL	7383	60.49
224	eGFP-RTAC (Mut)-ct-HA-6His-KDEL	7428	61.06
189	RTAC (Mut)-ct-HA-6His-KDEL	6624	31.77
175	HA-WT RTAC-6His	6636	32.06

3.3.2 Isolation of protein from 1000mL cultures

In order to isolate recombinant protein, the plasmid was isolated from the storage strain of *E. coli* Top10 and transformed into *E. coli* BL21*DE3. After characterising the plasmids, wild type RTAC (clone 175), rRTAC constructs (table 3.1) and rRTBC (clone 204) plasmids were separately transformed into *E. coli* BL21*DE3. As the plasmids had been well characterised, they were grown in 10mL of selective liquid media (2xYT containing ampicillin (200 μ g/mL) to saturation (overnight at 37°C, shaking at 200rpm).

These saturated cultures were used to inoculate 2000mL (2 x 1000mL) of 2xYT medium containing ampicillin (200 μ g/mL) (section 2.2.5). These cultures were grown at 37°C shaking at 200rpm utilising the optimum culture conditions (pre-induction growth time, IPTG concentration and post-induction time) determined by mini-induction experiments (sections 3.3.5) and also adopted from large-scale production of recombinant proteins. Even though the optimal conditions obtained herein (using mini-induction (1.5mL cultures)) may not translate to large-scale production (*i.e.* 1000+ mL cultures), they do give an indication of influence of the parameters examined on culture conditions and likely yield of protein. They also may help identify critical parameters.

Detergent-free bacterial lysis

After the bacteria harbouring the plasmid coding for the protein of interest had been grown and protein expression induced, the bacteria were subject to a further incubation period to allow protein expression (*i.e.* transcription and translation) to proceed. Following this the bacterial culture was harvested by sedimentation using a centrifuge. The bacterial cell suspension was harvested in 500mL aliquots subject to 6000 x g (rcf) at 4°C for 20minutes. The supernatant was discarded and the pellet re-suspended in 5mL of 1xPBS. Complete® EDTA free protease inhibitor cocktail was added to the re-suspended cells giving a final concentration of 5x. French pressing was performed (section 2.2.5.3) and sodium azide was added to a final concentration of 0.02% (w/v). The cell lysate was cleared by sedimentation, using an SS34 rota set to generate 20000 x g (rcf) for 20minutes at 4°C. The resulting supernatant was collected and 6His containing recombinant protein fractions obtained by affinity chromatography using Ni-Sepharose high performance (GE Healthcare Life Sciences, Buckinghamshire, UK) or TALON® Metal affinity resins (Clontech-Takara Bio Europe, Saint-Germain-en-Laye, France). A standard protocol was followed according to manufacturers instructions (section 2.2.5.4).

3.3.2.1 Affinity isolation/enrichment of recombinant proteins

The RTAC and RTBC construct contained 6His residues either N- or C-terminal to the RTAC or RTBC encoding region. As previously discussed (section 2.2.5.4) the 6His residues bind to Co^{2+} and Ni^{2+} ions. When high concentration of imidazole (100-150mM) solution applied onto the column the recombinant protein with 6His will be eluted from the column. After the purification of the protein by IMAC (section 2.2.5.4), fractions were collected and the Bradford assay (section 2.2.5.5) was performed to identify fractions containing protein. The fractions containing protein were mixed together and analysed by SDS-PAGE followed by Coomassie staining (A typical gel is shown. figure 3.9). The pooled fractions were subjected to dialysis against 4000mL of 1xPBS at 4°C for 2h. The 1xPBS dialysate was replaced with fresh 1xPBS and the dialysis was continued for 2 more hours under gentle mixing with the magnetic stirrer at 4°C, which brings the dilution of imidazole into picomole concentration range. At high concentrations (above 50mM) imidazole is toxic to cells (section 4.3.4).

The dialysed proteins were filter sterilised (using 0.2 μ m filters) and resolved using a 10% (w/v) SDS-PAGE gel. From the figure 3.9, it was observed that rRTAC proteins were detected at 32kDa (wells 2-7).

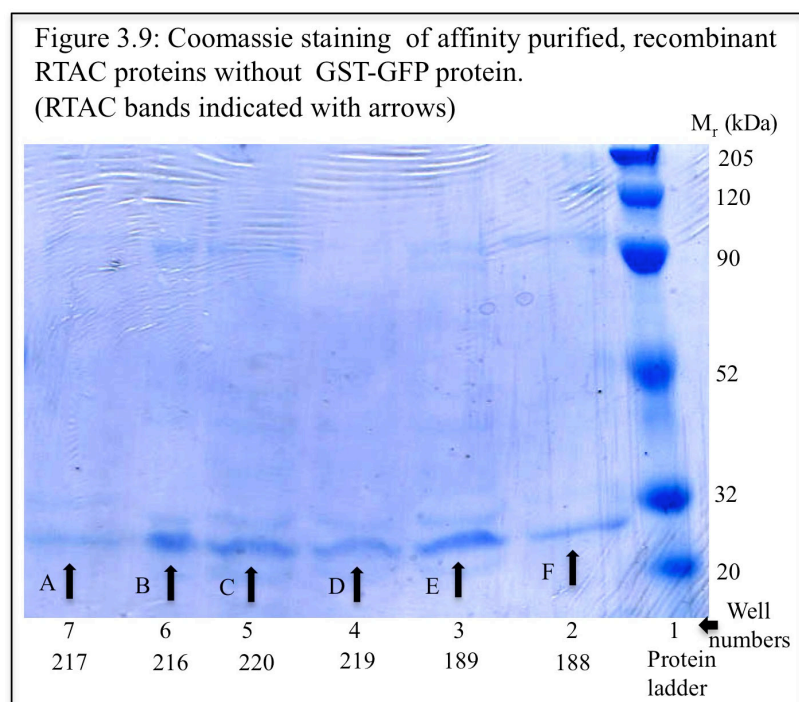
Table 3.3: RTAC plasmid constructs without GST-GFP

Clone number	Description
216	RTAC Mutation (Amino Acids 177-182 Gly) nt-HA
217	RTAC Deletion (Amino Acids 177-182) nt-HA
220	RTAC Deletion (Amino Acids 177-182) nt-HA KDEL
219	RTAC Mutation (Amino Acids 177-182 Gly) nt-HA KDEL
188	RTAC Deletion (Amino Acids 177-182) ct-HA KDEL
189	RTAC Mutation (Amino Acids 177-182) ct-HA 6H KDEL

More RTAC constructs were evaluated (table 3.4). From the figure 3.10, it was observed that GFP containing proteins were recorded with a molecular weight at 62kDa (wells 2-6).

Table 3.4: RTAC plasmid constructs with GST-GFP

213	RTAC Mutation (177-182 Gly) nt-GFP
224	RTAC Mutation (177-182 Gly) nt-GFP KDEL
192	RTAC Deletion (177-182) ct-eGFP KDEL
183	RTAC Mutation (177-182 Gly) ct-eGFP
182	RTAC Deletion (177-182) ct-eGFP



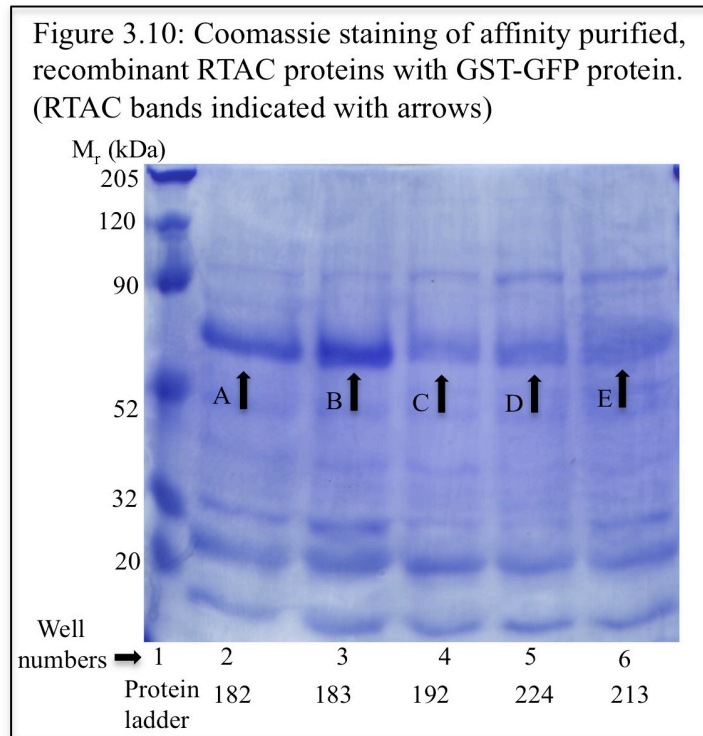
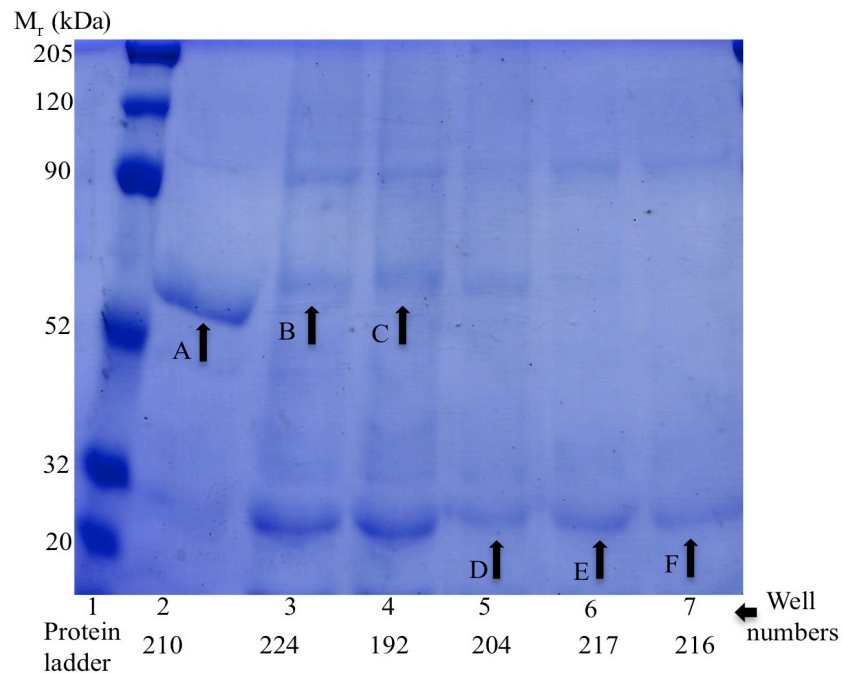


Figure 3.11 Coomassie staining of selected recombinant proteins purified by affinity chromatography. (GST-GFP, RTAC with GST-GFP detected above 52kDa (wells 2, 3 and 4), RTAC without GST-GFP seen below 32kDa (wells 5,6 and 7)).



Four RTAC constructs (table 3.3 and 3.4) as well as RTBC (clone 204) and a GST-GFP construct (clone 210) were selected for further evaluation. After expression and affinity enrichment, the recombinant proteins were identified on 10% (w/v) SDS-PAGE gel. From the figure 3.11, it was observed that, each protein was detected at the predicted molecular weight (predictions being made from an *in silico* interrogation of plasmid sequence information, table 3.2). Proteins bands of rRTAC proteins without GFP (clones 216 and clone 217) and rRTBC (clone 204) were detected at approximately 32kDa (monomers indicated with arrows D=204, E=217, F=216), figure 3.11; wells 5-7) and GFP containing RTAC proteins (clones 192, 224) and GST-GFP (clone 210) were detected at 62kDa (monomers indicated with arrows, A=210, B=224, C=192, figure 3.11, wells 2-4). From the above results, it can be concluded that RTAC, RTBC (clone 204) and GFP-GST (clone 210) constructs were expressed, purified by affinity chromatography and were detected at the predicted molecular weight after analysis by SDS-PAGE and Coomassie staining.

3.3.3 Protein detection

Wild type RTAC (clone 175) and rRTBC (clone 204) were produced and purified as described (section 3.3.2). The purified, dialysed and sterilised proteins were detected specifically by immuno-blotting.

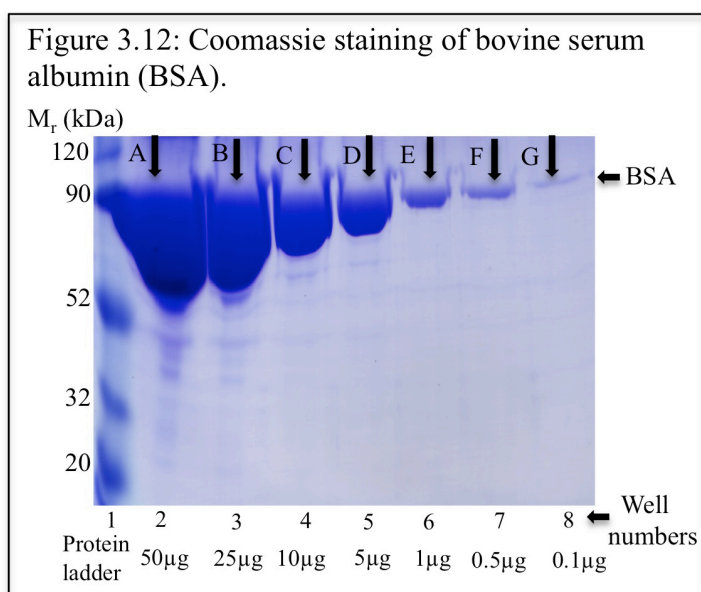
The detection of proteins by immuno-blotting required three steps:

- a). Separation of proteins by SDS-PAGE
- b). Transfer of proteins onto a solid phase support *i.e.* nitrocellulose membrane
- c). Immunological detection of proteins, usually in conjugation with ECL reagents.

a). Separation of proteins by SDS-PAGE

The first stage in establishing Western blotting as a reliable, reproducible methodology within the Richardson laboratory was to ensure the three areas identified above were all functioning. To put these controls in place, a model protein (bovine serum albumin (BSA)) was used. Initially, selected concentrations of BSA (0.1µg to 50µg) were resolved on a 10% (w/v) SDS-PAGE gel, which was then stained with Coomassie brilliant blue R-250 (section 2.2.6). It was of note that, after Coomassie staining, the BSA was overloaded and protein was running below 90kDa (figure 3.12, arrow A=50µg, B=25µg, C=10µg, D=5µg). In wells 6-8 (figure 3.12, arrow E, F and G) BSA was running at 90kDa. The predicted molecular weight of BSA is 66kDa however here it was documented with a higher apparent molecular weight, which may be attributable to BSA overloading. This overloading was deemed appropriate in

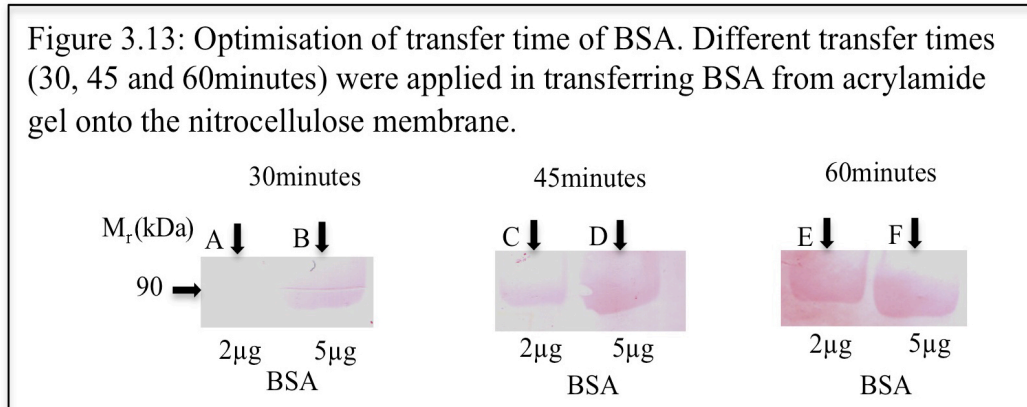
light of previous problems with signal to noise ratio (*i.e.* detecting proteins) and also in the interests of exploring the capacity of the SDS-PAGE gels to resolve a range of protein loading. Further, as the next phase of this investigation required the transfer of protein from the gel to a solid phase support, having protein at excess was considered useful in light of the possibility of incomplete or inefficient protein transfer or inefficient detection post-transfer.



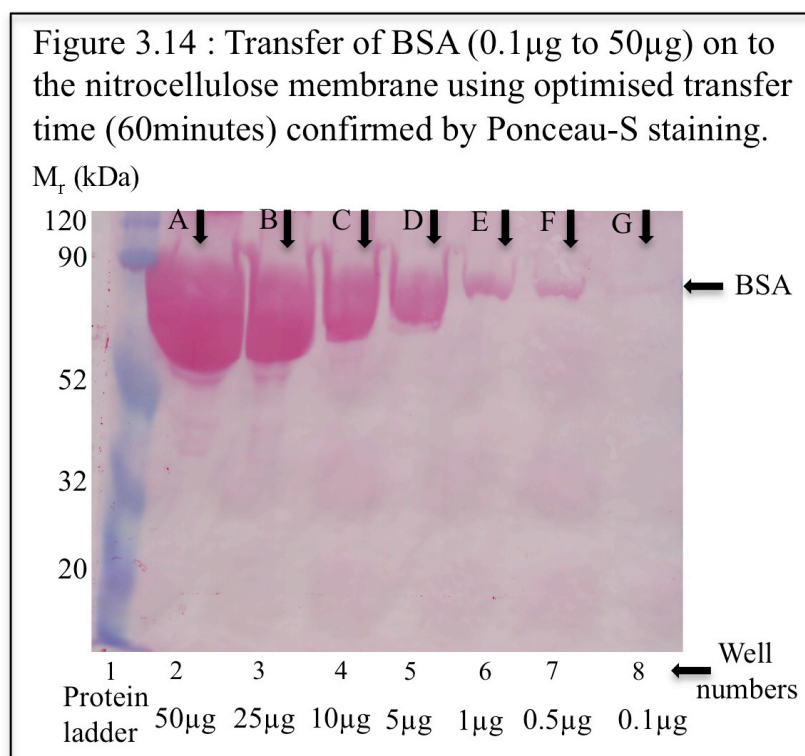
b). Optimisation of transfer time of BSA on to the nitrocellulose membrane

Using three identical 10%(w/v) SDS-PAGE gels, BSA was loaded into three separate wells each containing a final concentration of 0.5µg, 2µg and 5µg of BSA in each gel. After the resolution of the BSA on the gel, the transfer of BSA from the gel to the membrane was performed using three different time points (30minutes, 45minutes and 60minutes) using a mini-trans blot electrophoretic transfer cell (BioRad, Hemel Hempstead, UK) (Section 2.2.7) set at 400mA.

After the electrophoretic transfer of BSA onto the solid support (nitrocellulose membrane), the membrane was washed with water and was left in Ponceau-S solution for 120seconds (section 2.2.7). The membrane was then washed with distilled water and until stained BSA was visible. From the figure 3.13, it was clear that 60minutes transfer time was efficient in transferring the BSA from the gel onto the nitrocellulose membrane.

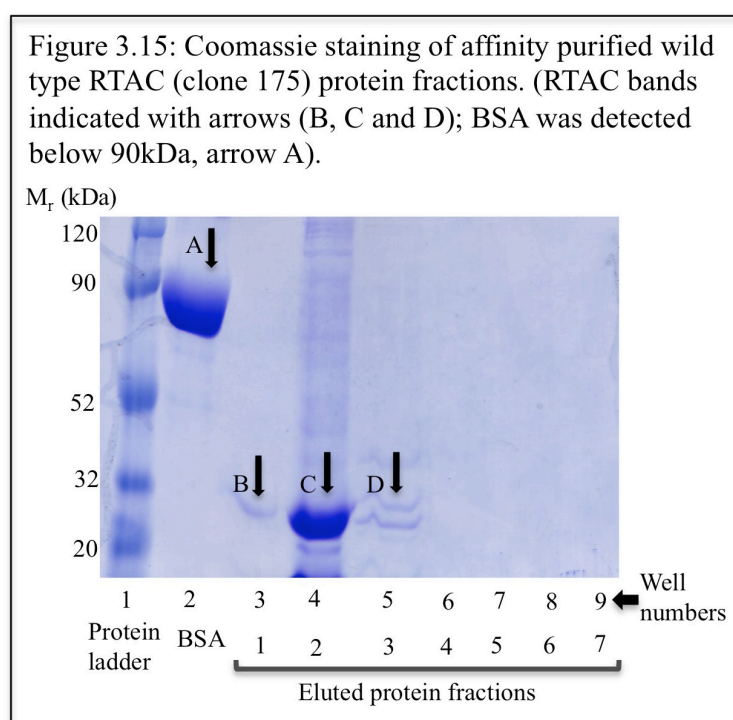


After optimising the transfer time, a gel identical to that in figure 3.12 was prepared and transferred onto the nitrocellulose membrane, using the optimum transfer time (60minutes). Figure 3.14 shows the BSA effectively transferred on to the nitrocellulose membrane. It was concluded (figure 3.13 and 3.14) that for BSA, a 60minutes transfer time was optimal. This transfer time was applied to rest of the immuno-blotting experiments as the proteins under investigation were of a comparable molecular weight.



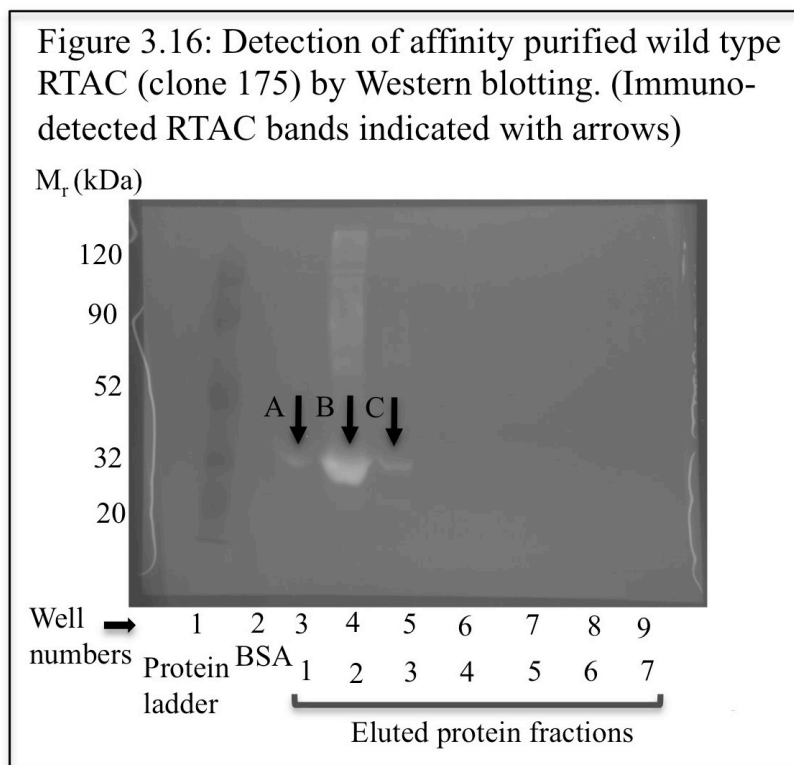
c) Detection of protein by immuno-blotting

Wild type RTAC (clone 175) protein fractions were collected from a Ni-Sepharose column and were resolved on 10% (w/v) SDS-PAGE gel. The gel was stained with Coomassie brilliant blue R-250 (figure 3.15) and it was observed that fractions 1, 2 and 3 (figure 3.15, arrows B, C and D in wells 3, 4, 5) contained protein of the predicted molecular weight. The same protocol was repeated and protein fractions were transferred onto the nitrocellulose membrane by utilising the optimum transfer conditions, using mini-trans blot electrophoretic transfer cell (BioRad, Hemel Hempstead, UK).



After the successful, reproducible transfer of proteins, a robust protocol for immuno-detection was required (section 2.2.8). The immuno-detection of wild type RTAC (clone 175), was initially undertaken using a commercial polyclonal primary antibody specific for RTAC at a 1:1000 dilution. This primary antibody was detected using an anti-rabbit IgG HRP-conjugated secondary antibody (used after a 1:500 dilution, see table 2.2). During the final step, 0.5mL of ECL detection reagents (A and B) were applied and the resultant signal detected, initially using an EpiChem BiImaging systems (UVP). From figure 3.16 it was observed that wild type RTAC (clone 175) was detected at the predicted molecular weight

(~32kDa) (figure 3.16, arrows A, B and C in wells 3,4 and 5). This technique was developed within the school of science for the first time.



The above methodology was also applied to the characterisation of rRTBC (clone 204). However, in this instance, instead of running pooled, eluted protein fractions, known amounts of rRTBC (clone 204) were used. When protein concentrations were verified using SDS-PAGE followed by Coomassie staining (figure 3.17, arrows A, B, and C), putative rRTBC (clone 204) bands were detected at the predicted molecular weight (32kDa). After known amounts of rRTBC (clone 204) had been transferred into nitrocellulose membrane, a primary polyclonal antibody specific for rRTBC (anti-RTBC) diluted 1:1000 (table 2.2) was used to decorate rRTBC (clone 204). The primary antibody was detected using a secondary antibody (anti-rabbit IgG conjugated with HRP) also diluted 1:500. From figure 3.18 it was observed that the rRTBC (5 μ g) could be seen at its predicted molecular weight (32kDa).

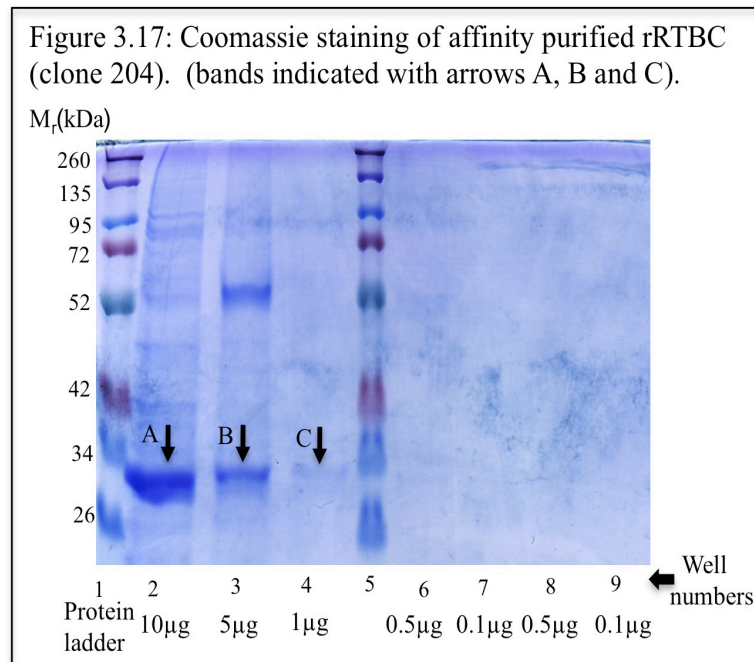
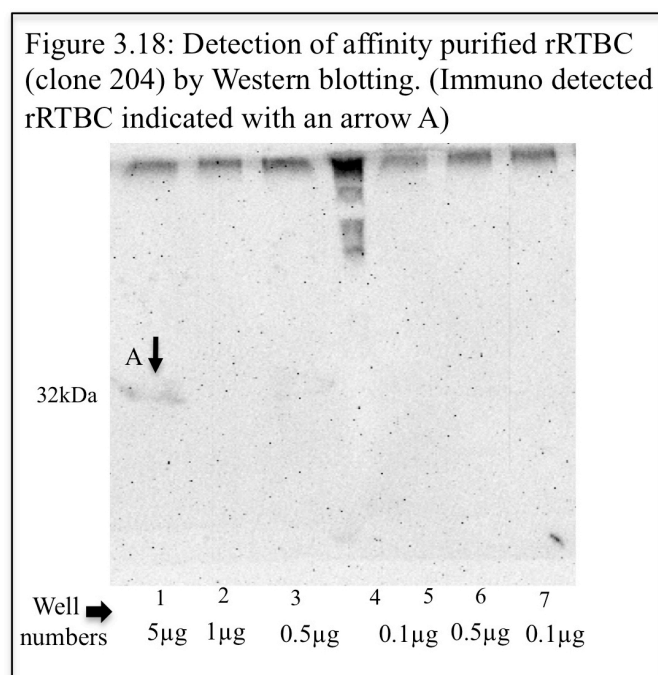
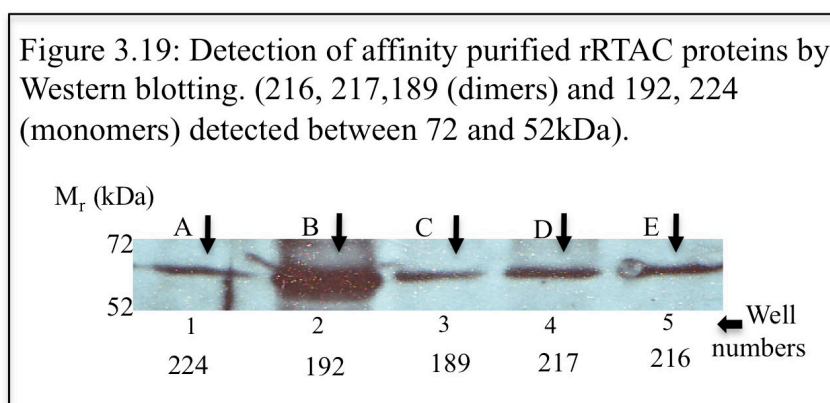


Figure 3.18 demonstrates that the detection of rRTBC (clone 204) by immuno-blotting was not adequate. Here, 5µg of rRTBC was detected (figure 3.18, arrow A in well 1) using the EpiChemi BioImaging system. As X-ray film had previously been used to characterise these antibodies, it was used in preference to the EpiChemi BioImaging systems (UVP) for ECL detection, as the immuno-detection of 1-5ng would be predicted (GE Health care, Buckinghamshire, UK).



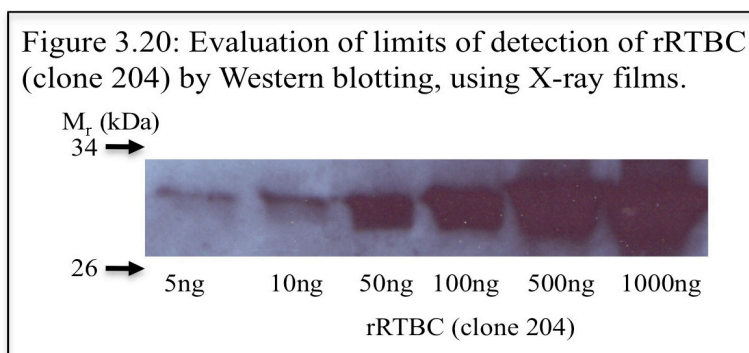
For the selected proteins (from table 3.3 and table 3.4), SDS-PAGE (figure 3.11) and Western blotting was performed using an anti-RTAC antibody (in 1:1000 dilution) and an HRP-conjugated anti-rabbit IgG antibody (in 1:1000 dilution) (table 2.2). In this instance X-ray films were used instead of the EpiChemi BioImaging system (UVP).

Figure 3.19, shows that RTAC analogues (table 3.2) were identified using the appropriate antibody at the predicted molecular weight. Proteins with GFP were detected at 62kDa (figure 3.19, arrows A (224) and B (192)). Proteins without GFP (216, 217 and 189) were also detected at approximately 62kDa, indicating that they may be running as dimers (figure 3.19, arrows C (189), D (217) and E (216)). Figure 3.19 shows successful immuno-detection of rRTAC proteins with Western blotting, validating the cloning using a commercially available antibody.



Establishing the limits of rRTBC immuno-detection by Western blotting

Recombinant RTBC (clone 204) was used to analyse the limits of detection of immuno-blotting. rRTBC (clone 204), having been characterised by previous rounds of immuno-blotting as well as Coomassie staining, and having had its protein concentration estimated using the densitometry, was loaded over a concentration range of 5ng to 1000ng and resolved on a 10% (w/v) SDS-PAGE gel. After the transfer of rRTBC (clone 204) onto a solid phase support, immuno-detection was performed as described (section 2.2.7) using a polyclonal anti-RTBC primary antibody (abcam, Cambridge, UK) and HRP-conjugated anti-rabbit IgG secondary antibody (GE healthcare, Buckinghamshire, UK) (1:1000 dilution). X-ray films were used to detect the HRP-label conjugated to the secondary antibody. From figure 3.20, it was observed that, up to 5ng of rRTBC (clone 204) could be detected using this method.



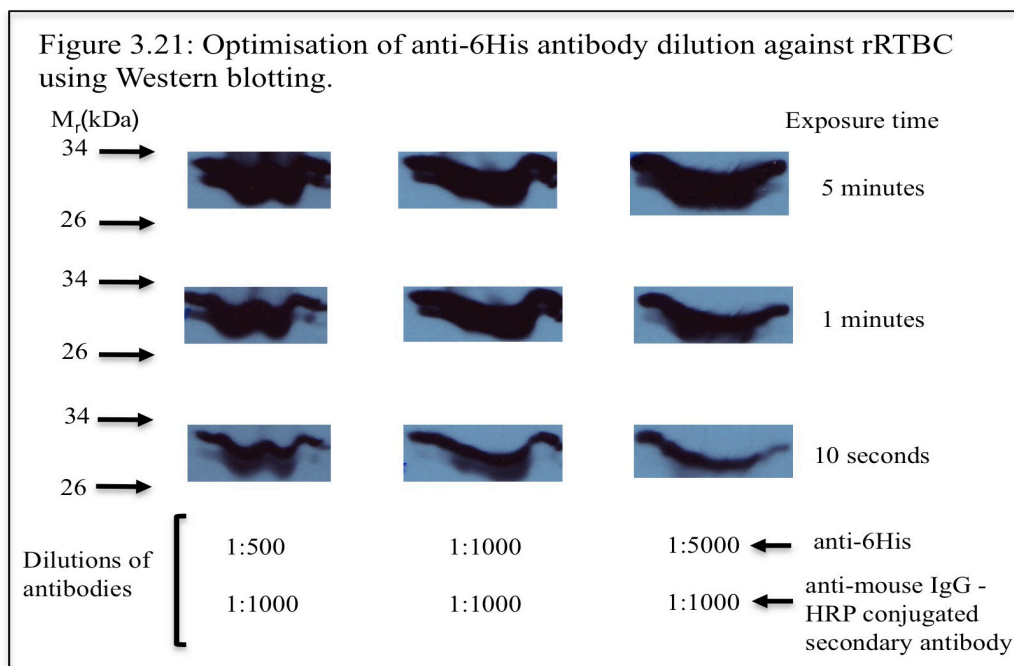
3.3.4 Optimisation of Western blotting

In order to optimise the signal to noise ratio associated with protein immuno-detection, an evaluation of antibody performance in relation to antibody dilution was undertaken. Both primary (anti-6His monoclonal antibody, anti-RTAC antibody, and anti-RTBC antibody, table 2.2) and secondary antibody (HRP-conjugated anti-mouse IgG antibody and HRP-conjugated anti-rabbit IgG-antibody (GE Health care, Buckinghamshire, UK)) dilutions were optimised for the detection of rRTAC (clone 189) and rRTBC (clone 204) proteins using Western blotting.

Mini-inductions were performed for both rRTAC (clone 189) and rRTBC (clone 204) constructs (section 2.2.9) by utilising 2h pre- and post- induction growth times and protein expression induced with 0.25mM IPTG (final concentration). The resultant culture was centrifuged at 6000 x g (rcf) at 4°C for 20minutes. The supernatant was discarded and the pellet dissolved in 180µL of LSB and 20µL of BME. SDS-PAGE and immuno-blotting experiments were performed as described in section 2.2.6 and 2.2.7. Instead of using the EpiChemi BioImaging systems (UVP), X-ray films were used for immuno detection of proteins.

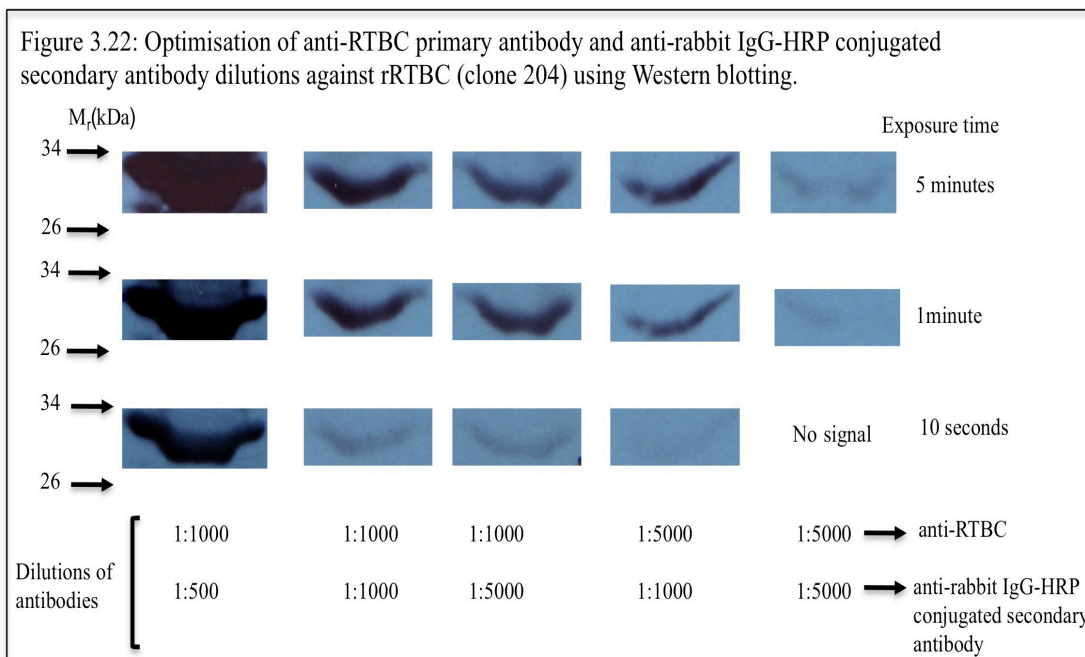
3.3.4.1 Optimisation of anti-6His primary antibody dilutions for rRTBC (clone 204) detection

Figure 3.21 shows that a 1:5000 dilution of anti-6His and 1:1000 dilution of anti-mouse HRP-conjugated IgG secondary antibody was sufficient to detect the target rRTBC (clone 204) after a 10seconds exposure time.



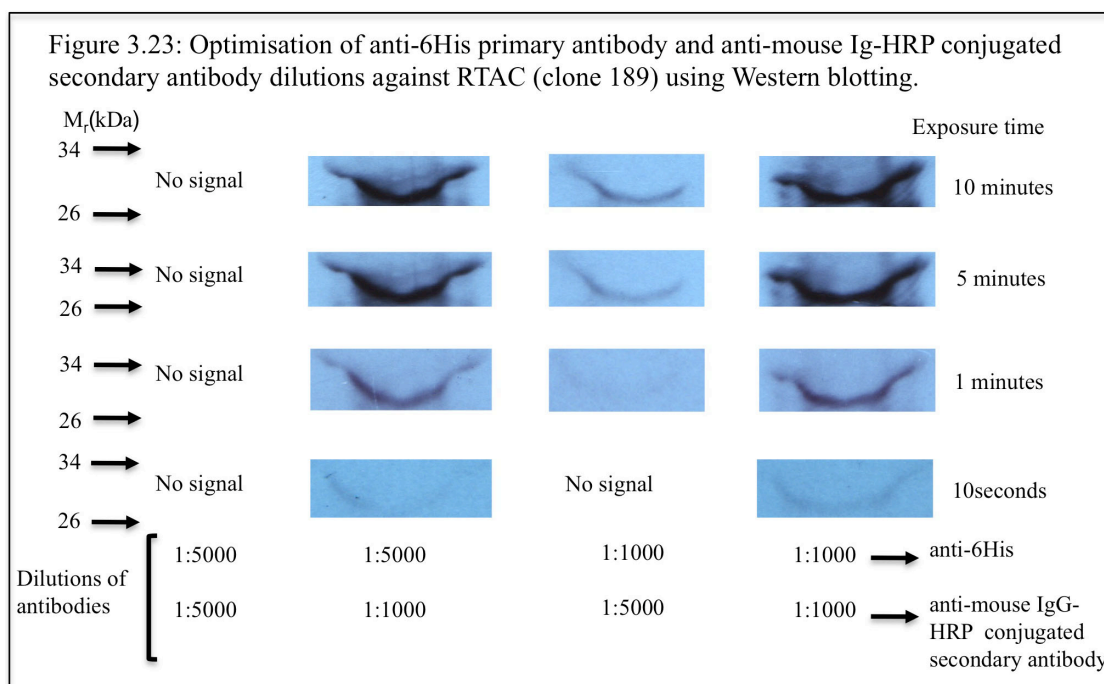
3.3.4.2 Optimisation of anti-RTBC primary and HRP-conjugated anti-rabbit IgG secondary antibody dilutions for rRTBC (clone 204) detection

Figure 3.22 shows that a 1:1000 dilution of anti-RTBC and a 1:5000 dilution of HRP-conjugated anti-rabbit IgG secondary antibody was sufficient to detect rRTBC (clone 204) after a 1minute exposure time. After a 10second exposure time rRTBC was detected but with lower intensity. Like with anti-6His antibody dilution, here also it was possible to achieve an adequate signal with a 1:5000 dilution of primary antibody (anti-RTBC) and 1:1000 secondary antibody dilution (HRP-conjugated anti-rabbit IgG antibody), after a 1minute exposure time.



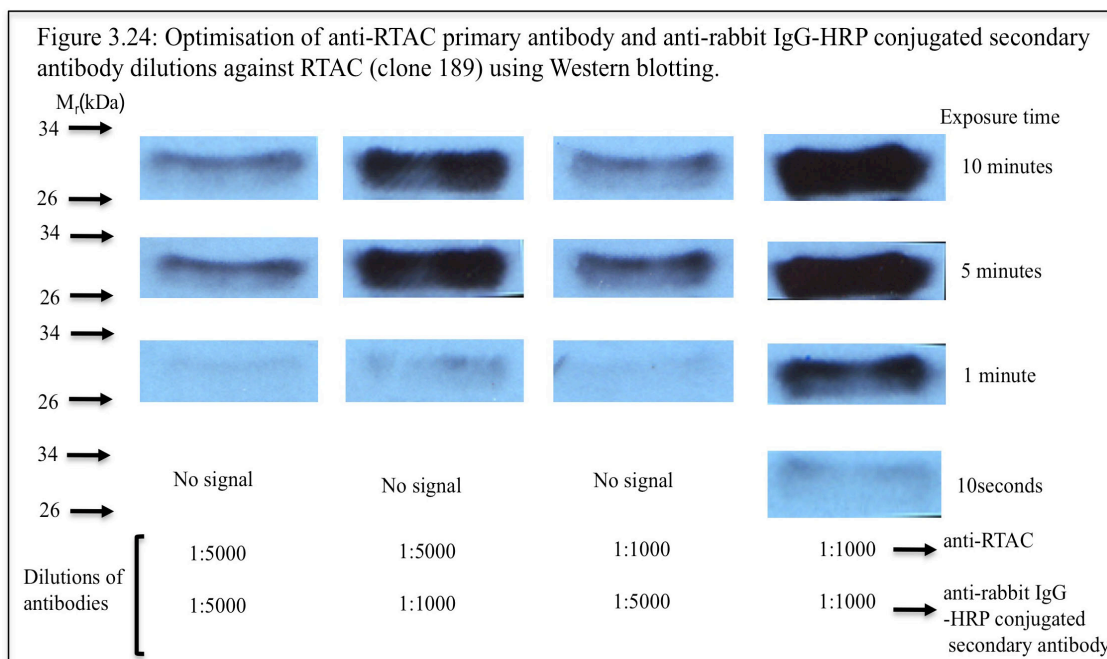
3.3.4.3 Optimisation of anti-6His primary antibody and HRP-conjugated anti-mouse IgG secondary antibody dilutions, for rRTAC (clone 189) detection

From figure 3.23, rRTAC protein (clone 189) was detected using anti-6His specific primary antibody (1:5000 dilution) and an anti-mouse HRP-conjugated IgG secondary antibody (1:1000 dilution) after a 1minute exposure time. Decreasing both primary and secondary antibody dilutions up to 1:1000 increased the sensitivity of the detection methodology (figure 3.23).



3.3.4.4 Optimisation of anti-RTAC primary antibody and HRP-conjugated anti-rabbit IgG- secondary antibody dilutions for rRTAC (clone 189) detection

Figure 3.24 shows that after a 1:1000 dilution of both anti-RTAC primary antibody and the HRP conjugated anti-rabbit IgG secondary antibody, rRTAC (clone 189) protein could be detected after a 1minute exposure time. At higher dilutions (1:1000 and 1:5000), it was also possible to detect the protein by increasing the exposure time to 5minutes (figure 3.24, 3rd row bands from right hand side).



3.3.5 Production and optimisation of recombinant protein culture conditions using mini-induction experiments

Mini-induction experiments were performed in order to optimise protein expression on a small scale and perform preliminary recombinant protein characterisation.

Three culture parameters were identified as being critical and these were: growth time (pre-induction) (PrIGT), IPTG concentration, growth time (post-induction) (PoIGT), which, were optimised at different temperatures 30°C (O'Hare *et al.*, 1987) and 37°C.

3.3.5.1. Growth time (pre-induction) (PrIGT)

Having ascertained that rRTBC and RTAC analogues could be reliably detected using immuno-blotting, culture conditions were optimised, using immuno-blotting as an indicator of success. Initially PrIGT growth times (2h, 3h and 4h), with constant IPTG concentrations (0.25mM) and post-induction growth time (PoIGT) (2h) were investigated as described in section 2.2.9, in order to ascertain the optimal culture conditions for RTAC constructs (clone 175, clone 189).

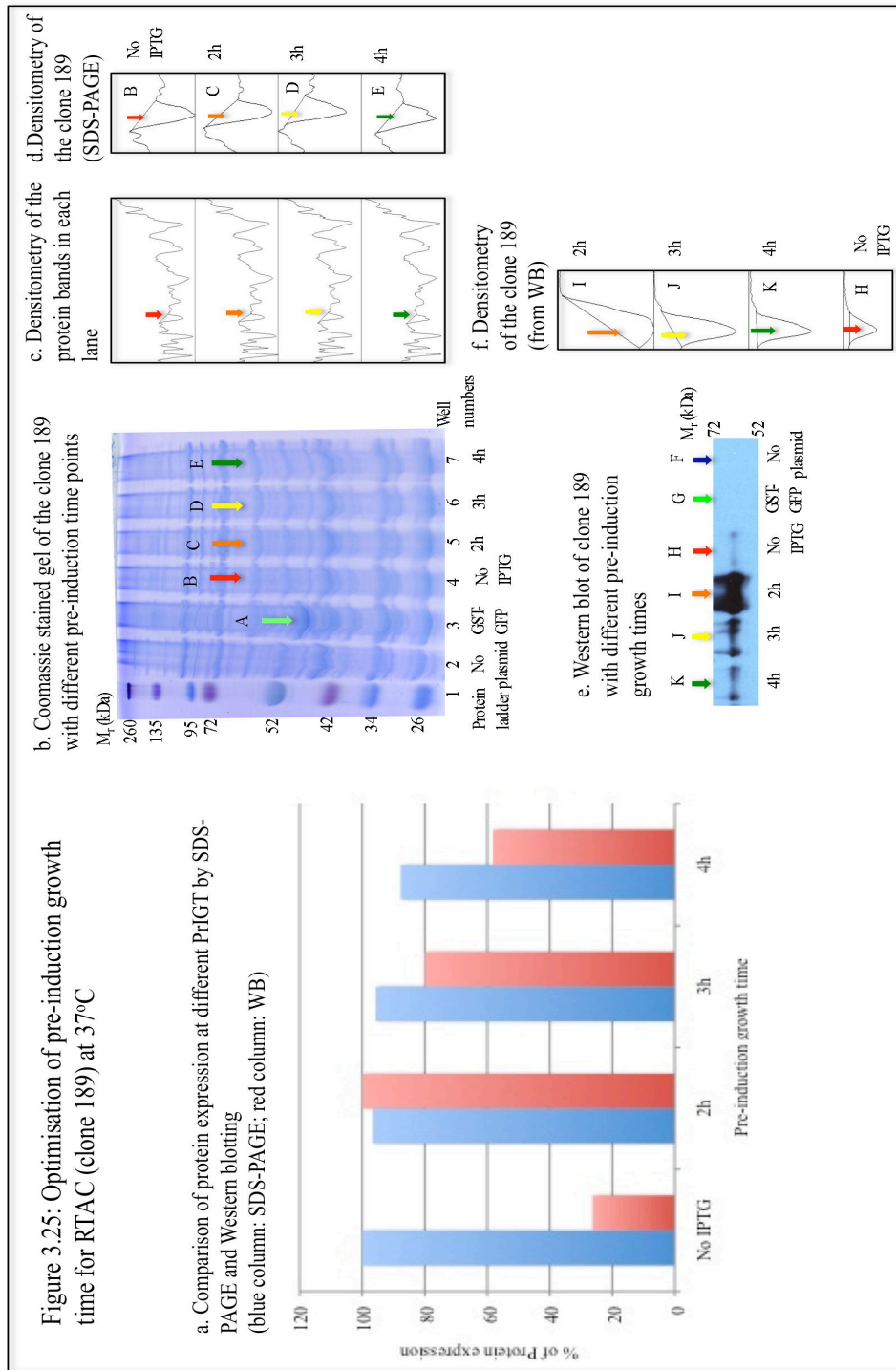
Figure 3.25a and b demonstrate that during rRTAC (clone 189) expression, there was a slightly higher (~10%) protein expression level after 2h and 3h growth time points (figure 3.25, arrows C, D and E, well numbers 5 to 7). Without IPTG, more expression was observed. This phenomenon can result from the promoter leakage, however the protein

expression was higher than all the three time points. This result cast doubt upon the reliability of this experimental methodology and the selection of the correct band representing the recombinant protein within the bacterial lysate. To assay specific protein expression level, Western blotting followed by immune-detection was performed. Occasionally recombinant proteins would resolve as dimers (62kDa,) a phenomenon often seen during SDS PAGE.

Different protein expression levels were clearly visible at different pre-induction growth time points relative to the controls (figure 3.25e, arrows from F to K). Densitometry was performed to quantify the amount protein detected during immuno-blotting. This methodology was not perfect however given the impurity inherent to these experiments, was deemed adequate.

When evaluating protein expression level at different time points, the highest protein expression was taken as 100% and other protein expression levels were compared to it (*i.e.* at different time points). In this experiment, the highest protein expression was observed at 2h time point and it was taken as reference (100%) to compare the expression levels of protein at 3h, 4h and controls. Figure 3.25 panels a and e demonstrate that at after a 2h incubation, protein expression was 20% higher than 3h and 42% higher than at 4h time point. Promoter leakage was also observed, but was less (26%) relative to the 2h time point (Protein bands labelled with arrows from F to K).

After SDS-PAGE, the GST-GFP protein band was documented at the predicted molecular weight relative to the molecular weight marker (figure 3.25b, lane 2, arrow A). As expected, after immuno-blotting, the GST-GFP protein and *E.coli* BL21*DE3 without a plasmid construct did not produce any immune-reactive bands, as they do not produce endogenous 6His containing proteins and serve as a negative control during this experiment (figure 3.25e, arrows F and G).



rRTAC (clone 189) expression at different pre-induction growth times was also evaluated at 30°C. SDS-PAGE and immuno-blotting was performed as above, except that here 10µL of sample was during the evaluation of protein expression.

Figure 3.26 shows that after incubation at 30°C, the proportion of protein expression at 2h was 30% higher than at 3h and 62% higher than at 4h (arrows D, E and F). The negative control, GST-GFP protein (clone 210) and non-transformed *E.coli* BL21*DE3 bacterial lysate didn't produce any bands (arrows A and B). Here the Coomassie staining of gels was undertaken but is not shown, as similar to the experiments performed above, it was difficult to draw a definite conclusion from it. However, immuno-detection of the recombinant protein also rectified the problem of identifying the recombinant protein within the lysate.

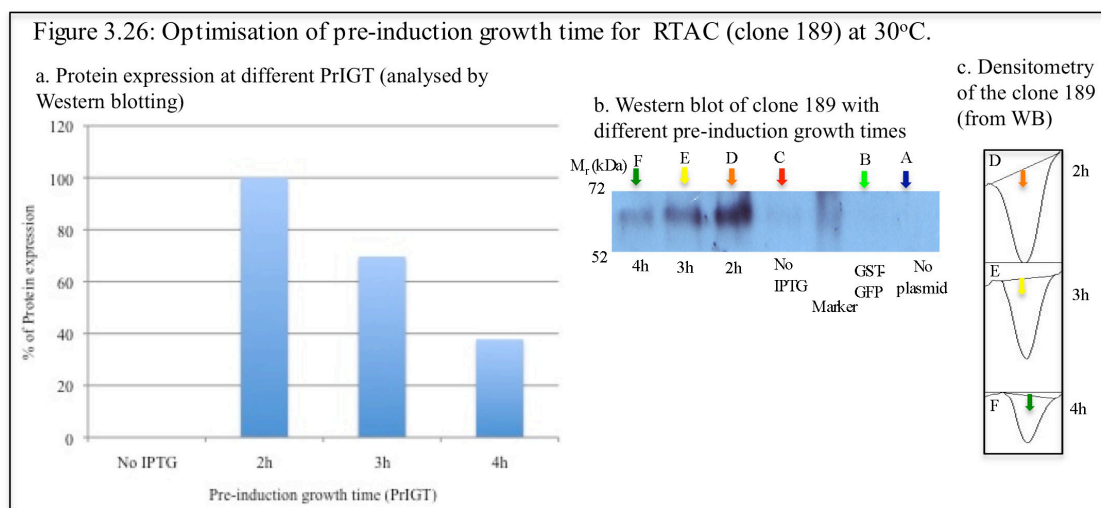
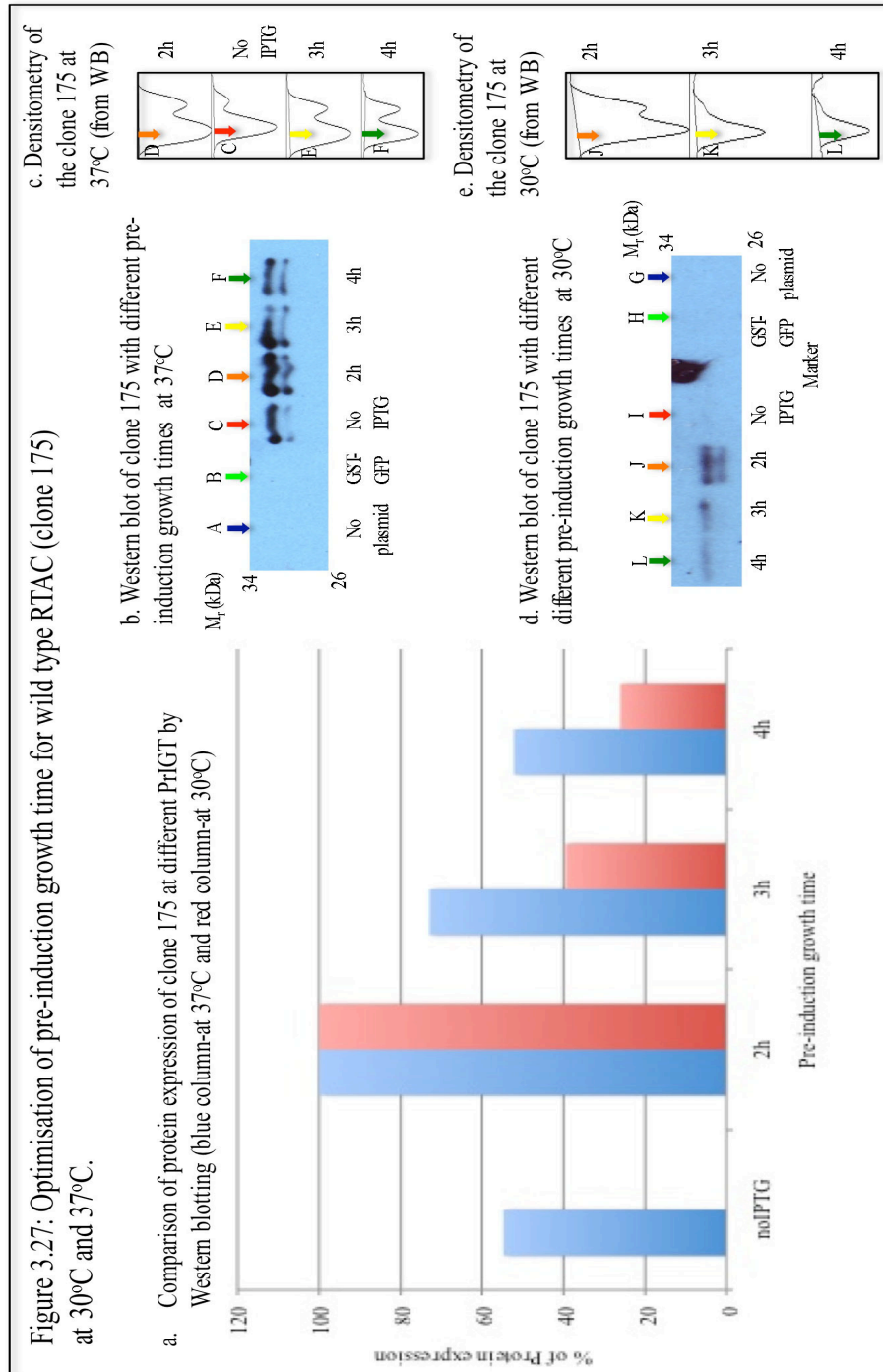


Figure 3.27a and d shows wild type RTAC (clone 175), after incubation at 30°C after a 2h pre-induction time and that these conditions produced 60% more protein than at 3h (arrows J and K)) and 73% more than 4h (arrow L). There was no promoter leakage observed (arrow I). Negative controls, GST-GFP (clone 210) (arrow H) and *E.coli* BL21*DE3 with no plasmid (arrow G) confirmed the specificity of the antibody (No bands detected).

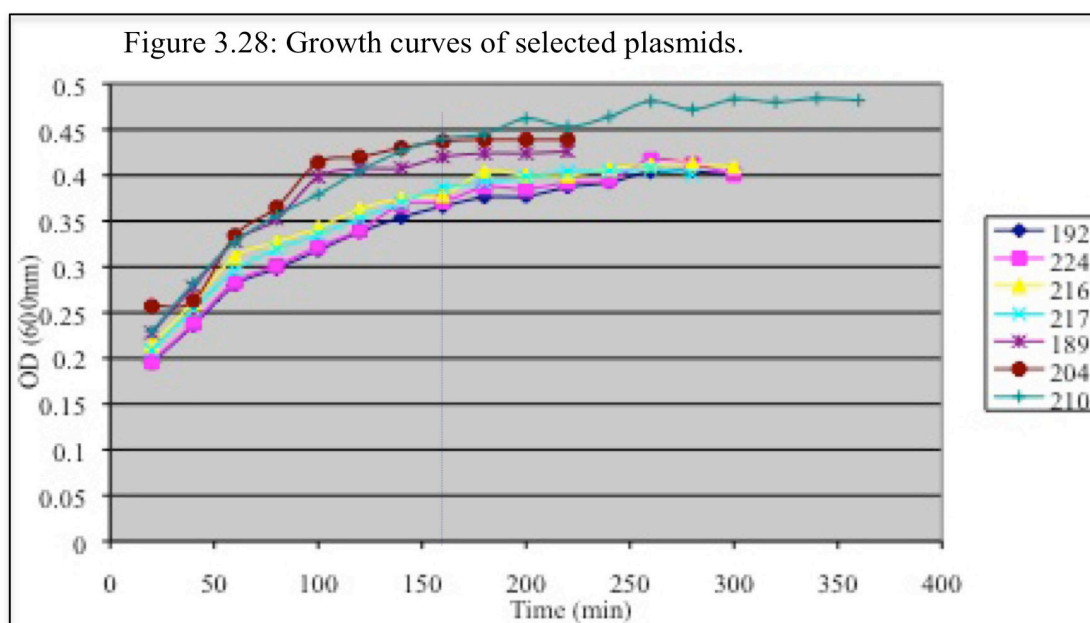
Figure 3.27a and b also shows wild type RTAC (clone 175) produced at 37°C. Recombinant RTAC (clone 175) expression after 2h (pre-induction) was 27% higher than after 3h (arrows D and E) and 47% higher than at 4h time point (arrow F). High promoter leakage was observed (54% protein expression without IPTG (arrow C)). Protein expression was highest after the 2h time point (arrow D) and it was taken as reference to compare the expression at different time points. At both incubation temperatures (30°C and 37°C), GST-GFP (clone

210) and *E.coli* BL21*DE3 without plasmid construct, did not produce any signal demonstrating antibody specificity (arrows A, B, G and H).



With both wild type RTAC (clone 175) and rRTAC (clone 189), protein expression was higher with 2h incubation at 37°C (figure 3.27, arrow D and figure 3.25, arrow I) than 2h at 30°C (figure 3.27, arrow J and figure 3.26, arrow D).

Identification of the optimal growth time was also performed by measuring the absorbance of bacterial culture containing plasmids coding for selected RTAC (from tables 3.3 and 3.4), rRTBC (clone 204), and GST-GFP (clone 210) as described in section 2.2.9. From figure 3.28 it was evident that the transformed bacterial cultures were reaching stationary phase after approximately 160minutes (figure 3.28, time indicated with a dotted line). From the Western blotting, it was concluded that the optimum pre-induction growth time was 120minutes (figure 3.25 and 3.27) and this was close to the time required for the bacterial cultures needs to reach stationary phase (160minutes).



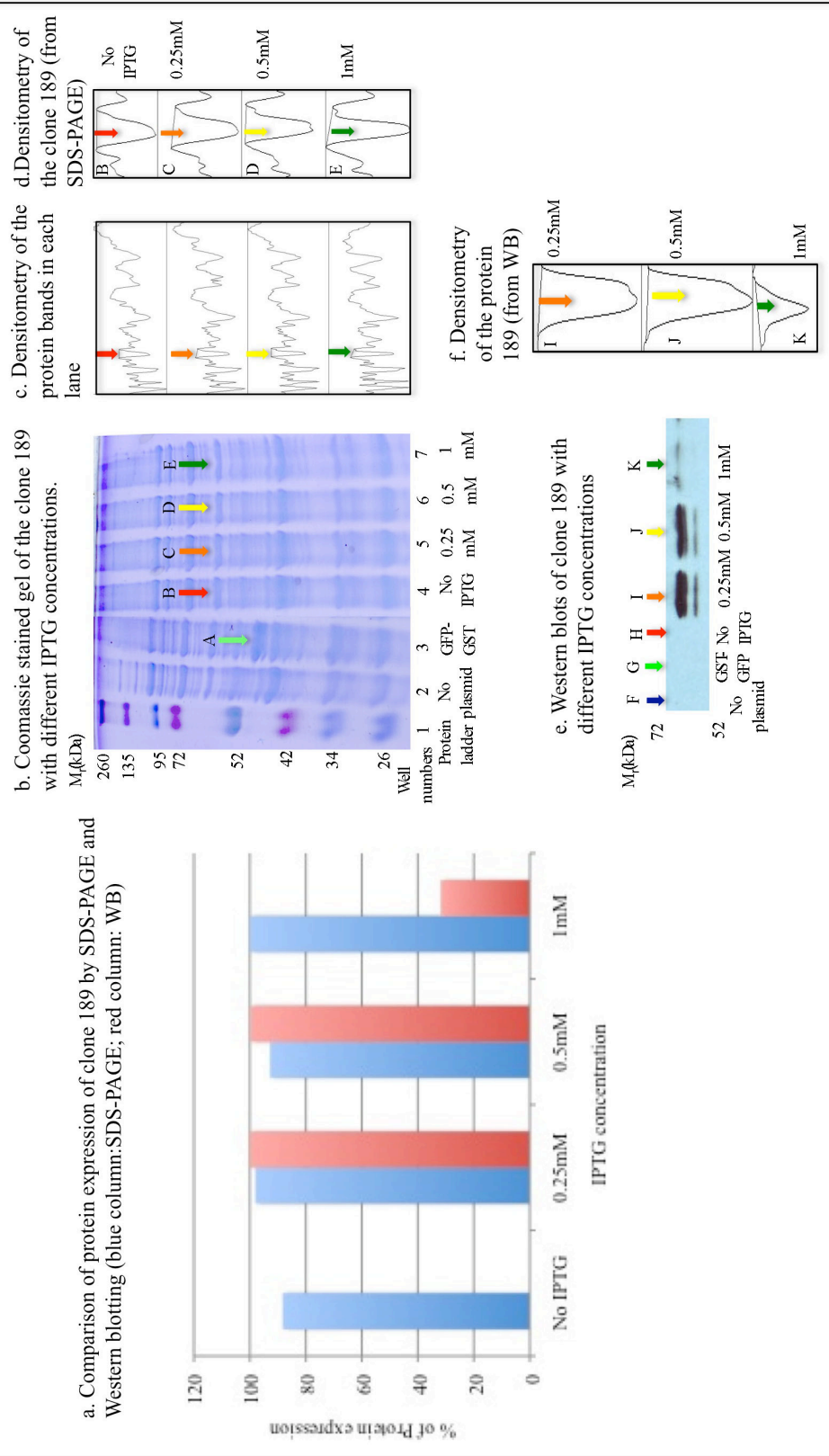
3.3.5.2 IPTG concentration

The concentration of IPTG was optimised using three different concentrations, 0.25mM, 0.5mM and 1mM. These three IPTG concentrations were used (separately) to induce protein expression of GST-GFP (clone 210) and RTAC (clone 175 and clone 189) whilst keeping constant PoIGT (120minutes) and PrIGT times (120minutes).

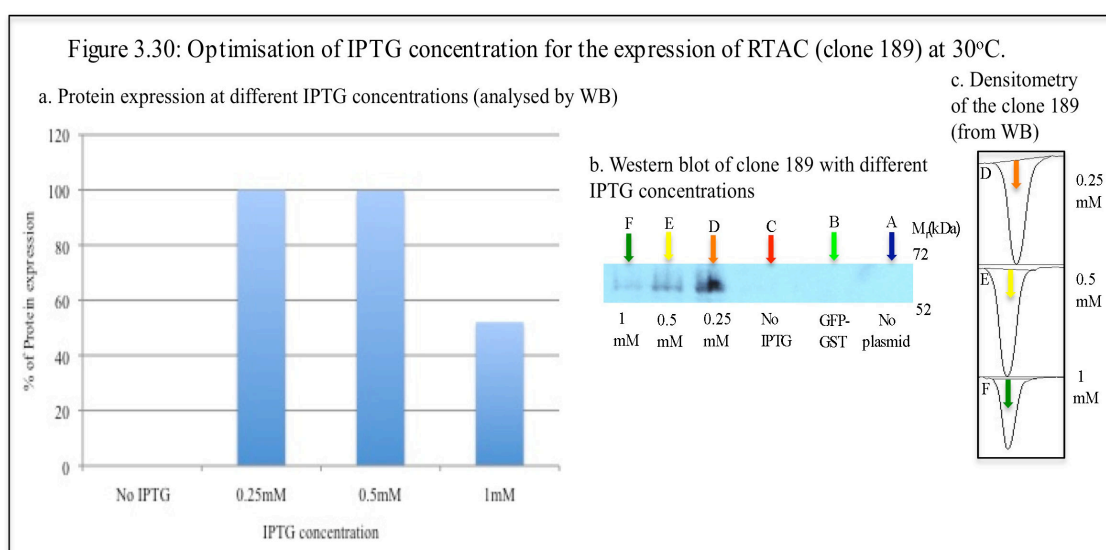
Figure 3.29a demonstrated that at 37°C, there was no obvious difference observed between the three different concentrations of IPTG used to induce the production of rRTAC (clone 189). Figure 3.29b identified expressed protein (lanes 4-6, bands indicated with arrows B, C,

D and E) at the predicted molecular weight (62kDa, dimer of the protein). Western blots show that with 0.25mM and 0.5mM IPTG concentrations, rRTAC (clone 189) (Figure 3.29e; arrow I and J) protein expression levels were equal and protein expression was 70% higher than 1mM IPTG concentration (arrow K). For the recombinant GFP-GST (clone 210), protein expression was observed after Coomassie staining (Figure 3.29a, arrow A). But in the Western blotting, GST-GFP (clone 210) and *E.coli* BL21*DE3 without plasmid construct, didn't show any bands, which was predicted as they serve as negative controls (arrows F and G).

Figure 3.29: Optimisation of IPTG concentration for the expression of RTAC (clone 189) at 37°C.

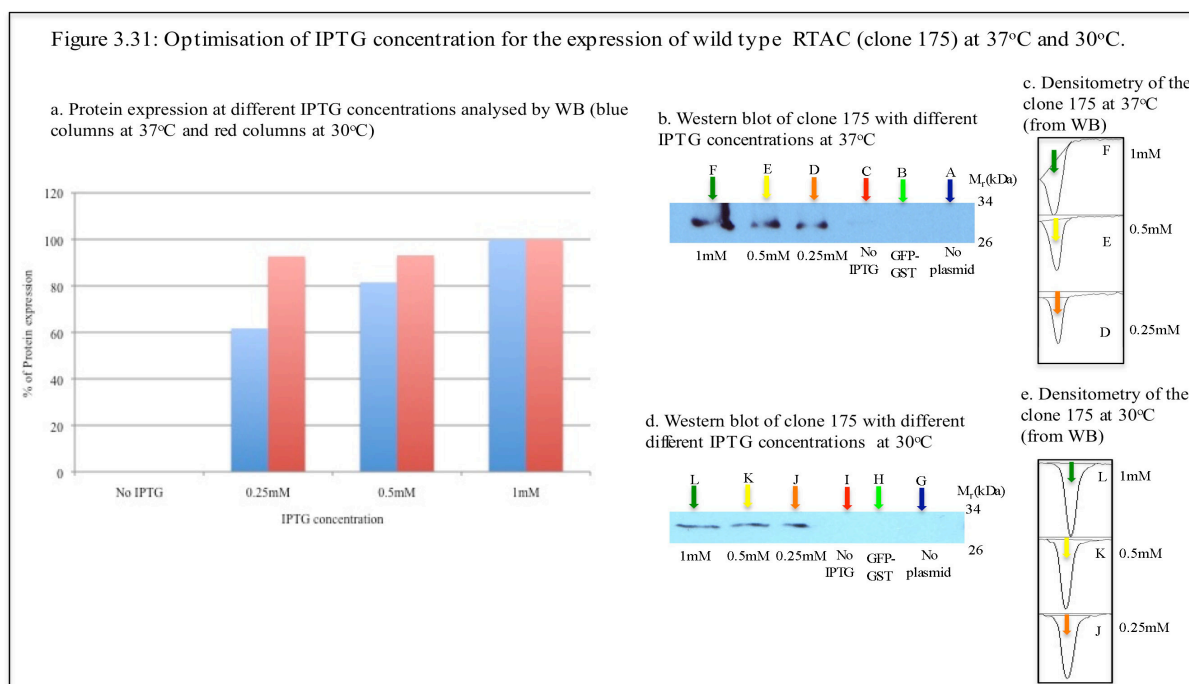


Mini-inductions and immuno-blotting were performed as previously described, using three concentrations of IPTG (as above) to induce the expression of rRTAC (clone 189) at 30°C. rRTAC (clone 189) protein expression levels were similar after incubation at 30°C and 37°C. Of note was that if a 1mM IPTG concentration was used after incubation at 30°C, the protein expression level was 48% lower than with 0.25mM and 0.5mM IPTG concentrations (figure 3.30, arrows D, E and F). Negative controls, GST-GFP (clone 210) and *E.coli* BL21*DE3 plasmid construct, didn't show any bands after immuno-blotting using a RATC specific primary antibody (arrows A and B).



It was observed that for wild type RTAC (clone 175) (figure 3.31a, and b), after incubation at 37°C, protein expression was higher when a 1mM IPTG concentration was used (arrow F). Protein expression (at 1mM IPTG) was 39% higher than at 0.25mM (arrow D) and 29% higher than at 0.5mM IPTG concentrations (arrow E). At 30°C, the level of protein expression of wild type RTAC (figure 3.31d) was higher after induction with 1mM IPTG (arrow L) relative to 0.25mM (arrow J) and 0.5mM (arrow K). For wild type RTAC (clone 175) the difference in protein expression levels at different IPTG concentrations was below 10%.

From the above experiments (section 3.3.5.2), it was observed that for wild type RTAC (clone 175), high protein expression was documented after induction with 1mM IPTG (figure 3.31) whereas optimal expression of rRTAC (clone 189) required a final concentration of 0.25mM IPTG at both the incubation temperatures (figure 3.29 and 3.30).



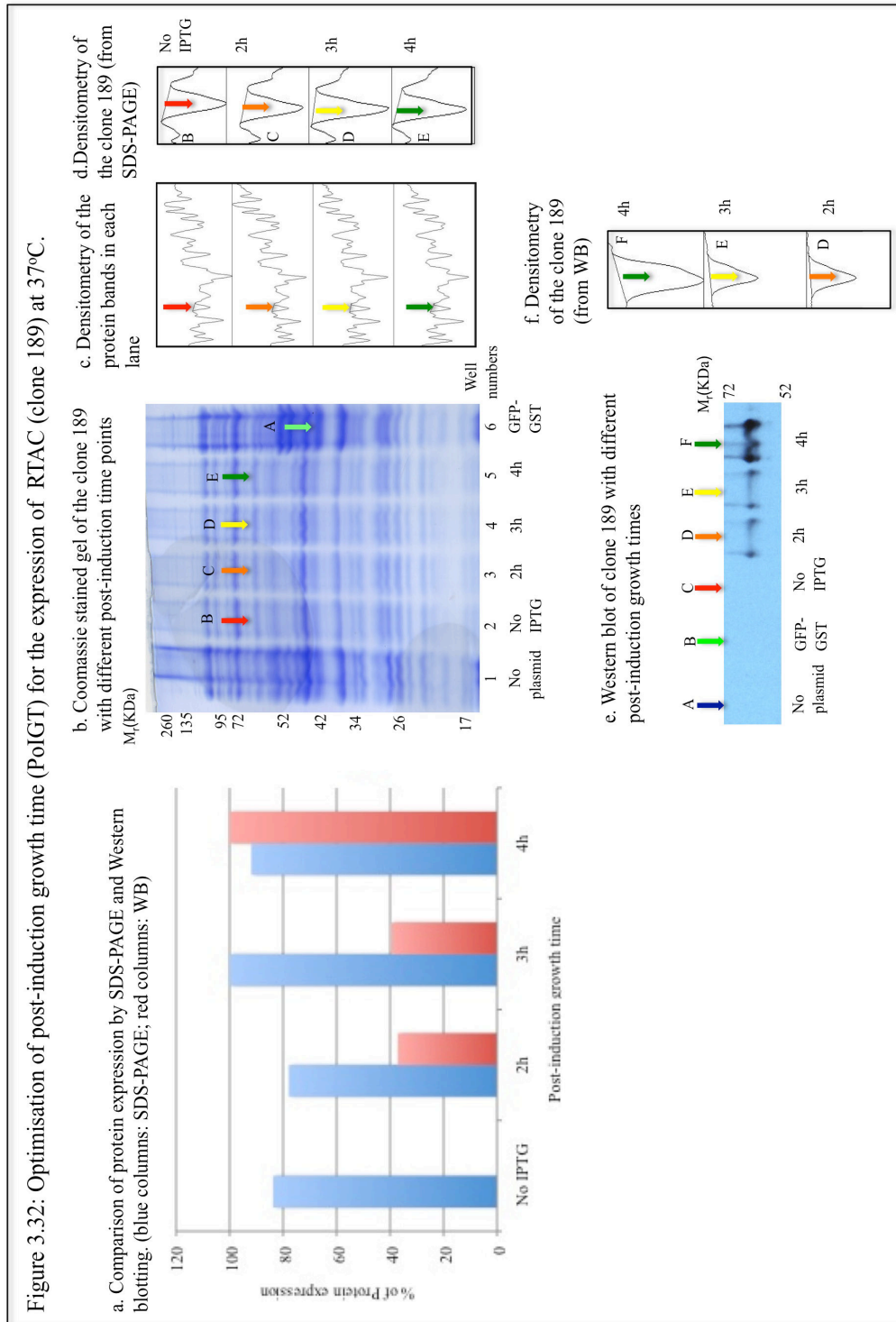
3.3.5.3 Post induction growth time (PoIGT)

It was observed that a 2h pre-induction growth time (figure 3.25) using 0.25mM IPTG (figure 3.29) was required for optimal protein expression (clone 189).

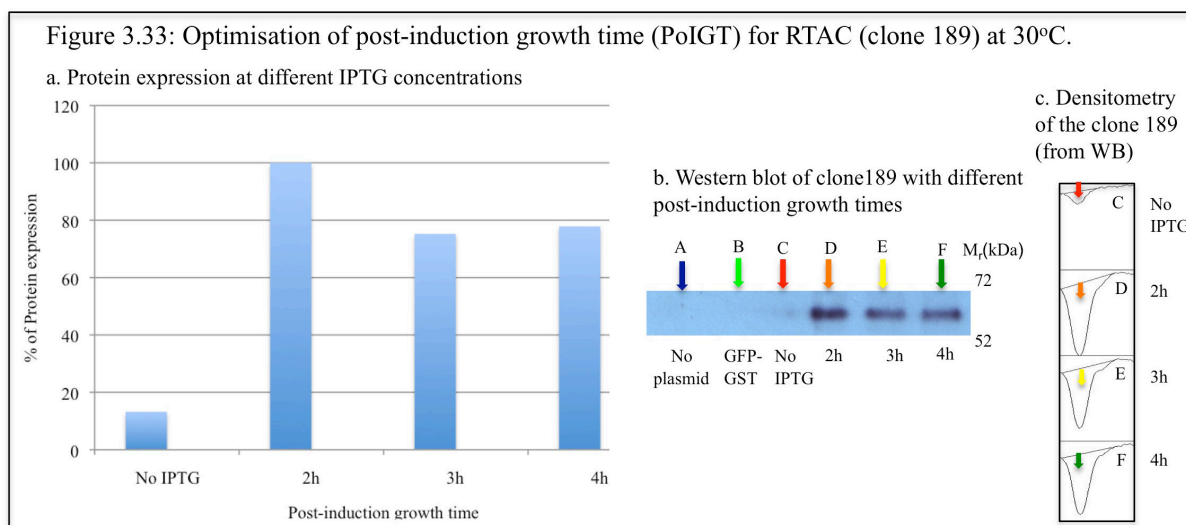
By keeping the PrIGT (2h) and IPTG concentrations (0.25mM) constant, three different PoIGT time points (2h, 3h and 4h) were examined by monitoring the production of GST-GFP (clone 210), rRTAC (clone 189) and wild type RTAC (clone 175) proteins from their respective plasmid constructs. Mini-inductions, Coomassie staining and immuno-blotting were performed as above (sections 3.3.5.1 and 3.3.5.2). From the Coomassie stained gel (figure 3.32a and b), it was observed that a 3h post-induction growth time (arrow D) was optimal relative to 2h (arrow C) and 4h (arrow E) when expressing rRTAC (clone 189). Without induction with IPTG 83% expression (arrow B) was observed relative to expression levels at 3h (arrow D). This may indicate that the experimental conditions investigated had little effect upon protein expression (section 3.3.5.1).

In order to look at the expression of a specific protein, immuno-blotting was performed. rRTAC (clone 189) (figure 3.32e) was expressed a higher level after a 4h post-induction growth time (arrow F) relative to the 3h (arrow E) and 2h (arrow D) time points. Protein expression at 4h (arrow F) was 62% higher than 2h (arrow D) and 60% higher than at 3h post-induction times (arrow E). Negative controls, GST-GFP (clone 210) (arrow B) and

E. coli BL21*DE3 without a plasmid didn't express any detectable protein after immunoblotting (arrow A) and acted as a negative control.



Mini-induction experiments and immuno-blotting were performed as above at 30°C for to investigate the optimal expression of rRTAC (clone 189) with 2h, 3h and 4h post-induction times. From the figure 3.33, it was observed that rRTAC (clone 189) expression was optimal at 2h post-induction time (arrow D) and this level was taken as reference to compare the expression of other time points. RTAC protein expression was 25% higher relative to 3h (arrow E) and 23% to 4h (arrow F) post-induction time point.

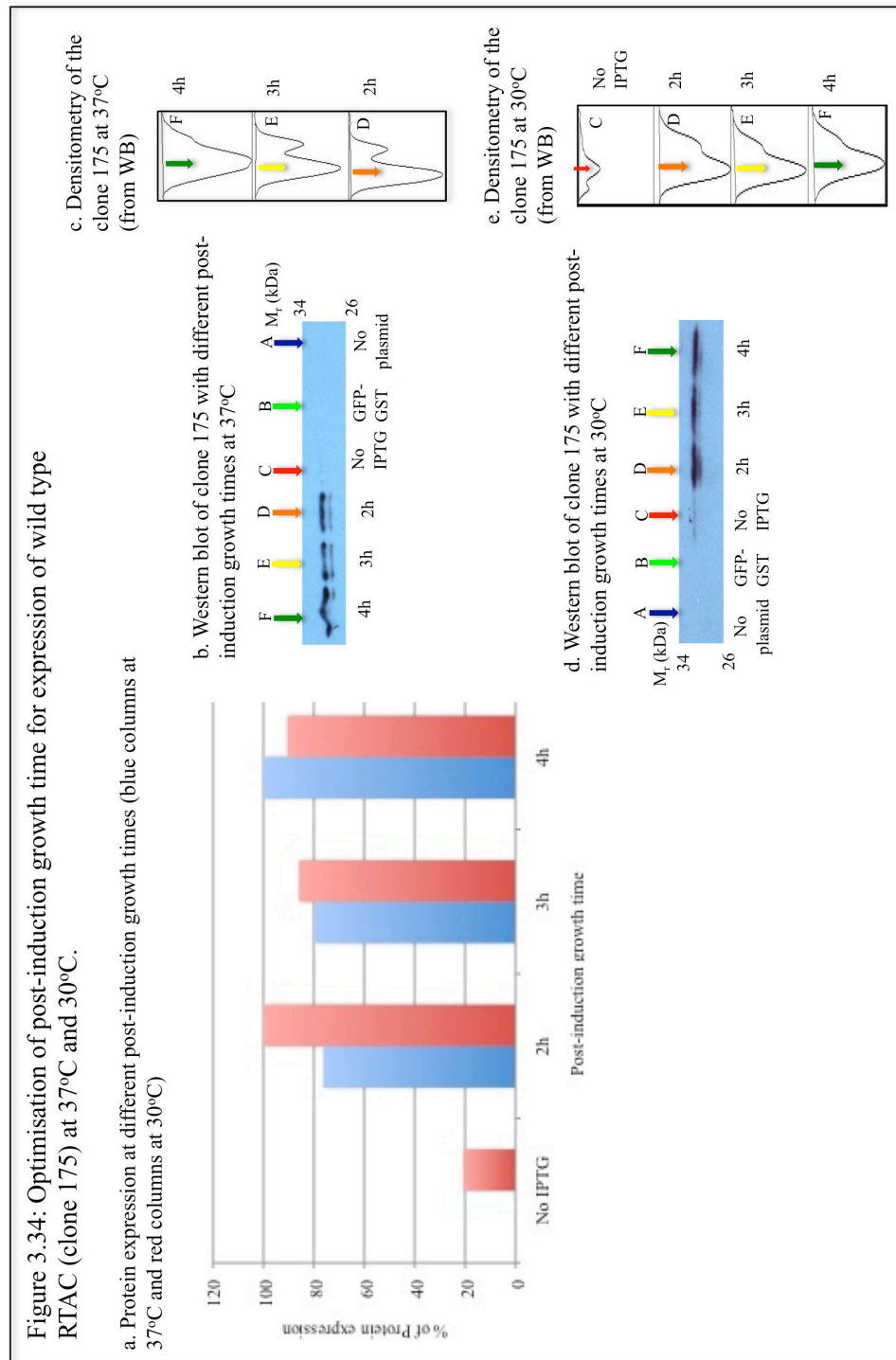


When evaluating the optimum post-induction growth time for wild type RTAC (clone 175), mini-induction and immuno-blotting was performed as above. Figure 3.34, demonstrates that, for wild type RTAC (clone 175) (figure 3.34a and d), after incubation at 30°C protein production was higher at 2h post induction growth time (arrow D) relative to the 3h (arrow E) and 4h (arrow F). At 2h, wild type RTAC (clone 175) production was 14% higher relative to 3h and 10% higher than 4h post-induction time.

After grown at 37°C, wild type RTAC (clone 175) expression after a 4h post-induction time (figure 3.34b, arrow F) was 24% higher relative to a 2h post-induction time (figure 3.34b, arrow D) and 21% higher than 3h (figure 3.34b arrow E).

After being grown at 37°C, both rRTAC (clone 189) (figure 3.32) and wild type RTAC (clone 175) (figure 3.34), show higher protein expression levels after a 4h post-induction growth time relative to 2h and 3h post-induction growth time. However after being grown at 30°C, a 2h post-induction growth time was optimal for recombinant protein production for both constructs. Protein expression levels at 37°C (figure 3.32) were higher than at 30°C

(figure 3.33) and this conclusion was drawn from the fact that the immuno-blotting experiments were performed using 5 μ L of lysate and detection was performed using a 1min exposure (37 $^{\circ}$ C experiments), whereas 10 μ L of sample was used and 30minute exposure time were required to generate an equivalent signal for samples grown at 30 $^{\circ}$ C.



3.4 Discussion

3.4.1 Characterisation of the plasmid constructs

Plasmid constructs were characterised by generating plasmid maps and by agarose gel electrophoresis. Plasmid maps were drawn for each of these plasmids listed in table 3.2 and were generated from sequence data.

3.4.1.1 Plasmid maps

The primers deployed to sequence the plasmids made in Iowa were chosen to provide information about both the open reading frame (ORF) and the junctions between the PCR product (insert) and the vector. Primers were designed to provide a description of vector – insert junctions in a 5' to 3' and a 3' to 5' direction. This was important as it was anticipated that from ~800 to 1000bp of sequence data, the distal and proximal ends would contain errors. Consequently, a strategy requiring having multiple overlapping contiguous data sets that span critical regions (*i.e.* junctions) was adopted.

Plasmid maps were generated from the sequencing data (figure 3.1 to 3.7). These maps were pictorial representations of the vectors and the PCR inserts (table 3.5). What was of particular importance, within the context of the plasmids, was that (from the sequence data used to produce the maps) the junctions between the PCR product (insert) and the vector showed that the open reading frame (ORF) was in frame with the relevant sequence coding and the predicted epitope motifs as well as the start and stop codons.

Table 3.5 Predicted molecular weights and sequences of open reading frames (ORFs) of selected clones

Clone number	Protein sequence	M _w (kDa)
204	MHHHHHHHGKPIPNPLGLDSTENLYFQGIDPFTADVCMDEPIVIRIVGRNGLCVDVDRDGRFHNGNAIQLWPCKSNTDANQLWTLKRDNTIRSNKGKCLTTYGYPSGVVYMIYDCNTAATDATRWQIWDNGTIINPRSSLVLAATSGNSGTTLVQTNIIYAVSQGWLPNTNTQPFVTTIVGLYGLCLQANSQVWIEDCSSEKAEQQWALYADGSIRPQQNRDNCLTSDSNIRETVVKILSCGPASSGQRWMFKNDGTILNLYSGLVLDVRASDPSLKQIILYPLHGDPNQIWLPLF.	32.75
216	MYPYDVPDYAMIFPKQYPIINFTTAGATVQSYTNFIRAVRGRLTTGADVRHEIPVLPNRVGLPINQRFILVELSNHAELSVTLALDVTNAYVVG YRAGNSAYFFHPDNQEDAEAIHLFTDVQNR YTFAFGGNYDRLEQLAGNLRENIELGNGPLEE AISALYYYSTGGTQLPTLARSFII CIQMIGGGGGGQYIEGEMRTRIRYNRRSAPDPSVITLENSWGR LSTAIQESNQGAFASPIQLQRRNGSKFSVYDVSILIPIIALMVYRCAPPPSSQFHHHHHH.	31.76
217	MYPYDVPDYAMIFPKQYPIINFTTAGATVQSYTNFIRAVRGRLTTGADVRHEIPVLPNRVGLPINQRFILVELSNHAELSVTLALDVTNAYVVG YRAGNSAYFFHPDNQEDAEAIHLFTDVQNR YTFAFGGNYDRLEQLAGNLRENIELGNGPLEE AISALYYYSTGGTQLPTLARSFII CIQMIIQYIEGEMRTRIRYNRRSAPDPSVITLENSWGR LSTAIQESNQGAFASPIQLQRRNGSKFSVYDVSILIPIIALMVYRCAPPPSSQFHHHHHH.	31.42
192	MIFPKQYPIINFTTAGATVQSYTNFIRAVRGRLTTGADVRHEIPVLPNRVGLPINQRFILVELSNHAELSVTLALDVTNAYVVG YRAGNSAYFFHPDNQEDAEAIHLFTDVQNR YTFAFGGNYDRLEQLAGNLRENIELGNGPLEE AISALYYYSTGGTQLPTLARSFII CIQMIIQYIEGEMRTRIRYNRRSAPDPSVITLENSWGR LSTAIQESNQGAFASPIQLQRRNGSKFSVYDVSILIPIIALMVYRCAPPPSSQFHHHHHHKGFQCRYPAQWRPLESRMASKGEELFTGVVPILEVELDGDVNGHKFSVSGEGEDATYGKLT LKFICTTGKLPVPWPTLVTTFSYGVQCFSRYPDHMKRHDFKFSAMPEGYVQERTISFKDDGNYKTRAEVKFEGDTLVNRIELKIDFKEDGNILGHKLEYNYNSHNVYITADKQKNGIKANFKIRHNIEDG SVQLADHYQQNTPIGDGPVLLPDNHYLSTQSALS KDPNEKRDMVLEFVTAAGITHGMDELYKHHHHHHHREDL.	60.5
189	MIFPKQYPIINFTTAGATVQSYTNFIRAVRGRLTTGADVRHEIPVLPNRVGLPINQRFILVELSNHAELSVTLALDVTNAYVVG YRAGNSAYFFHPDNQEDAEAIHLFTDVQNR YTFAFGGNYDRLEQLAGNLRENIELGNGPLEE AISALYYYSTGGTQLPTLARSFII CIQMIIQYIEGEMRTRIRYNRRSAPDPSVITLENSWGR LSTAIQESNQGAFASPIQLQRRNGSKFSVYDVSILIPIIALMVYRCAPPPSSQFYYPYDVPDYAHHHHHHKDEL.	31.77
224	MASKGEELFTGVVPILEVELDGDVNGHKFSVSGEGEDATYGKLT LKFICTTGKLPVPWPTLVTTFSYGVQCFSRYPDHMKRHDFKFSAMPEGYVQERTISFKDDGNYKTRAEVKFEGDTLVNRIELKIDFKEDGNILGHKLEYNYNSHNVYITADKQKNGIKANFKIRHNIEDG SVQLADHYQQNTPIGDGPVLLPDNHYLSTQSALS KDPNEKRDMVLEFVTAAGITHGMDELYKSGSGPVLA VPSDPLVQCGGIALMIFPKQYPIINFTTAGATVQSYTNFIRAVRGRLTTGADVRHEIPVLPNRVGLPINQRFILVELSNHAELSVTLALDVTNAYVVG YRAGNSAYFFHPDNQEDAEAIHLFTDVQNR YTFAFGGNYDRLEQLAGNLRENIELGNGPLEE AISALYYYSTGGTQLPTLARSFII CIQMIGGGGGGQYIEGEMRTRIRYNRRSAPDPSVITLENSWGR LSTAIQESNQGAFASPIQLQRRNGSKFSVYDVSILIPIIALMVYRCAPPPSSQFYYPYDVPDYAHHHHHHKDEL.	61.07
175	MYPYDVPDYAMIFPKQYPIINFTTAGATVQSYTNFIRAVRGRLTTGADVRHDIPLVLPNRVGLPINQRFILVELSNHAELSVTLALDVTNAYVVG YRAGNSAYFFHPDNQEDAEAIHLFTDVQNR YTFAFGGNYDRLEQLAGNLRENIELGNGPLEE AISALYYYSTGGTQLPTLARSFII CIQMISEAARFQYIEGEMRTRIRYNRRSAPDPSVITLENSWGR LSTAIQESNQGAFASPIQLQRRNGSKFSVYDVSILIPIIALMVYRCAPPPSSQFHHHHHH.	32.05

3.4.1.2 Isolating plasmids

Plasmids in *E.coli* TOP10 were purified using a QIAprep® spin Miniprep Kit (Qiagen). High-purity and quantity plasmid DNA, was produced relatively quickly in relation to other techniques such as alkali lysis (Birnboim and Doly, 1979) or the cleared lysate and cesium chloride gradient purification method. Whilst there is circumstantial evidence that the purity of DNA from cesium chloride preps is better than that of the DNA isolated from Qiagen kits, it is likely that DNA purity at this level is only rate limiting during experiments requiring the high efficiency transfection of plasmid libraries. As these DNA preps were used for physicochemical analysis and transformation, this extra level of purity was deemed unnecessary.

According to the manufacturer (QIAprep® Spin Miniprep Kit, Qiagen), 10mL of saturated, low copy plasmid overnight culture yields 5-10µg of plasmid DNA. According to table 3.1, the yield of the most of the clones were relative to the manufacturers expectations, it was reasonable to assume that the experimental parameters outlined in the methods section (section 2.2.2) were close to the optimum conditions for these experiments. Having obtained acceptable yields of plasmid DNA that was also characterised by sequencing, further characterisation was undertaken by gel electrophoresis (section 3.3.1.3).

3.4.1.3 Agarose gel electrophoresis of purified plasmid DNA

From the plasmid maps and sequencing data sets, it was predicted that all the plasmids characterised herein were between 6.5 to 7.5 kilobase pairs (kbp) (table 3.2 and figures 3.1-3.7). When the plasmid DNA was resolved by agarose gel electrophoresis, the bands observed were at predicted molecular weight given the conformation of the plasmid DNA as previously discussed (section 3.3.1.3). Occasionally the super helical circular form of the plasmid was observed running in front of the nicked circular form of plasmid DNA (figure 3.8). However the relative speed of the migration of these two bands was dependent upon the conformation and radius of gyration (R_g) of the DNA, which is a function of ethidium bromide intercalation into the super-helical circular form, driving conformational relaxation, increasing the R_g of the plasmid, altering the speed of migration relative to the nicked circular form (Sambrook *et al.*, 1989).

These experiments confirmed that plasmid DNA obtained from the Qiagen Minipreps behaved as predicted when subject to electrophoretic separation. A linear band was obtained that was of the predicted molecular weight. Majority of the plasmid DNA appeared to be in

the super helical circular form, indicative of a high quality yield (*i.e.* containing little in the way of contaminating endonucleases and isolated in a non-digested form). Having shown that the plasmid DNA contained the predicted sequence and had been isolated and characterised by agarose electrophoresis, the next stage in their characterisation was thought to be to ask the questions:

- 1) Can these plasmids be used to generate recombinant proteins?
- 2) Are the recombinant proteins produced of the correct molecular weight?
- 3) Do these recombinant proteins behave in an immunologically predictable way?

3.4.2 Isolation of protein from 1000mL cultures

To know whether the characterised plasmid constructs express the recombinant proteins, experiments were designed to examine the production of soluble recombinant proteins. These experiments were particularly important, as they would produce data pertinent to the usefulness of the proteins in question within the context of a drug delivery system. If a protein was produced and trafficked into a bacterial inclusion body, it would be highly likely that the protein was not folded correctly and consequently may not have appropriate biological function. This may mean, in the case of the attenuated RTAC analogues, that toxicity was not going to be an issue, as the protein construct would not traffic to the cytosol. This may be due to several factors however, as the domains within the RTAC analogues responsible for ER to cytosol transfer have yet to be identified. It may be possible that incorrect folding of the protein would mask these putative regions, thus interfering with the exit of the RTAC from the ER. Consequently, an experiment to not only scale up the production of the protein but also to give a binary answer to the question “can soluble recombinant protein be enriched from a bacterial culture?” was also posed.

During the production of recombinant protein, 10mL of a saturated overnight bacterial culture was added to 2 x 1000 mL 2xYT with ampicillin (200µg/mL) and left to grow for the optimal pre-induction time (3h) (section 3.3.5.1). Protein production was then induced using the optimal concentration (0.25mM) of IPTG (section 3.3.5.2) and the culture subject to a further optimal incubation time (4h) (section 3.3.5.3).

After the purification, dialysis and sterilisation of the enriched recombinant proteins, the resultant preparations were characterised by SDS-PAGE and Coomassie staining (section 3.3.2.1). After Coomassie staining, recombinant proteins were identified at approximately the

predicted apparent molecular weight (figure 3.9, 3.10 and 3.11). Some deviation from the predicted molecular weight was observed and this reflected the nomenclature “apparent molecular weight” adopted by the manufacturers of the pre-stained proteins used to calibrate the SDS gels (*i.e.* the molecular weight markers). This designation refers to the tendency to proteins to run at “approximately” the correct molecular weight and that the electrophoretic retention time of protein samples may also be effected by residual secondary and tertiary structure remaining after SDS and 2-Mercaptoethanol denaturation. Residual secondary and tertiary structure will influence the radius of gyration (R_g) of the protein and its resistance to movement through an acrylamide matrix *i.e.* the SDS-PAGE gel. Consequently very stable proteins may run with an apparently “smaller” molecular weight relative to the molecular weight markers without being degraded. Destruction of acrylamide cross links within the gel matrix can also, in a lane specific manner, also cause proteins to run with a lower apparent molecular weight, as a lack of cross links can lead to a locally larger pore size and hence less resistance to the passage of the protein through the gel. For this reason it is important not to overload the gels, a factor thought to contribute the breaking of bonds within the acrylamide matrix. These factors may have contributed to the molecular weight markers running at slightly different speed from the protein. By using known amounts of bovine serum albumin (BSA) as a standard, densitometry was used to calculate the concentration of recombinant protein.

Various RTAC constructs containing 6His, KDEL or GFP, were expressed and purified. The GFP containing proteins (figure 3.10) were identified at 32kDa and 20kDa, which indicate protein degradation or prematurely truncated protein transcripts (figure 3.10).

3.4.3 Protein detection

Experiments investigating the immunological detection of wild type RTAC (clone 175) and rRTBC (clone 204) proteins were carried out by Western blotting and immuno-detection. However, before the detection of these toxins, bovine serum albumin was used to optimise the transfer conditions utilised during Western blotting. This was deemed necessary after the transfer of material during Western blotting was identified as a rate-limiting step after several unsuccessful attempts to detect rRTAC and rRTBC (clone 204).

In order to optimise the electrophoretic transfer of protein onto a solid phase support (*i.e.* the nitrocellulose membrane), experiments were undertaken using BSA as a substrate as it was: 1) of a constant molecular weight, 2) very ease to obtain in large quantities (aiding detection)

and 3) relatively inexpensive. BSA (figure 3.12) was resolved on two identical 10% (w/v) SDS-PAGE gels. The first gel was subject to Coomassie staining and was documented digitally. The second gel was subjected to Western blotting and stained using Ponceau S. As is evident the proteins were easily detectable and were visible in approximately the same quantities and with approximately the same molecular weight distribution as the Coomassie stained gel (figure 3.12 and 3.14). Further, the transfer time (duration) and protein concentration were also optimised for Western blotting and Ponceau-S staining (figure 3.13). Three identical BSA containing 10% (w/v) SDS-PAGE gels were prepared (figure 3.14) and all three gels were subject to electrophoretic transfer using constant current (400mA) and three different time points (30, 45 and 60minutes). The nitrocellulose membranes were stained with Ponceau-S (figure 3.13) and it was concluded that the 60minute transfer time was optimal when transferring BSA from an SDS PAGE gel to a nitrocellulose membrane.

3.4.3.1 Immuno-detection

Using the anti-RTAC polyclonal primary antibody and an appropriate secondary antibody (HRP-conjugated anti-rabbit IgG) wild type RTAC (clone 175) was detected (figure 3.16). Using an anti-RTBC specific polyclonal primary antibody and an appropriate secondary antibody (HRP-conjugated anti-rabbit IgG) RTBC was detected using the EpiChem BioImaging systems (UVP) (figure 3.18). The manufacturers of the EpiChem BioImaging systems (UVP) state that it should be able to detect up to 2.5ng of protein, however empiric investigation found the system to be sensitive to μg quantities of protein (section 3.3.3, figure 3.16). The sensitivity of the EpiChem BioImaging system (UVP) was of very limited use for our intended application, given that the normal range and limit of detection for proteins by Western blotting and immuno-detection is 1-10ng. Consequently further immuno-blotting experiments were performed using X-ray film to detect photons emitted by the hydrolysis of the ECL reagent by (the secondary antibody conjugated-) HRP. Relative to the EpiChem BioImaging system (UVP), the immuno-detection of recombinant protein using X-ray film was more than three orders of magnitude more sensitive.

3.4.3.2 Optimisation of immuno-detection

Western blotting and immuno-detection is a commonly used method to identify specific proteins within a complex mixture of proteins. This technique has many limitations, such as, without the use of a radioactive secondary, only being able to semi-quantify the amount of

protein detected. During the identification of RTAC and RTBC proteins, three types of primary antibodies and two types of secondary antibodies were used. The primary anti-bodies tested were: anti-6His (monoclonal), anti-RTBC and anti-RTAC (polyclonal) antibodies. The secondary antibodies were: anti-mouse-IgG with and anti-rabbit IgG, both conjugated to HRP.

There are several factors which influences the out come of immuno-blotting experiments, such as polyacrylamide gel composition (% of polyacrylamide, age, buffers), the transfer of resolved proteins onto a nitrocellulose membrane (buffer type, applied current and time), choice of blocking buffer, antibody avidity, washing steps between the incubation periods and detecting method (imaging instrument, X-ray films, exposure time and volume of ECL detection reagents). All the above factors were carefully considered and used to optimise of the conditions and dilutions of both primary and secondary antibodies for successful detection of RTAC and RTBC proteins. The optimum dilutions of each primary and secondary antibodies were determined using bacterial lysates generated from mini-induction experiments.

Anti-6His primary antibody: The manufactures recommended dilution was 1:2000. After applying different dilutions and exposure times to identify rRTBC (clone 204), it was concluded that a 1:5000 dilution of anti-6His and a 10seconds exposure time was sufficient to detect the RTBC and 1:1000 dilution of anti-6His and with 1minute exposure time was required to detect rRTAC (clone 189).

Anti-RTBC and anti-RTAC primary antibodies: The manufactures recommended a dilution of 1:2000. But both antibodies detected rRTBC (clone 204) and rRTAC (clone 189) proteins at a 1:1000 dilution with a 1minute exposure time.

HRP-conjugated anti-mouse IgG secondary antibody: The manufactures recommended dilution was 1:1000 to 1:5000. For both rRTAC (clone 189) and rRTBC (clone 204), 1:1000 ratios were sufficient to detect the proteins.

HRP-conjugated anti-rabbit IgG secondary antibody: The manufactures recommended dilution was 1:5000. For rRTBC (clone 204) 1:5000 ratio and for rRTAC (clone 189) 1:1000 ratios were sufficient for the detection of the target proteins.

3.4.4 Optimisation of bacterial culture conditions using mini-induction experiments

Initially experiments were performed to answer the three questions posed (section 3.4.1.3). However it was also postulated that if indeed recombinant proteins of the predicted molecular weight could be identified, and then it might also be prudent to investigate optimal culture conditions.

As proteins of the predicted molecular weight were identified (in each instance) (section 3.3.5, figures 3.25-3.34), and as these proteins were recognised by the appropriate antibodies after immuno-blotting, the optimisation of culture conditions was undertaken. It should be noted that the mini-induction experiments have limitations and they do not give any insight as to the solubility of the recombinant protein and will only give data pertinent the amount of protein produced by the bacteria. In order to find the optimal conditions for the expression of the desired recombinant proteins (table 3.1), three conditions were optimised at two incubation temperatures (30°C and 37°C).

3.4.4.1 Growth time (pre-induction) (PrIGT)

During the first stage of bacterial growth (lag phase), bacteria adapt to their environment and induce the production of gene products necessary to utilise available carbon and nitrogen sources. In second stage, (log phase or exponential growth phase), bacteria start dividing at an optimal rate. The generation time for *E.coli*, is typically one division every 20minutes under optimal culture conditions during exponential growth phase. The third stage, referred to as stationary phase is characterised by the growth rate of bacteria slowing down due to the depletion of nutrients and the accumulation of toxic metabolic by-products (Nyström, 2004). In the fourth stage, which is a death phase, bacteria die due to the depletion of nutrients and the further accumulation of toxic metabolic by-products.

Generally, during recombinant protein production, the induction of protein expression was initiated in mid or late log phase. Some proteins show high-yield when initiated in early log phase compare to stationary phase. Consequently, it was decided that determining the growth phase of the bacteria would be useful relative to optimising protein yield.

From the bacterial growth curves (figure 3.28), it was determined that, the bacteria reached stationary phase after 2-3h of culture and that this growth was dependent upon the plasmid that the bacteria were carrying (figure 3.28, section 3.3.5.1). This would suggest that the plasmid was influencing bacterial growth.

When optimising the growth time, three time points 2, 3 and 4h were selected. Mini-induction experiments using RTAC encoding plasmids (clones 175 and 189) were performed. SDS-PAGE gels were used to resolve bacterial lysate in order to estimate RTAC protein production at the three time points stated. Protein bands clearly representative of the recombinant RTAC proteins predicted were not clearly distinguished relative to cultures without IPTG (figure 3.25a and b). To overcome this problem, Western blotting followed by immuno-detection was performed (section 3.3.5.1). An anti-6His specific antibody was used to detect rRTAC (clone 189) and wild type RTAC (clone 175) under different growth conditions. The target protein was detected specifically at the predicted molecular weight (monomers at 32kDa and dimers at 62kDa) (figures: 3.25, 3.26 and 3.27). Importantly there were no RTAC bands detected within the GST-GFP (clone 210) expressing culture and in lysate from *E.coli* BL21*DE3 containing no plasmid. When densitometry was used to compare recombinant protein production at different growth times, the optimum growth time for both rRTAC (clone 189), and wild type RTAC (clone 175) at 37°C and 30°C was found to be 2h.

3.4.4.2 IPTG concentration

Unlike lactose and other galactosides, IPTG is a galactose analogue (Herzenberg, 1985). Since it is not metabolised by the cell, the level of induction remains constant following the addition of IPTG to the growth medium (Donovan *et al.*, 1996).

Several factors influence the level of IPTG needed for optimal induction (Donovan *et al.*, 1996). Different range of IPTG concentrations (from 0.1mM to 1mM) were used in expressing the heterogenous protein expression. Here three different concentrations of IPTG were analysed (0.25mM, 0.5mM and 1mM) to induce the expression of rRTAC (clone 189) and wild type RTAC (clone 175). Coomassie stained SDS-PAGE gels (figure 3.29a, and b), displayed no difference in RTAC expression levels in response to varying the IPTG concentration over the range tested. Immuno-blotting was performed (3.3.5.2) using a monoclonal anti-6His-specific antibody. Recombinant proteins were detected at the predicted molecular weight for both rRTAC (clone 189) (figure 3.29e) and wild type RTAC (clone 175) (figure 3.31). At both the temperatures (30°C and 37°C), rRTAC (clone 189) produce a high protein production using 0.25mM IPTG final concentration when compare to 0.5mM and 1mM IPTG concentrations (figure 3.29 and 3.30). For wild type RTAC (clone 175), at both temperatures, 1mM IPTG concentration gave high protein yield (figure 3.31). It was

concluded that the optimal concentration of IPTG was dependent on the biology of the protein being expressed.

3.4.4.3 Post induction growth time (PoIGT)

After protein induction, post-induction growth time (PoIGT) was also investigated. If the PoIGT was short, there was the possibility of low expression levels and if the PoIGT was too long, it may be possible that the depletion of amino acids and the formation of toxic products may result in reduced cell growth rates and bacterial stress response, characterised by enhanced production of protease (which can degrade the expressed protein).

The three post induction growth time points (2h, 3h and 4h) were used to examine the influence of increased PoIGT upon the expression of rRTAC (clone 189). After 4h higher protein expression levels (60%) relative to the 2h and 3h PoIGT were documented (figure 3.32a and b).

After growth at 30°C for both rRTAC (clone 189) and wild type RTAC (clone 175), a 2h PoIGT was optimal. After growth at 37°C, a 4h time point was optimal for both constructs.

Generally the maximum specific growth rate of *E.coli* occurs at temperature of 37-39°C (Donovan *et al.*, 1996). The maximal activity of *lac* and *tac* promoters also occurs at 37-39°C. During these expression experiments, two incubation temperatures were analysed, 30°C and 37°C. It was documented that in all experiments (PrIGT, IPTG concentration and PoIGT) at 37°C, protein production was higher than 30°C. Lower temperatures are favourable, if the proteins are forming aggregates at high temperatures.

The data presented here shows that the culture conditions investigated herein did not provide an obvious increase in recombinant protein yield.

3.5 Conclusions

Plasmids were isolated, sequenced and this data used to produce plasmid maps.

Recombinant RTAC (containing a panel of epitope tags and either the 'Mut' or 'Del' mutations (AA177-182)) and rRTBC (clone 204) were produced and the resulting proteins were soluble and immuno-reactive being recognised by commercial anti-RTAC or anti-RTBC specific antibodies. These constructs displayed immuno-reactive C-terminal epitopes indicating that the transcripts were complete. Examining the apparent molecular weight of

the immuno-reactive constructs (after SDS PAGE and Western blotting) further substantiated this conclusion.

The Western blotting and immuno-detection was optimized using X-ray films and the detection of specific proteins was reproducible. Up to 5ng of target protein was detected using this technique.

After investigating the optimum culture conditions for transgene expression, it was concluded that, for rRTAC (clone 189), a 2h pre-induction growth time, 0.25mM of final IPTG concentration, 4h post induction growth time and 37°C incubation temperature were optimal. For wild type RTAC (clone 175), optimised culture conditions were similar to rRTAC (clone 189), except that 1mM IPTG was optimal than 0.25mM IPTG at both the incubation temperatures.

Protein production was higher at 37°C than at 30°C though a direct comparison of protein production at 37°C and 30°C was not performed.

Chapter 4
Biological Evaluation of Ricin Toxin Proteins

4.1 Introduction

In 1908, Paul Ehrlich introduced the concept of the magic bullet, which proposed the targeting of very specific cell populations prior to exerting a toxic effect (Strebhardt and Ullrich, 2008). A plethora of concepts have been proposed to target a specific population of cells however, to date, all have been found lacking. Examples of cell specific targeting strategies include: using antibodies specific for target cell enriched antigens, targeting receptor populations enriched upon the target cell population using a ligand or through focusing upon another physiologically distinctive phenomena that delineate the target cell population from the rest of the non-target healthy cells within the body *i.e.* an increased doubling time.

Besides having the applications detailed here in (*i.e.* mediating the cytosolic delivery of peptides and proteins), RT has been widely used during the construction of immunotoxins (Shapira and Benhar, 2010). However limited success was achieved utilising this approach. It may be due to the preparation of the immuno-toxins, which often calls for the removal of the binding moiety (*i.e.* RTBC). In the instance of RT based immunotoxin, in the wild type, the binding moiety is critical for A chain internalisation and trafficking of whole toxin to the ER, facilitating the translocation of the A chain into the cytosol. Whilst RTAC displays some toxicity on its own it is several orders of magnitude less toxic than the wild type holotoxin (section 4.3.4) (Virgillo *et al.*, 2010).

In this study recombinant RTAC and RTBC proteins produced in *E.coli* (as discussed and characterised in chapter 3) were tested for cytotoxicity (evaluated *in vitro*). These experiments were designed to test the hypothesis that the mutations made within the active sites of the RTAC mutants would reduce the toxicity of the molecules.

There were several methods available to test the catalytic activity of the recombinant toxins. These include a 28S ribosomal RNA depurination assay (Simpson *et al.*, 1995), an inhibition of protein synthesis assay (Press *et al.*, 1986), LDH assay (Rao *et al.*, 2005) and the MTT assay (Mossman, 1983). RTAC shows catalytic activity when it depurinates the 28S ribosomal subunit (rRNA) at the α -sarcin/ricin loop (A4256). This results in ribosome inactivation, the inactivation of protein synthesis and cell death (Endo and Tsungi, 1986). By estimating the rate of depurination of 28S ribosomal RNA, activity of RTAC can be measured. Equivalently the inhibition of protein synthesis by toxins has been evaluated by applying radiolabelled lucine or methionine onto cells. The principle behind the assay was living cells incorporate radio labelled amino acids into newly synthesized macromolecules

and the amount of incorporation will reflect the synthetic activity and cell number in the well (Spooner *et al.*, 2004). In this study, the MTT assay was performed to estimate the cell viability after treating cells with the recombinant toxins.

During the MTT assay, a water soluble yellow tetrazolium salt (MTT reagent), is reduced by pyridine cofactors like NADH, NADPH (Berridge and Tan, 1999) and mitochondrial dehydrogenases in living cells. This reduction is mediated by opening of a ring structure, which results in the formation of an insoluble, purple, formazan salt. Solvents such as dimethyl sulphoxide (DMSO) can be applied to the cell monolayer at the end of the experiment to dissolve the formazan crystals. Formazan salt production is proportional to viable cell density. Compared to other methods, the MTT assay is rapid and easily accommodates many (*i.e.* 10 x 96 well plates) samples. The absorbance of the formazan in solution can be assayed at 540nm (Mosmann, 1983). The protocol for the MTT assay was described in section 2.2.10.

If the RTAC and RTBC proteins not in an appropriate conformation *i.e.* heterodimers, it was possible that they may not exert optimal toxicity when applied to the cells. By using cRTAC and cRTBC a re-association protocol was established and optimised (Smith *et al.*, 2003). Sub-cellular fractionation was used to confirm the cytosolic location of the RTAC molecule testing the hypothesis that any lack of toxicity resulted after RTAC cytosolic translocation.

Lectinic activity of RTBC was essential not only for cell surface binding but it also play crucial role in intracellular trafficking and ricin cytotoxicity (Newton *et al.*, 1992). RTBC contains three galactose binding sites located in B chain subdomains, through which it binds to galactose molecules on cell surface. When mutations introduced into the B chain binding sites, the cytotoxicity of mutant RTBC-RTAC was reduced 20 times (Frankel *et al.*, 1996). Due to the importance of RTBC lectinic activity during cell intoxication, in this study rRTBC (clone 204) and cRTBC were analysed for their lectinic activity.

Fluorescence microscopy has wide applications during the imaging of fluorescently labelled lipids, proteins and polymers within specific sub-cellular compartments. In this study, immuno-fluorescence microscopy was used to evaluate the intracellular localisation of RTBC. Inside the cell, immuno-reactive proteins (EEA-1, GM130 and TfR etc), which delineate specific organelle function, were used as markers to define intracellular compartment(s). Generally two strategies were used during the fluorescence identification of sub-cellular compartment. The first strategy required the direct identification of a compartment by detecting a fluorescent physiological probe or fluorophore conjugated to antibody. The second required the indirect identification by immuno-labelling of the sample

with primary antibody, present within the target compartment. The primary antibody was then detected using a fluorophore labelled secondary antibody (Richardson *et al.*, 2004; Ramos-Vara, 2005; Watson *et al.*, 2005).

Sub-cellular fractionation was developed to monitor the translocation of material through (and delineate) specific intracellular compartments (Richardson *et al.*, 2010). This technique has wide application during the characterisation of intracellular trafficking pathways such as the endocytic and secretory pathways. Here, sub-cellular fractionation was used to investigate the trafficking of a heterodimeric mix of RTAC and RTBC using the Vero cell line. Western blotting was used to detect the presence of RTAC and RTBC chain within specific fractions over time. Here, as internal controls three antibodies specific for: the transferrin receptor (TfR), lactate dehydrogenase (LDH), and early endosome antigen-1 (EEA1) were used to monitor the success of the fractionation procedure. These antibodies were produced commercially.

Transferrin receptor (TfR) is a receptor for the iron carrier protein transferrin. It is expressed in most cells and tissues, especially proliferating cells. Transferrin is responsible for the import of iron into the endocytic pathway where, under acidic pH iron associated molecules disassociate from the transferrin carrier protein (Feelders *et al.*, 1999). Typically the TfR occupies the early sorting endosome and recycling endosome and is an integral membrane protein, which may be used to denote the presence of membrane components.

Human lactate dehydrogenase (LDH) is an enzyme, which catalyzes the interconversion of pyruvate and lactate with concomitant interconversion of NADH and NAD⁺. It exists in four distinct enzyme classes. LDH is immuno-specific for LDH isoenzymes containing the H-subunit. It acts as a cytosolic marker (Seedorf *et al.*, 1986).

Early endosome antigen 1 (EEA1) is a peripheral membrane protein present in cytosol and membrane fractions. EEA1 forms homo oligomers acting as a tethering protein between perspective fusion partners (Mu *et al.*, 1995). EEA1 is also an effector of the small GTPase Rab5, which regulates homo- and heterotypic fusion to the early sorting endosome.

Even though sub-cellular method is labour intensive and possibility of cross-contamination of different fractions (*i.e* membrane and cytosolic fractions) it is possible to quantify the polymer or protein concentration in different cellular compartments inside the cell (Richardson *et al.*, 2008). The protocol adopted herein eliminates some of the more labour intensive parts of classic, DeDuvian sub-cellular fractionation and eliminates some of the possible shortcomings at the cost of resolution (Richardson *et al.*, 2008).

The growth characteristics of cells grown in culture can be described by plotting cell number against time. The “growth curve” that this data describes can yield information about the doubling time of the cells. Different cell types grow at different rates and cell number can be estimated either by direct counting or via the MTT assay. The MTT assay can also be used to assess cytotoxicity (section 2.2.10)

In this chapter following questions were addressed:

1. Does recombinant RTBC have lectininc activity?
2. Is recombinant RTAC non-toxic?
3. Can recombinant RTAC re-associate with commercial RTBC?
4. Does recombinant RTAC traffic to the cytosol?

4.2 Materials and methods

Growth curve

The MTT assay was used to calculate the doubling time of B16 and Vero cells as follows: After trypsinization, cells were seeded into sterile, flat-bottomed 96 well microtiter plates at density of 1000 cells per well and were grown using standard incubation conditions (37°C, 5% (v/v) CO₂). After 24h, 10µL (50µg) of MTT reagent (5mg/mL in sterile PBS) was added to the 2nd row of a 96 well plate and the plate left under standard incubation conditions for 4h. After the incubation period, media was removed from the wells containing MTT (2nd row) and 100µL of dimethylsulphoxide (DMSO) was added (under aseptic conditions). Cells were incubated using standard incubation conditions for a further 30minutes prior to the absorbance of the purple formazan salt being measured at 540nm using a Multiskan EX Microplate Photometer (Thermo Scientific, Essex, UK). During the above procedure good aseptic technique was practiced in order to exclude any contaminants. The same procedure was applied to the rest of the wells (each day one well up to 10 wells). A graph depicting absorbance and time (number of days) was plotted. Error bars were plotted showing the standard error of the mean (n=8).

Measuring *in vitro* cytotoxicity of enriched recombinant proteins using MTT assay

The cytotoxicity of the recombinant RTAC analogues, recombinant RTBC analogue (clone 204), commercial RTAC (Sigma Dorset, UK), commercial RTBC (Vector laboratories, CA, USA), re-associated mutant RTAC-commercial RTBC heterodimers and commercial RTAC-commercial RTBC heterodimers was assessed in both B16 and Vero cells as described in the methods section (section 2.2.10).

Re-association of RTAC and RTBC

If RTAC and RTBC were mixed together, there was the possibility of forming heterodimers (RTAC-RTBC) and homodimers (RTAC-RTAC, RTBC-RTBC). This would potentially reduce the signal to noise ratio from any experiment in which the mixture was used, as potentially 66% of the added protein could be associated as a homodimer. To obtain an enriched heterodimeric preparation (RTAC-RTBC), the re-folding of the A and B chains was explored. The protocols for re-association were described in the methods section 2.2.11.

Establishing the intracellular localization of RTAC using crude Sub-cellular fractionation

The sub-cellular distribution of rRTAC (clone 189)-rRTBC (clone 204) molecules was established in Vero cells over time. The seeding of the Vero cells, applying the rRTAC (clone 189)-rRTBC (clone 204) and sub-cellular fractionation was performed as described in methods section (section 2.2.12). After sub-cellular fractionation, the pellet (which contains membrane bound organelles) and supernatant fraction (a crude cytosolic, soluble fraction) were separated. The supernatant fraction was subjected to trichloroacetic acid (TCA) precipitation and the resulting pellet dissolved in 100 μ L LSB and 20 μ L of BME. The pellet was dissolved in 100 μ L LSB and 20 μ L of BME. Each fraction (20 μ L) was resolved using a 10% (w/v) SDS-PAGE gel after electrophoretic separation (100V for 80 minutes) prior to the proteins being transferred onto nitrocellulose membrane (Western blotting). After protein transfer to the nitrocellulose membrane, non-fat dried milk (Marvel; TESCO, Kent, UK) (5% (w/v) dissolved in PBS containing TWEEN 20 (0.01 % (v/v))) was applied as a block. The blocking solution was also used to dilute (individually) the primary antibodies used to characterise the fractionation as well as those used to detect the RTAC and RTBC proteins. Anti-RTAC, anti-RTBC, anti-LDH, anti-TfR, anti-EEA1 were diluted as described in the methods section (section 2.2.7). Membranes were incubated with each antibody dilution for

1h at 37°C in an orbital shaker (200rpm). The blots were removed and washed three times with PBS-TWEEN 20 (0.01%). Secondary antibodies were also diluted in non-fat dried milk as before and applied to the blots. The blots were incubated for 1h at 37°C in the incubator as before. After the incubation blots were washed three times with PBS-TWEEN 20 (0.01% (v/v)). Equal volumes (0.5mL each) of ECL detection reagents (GE Healthcare, Buckinghamshire, UK) were added to the blots as per the manufacturers instructions and resulting signal was captured using X-ray films (Scientific Laboratory Supplies Ltd, Nottingham, UK) and bands were observed after developing the X-films in dark room as described in section 2.2.8.

The position of the bands reviewed by ECL detection was recorded relative to the positions of pre-stained molecular weight markers (Spectra Multi-colour Broad-range protein ladder, Fermentas, Cambridgeshire, UK).

Evaluation of lectinic activity of recombinant and commercial RTBC

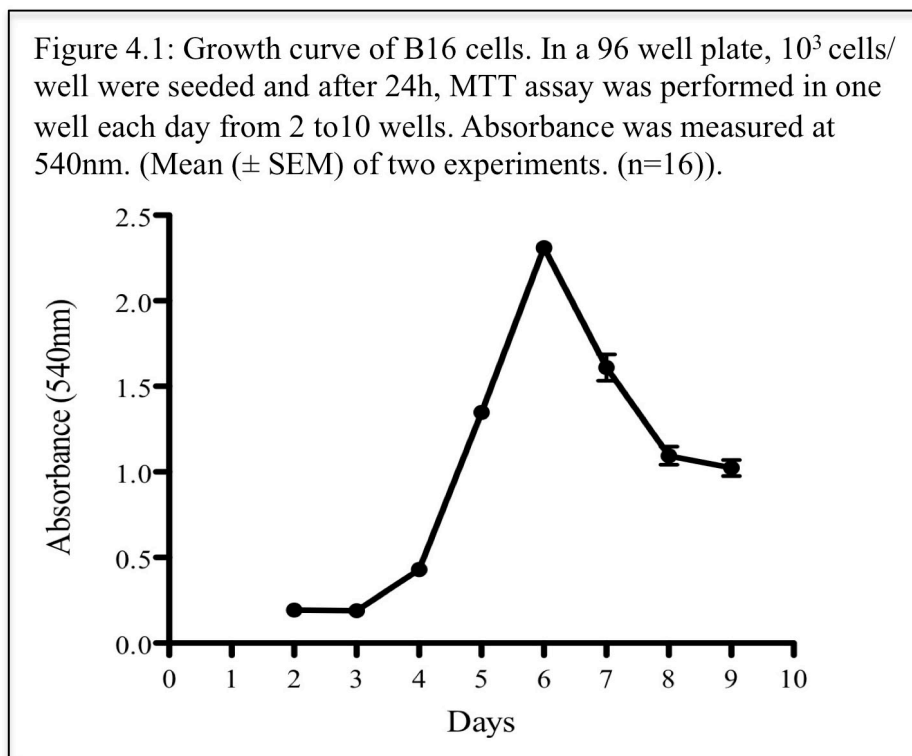
α -Lactose-agarose saline suspension (Sigma, Dorset, UK) was used to evaluate the lectinic property of rRTBC (clone 204) and cRTBC. Stock solutions both cRTBC (Vector laboratories Ltd, Peterborough, UK) and rRTBC (clone 204) (10 μ g/mL) were prepared separately in 1xPBS. From each stocks solution, 10 μ L was collected as input (100ng) and transferred into fresh Eppendorf tubes and labelled them as input. In two fresh Eppendorf tubes, 50 μ L of α -Lactose-agarose saline suspension was transferred and washed three times with 1xPBS before adding to rRTBC (clone 204) and cRTBC separately to each Eppendorf tube. After 10minutes incubation at room temperature with gentle shaking, two Eppendorf tubes were centrifuged for 1minute using table micro centrifuge. Supernatant from each Eppendorf tube was collected separately into fresh Eppendorf tubes and labelled them as depleted. 5 μ L of beads from each Eppendorf tube were collected and transferred into fresh Eppendorf tubes and labelled them as beads before elution. Rest of the beads in each Eppendorf tube were washed three times with 1xPBS and to each tube 80 μ L of 75mM lactose was added and incubated for 10minutes at room temperature. Again centrifugation was performed for 1minute and the supernatant (elution) was collected from each tube and transferred into fresh Eppendorf tubes. Again 5 μ L of beads were also collected from each tube and labelled them as beads after elution. Each collected fractions from both Eppendorf tubes were dissolved in suitable volumes of LSB and BME to give final concentration of

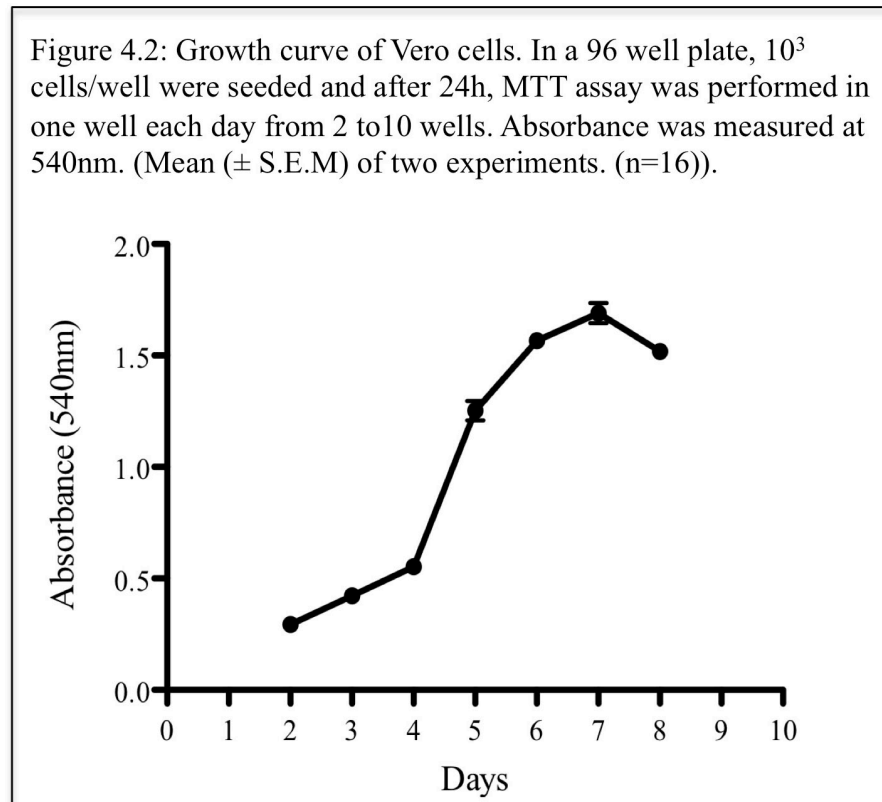
RTBC (approximately) 100ng for evaluation using SDS-PAGE and Western blotting (section 2.2.6 and 2.2.7).

4.3 Results

4.3.1 Assessing B16 and Vero generation time

Growth curves of both B16 and Vero cells were plotted using the values obtained from the MTT assay, which was performed as described in section 4.2. Initially, growth rate of B16 cells was slow (lag phase) but after 3 days, growth was increased exponentially (from day 4 to day 5). The doubling time was calculated using the increase in absorbance (from 0.45 to 1.35), in exponential phase, which was 24h. For Vero cells also the initial growth was slow, but after 3 days the growth was increased exponentially. The doubling time was 24h, as the absorbance increased from 0.6 to 1.2 in exponential phase (from day 4 to 5).



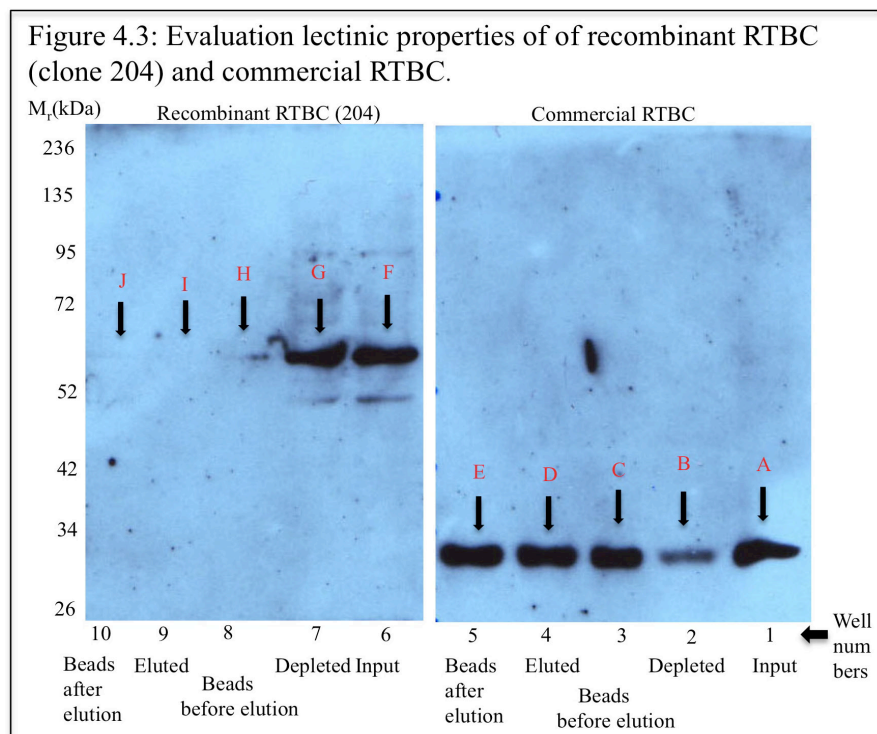


4.3.2 Evaluation of RTBC lectinic activity

During the assessment of rRTBC (clone 204) and cRTBC (Vector laboratories Ltd, Peterborough, UK) lectinic activity, α -Lactose-agarose saline suspension (Sigma, Dorset, UK) was used to immobilize the RTBC protein. Here commercially available, fully glycosylated RTBC was used as a positive control relative to rRTBC (clone 204) made in *E.coli*. A detailed protocol describing the immobilisation (binding), eluting and detecting of the protein to and from a solid-phase support was previously described (section 4.2). After elution with 75mM galactose, RTBC was detected by Western blotting using a 1:1000 dilution of a RTBC specific primary antibody (table 2.2) followed by a 1:2000 dilution of a anti-rabbit IgG specific secondary antibody conjugated with HRP (table 2.2).

It was observed that (figure 4.3) the non-glycosylated rRTBC (clone 204) lacked lectinic activity, which was concluded from the fact that initially the rRTBC (clone 204) could only be detected after hybridisation with the solid phase support at a very low level (figure 4.3, well 8, arrow H) relative to both the input and the control (figure 4.3, well 6, arrow F) and that the eluted fractions (figure 4.3, well 9, arrow I), contained no detectable rRTBC (clone

204). The cRTBC could be detected binding to the solid phase support (figure 4.3, well 3, arrow C) and this interaction was seen to be specific as the cRTBC could be eluted in a predictable way, using a binding competitor introduced to the mobile liquid phase (75mM galactose) (figure 4.3, well 4, arrow D). This empirical result indicates that the positive control (cRTBC) demonstrated specific lectinic activity whereas the rRTBC (clone 204) did not.



4.3.3 Re-association of mutant RTAC and commercial RTBC

As the rRTBC (clone 204) displayed significantly reduced lectinic activity relative to commercially available RTBC, the decision was taken to use the commercially available protein when lectinic activity (*i.e.* cell binding and Golgi and ER translocation) to evaluate RTAC cytotoxicity. Whilst some lectinic activity was demonstrated by the rRTBC (clone 204) it was likely that this protein would give an unacceptably low level of ER translocation (potentially giving rise to false negative results).

In order to provide a positive control describing wild type RTAC and RTBC association, *i.e.* making an enriched preparation of heterodimeric RTAC and RTBC (wild type RT), cRTAC and RTBC were re-associated (section 2.2.11.). To achieve this, cRTAC (Sigma, Dorset, UK) was used to re-associate with cRTBC (Vector laboratories Ltd, Peterborough, UK). As this

would generate a substance regulated by both the Chemical Weapon Convention and part 7 of the Anti-Terrorism Crime and Security Act 2001, licences were obtained and the appropriate records kept.

After the elution of re-associated protein using 75mM galactose, samples were analysed by Western blotting and immuno-detection were used to analyse the presence of RTAC or RTBC in the following fractions: input (100ng), beads before elution (20 μ L), eluted fractions (20 μ L), beads after elution (20 μ L), and wash (20 μ L)) using primary antibodies specific for both RTAC (1:1000 dilution) and RTBC (1:1000 dilution) (section 2.2.6 and 2.2.7). A 1:2000 dilution of the anti-rabbit IgG-conjugated secondary antibody was used.

The empirical data presented here (figure 4.4), shows that the eluted fractions contained re-associated, heterodimeric protein as detected by Western blotting *i.e.* cRTBC (figure 4.4, well 3, arrow C) and cRTAC (figure 4.4, well 8, arrow H).

Having achieved the re-association and isolation of a heterodimeric cRTAC and cRTBC complex and its successful characterisation by Western blotting, the next step in characterising mutant, recombinant, de-toxified RTAC was taken. This was to form heterodimers containing, instead of cRTAC, detoxified, rRTAC (clone 189).

Initially rRTAC (clone 189) was chosen, as it contained a C-terminal KDEL sequence as well as a 6His motif. The literature describes a C-terminal KEDL sequence enhancing the cytotoxicity of RT constructs (Wales *et al.*, 1993). Here it was hypothesized that presence of KEDL may enhance the trafficking of rRTAC constructs from Golgi to ER.

When the re-association of rRTAC (clone 189) and cRTBC was performed, the same protocol was followed as previously described (section 2.2.11) except that in this instance 10 μ g of cRTBC and 50 μ g of rRTAC (clone 189) were used. SDS-PAGE and Western immuno-blotting was performed as described in section 2.2.6 and 2.2.7 to analyse the samples: input (100ng), beads before elution (20 μ L), eluted fractions (20 μ L), beads after elution (20 μ L), and wash (20 μ L). From the figure 4.5, it was observed that in eluted fraction from the solid-phase support, both cRTBC (figure 4.5, well 3, arrow C) and rRTAC (figure 4.5, well 8, arrow H) were detected at their predicted molecular weight. Having now demonstrated that it was possible to re-associate enriched hetero dimeric rRTAC and cRTBC proteins, their cytotoxicity could be tested *in vitro*.

Figure 4.4: Re-association of commercial RTAC and RTBC. Re-associated protein was eluted with 75mM Galactose and cRTAC and cRTBC were detected in eluted fractions using Western blotting using specific antibodies (anti-RTAC and RTBC).

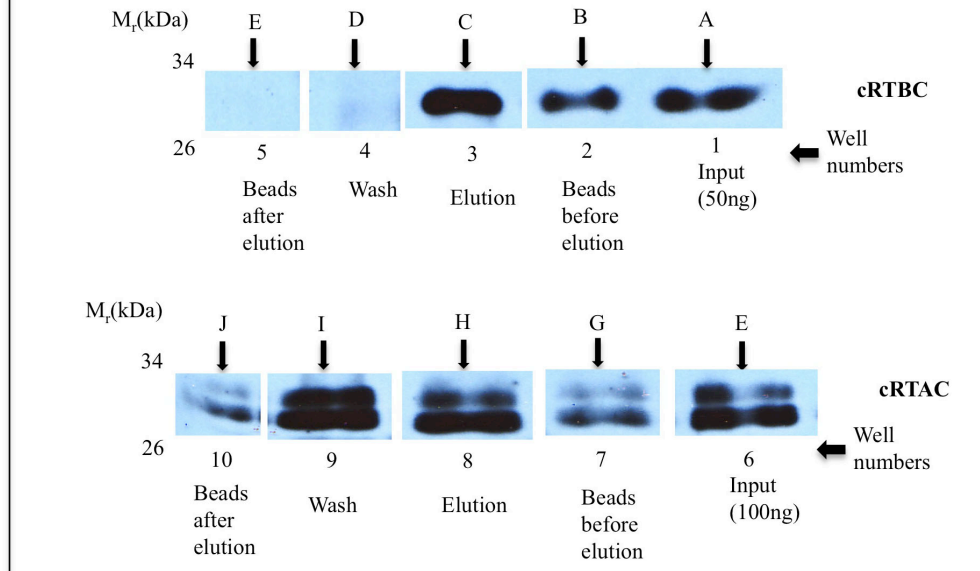
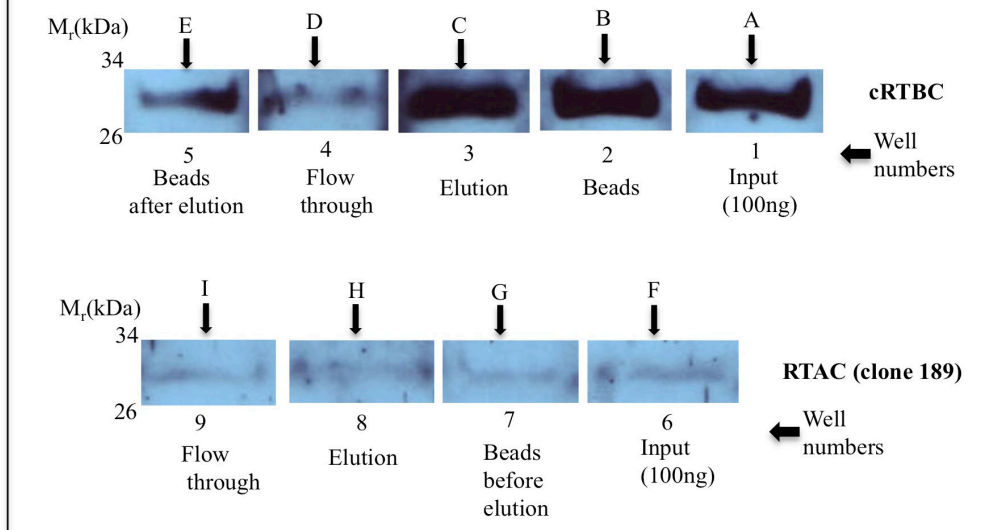
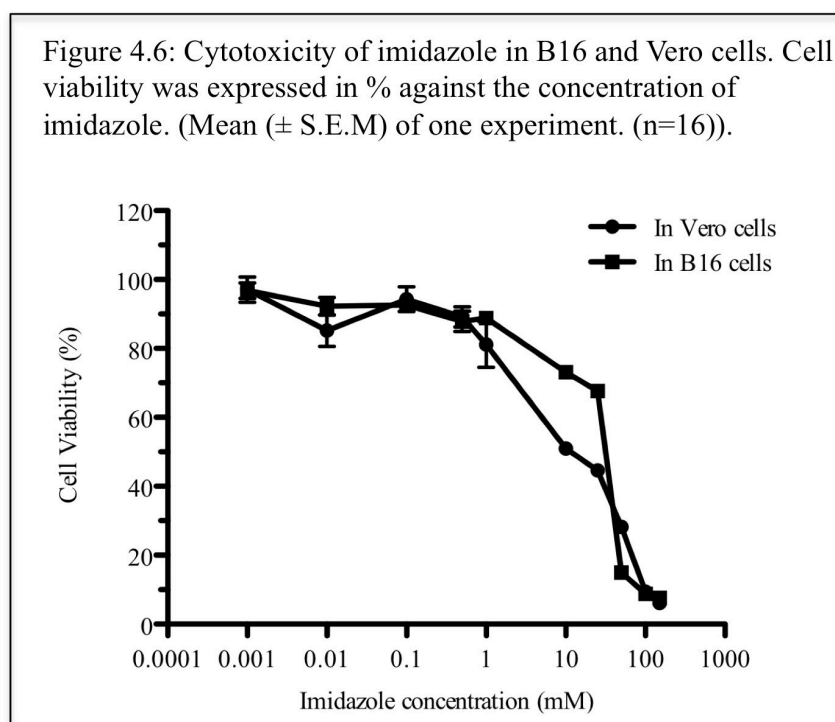


Figure 4.5: Re-association of mutant RTAC (clone 189) and cRTBC. Re-associated protein was eluted with 75mM Galactose. RTAC and cRTBC were detected in eluted fractions using Western blotting using specific antibodies (anti-RTAC and RTBC).



4.3.4 Toxicity studies of recombinant proteins

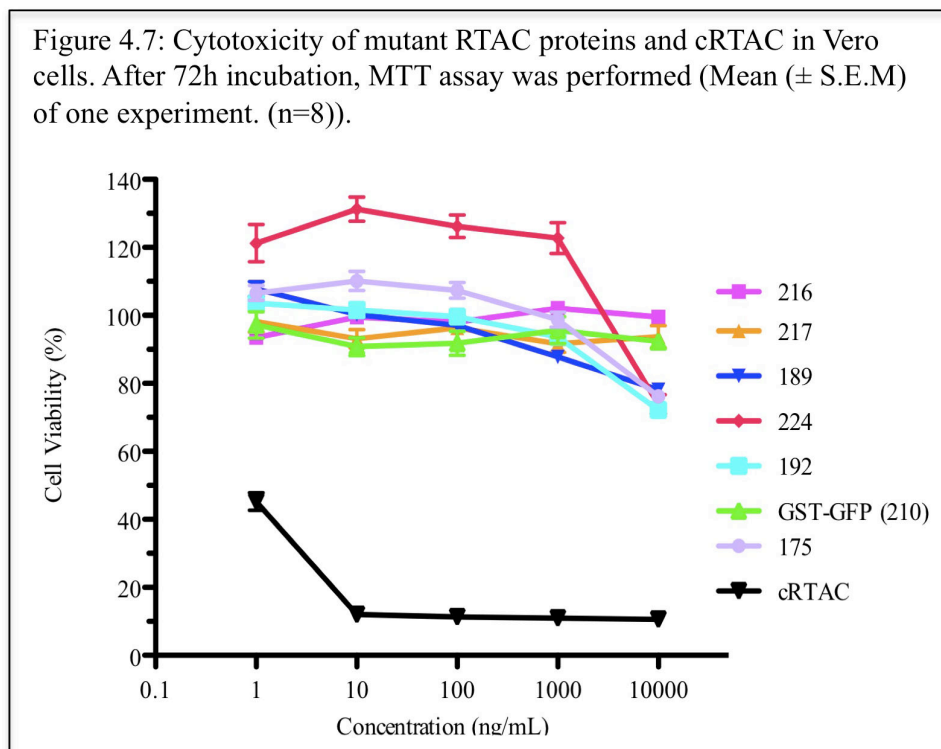
During the purification of 6His tagged recombinant proteins, imidazole (100mM to 150mM) was used to elute the proteins from the solid phase support (both Talon-coupled cobalt (CLONTECH, Takara Bio Europe S.A.S, France) or Ni-sepharose resin (GE healthcare, Buckinghamshire, UK) were used). Before performing the cytotoxicity studies (section 2.2.10) of recombinant proteins, imidazole toxicity was evaluated at different concentrations (0.5mM to 100mM) in B16 and Vero cells. The MTT assay was performed as described in section 2.2.10. From the figure 4.6, it was observed that, at a concentration of 150mM (6.8mg/100 μ L), imidazole was highly toxic to both B16 and Vero cells. With lowering concentrations, the toxicity was decreased. IC₅₀ of the imidazole was 53.64(\pm 3.74)mM in B16 cells and 16.44(\pm 1.92)mM in Vero cells.



As these molecules (rRTAC, rRTBC) were being evaluated within a therapeutic context, toxicity was evaluated under a variety of conditions:

Recombinant RTAC constructs: The main objective of this experiment was to analyse, if the mutated RTAC constructs has any cytotoxicity compared to cRTAC. After 72h incubation with Vero cells, RTAC toxicity was evaluated using MTT assay (section 2.2.10). From the figure 4.7, it was observed that rRTAC constructs did not show cytotoxicity up the

concentration ranges tested (10 μ g/mL). But the cRTAC showed high cytotoxicity. IC₅₀ was recorded as 1.81(\pm 0.15)ng/mL.



Cytotoxicity of heterodimers: By combining the rRTAC and rRTBC in stoichiometrically equal quantities (10 μ g/mL of both rRTAC and rRTBC), the cytotoxicity was evaluated in both B16 and Vero cells with 48h incubation time (1h pulse in presence of 1xPBS, then cells were incubated in complete media) (section 2.2.10).

From the figure 4.8 and 4.9, it was observed that all mutant RTAC constructs when applied together with rRTBC (clone 204) were non-toxic in both Vero and B16 cells. Here rRTBC (clone 204) alone was also analysed and did not show any cytotoxicity over the concentration ranges tested. This preliminary data was generated using proteins that were not re-associated but mixed together in the interests of time.

Recombinant, enriched green fluorescent protein expressed in frame with glutathione-S-transferase (GST-GFP) didn't show any cytotoxicity when exposed to B16 and Vero cells over a similar concentration range to RT, and served as negative control. PEI and dextran (section 6.3.1) have also been used as a positive and negative control for cell toxicity and were used to standardise these assays.

Figure 4.8: Cytotoxicity of mutant RTAC and rRTBC in Vero cells. After 48h incubation, MTT assay was performed (Mean (\pm S.E.M) of one experiment. (n=8)).

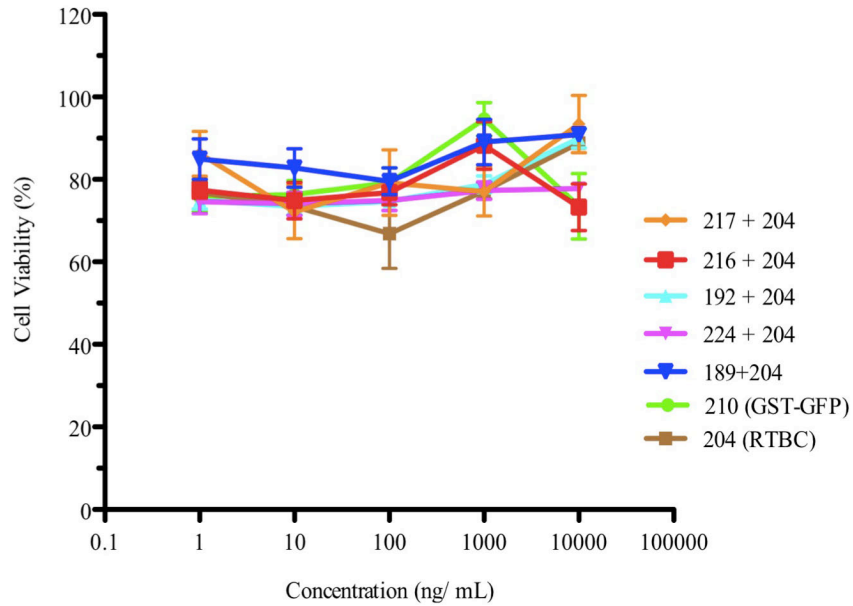
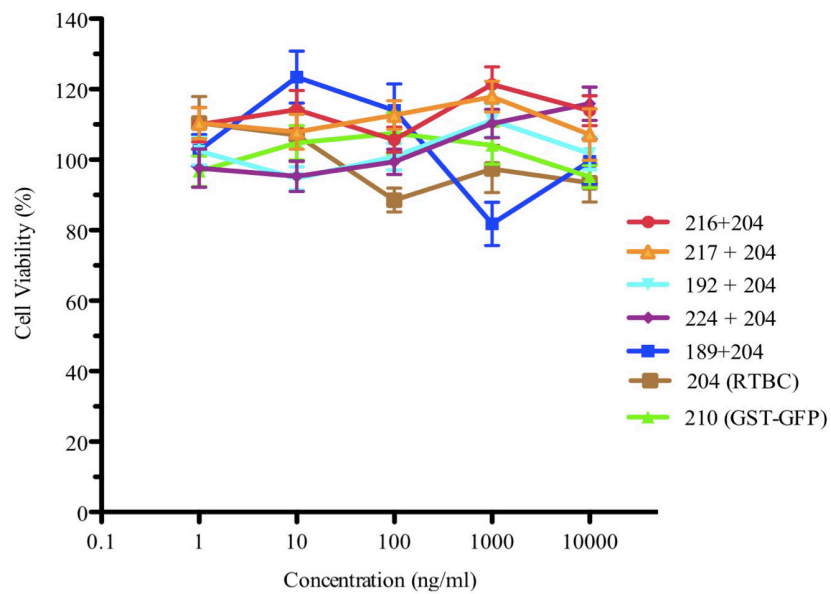
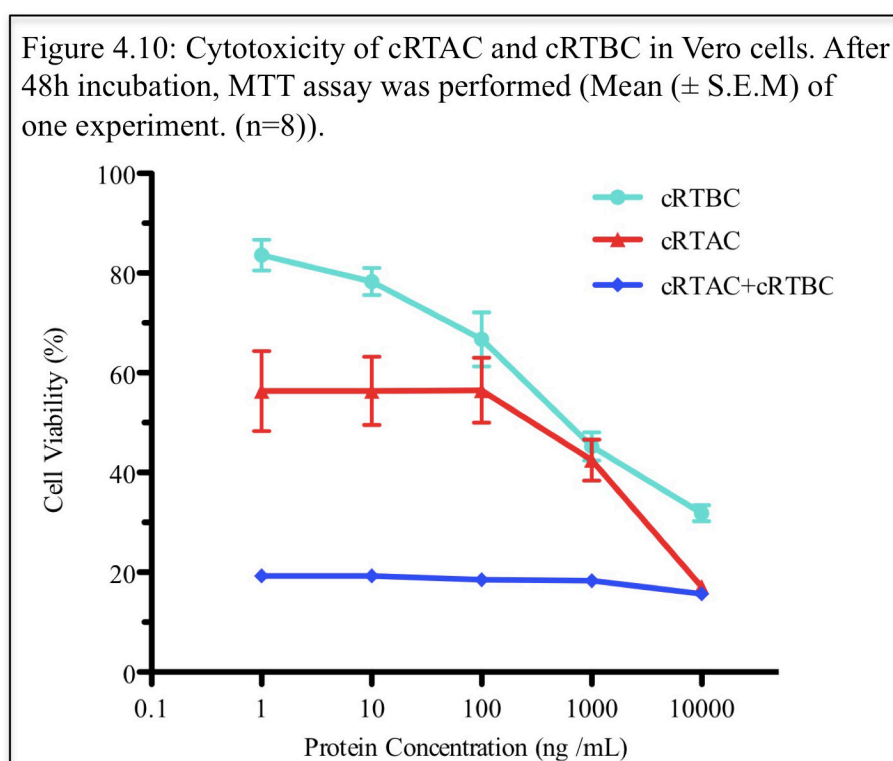


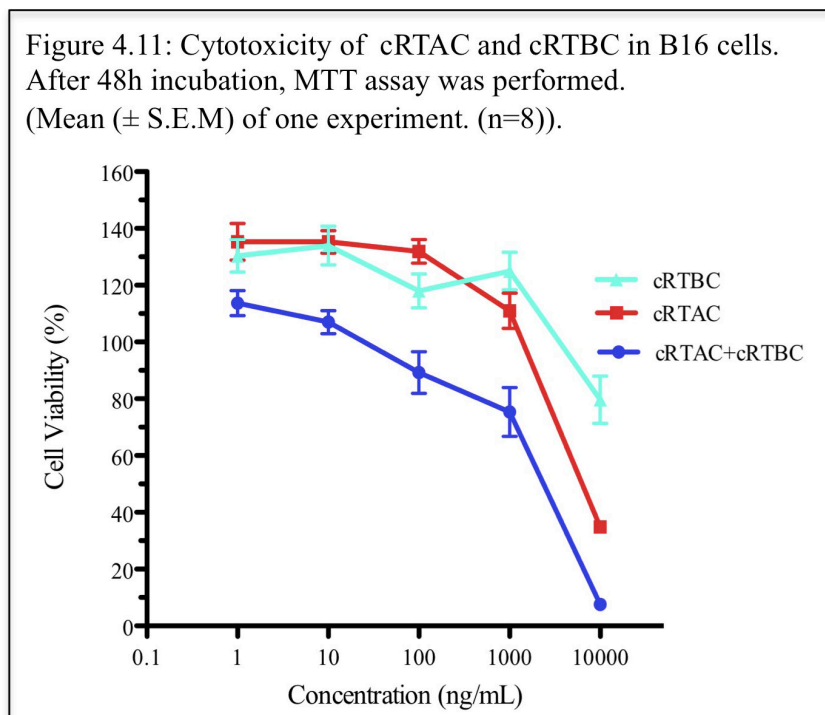
Figure 4.9: Cytotoxicity of mutant RTAC and rRTBC in B16 cells. After 48h incubation, MTT assay was performed (Mean (\pm S.E.M) of one experiment. (n=8)).



Using cRTAC and cRTBC, a similar experiment to that described above was performed. From the figure 4.10, it was observed that cRTAC together with cRTBC (10 μ g each) was highly toxic to Vero cells. The cRTAC alone was also cytotoxic (figure 4.7). The cRTAC preparation was documented with an IC₅₀ value of 1.7(\pm 1.16) μ g/mL. The cRTBC showed some degree of cytotoxicity as 50% cell growth was inhibited at 2.80(\pm 1.32) μ g/mL. The IC₅₀ of the mixture of cRTAC and cRTBC was below 1ng/mL (figure 4.10).



When assayed in B16 cells, cRTAC together with cRTBC was also highly toxic (IC₅₀: 4.15(\pm 0.12) μ g/mL) (figure 4.11). The cRTAC preparation also showed considerable cytotoxicity (IC₅₀: 8.55(\pm 0.35) μ g/mL). The cRTBC preparation didn't show as much toxicity as it exerted in Vero cells.



Cytotoxicity of re-associated, isolated, enriched heterodimers of rRTAC (clone 189) and cRTBC: These experiments were performed in order to assess the effect of re-associated between rRTAC (clone 189) and cRTBC upon mammalian cells. It was hypothesized that after introducing mutations and deletions in active site region (AA 177-182) the rRTAC should not show cytotoxicity. From the figure 4.12, it was observed that in Vero cells, re-associated rRTAC (clone 189)-cRTBC showed IC_{50} of $0.39(\pm 0.04)\mu\text{g/mL}$. The cytotoxicity was partly attributed to cRTBC, which was also showing some degree of cytotoxicity (IC_{50} of $0.70(\pm 0.04)\mu\text{g/mL}$). Re-associated cRTAC-cRTBC was highly toxic even at 0.1ng/mL concentration. IC_{50} could not be determined as the cell viability was below 50% even at 0.1ng/mL .

In B16 cells, re-associated rRTAC (clone 189)-cRTBC was not toxic over the concentration range tested ($1\mu\text{g/mL}$), whereas re-associated cRTAC-cRTBC was highly toxic to B16 cells (IC_{50} of $0.79(\pm 0.01)\mu\text{g/mL}$).

Figure 4.12: Cytotoxicity of re-associated cRTAC-cRTBC and rRTAC (clone 189)-cRTBC in Vero cells. After 72h incubation, MTT assay was performed. (Mean (\pm S.E.M) of one experiment (n=8)).

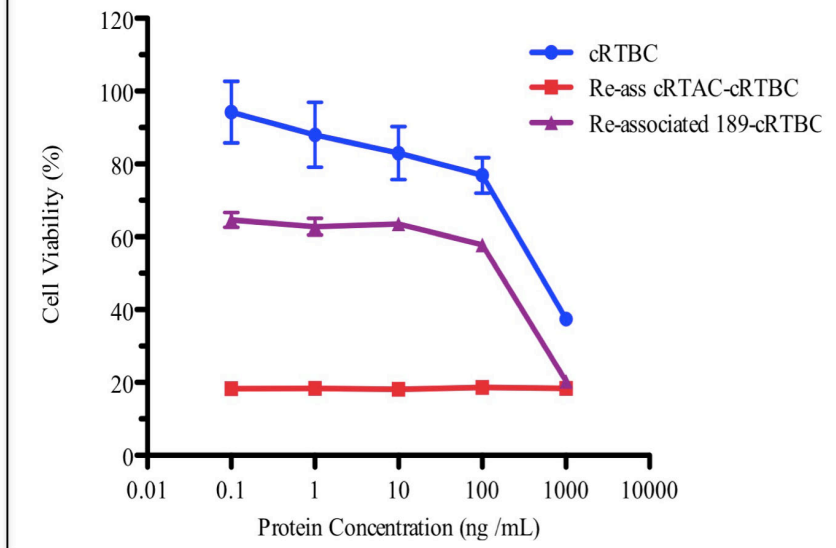
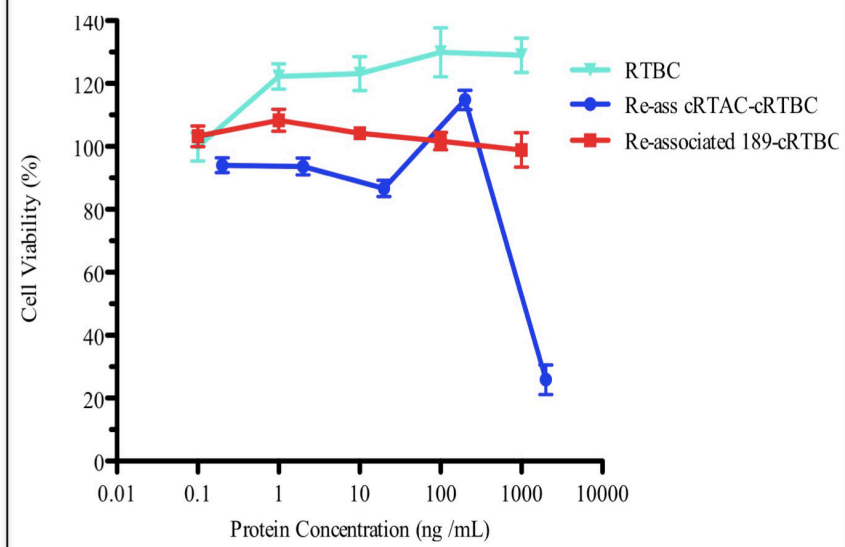
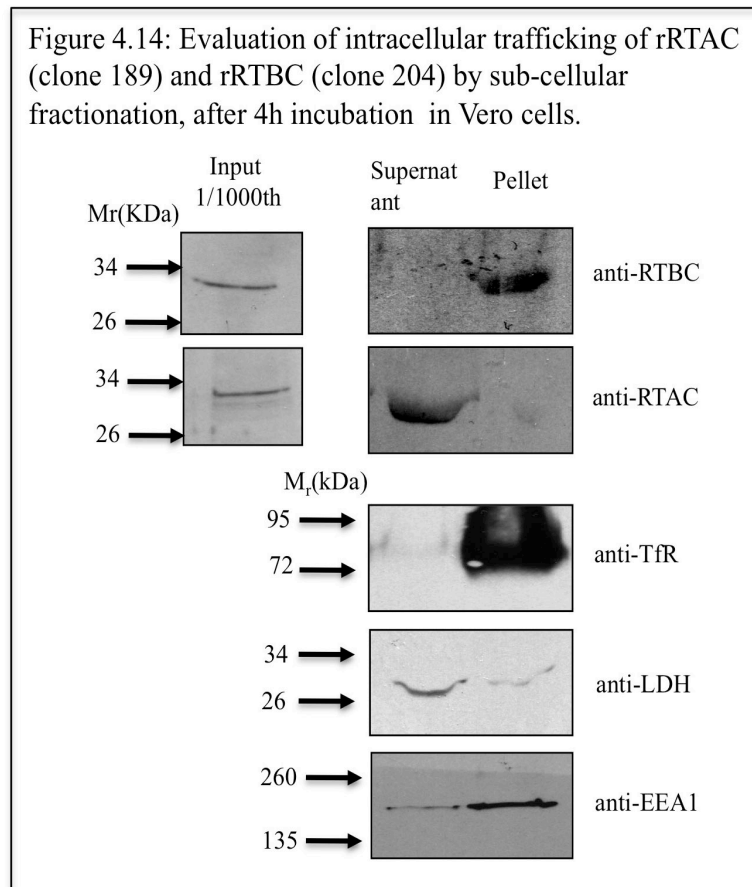


Figure 4.13: Cytotoxicity of re-associated cRTAC-cRTBC and rRTAC(clone189)-cRTBC in B16 cells. After 72h incubation, MTT assay was performed. (Mean (\pm S.E.M) of one experiment (n=8)).



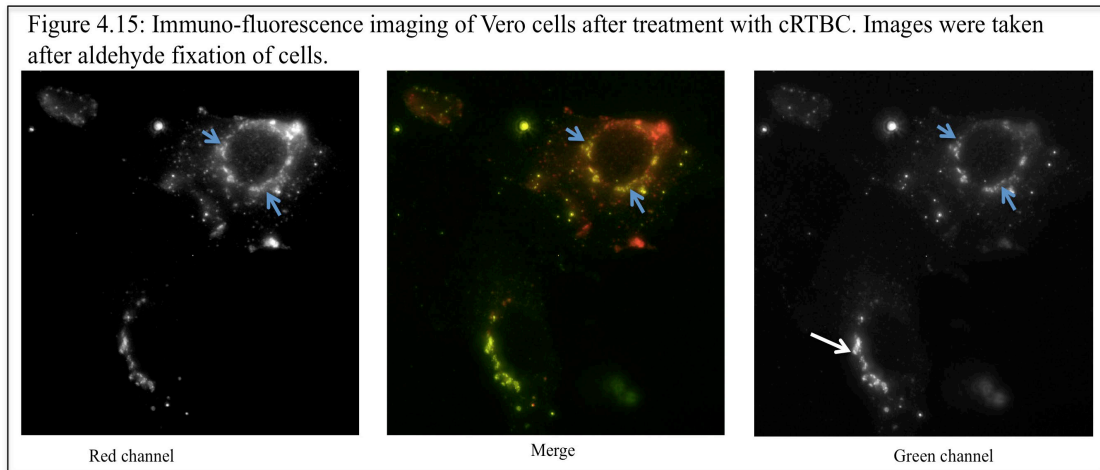
4.3.5 Sub-cellular fractionation

Sub-cellular fractionation and further analysis of the membrane and pellet fractions were performed as described in section 2.2.12. After 4h, rRTAC (clone 189) was detected in the cytosolic fraction and rRTBC (clone 204) was detected in membrane fraction (figure 4.14). Compared to cytosolic fraction, rRTAC (clone 189) can also be found in membrane fraction at very low levels (4.4%). The similar pattern observed with rRTBC (clone 204), it was found in cytosolic fraction at low level (1.9%). Controls used to characterise the degree of enrichment within each fraction showed that there was some cross-contamination of membrane proteins in the cytosolic fraction and cross-contamination of the cytosolic marker within the membrane fraction. It is likely that introducing a washing step to remove any co-fractionation of cytosolic proteins and keeping the experiment at 4°C may solve this problem. Even in light of the low marker contamination (*i.e.* LDH, TfR and EEA1) what is obvious is the localisation of RTAC to the cytosol and its enrichment beyond the level of membrane protein contamination (figure 4.14). This experiment needs to be repeated before these results can be published, however to do give a preliminary indication that the trafficking of the RTAC mutants generated herein is similar to that of the wild type RTAC. As predicted the integral membrane protein and membrane marker TfR, was enriched predominantly within the membrane fraction. Compared to membrane fraction there was small amount of TfR was documented in cytosolic fraction (2%). The soluble protein lactate dehydrogenase (LDH) was enriched within the soluble (cytosolic) fraction and LDH (25%) was also detected in membrane fraction. The peripheral membrane protein early endosome antigen-1 (EEA-1), which served as a positive control, was detected (as would be predicted) both in membrane and cytosolic fraction.



4.3.6 Immuno fluorescence microscopy

The trafficking of both cRTBC and rRTBC (clone 204) was analysed using Vero cells by fluorescent microscopy. Cell seeding, the dosing of proteins and fixing of cells were performed as described in 2.2.14. From the figure 4.15, it was observed that after 20minutes incubation, cRTBC was co-localising with the trans-Golgi marker TGN46 (Prescott *et al.*, 1997) (figure 4.15). When rRTBC (clone 204) was applied to cells it did not show any co-localisation with TGN46 (data not shown).



4.4 Discussion

4.4.1 Growth curve

The growth of mammalian cells in culture can be divided into four stages: lag phase, log phase, stationary phase and death phase. Lag phase, shows a slow increase in cell number. During this period cells adapt to the culture conditions and replace elements of the glycocalyx lost during trypsinization. Cells in lag phase may also up-regulate genes that are able to more efficiently utilize the available carbon and nitrogen sources. In log phase cells grow exponentially, having attained optimal the gene expression to utilise available resources. The length of the log phase depends on several factors like cell density and the growth rate (doubling time) of the cells as well as the availability of resources. It is the optimal period for sampling since viability is high. During stationary phase, cells are normally confluent and growth rate drops to between 0-10% of its optimal level. Once space, nutrients and toxic metabolic products become rate limiting, cells enter a death phase. Decrease in growth rate can be caused by density dependence and density independent factors. Density dependent factors include growth factors and nutrients, which deplete when cell population increases. A steady state in cell number can also be regulated by contact inhibition.

As doubling time is an important characteristic and individual to all cell types, it was determined for all of the cell lines used herein. This allowed an accurate estimation of cell seeding densities for subsequent experiments and the establishment of culture conditions that prevented the cells from becoming overgrown.

B16 (Murine melanoma) cells were well characterised in the literature and have been used for the study of experimental cancer therapies. B16F1 and B16F10 cells originate from B16 melanoma cells but differ in number of selections performed *in vivo* and *in vitro*. B16 F10

metastasized exclusively in the lung whereas B16F1 can form secondary tumours in multiple organs. Here B16 cells were used as they are well characterised and cytotoxicity of parent PAA polymers was performed in this cells and it will be useful to compare the cytotoxicity of novel PAA polymers in this cells. From the growth curve (figure 4.1), it was observed that, there was small increase in absorbance (which corresponds to the cell growth) in lag phase. But in the log phase, there was huge increase in absorbance (1.0), which indicate the exponential growth of the cells. After 48h, log phase begins and then in 24h the absorbance reaches from 0.4 to 1.4. From the graph it was concluded that the doubling time required for B16 cells in exponential phase was approximately 24h.

Vero cells were originally from squamous epithelia from the African green monkey *Cercopithecus aethiops* kidney. (ECCAC catalogue number 84113001). Vero cells have been widely used during the production of vaccines and biopharmaceuticals (Barret *et al.*, 2009). They also serve as models for evaluating the toxicity of potential drugs for cancer. Intracellular trafficking of PAA polymers already performed in B16 cells and it will be interesting to observe their trafficking in Vero cells. From the figure 4.2, it was concluded that the doubling time for Vero cells was approximately 24h during log phase

4.4.2 Lectinic activity of RTBC

Figure 4.3 documents rRTBC (clone 204) lack of lectinic activity, which was concluded from the fact that in elution fractions, rRTBC (clone 204) was not detected. Commercial RTBC showed high lectinic activity, which was to be expected. Due to this reason, rRTBC (clone 204) was not used in re-association studies, instead cRTBC (Vector laboratories Ltd, Peterborough, UK) was used.

4.4.3 Re-association of RTAC and RTBC

When recombinant RTAC and RTBC chains were mixed together using a controlled environment, they have been reported to form an A-B chain heteromeric complex associated through a disulphide bond. Wild type RTAC, Cys²⁵⁹ forms the inter-chain disulphide bond with Cys⁴ of RTBC (Argent *et al.*, 1994). If the environment in which the association takes place was not carefully controlled, there exists the possibility of homooligomeric complexes *i.e.* the binding of another RTAC to another RTAC. Consequently, the re-association of RTAC and RTBC was performed according to the protocol described (section 2.2.11), which is loosely based on those of the Lord Laboratory at Warwick University (Smith *et al.*, 2003). Here the lectinic property of the RTBC was used to immobilise the B chain upon a lactose-

agarose solid phase support (sepharose beads). Under reducing conditions (2% (v/v) BME) the RTAC was added to excess. The homomeric complexes formed (RTAC bound to RTAC) was then removed by washing the immobilised solid phase support. The heteromeric complexes were then recovered by elution with 75mM galactose in PBS. This produced a high activity heteromeric RTA/B chain complex that had the capacity to traffic through the endomembrane system with kinetics similar to wild-type toxin.

Commercial RTAC was used to optimise the re-association of cRTAC and cRTBC. In the wild the problem of homo oligomeric complexes is overcome by the production of pro-ricin which is a single peptide chain composing of both the A and B chains, which are produced from one open reading frame. Intra-molecular bonds are allowed to form between what will become the A and B chains prior to the proteolytic cleavage of “spacer” sequences of amino acid at the (C/N)-terminus of the pro-ricin and also between the A and B chains. To mimic this process in the lab would require the A and B chains of the Ricin toxin to be encoded by the same plasmid, which would breach currently implemented HSE guidelines.

4.4.4 Toxicity studies using MTT assay

Before evaluating the toxicity of rRTAC constructs, imidazole cytotoxicity was evaluated. Imidazole was used to elute 6His tagged proteins. At low concentrations, imidazole (10mM), removes cellular proteins, which loosely bind un-specifically to the column. But at high concentrations (150mM), it competes with 6His motifs binding to Ni^{+2} ions forming the column. It was important to know the cytotoxic effect of imidazole on the cells before evaluating the cytotoxicity of recombinant proteins. Dialysis of the purified protein was performed to remove the imidazole. Knowing the cytotoxicity of the imidazole, allowed the optimisation of the dialysis. From the imidazole toxicity data, it was concluded that IC_{50} of imidazole was $16.44(\pm 1.92)\text{mM}$ in Vero cells and $53.64(\pm 3.74)\text{mM}$ in B16 cells (figure 4.6). Vero cells were more sensitive than B16 cells to imidazole. After dialysis (2 x 4000mL of 1xPBS), the concentration of imidazole was reduced to 6.25pM, which was non-toxic to both B16 and Vero cells.

The cytotoxicity of rRTAC constructs was evaluated. In Vero cells, all of the rRTAC constructs tested didn't show any cytotoxicity over a 72h time span. During this experiment, cRTAC (Sigma, USA) and GST-GFP (210) were used as positive and negative controls. As predicted, cRTAC was highly toxic to Vero cells. The cell viability was diminished to 10%

(IC₅₀ of 1.81(±0.15)ng/mL). Conversely, no toxicity was observed when the GST-GFP (clone 210) was incubated with either cell line at all concentrations tested (*i.e.* up to 10µg/mL).

When mixed with rRTBC (clone 204), the rRTACs did not show any measurable toxicity up to 10µg/mL in both B16 and Vero cells. At the same time, the cRTAC together with cRTBC was highly toxic to both the cells. This lack of toxicity of rRTAC-rRTBC may be attributable to several factors. The first may be that the rRTAC and rRTBC were not correctly associated. This possibility was being investigated. The second possibility was that the RTAC and RTBC were not correctly folded when produced in bacteria and as such were unable to translocate to the cytosol so limiting toxicity via spatial exclusion from their targets. As this system was being developed as a gene delivery system, the proteins not being able to reach the cytosol would be disastrous. This possibility is addressed before in this document (section 4.4.3). The third possibility may be due to lack of lectinic activity of rRTBC (clone 204), the trafficking of rRTAC constructs may be not as effective as they could in presence of RTBC which has lectinic activity (figure 4.3).

Re-associated cRTAC-cRTBC was highly toxic to both B16 and Vero cells. At 0.1ng/mL concentration cell viability was only 20% in Vero cells, which was close to the published holotoxin data (IC₅₀: 0.13ng/mL) (Simpson *et al.*, 1995). In B16 cells also re-associated cRTAC-cRTBC showed high toxicity (IC₅₀: 0.79(±0.01)µg/mL), which was close to published data (IC₅₀: 0.3µg/mL) (Patrick *et al.*, 2001). Toxicity of re-associated rRTAC (189)-cRTBC was evaluated. It was non-toxic in B16 cells but showed only 55% cell viability (IC₅₀ of 0.39(±0.04)µg/mL) in Vero cells. The decrease in cell viability was might be due to the toxicity of caused by cRTBC (IC₅₀ of 0.70(±0.04)µg/mL). Even though cRTBC does not have the catalytic sites like RTAC but showed some cytotoxicity. The reason for the cytotoxicity of cRTBC was not known, but may have been due to RTAC contamination.

4.4.5 Sub-cellular distribution preliminary results

Sub-cellular fractionation was developed to monitor the translocation of material through (and delineate) specific intracellular compartments (Richardson *et al.*, 2008). This technique has had wide application during the characterisation of intracellular trafficking pathways such as the endocytic and secretory pathways. Here, it was used to investigate the trafficking of rRTAC (clone 189) and rRTBC (clone 204) in the Vero cells. Three antibodies were used to monitor the success of the fractionation procedure. The antibody specific for EEA-1 denotes the presence of both membrane proteins and cytosolic proteins whereas the LDH specific

antibody confirms the presence of soluble cytosolic proteins. The TfR specific antibody was used to characterise the distribution of integral membrane proteins. This data can be used to assess the levels of contamination between the crude “membrane” and crude “cytosolic” fractions generated through our fractionation protocol.

Figure 4.14, depicts rRTBC (clone 204) within the membrane fraction and the rRTAC (clone 189) within the cytosolic fraction. The controls were consistent with an adequate fractionation procedure, with the markers for the various fractions were in the predicted fractions *i.e.* the vast majority of the marker for the membrane fraction (an integral membrane protein, TfR) was detected within the membrane fraction. Similarly the majority of the marker for the soluble fraction (*i.e.* LDH) was detected in the “soluble” supernatant fraction.

The majority of the rRTAC (clone 189) was detected in cytosolic fraction, which indicates that even after the deletions or mutations documented, the rRTAC (clone 189) retained its trafficking properties. This distribution also substantiates the fact that the lack of toxicity observed was not due to the toxin being unable to assimilate its target (*i.e.* ribosomes within the cytosol). It is of note that single RTAC is capable of accessing the cytosol without the aid of ricin B chain all be it much less efficiently than the hetero oligomeric complex both *in vitro* and *in vivo*. It is also possible that the mutations introduced herein allowed a much greater accumulation of RTAC over time as the molecules were not exerting a toxicity that would, in the instance of the wild type toxins prevent the cytosolic accumulation of the A chain, on account of the cell being in the process of initiating apoptotic mechanisms resulting ultimately in the death of the cell.

Further investigations are necessary to substantiate the preliminary results obtained.

4.4.6. Immuno fluorescence microscopy

It was observed that (figure 4.15), cRTBC was co-localising with TGN46 after 20minutes. TGN46 acts as a Golgi marker. It has been published that after 30minutes RTBC could be detected in the Golgi apparatus (Richardson *et al.*, 2008). After reduction and re-association, the toxicity and immuno fluorescence data would indicate that cRTBC was functionally and biologically active. The rRTBC (clone 204) did not show any detectable co-localisation with TGN46, as it lacked lectinic activity which might impaired its endocytic and intracellular trafficking properties. Even though rRTBC (clone 204) can be produced recombinantly and can be detected immuno-specifically, it did not show the necessary functional properties.

4.5 Conclusions

From the growth curves the doubling time of both B16 and Vero cells were calculated, which was 24h for both cell lines.

Lectinic properties of rRTBC (clone 204) and cRTBC were evaluated and it was concluded that rRTBC (clone 204) lack the lectinic property.

Re-association of cRTAC-cRTBC was achieved successfully and applied the optimised conditions to re-associate rRTAC (clone 189) with cRTBC.

Compared to cRTAC, rRTAC constructs were relatively non-toxic in Vero cells.

Re-associated cRTAC-cRTBC was highly toxic to both Vero and B16 cells, whereas re-associated rRTAC (clone 189)-cRTBC was non-toxic in B16 cells and showed some degree of cytotoxicity in Vero cells, which may be attributed to cRTBC.

From the sub-cellular fractionation experiments it was concluded that rRTAC (clone 189) was reaching the cytosol. More work is needed to substantiate this conclusion.

The cRTBC was able to localise with Golgi markers where as rRTBC could not.

Chapter 5
Cloning, Expression, Characterisation and Biological Evaluation
of Gelonin Constructs

5.1 Introduction

Lectins compose of a class of substance that bind to material (*i.e.* a sugar, protein or a lipid). Thus, lectinic binding provides opportunities for drug delivery to targets presenting enriched levels of lectinic target. Further if the lectin is proteinationous, it may be manipulated using genetic recombination technology (Bies *et al.*, 2004). Lectinology begun in 1888, when Herman Stillmark described the agglutinating properties of ricin. Subsequently, lectins were found in prokaryotes and eukaryotes, though most have been found in plants. Given that the cell outer surface (the glycocalyx) is composed of glycans (carbohydrates) and glycosylated membrane phospholipids, ample targets for lectinic binding and can induce the initiation of endocytic capture (Bies *et al.*, 2004). Material conjugated to the lectin may also be subject to cellular uptake, promoted within specific populations of cells. Specific lectins exhibit non-standard post-internalisation intracellular trafficking and one of the overarching aims of this investigation is to test the hypothesis that this property can be used for the delivery of macromolecules to the cytosol.

Further, diseased and healthy tissues selectively express specific glycans (Dube and Bertozzi, 2005) and this difference may also be used to select a lectin that can be used as a carrier to target a drug specifically to desired tissue or cell surface. Beyond limiting drug off target side effects this property may also be used to ensure a therapeutic dose of a “gene specific” drug reaches its target destination. Here targeting is intrinsically specific to the drug.

Ricin B chain is a galactose/*N*-acetyl-galactosamine specific lectin, which is required for the delivery of RTAC into the cytosol (Spooner *et al.*, 2004). In this study, cRTBC was evaluated for its ability to deliver both rRTAC and a type I RIP (gelonin) which contained a conserved active sight (relative to RTAC) into the cytosol.

Gelonin belongs to the class I family of RIP proteins, which lacks a lectinic cell-binding moiety (Stripe *et al.*, 1980). Gelonin is interesting as it does not cause cytotoxicity below 1.4µg/mL in B16 cells (Patrick *et al.*, 2001). The limited cytotoxicity of gelonin relative to RT (when incubated with intact cells) is thought to be due to gelonin inability to reach the ribosomes within the cytosol. Like ricin, gelonin is thought to depurinate the 60S ribosome, which results in inhibition of protein synthesis (Sperti *et al.*, 1991). RTAC and gelonin share approximately 30% sequence identity (Rosenblum *et al.*, 1995).

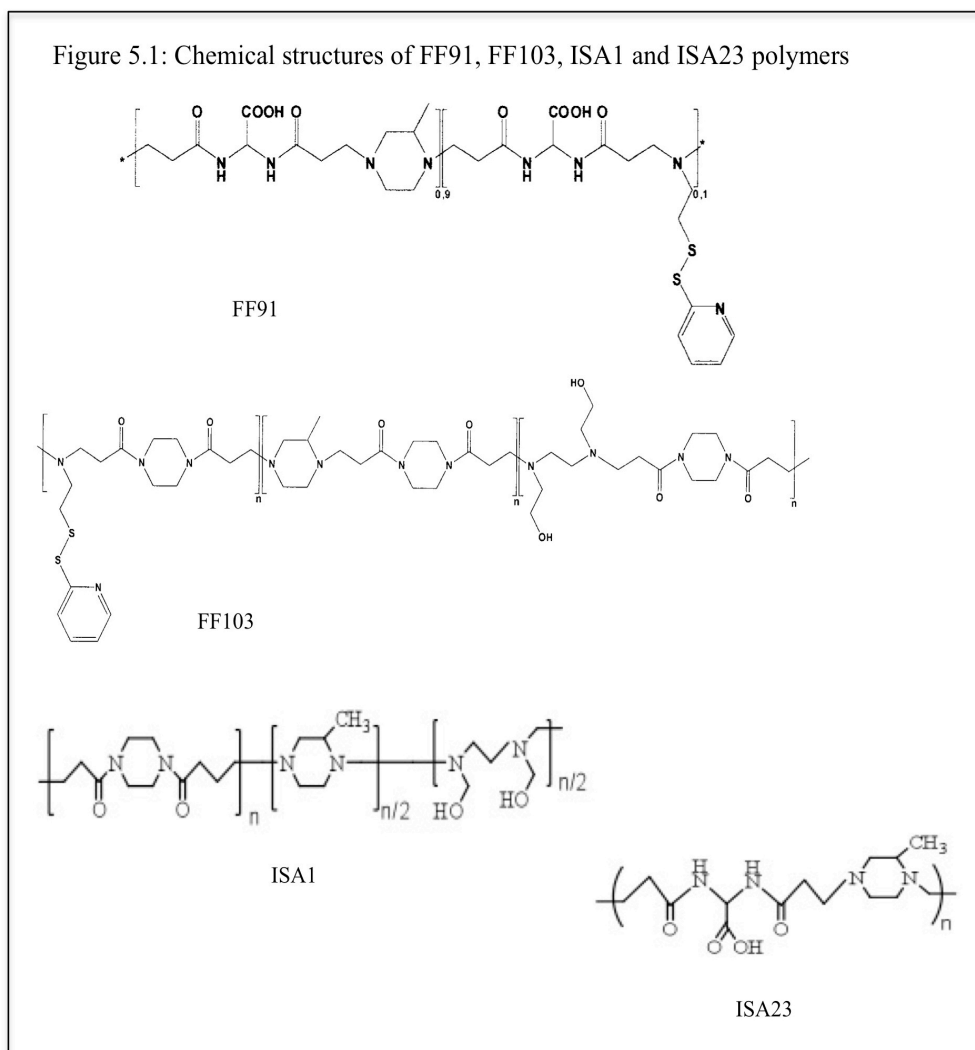
Previously, sub-lethal concentrations of gelonin, when co-incubated with increasing concentrations of the poly(amidoamine) ISA1 exerted toxicity *in vitro* in a polymer concentration dependant manner (Patrick *et al.*, 2001). Further, when gelonin was linked to

concanavalin A, the complex was toxic to intact cells, whereas gelonin alone was not (Stripe *et al.*, 1980). Consequently, gelonin was thought to be an excellent candidate as model proteins to evaluate and compare the abilities of different vectors to deliver macromolecules to the cytosol. It is also possible to think of sub-lethal concentrations of gelonin as a pro-drug, inactive until it is delivered to the target population of cells in order to treat disease such as cancer.

Several poly(amidoamines) (PAA) have been evaluated as carriers for anticancer drugs, proteins and genes. PAAs show endosomolytic properties at low pH, a property can be used in delivering biologics to the cytosol (Dyer and Richardson, 2011). Recently it was showed that linear PAAs containing intra-molecular disulphide bonds delivered siRNA to the cytosol (van der Aa *et al.*, 2011). It was already established that PAAs can deliver proteins like RTAC and gelonin into the cytosol *in vitro* (Pattrick *et al.*, 2001). Here two polymers FF91 and FF103 were evaluated for their ability to deliver recombinant and commercial gelonin into the cytosol. FF91 is based upon the monomeric architecture of ISA23 polymer, whereas FF103 is based upon the monomeric architecture of ISA1 with the exception of the inclusion of ethenyldithio pyridine (-SSPy) monomers within the polymer backbone (figure 5.1). The properties and characterisation of both FF91 and FF93 is summarised in table 5.1. Both FF91 and FF103 polymers were synthesized and characterised by Prof. Paolo Ferruti's research group at the University of Milan, Italy. The SSPy monomers were incorporated in order to foster intermolecular thiol bonding between the PAAs and rGel.

Table 5.1: Molecular weights of FF91, FF103, ISA1 and ISA23 polymers.

Polymer code	M_n	M_w
FF91 (ISA23-SSPy)	12700	23600
FF103 (ISA1-SSPy)	1800	3000
ISA1	5000	
ISA23	10500	



In this chapter the following questions were addressed:

- 1). Was it possible to clone gelonin with specific motifs introduced into it (6His, V5 and cysteine)?
- 2). Was it possible to express, purify and detect recombinant gelonin constructs?
- 3). Was recombinant gelonin proteins toxic to mammalian cells?
- 4). Was it possible to enhance the cytotoxicity of recombinant gelonin constructs by cRTBC and Poly(amidoamine) polymers?

5.2 Materials and methods

Isolation of plasmid containing gelonin ORF by Miniprep


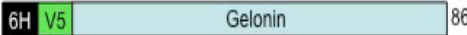
Gelonin sequence was identified using the BLAST search tool within the NCBI gene bank database and sequence was taken from gene bank accession L12243. This sequence was sent to BBI (Ontario, Canada) for codon optimisation for expression in *E.coli*. Codon optimised gelonin sequence was inserted into pUC57 vector by BBI. Once the vector was received from BBI, it was reconstituted in sterile H₂O and was transformed into *E.coli* TOP10, which were plated onto 2xYT plates (ampicillin: 200µg/mL) and left overnight at 37°C. Next day one of the colonies was selected and grown over-night in 10mL of 2xYT media (ampicillin: 200µg/mL) at 37°C. Next day a stock of the culture was prepared by mixing sterile 2xYT media (without ampicillin and with 14%DMSO) in a 1:1 ratio with the over night bacterial culture. This preparation was labelled, the details entered into the Richardson Laboratory plasmid database and the DMSO containing culture was stored at -80°C.

The *E.coli* TOP10 culture stock (which has the plasmid carrying gelonin ORF), was added to fresh, 10mL of 2xYT medium containing ampicillin (200µg/mL) and was grown over night at 37°C on orbital shaker set at 200rpm. The plasmid was purified from the overnight bacterial cell culture as described in section 2.2.2. The concentration of plasmid DNA was calculated using UV-Spectrophotometer (section 2.2.3).

Polymerase chain reaction (PCR) amplification of the gelonin open reading frame (ORF)

The plasmid previously isolated (carrying gelonin ORF) was used as a template for two PCR reactions were performed using oligonucleotide primers engineered to introduce specific epitope motifs (6His, V5, HA and cysteine) into the gelonin ORF on different terminals (N- or C- terminal). The components used in the PCR reactions were *Taq* DNA polymerase (0.5µL), dNTP (5mM) (5µL), 10xBuffer (10µL), oligo1 (1.25µL), oligo2 (1.25µL), template (1µL), water (81µL). Listed components were purchased from Fermentas (Cambridgeshire, UK). The PCR reaction was performed using 30cycles, a 1minute extension time and an annealing temperature of 55°C (1kb programme).

Table 5.2: Oligonucleotide primers used for PCR amplification. (gelonin constructs with (first column) and without cysteine (second column)).

87  89	90  86
cacctaaaggaggaaaggatccatgaaaggtaatatgaaagtg (87)	caccatgaaaggtaatatgaaagtg (90)
gaatccctggttgcttcgattatccttacgacgtaccagattacg caagatgcgcacatcatcatcatcattaa (89)	tccttggttgcttcgattaa (86)

Here cysteine was introduced into C-terminal of one rGel construct and in another it was not included (to serve as a control). It was hypothesized that presence of cysteine may increase the binding affinity with poly(amidoamine) polymers which have ethenyldithio pyridine (-SSPy) group for disulphide bond formation. This disulphide bond between the gelonin and PAA may enhance the intracellular delivery of gelonin than just merely mixing PAA (without SSPy group) with rGel.

Electrophoresis of PCR products

After PCR amplification, the PCR product was analysed by agarose gel electrophoresis. Following the preparation of the agarose gel (1% (w/v)) containing 2.5µg/mL ethidium bromide, samples were prepared (see below) and loaded into individual wells. PCR product (20µL) was added to loading buffer (Fermentas, Cambridgeshire, UK) (3µL). Molecular board range weight marker (Fermentas, Cambridgeshire, UK) (6µL) was loaded into a separate well and the running conditions were followed as previously described (section 2.2.4).

Gel extraction of the PCR product

After gel electrophoresis, the PCR product was excised from the agarose gel and transferred into a fresh, sterile microcentrifuge tube. The excision of the PCR product was performed by using a PCR product gel extraction kit from Qiagen. Following the manufactures instruction, the excised gel fragment containing the PCR product was weighed and 3 equivalents of buffer QG was added to 1 equivalent gel. This preparation was sealed and incubated at 50°C for 10minutes to dissolve the gel completely. The mix was transferred into QIA quick spin column, which was placed into a 2mL collection tube. This was then centrifuged (21 000 x g (rcf) for 60seconds at 4°C). Flow-through (buffer) was discarded and the QIAquick column

was placed back into a collection tube. Buffer QG (0.5mL) was added to the QIAquick column and also centrifuged for 1minute as before. The flow-through was also discarded. To the QIAquick column 0.75mL of buffer PE was added and the tube centrifuged as before. Again flow through was discarded and the column subject to an additional 1minute at 21 000 x g (rcf). The QIAquick column was placed into a sterile, 1.5mL microcentrifuge tube and 25µL of sterile water was added. The tube was left for 1minute at room temperature and then centrifuged as before. The water containing the PCR product was collected and the insert disposed of. The purified PCR product was stored at -20°C.

PCR product ligation into the cloning vector (using a “TOPO” reaction)

Before the ligation, 50µL of *E.coli* TOP10 bacteria were placed on ice to thaw (15minutes). The ligation reaction was initiated by adding PCR product (2µL), de-ionised water (sterile) (2.5µL), salt (buffer) (1µL), TOPO vector (pET151/D) (0.5µL) in an Eppendorf tube. The complete ligation reaction was incubated for 20minutes at room temperature and then chilled to 4°C for 5minutes. After this incubation period, 25µL of *E.coli* TOP10 was added and incubated for a further 30minutes on ice. After that, TOP10 *E.coli* was briefly heated to 42°C for 30seconds before being placed back on ice for 5minutes. Next 100µL of sterile SOC medium (Appendix I) was added and the bacteria incubated at 37°C for 45minutes. Finally the entire culture was plated on 2xYT agar plates containing ampicillin (200µg/mL) as a lawn using sterile wooden applicators. The plates were incubated at 37°C in an incubator over night. Next day, bacterial colonies were observed on the plates. From the plate, 30-40 individual colonies were picked and PCR was performed to screen the colonies, which carry the insert in pET151/D-TOPO vector.

PCR screening of transformants containing the ligated vector and PCR product

Having selected a single individual clonal colony, a small portion of bacteria was scraped into PCR tube before the same tip was used to transfer the remaining bacteria on the tip onto a labelled 2xYT agar “patch” plate containing ampicillin (200µg/mL). The colonies forming patches were labelled using the bottom of the agar plate. To each PCR tube 12.5µL of DreamTaq PCR master mix (which already contains dNTPs, buffer and MgCl₂) (Fermentas), 0.3µL of each forward 5', reverse 3' oligonucleotide and 11.9µL of de-ionised sterile water were added. Oligonucleotides were chosen that would hybridise to either the vector or the insert effectively screening for PCR insert orientation and presence (table 5.3).

Table 5.3: Oligonucleotide primers used during the screening of colonies generated after TOPO reaction using PCR.

Oligonucleotide	Sequence
T7 forward	5'-TAATACGACTCACTATAGGG-3'
T7 reverse	5'-TTCCTCGACGCTAACCTG-3'
92	5'-CCACCGAAGTGCAGACGGGTC-3'
V5 forward	5'-V5- GGTAAGCCTATCCCTAACCT-3'

The PCR reaction was performed using the conditions previously described (1minute extension time, annealing temperature 55°C, 30cycles). After completing the PCR reaction, the products were analysed by agarose gel electrophoresis as described in section 2.2.4.

The colonies yielding PCR products at the predicted molecular weight were grown over night in 2xYT medium (with ampicillin: 200µg/mL) at 37°C on orbital shaker (200rpm) prior to the isolation of the plasmids contained therein. Selected candidates were then sequenced.

After receiving sequencing data from Dnaseq, University of Dundee, Scotland, plasmid maps were generated as described (section 2.2.1).

Large scale production (1000mL culture) and purification of recombinant protein

In a sterile 1.5mL Eppendorf tube, 10µL of *E.coli* BL21*DE3 was taken and thawed for 10minutes and 5ng of purified plasmid was added and left on ice for 30minutes. After the incubation, bacterial cells exposed to heat shock for 30seconds at 42°C and then immediately transferred onto ice. After 2minutes of incubation 100µL of SOC medium was added and transformed bacteria was incubated at 37°C for 1h on orbital shaker with 200rpm. After the incubation, bacterial cells were transferred into 10mL of fresh 2xYT medium (with ampicillin: 200µg/mL) and grown overnight at 37°C on incubator with 200rpm. The 10mL-transformed culture was added to fresh, 1000mL 2xYT medium (with ampicillin: 200µg/mL) and protein expression was initiated using optimised culture conditions, which were obtained during production of RTAC (section 3.3.5.1). Separation of the pellet, French pressing and

protein purification of the recombinant protein by affinity chromatography were performed as described in section 2.2.5.

Characterisation of recombinant gelonin by SDS-PAGE and Western blotting

Purified recombinant gelonin (with and without cysteine), mature gelonin and commercial gelonin were characterised by SDS-PAGE (section 2.2.6). Except commercial gelonin, Western blotting (as described in section 2.2.7) was used to detect the gelonin immunospecifically by 6His and V5 antibodies.

Re-association of cRTBC and rGel proteins

Re-association of cRTBC and rGel with cysteine was performed as describe in section 2.2.11.

Evaluation of cell viability in response to exposure to gelonin by MTT assay

When assessing the cytotoxicity of rGel (with and without cysteine), cGel, cRTBC, PAA polymers (FF103, FF91) dextran and PEI, the MTT assay was used (Sgouras *et al.*, 1990). From seeding the cells to applying the proteins and polymers was performed as described in section 2.2.10.

Mixtures of gelonin and PAA were also incubated with cells using a non-toxic concentration of recombinant and commercial gelonin (1.4 μ g/mL). In addition rGel (with C-terminal cysteine) was also mixed with the PAAs at a higher concentration (also non-toxic), which was 14 μ g/mL.

5.3 Results

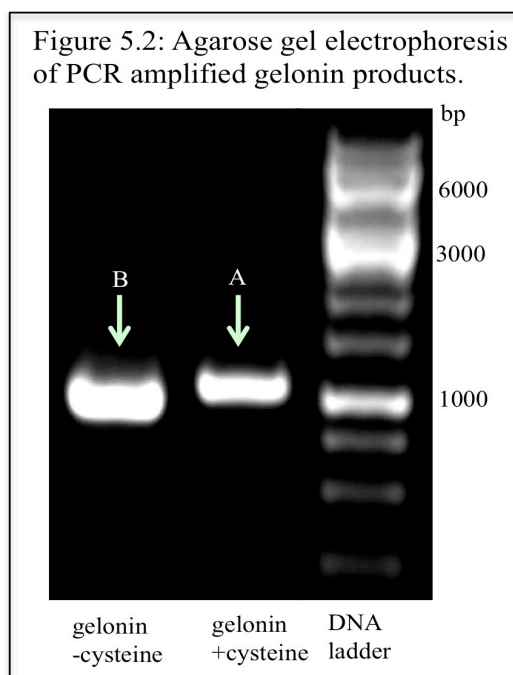
5.3.1 Isolation of gelonin template plasmid from *E.coli* TOP10

From the saturated, 10mL, over night bacterial culture which was harbouring the gelonin template plasmid was obtained by performing Miniprep plasmid isolation (as described in section 2.2.2). The yield of the plasmid was 2 μ g/mL, which was within the manufactures specified range.

5.3.2 PCR using specific oligonucleotide

Two different gelonin constructs (with and without cysteine) were generated using PCR. To incorporate specific motifs (6His, V5 and HA) into the gelonin ORF, different oligonucleotides were used in PCR reaction (oligonucleotide sequence and use are given in table 5.2). For the purification of recombinant proteins, 6His tag was incorporated. V5, HA and also 6His tags were used for detecting recombinant protein by Western blotting. The V5 and 6His epitopes were integral to the 5' end of the ORF within vector upstream of the insert integration sight.

From the figure 5.2, it was observed that DNA bands were documented at the predicted molecular weight (close to 1000bp) for both gelonin constructs (with (arrow A) and without cysteine (arrow B)). This indicates that PCR was successful and the PCR products could be used for sub-cloning.



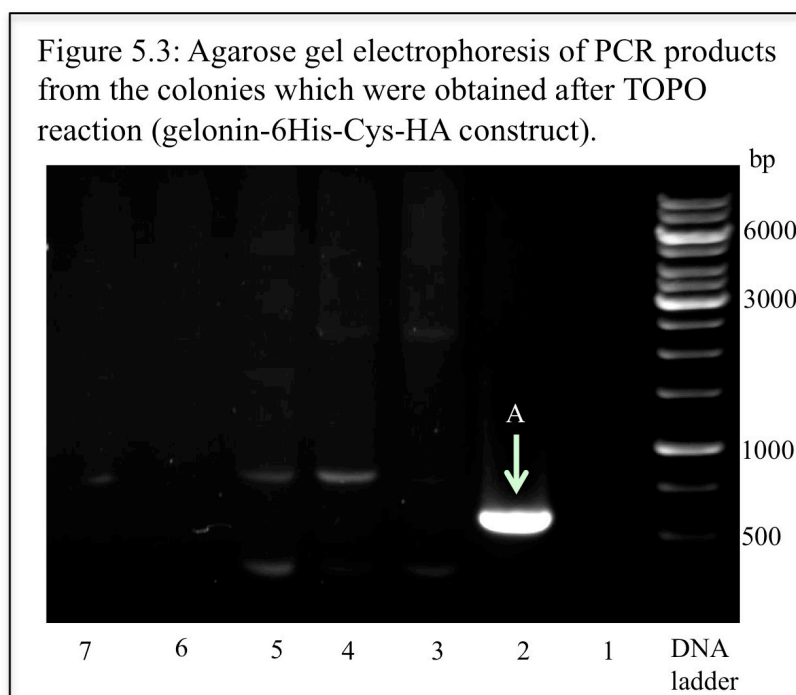
5.3.3 Ligation of PCR products into the expression cassette

Having successfully amplified the desired regions of the gelonin ORF, PCR products were purified and inserted into pET151/D-TOPO expression vector. TOPO reactions (Invitrogen, Paisley, UK) were performed as described in the section 5.2. After the final incubation period with SOC medium associated with the bacterial transformation of the ligation products, the reaction mix was spread as a lawn onto a 2xYT agar plate (ampicillin: 200µg/mL) and left over night, upside down in an incubator at 37°C.

The following day the bacterial lawns were scrutinised and single colonies screened (using PCR) for the presence of both the PCR insert and its orientation within the vector (section 5.2). The PCR screen was subject to agarose electrophoresis (section 3.3.1.3) in order to detect PCR product of the predicted molecular weight.

The colonies which showed bands at the predicted molecular weight (figure 5.3, well no.2, arrow A (at 500bp) and in figure 5.4, well no.6, arrow A (at 1kb)) were grown overnight in fresh, saturated, 10mL 2xYT medium and the plasmid was isolated (section 2.2.2) and sent for sequencing (Dnaseq, University of Dundee, Scotland). Overnight culture with desired plasmid was stored using sterile 2xYT medium (no ampicillin and contains 14% DMSO) in 1:1 ratio and stored at -80°C.

Once the sequencing data received, plasmid maps were generated using DNASTar (Madison, WI, USA) as described in section 2.2.1.



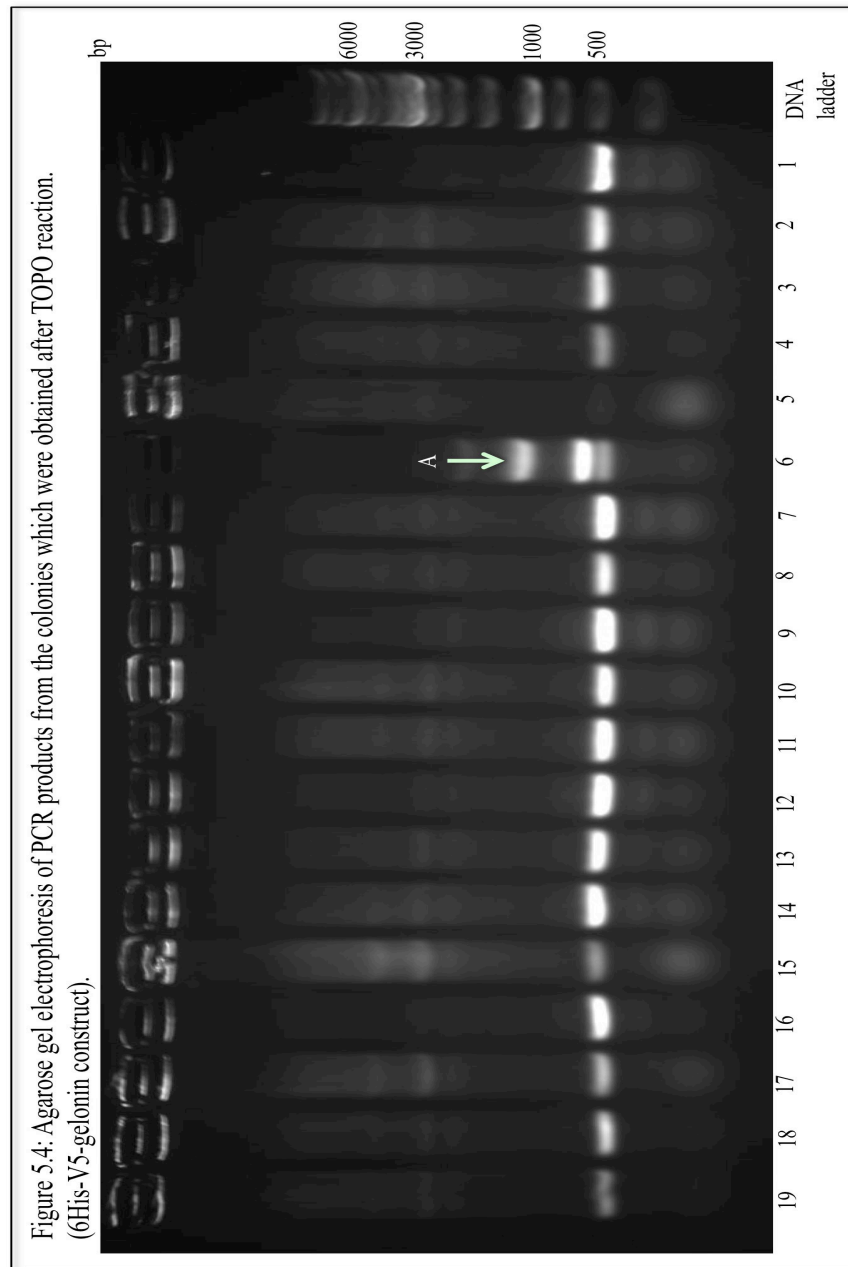
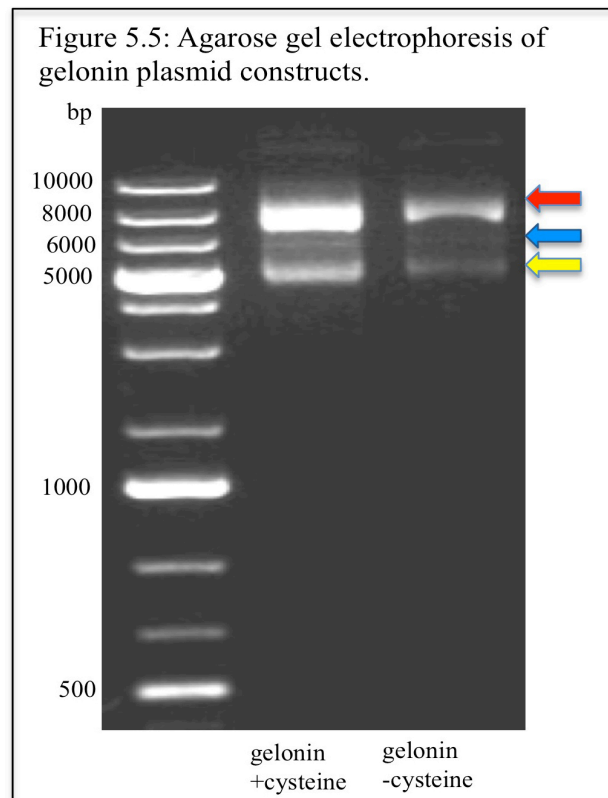


Figure 5.4: Agarose gel electrophoresis of PCR products from the colonies which were obtained after TOPO reaction. (6His-V5-gelonin construct).

5.3.4 Characterisation of gelonin constructs

Approximately 5 μ L of frozen *E.coli* culture (section 5.2) was transferred into, 10mL of sterile 2xYT media (ampicillin: 200 μ g/mL), which was grown over night at 37°C on an orbital shaker set at 200rpm. The following day plasmid isolation was performed as described in section 2.2.2. The concentration of plasmid DNA was measured using a UV-Spectrophotometer at OD_{260nm}. The yield of the plasmid constructs for gelonin with cysteine was 4 μ g and for gelonin without cysteine was 4.5 μ g (both isolated from 5mL of the bacterial

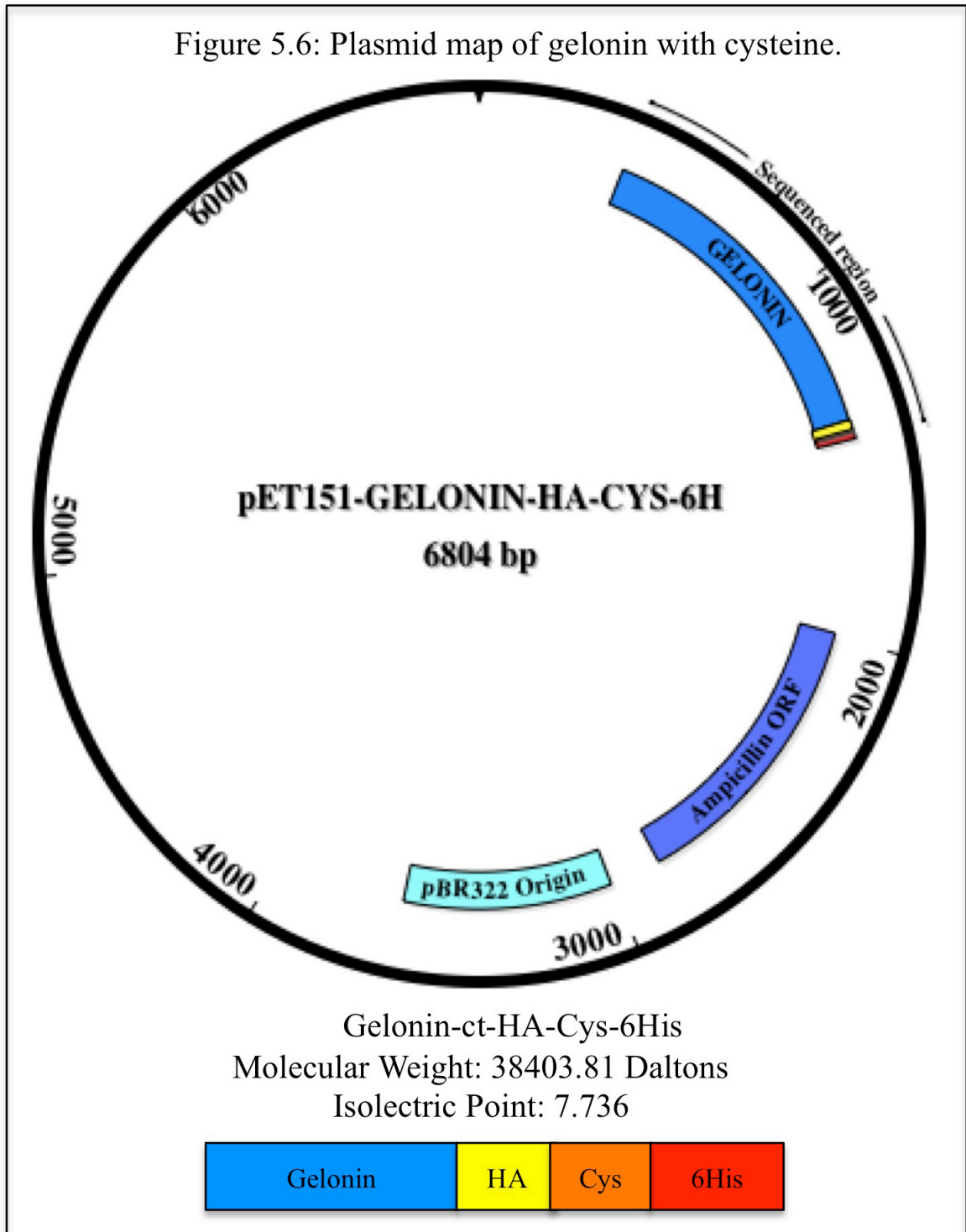
culture) and was within in the range specified by the manufacturer. Both purified plasmids were analysed by agarose gel electrophoresis (section 3.3.1.3) (figure 5.5). Plasmids were detected at the predicted molecular size (6500bp) and they appear in 3 forms (see section 3.4.1.3). The plasmid DNA that was close to 8000bp (indicated with red arrow) was running in linear form and the one close to 6000bp (indicated with blue arrow) was probably in the nicked, open circular form. Finally the plasmid DNA at 5000bp (indicated with yellow arrow) was in super helical circular form, which runs quickly through the gel due to its coiled structure.

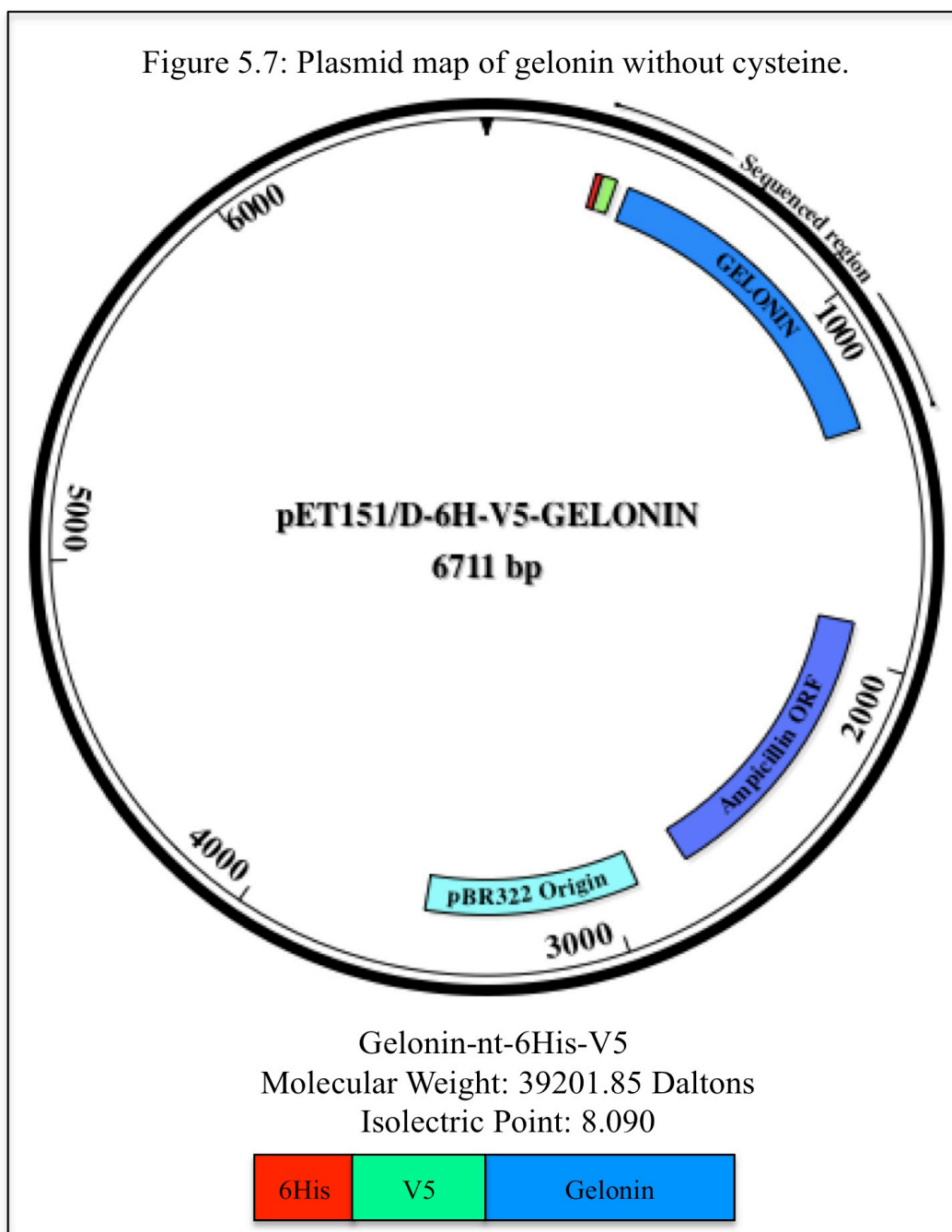


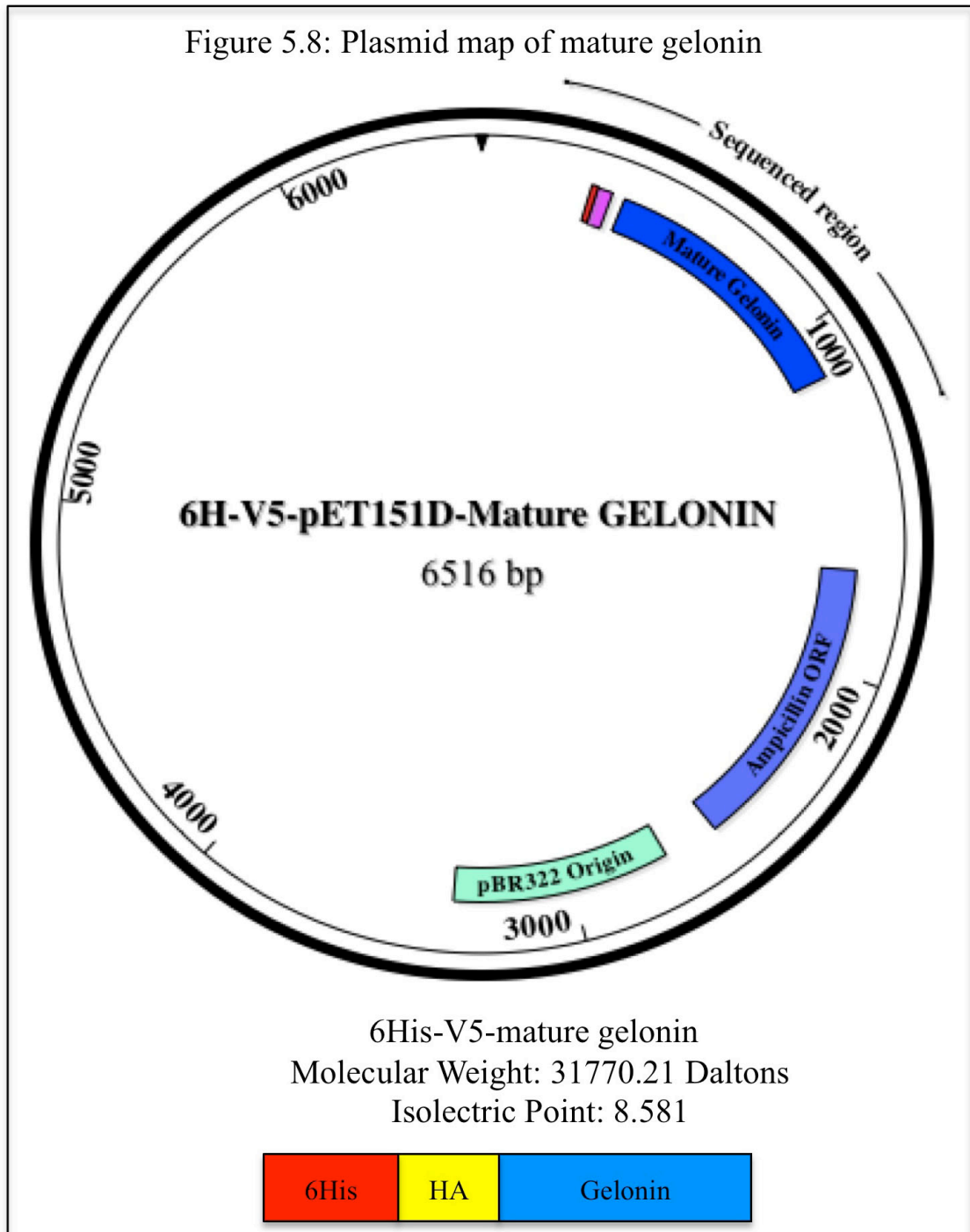
5.3.5 Plasmid maps of gelonin constructs:

Plasmid maps of the both gelonin constructs (with and without cystine) along with mature gelonin were made as previously discussed (section 2.2.1). Gelonin with and without cystine cloned and sequenced by Dr. Fabio Felini (University of Milan, Italy) and mature gelonin was cloned, sequenced by Marie Pettit, University of Greenwich. From the plasmid maps (figure 5.6 to 5.8), it was observed that, theoretical molecular weight is close to the actual molecular weight.

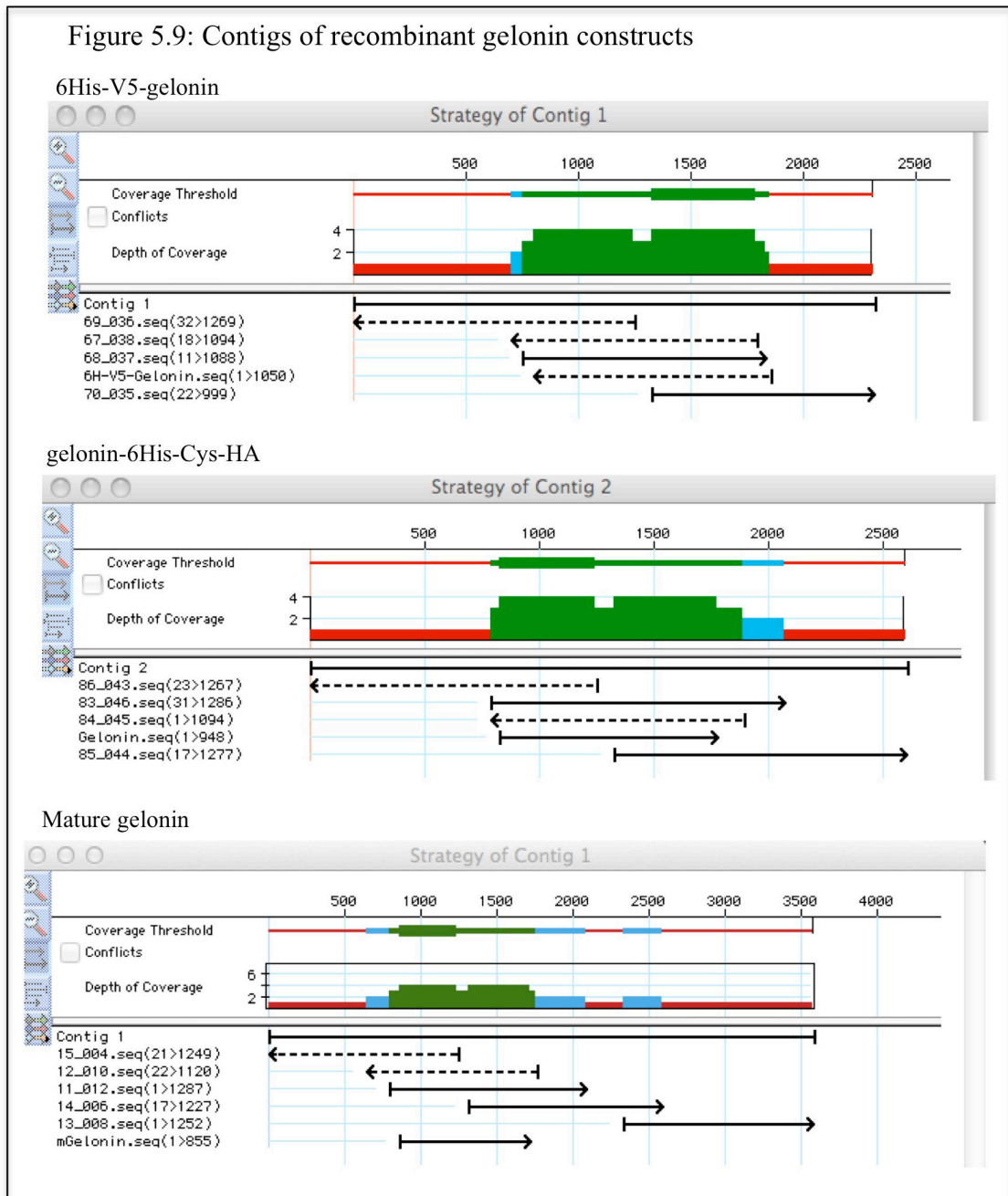
Figure 5.6: Plasmid map of gelonin with cysteine.







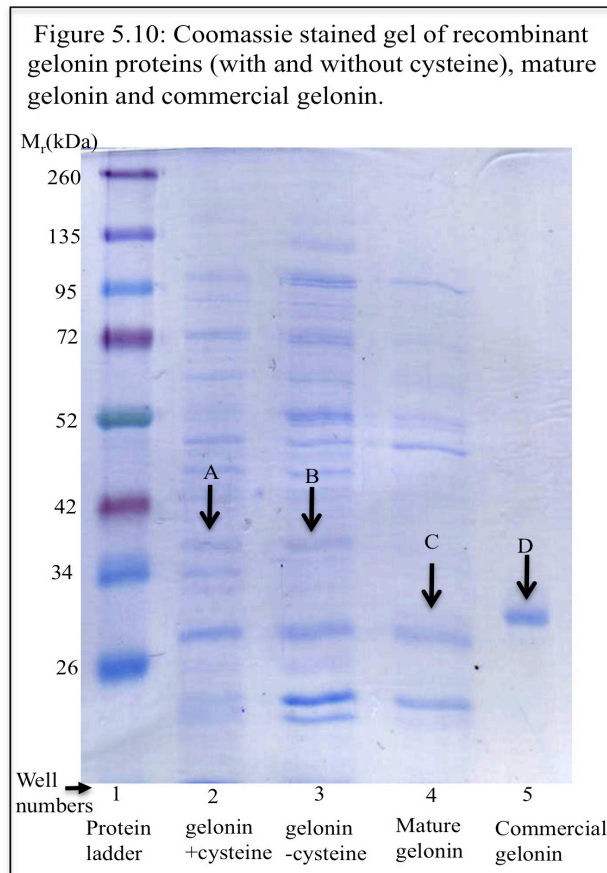
Contiguous sequences of three gelonin constructs (gelonin with and without cysteine, mature gelonin) were generated (figure 5.9). The green region in the figure shows the sequence alignment.



5.3.6 Gelonin protein expression and purification

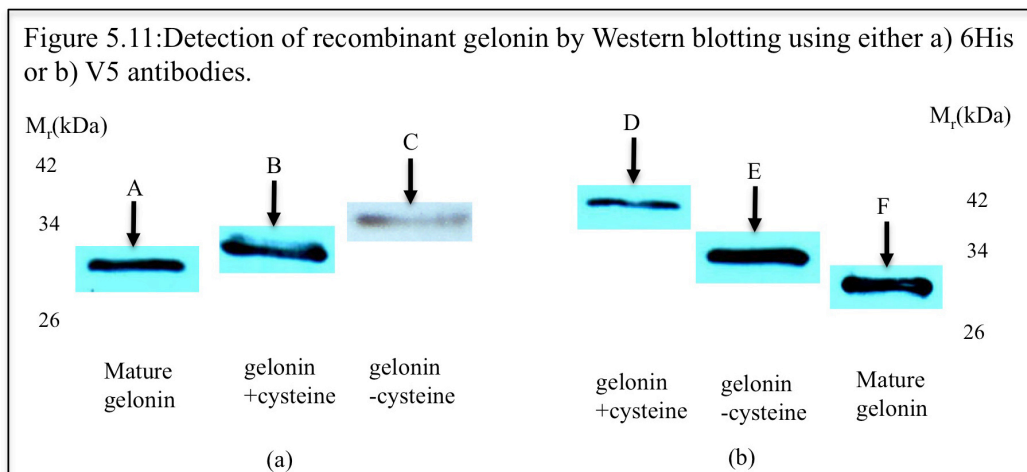
Gelonin constructs (with and without cysteine) and mature gelonin were transformed separately into *E.coli* BL21*DE3 for the protein expression (section 5.2) and proteins were expressed in large culture volume (1000mL) using 3h and 30minutes pre- and post-induction time with final concentration 0.25mM IPTG. Expressed proteins were separated and purified by affinity chromatography as described in section 2.2.5.4. After dialysis and sterilization using 0.2 μ m filter, proteins were characterized by SDS-PAGE and Western blotting as described in section 2.2.6 and 2.2.7.

From the figure 5.10, it was observed that gelonin proteins were detected at predicted molecular weight. Bands for gelonin with (38.4kDa) and without cysteine (39.2kDa) were seen above 34kDa marker band, whereas mature gelonin (31.7kDa) was detected between 26 and 34kDa. Commercial gelonin, which has a molecular weight of 30kDa, can be detected above 26kDa. For SDS-PAGE analysis 150ng of each gelonin protein was used.



5.3.7 Detection of gelonin proteins

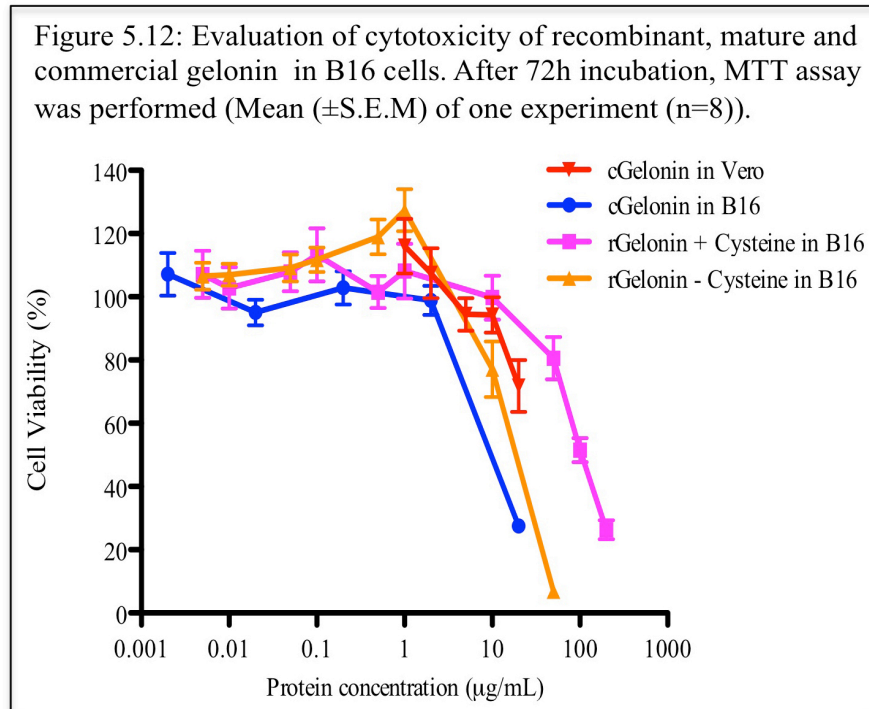
After performing SDS-PAGE, gelonin proteins (150ng each) (rGel with and without cysteine, mature gelonin) were transferred onto a nitrocellulose membrane and immuno-detection was performed using the protocol described earlier (sections 2.2.7 and 3.3.3). Here anti-V5 (1:1000 dilution) and anti-6 His (1:1000 dilution) primary antibodies were used after dilution in PBS-TWEEN 20 containing 5% (w/v) none fat dried milk. Anti-mouse-HRP-conjugated secondary antibody was used after a 1:1000 dilution also using PBS-TWEEN 20 containing 5% (w/v) none fat dried milk. From the figure 5.11, it was observed that mature gelonin (arrow A) was detected between 26kDa and 34kDa. Gelonin with cysteine (arrow B) was detected below 34kDa, where as gelonin without cysteine was detected just above 34kDa (arrow C) by 6His primary antibody. These proteins were also detected by anti-V5 primary antibody. Here gelonin with cysteine protein (arrow D) was detected above 34kDa and gelonin without cysteine (arrow E) was detected at 34kDa. Mature gelonin was detected at above 26kDa (arrow F). Currently there were no antibodies available against cGel in the laboratory, that's why it was not used in Western blotting experiments.



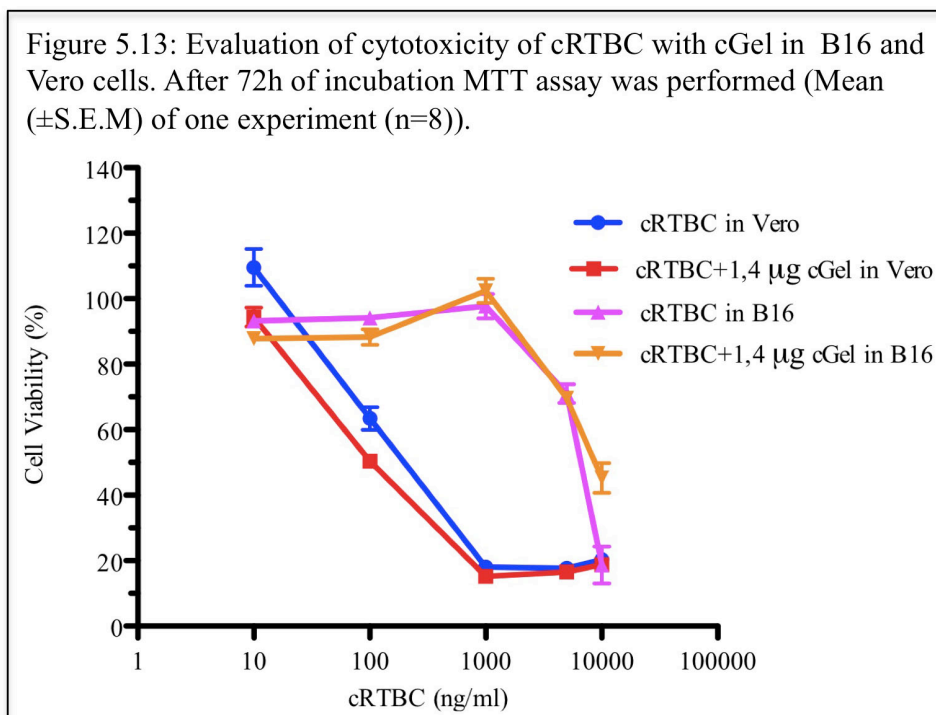
5.3.8 Cytotoxicity of recombinant gelonin (with and without cysteine), cGel and cRTBC

After characterizing the rGel constructs with and without cysteine, toxicity in B16 cells was analysed. From the figure 5.12, it was observed that in B16 cells, gelonin with cysteine showed IC_{50} value of $155.62(\pm 39.37)\mu\text{g/mL}$ and gelonin with 6H-V5 showed IC_{50} of $36.62(\pm 6.34)\mu\text{g/mL}$. cGel showed IC_{50} value of $19.75(\pm 0.2)\mu\text{g/mL}$ in B16 cell. Mature

gelonin showed 60% cell viability at 10 μ g/mL. Statistical comparisons were made between the toxicity of the gelonin constructs assayed here (based upon IC₅₀) in Chapter 7.



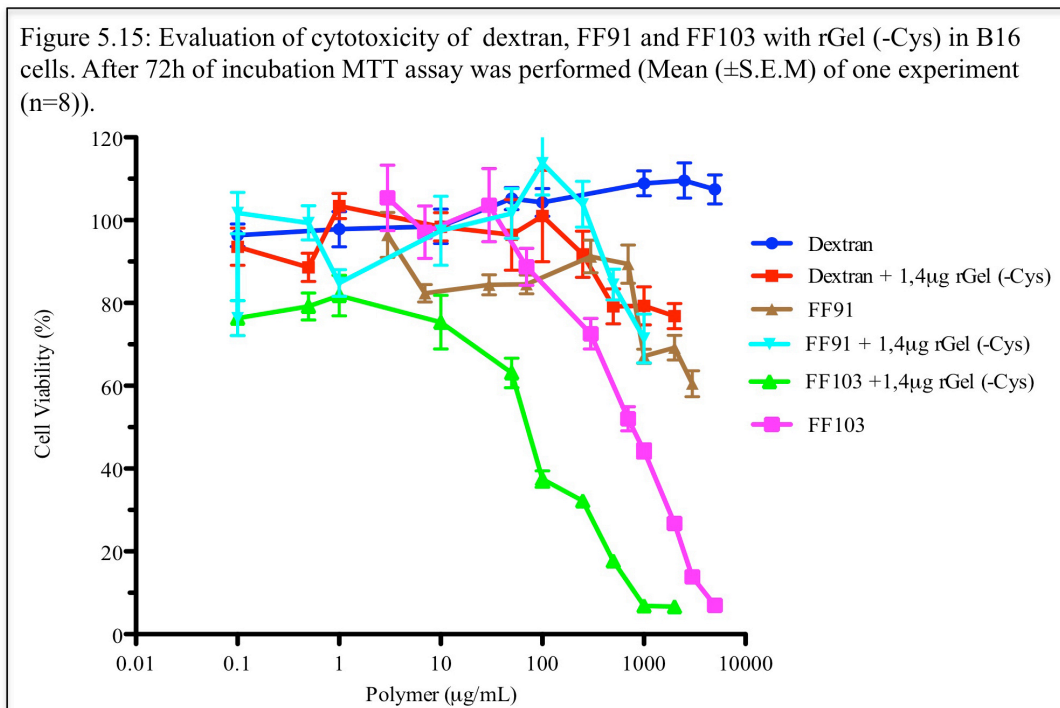
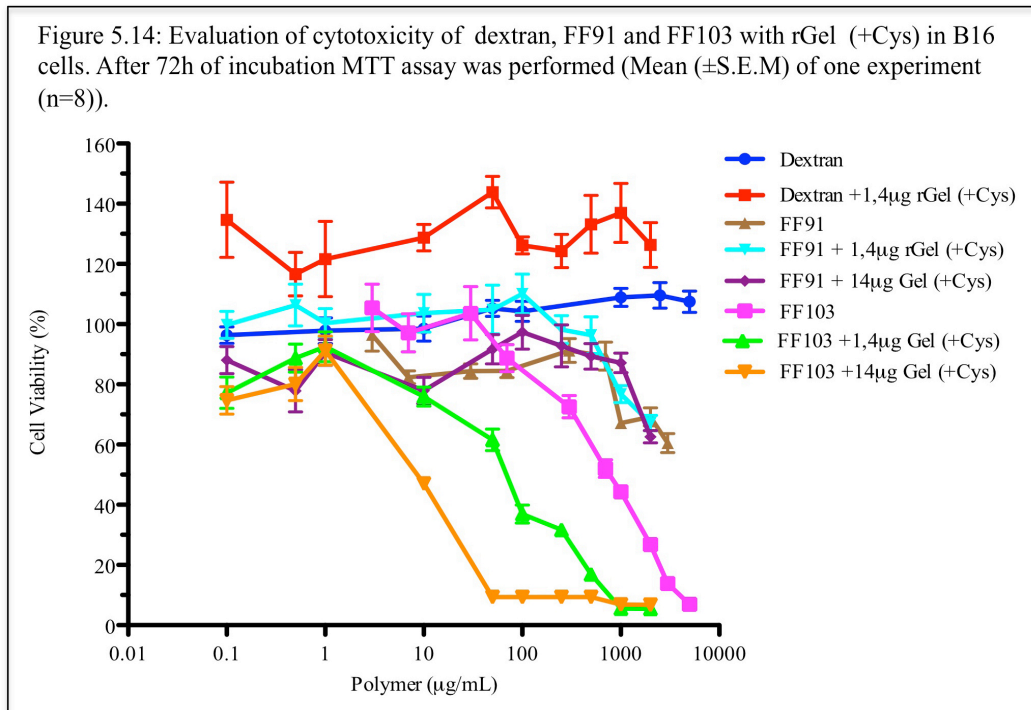
When cRTBC (ranging from 0.01 μ g/mL to 10 μ g/mL) and cGel (1.4 μ g/mL) were mixed and evaluated the cytotoxicity in B16 and Vero cells, there was not much influence of cRTBC was observed on cGel uptake. From the figure 5.13 it was observed that the difference in IC₅₀ values of cRTBC (8.657(\pm 0.58) μ g/mL) and cRTBC with cGel (8.875(\pm 0.15) μ g/mL) in B16 was less than 1%. In Vero cells, difference in IC₅₀ values of cRTBC (0.324(\pm 0.01) μ g/mL) and cRTBC with cGel (0.29(\pm 0.02) μ g/mL) was also less than 1%. It was noticed that cRTBC was more cytotoxic in Vero cells than B16 cell lines.



Evaluation of cytotoxicity of FF91 and FF103 polymers together with gelonin proteins

FF91 and FF103 polymers and dextran cytotoxicity was established with and without recombinant and cGel in B16 cells. From the figures 5.14-5.17, it was observed that dextran did not show any cytotoxicity in concentration ranges tested (up to 3mg/mL) alone or together with either recombinant or cGel (1.4µg/mL). Here dextran used as a negative control, as it does not show any cytotoxicity and did not enhancing gelonin uptake.

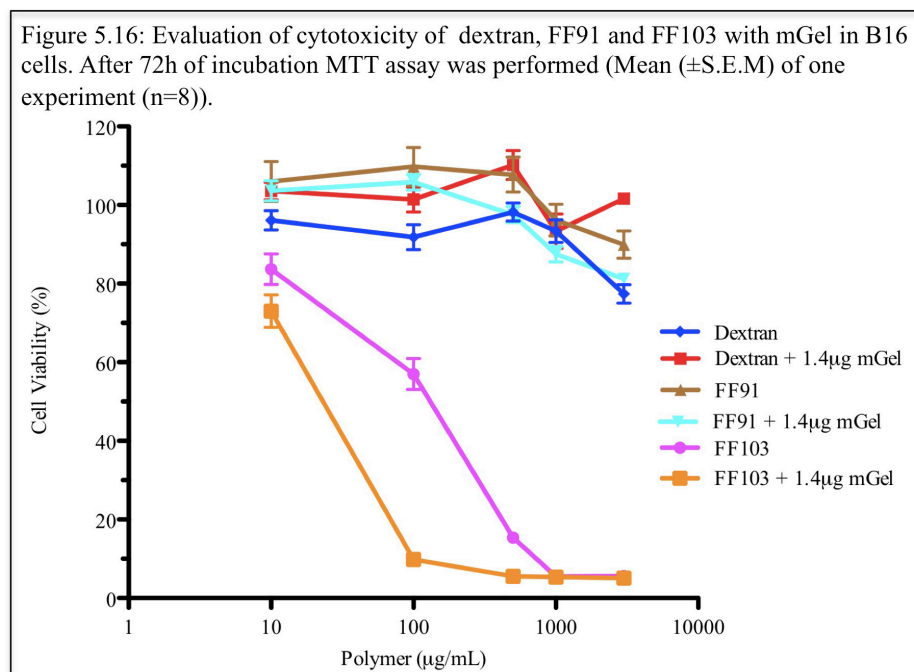
FF91, (similar to ISA23) showed low cytotoxicity up to the concentration ranges tested (3mg/mL) (figures 5.14 to 5.17) alone or together with either recombinant or cGel (cell viability was above 50% in all cases).

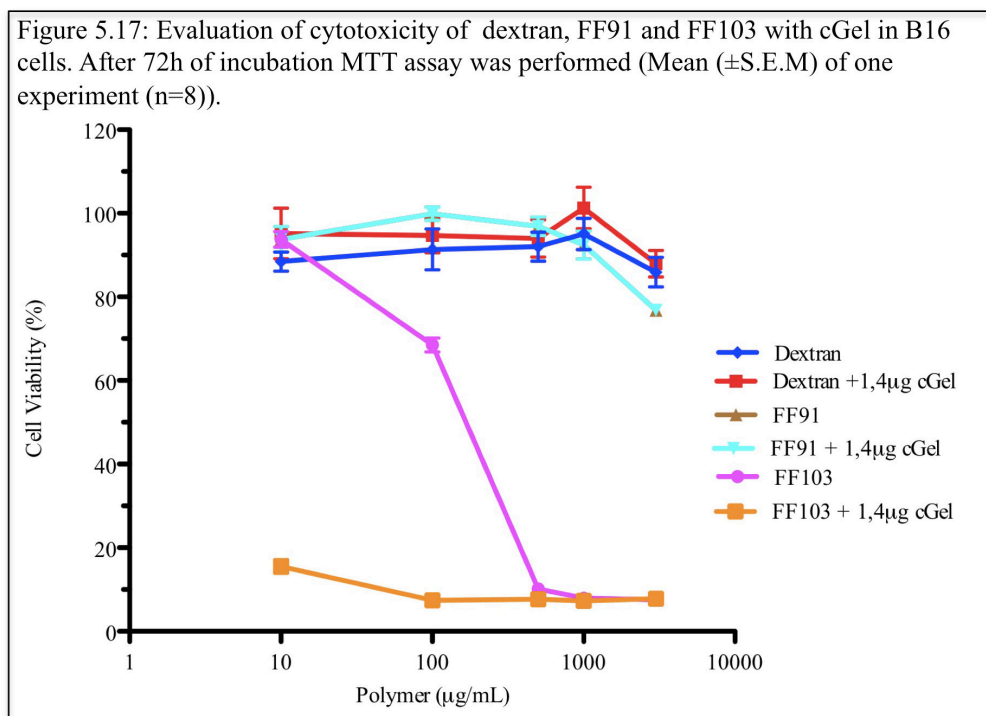


FF103 showed higher toxicity than FF91. It was expected as it is similar to the PAA ISA1 (Pattrick *et al.*, 2001), which showed a slightly higher toxicity than ISA23 polymers. IC₅₀ value of ISA1 was 890(±53.4)µg/mL (figure 5.14) (analysed by Dr. Fabio Felini). When FF103 applied onto cells together with rGel (with cystine) (1.4µg/mL, figure 5.14), the IC₅₀ value of FF103 was decreased 10 folds (88.25(±3.17)µg/mL and without cysteine also same pattern of IC₅₀ value observed (89(±5.20)µg/mL) (figure 5.15). When the concentration of rGel (with cysteine) was increased to 14µg/mL, the cytotoxicity of FF103 was increased approximately 65 folds (IC₅₀ of ISA103/rGel: 13.8(±1.79)µg/mL) when compared to FF103 alone.

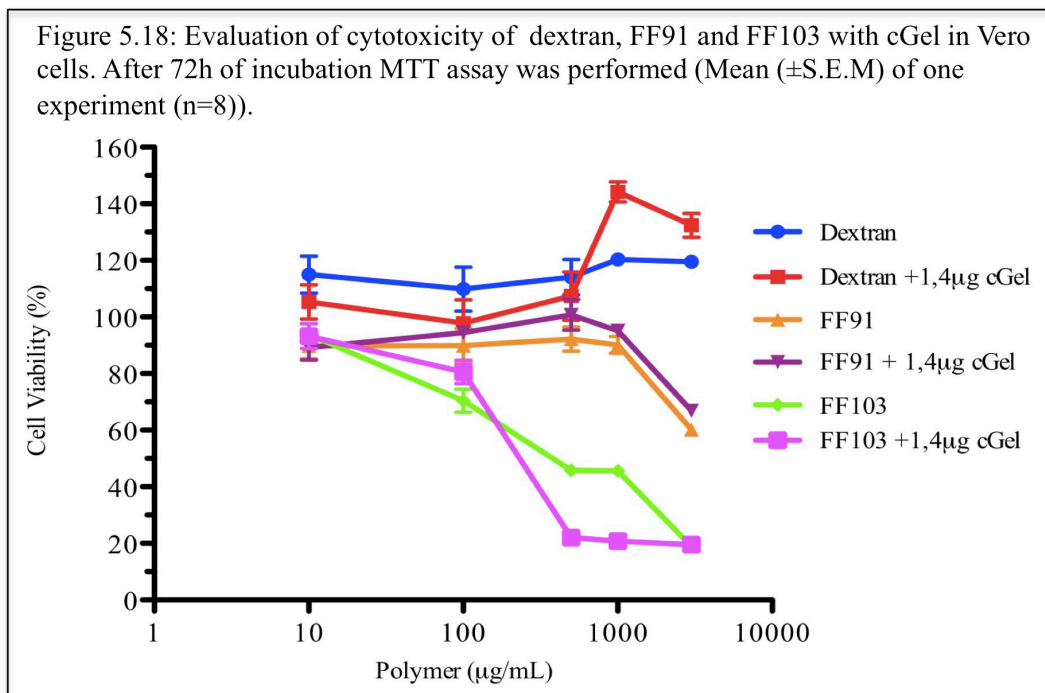
When FF103 (IC₅₀: 350(±24))µg/mL (figure 5.17)) was applied onto cells along with cGel (1.4µg/mL), cytotoxicity was increased dramatically. The cell viability decreased to 20% (10µg/mL of FF103+1.4µg/mL cGel) when compared to FF103 at the same concentration (10µg/mL).

FF103 polymer together with mGel (1.4µg/mL) showed increase in cytotoxicity (IC₅₀: 40(±0.8)µg/mL when compared to FF103 alone (IC₅₀: 310(±30.2)µg/mL) (figure 5.16).





The cytotoxicity of FF91, FF103 and dextran polymers and together with cGel was also evaluated in Vero cells. Dextran was non-toxic, in the concentration ranges tested (up to 3mg/mL). FF91 was slightly toxic (60% viability) to Vero cells in the concentration range used (3mg/mL). When applied together with cGel, FF91 didn't promote an increase in cytotoxicity over the range of polymer concentrations tested. However, when FF103 was co-incubated with cGel, the polymer promoted enhanced cytotoxicity in Vero cells. The IC_{50} value of FF103 was 625(\pm 10.2) $\mu\text{g/mL}$. When applied together with cGel, the cytotoxicity was increased, which was concluded from the fact that IC_{50} of FF103 was decreased to 445(\pm 17.4) $\mu\text{g/mL}$.



5.4 Discussion

5.4.1 Sequencing of gelonin constructs

In this study two modified (containing C- or N-terminal epitopes) rGel constructs were sub-cloned into bacterial expression cassettes. One, which contains C-terminal HA-Cys-6His, and another gelonin construct, which has N-terminal 6His-V5 tags, does not contain cysteine. After performing cloning and sequencing, it was concluded that it was possible to generate gelonin constructs with specific epitope tags introduced into them. From the plasmid sequence data, (nucleotide) plasmid maps (figure 5.6 to 5.8) and the amino acid sequences of the rGel constructs were determined.

Table 5.4: Amino acid sequences of gelonin constructs

Construct	Amino acid sequence	Mw (kDa)
6His-V5-gelonin	MHHHHHHGKPIPPLLGLDSTENLYFQGIDPFTMKGNMKVY WIKIAVATWFCCTTIVLGSTARIFSLPTNDEEETSKTLGLDVS FSTKGATYITYVNFLNELRVKLPKPEGNSHGIPLLRKKCDDPGK CFVLVALSNDNGQLAEIAIDVTSVYVVGYYQVRNRSYFFKDAP DAAYEGLFKNTIKTRLHFSGSYPSLEGEKAYRETTDLGIEPLRI GIKKLDENAIIDNYKPTIASSLLVVIQMVSEAAARFTFIENQIRN NFQQRIRPANNTISLENKWGKLSFQIRTSGANGMFSEAVELER ANGKKYYVTAVDQVKPKIALLLKFVDKDPKTSLAAELIIQNYE SLVGF	39.201
gelonin-6His-Cys-HA	MKGNMKVYWIKIAVATWFCCTTIVLGSTARIFSLPTNDEEETS KTLGLDVSFSTKGATYITYVNFLNELRVKLPKPEGNSHGIPLLR RKKCDDPGKCFVLVALSNDNGQLAEIAIDVTSVYVVGYYQVR NRSYFFKDAPDAAYEGLFKNTIKTRLHFSGSYPSLEGEKAYR ETDLGIEPLRIGIKKLDENAIIDNYKPTIASSLLVVIQMVSEA ARFTFIENQIRNRFQQRIRPANNTISLENKWGKLSFQIRTSGAN GMFSEAVELERANGKKYYVTAVDQVKPKIALLLKFVDKDPK SLAAELIIQNYESLVGFDESLVGFDPYDPYARCAHHHHH H	38.403
6His-V5-Mature gelonin	MHHHHHHGKPIPPLLGLDSTENLYFQGIDPFTLDTVSFSTKG ATYITYVNFLNELRVKLPKPEGNSHGIPLLRKKCDDPGKCFVLV ALSNDNGQLAEIAIDVTSVYVVGYYQVRNRSYFFKDAPDAAYE GLFKNTIKTRLHFSGSYPSLEGEKAYRETTDLGIEPLRIGIKKL DENAIIDNYKPTIASSLLVVIQMVSEAAARFTFIENQIRNRFQQR IRPANNTISLENKWGKLSFQIRTSGANGMFSEAVELERANGKK YYVTAVDQVKPKIALLLKFVDKDP	31.770

5.4.2 Characterisation of gelonin proteins by SDS-PAGE and Western blotting

In production of rGel proteins, mini-inductions were not performed. The optimal conditions (IPTG concentration, pre and post-inductions times) from RTAC productions were applied. After recombinant production and affinity purification of rGel proteins, they were characterised by SDS-PAGE and Western blotting. In SDS-PAGE, rGel proteins along with cGel were detected below the expected molecular weight marker. It may be caused by residual protein confirmation.

After Western blotting, rGel proteins were detected by commercial antibodies against 6His and V5 epitope tags present in the proteins. The optimized Western blotting conditions, which were obtained from RTAC, were applied in these experiments and they were successful in detecting the rGel proteins at predicted molecular weight.

Mature gelonin (31kDa) was detected close to predicted molecular weight (band was detected between 26kDa and 34kDa), whereas rGel without cysteine (39.2kDa) (against anti-

6His) and rGel with cysteine (38.4kDa) (against anti-V5) were detected slightly above 34kDa, where as rGel without cysteine (39.2kDa) (against anti-V5) and rGel with cysteine (38.4kDa) (against anti-6His) were detected slightly below 34kDa. C-terminal 6His epitope identification by immuno-blotting dictated that the full-length protein transcripts were generated.

5.4.3 Evaluation of cytotoxicity of rGel, cGel, cRTBC and polymers

Characterising gelonin toxicity in B16 cells

The rGel construct expressing a protein with an additional three, C-terminal, amino acids including a cysteine residue (C-terminal HA-Cys-6His) had an IC_{50} value ($155.62(\pm 39)\mu\text{g/mL}$) after 72h exposure to B16 cells. The rGel construct without cysteine (N-terminal 6His-V5) had an IC_{50} value of $36.62(\pm 6.34)\mu\text{g/mL}$. Commercial gelonin (Enzo life Sciences, Exeter, UK) had an IC_{50} value of $19.75(\pm 0.12)\mu\text{g/mL}$. This would indicate that the C-terminal cysteine residue was reducing toxicity (see chapter 7 for a statistical comparison) (figure 5.12). It had been previously published that gelonin was non-toxic up to a concentration of $1.4\mu\text{g/mL}$ in B16 cells (Patrick *et al.*, 2001). Compared to rGel, cGel was more toxic ($19.75(\pm 0.12)\mu\text{g/mL}$), as the cGel was subject to proteolytic activation (mature). The decision to compare rGel (with and without cysteine) cloned into a pre-gelonin ORF was taken in order to control for the addition of epitopes limiting toxicity by masking possible C- or N- terminal active amino acid sequence.

Gelonin intracellular delivery

Gelonin belongs to ribosome inactivation protein (RIP-I) family, lacks a cell-binding domain as such, is unable to translocate out of the endocytic system with the efficiency of RT. Consequently, at concentrations under $1.4\mu\text{g/mL}$ it demonstrated very little toxic to intact eukaryotic cells in agreement with the literature (Patrick *et al.*, 2001). But they were highly potent in cell free system (Stirpe *et al.*, 1980). However underscoring the idea that intracellular trafficking of gelonin is rate limiting relative to its cytotoxicity is the published data that characterises commercial gelonin (Enzo life Sciences, Exeter, UK) when introduced to a reticulocyte assay, as having an IC_{50} of 4ng/mL . Commercial gelonin has also been published to be slightly less toxic (below 50%) in HeLa cells ($100\mu\text{g/mL}$ relative to the Vero and B16 cells examined herein (Stripe *et al.*, 1980). It is likely that discrepancies in basil

rates of endocytosis and the cell specific efficiency of membrane recycling is responsible to this cell line specific variation in cytotoxicity.

Commercial RTBC delivery system

The cRTBC preparation can bind to galactose receptors on cell membranes and it plays vital role in RT intoxication. Here cRTBC was analysed for its ability to deliver cGel. Here, an increase in cytotoxicity was considered an indication of cRTBC's ability to deliver cGel. After analysing the cytotoxicity of cRTBC and cGel mixture (10µg/mL each protein) in both Vero and B16 cells there was not much increase in cytotoxicity of cRTBC (figure 5.13). This indicated that the re-association of cRTBC-cGel might be appropriate. However this would bias the experiment in favour of the cRTBC delivery system, as it would be very difficult to isolate re-associated cGel and PAA, PAA not having a specific lectinic activity. During this particular experiment, only cGel was analysed as it showed high cytotoxicity alone and together with FF103 polymer.

Poly(amidoamine) delivery systems

Poly(amidoamine)s have been documented as having the ability to form polyelectrolyte complexes with DNA and they have also been used to mediate transient transfection (Richardson *et al.*, 2001). FF91 did not increase the toxicity of RTAC or gelonin (Patrick *et al.*, 2001). This result was mirrored by the experiments performed here in that FF91 did not increase the cytotoxicity associated with a static non-toxic concentration of either recombinant or cGel, which given the previous published data is not contradictory (Patrick *et al.* 2001). It is possible that, this is a result of polymer charge and concomitant reduced polymer cellular uptake (Richardson *et al.*, 2010).

Similar to ISA1, it is likely that FF103 carries a net positive charge at neutral pH. This is reflected in the toxicity profile of FF103 relative to FF91 (Richardson *et al.*, 1999). When applied together rGel and FF103 showed higher toxicity than FF103 alone in B16 cells. When the rGel concentration was increased to 14µg/mL, the toxicity was increased 100 folds, which indicates that increasing the gelonin concentration results in high cytotoxicity (figure 5.14). This maybe interpreted as gelonin delivery still being suboptimal.

From the literature FF103 promotes increased cytotoxicity when mixed with rGel than parent ISA1 polymers, as FF103/rGel IC₅₀ is 88µg/mL relative to ISA/cGel IC₅₀ was 650µg/mL.

The inclusion of a C-terminal cysteine group in rGel did not appear play role in enhancing the cytotoxicity of rGel constructs. It was evident by the fact that IC₅₀ values of FF103 polymers were similar with both (+ or – C-terminal Cys) rGel constructs (figure 5.14 and 5.15). It may be possible that intrachain cysteine bonds within rGel might associate with the FF103 polymer.

Mature gelonin was also toxic when applied together with FF103. The IC₅₀ value of FF103 decreased 7 times (figure 5.16) when applied together with mature gelonin. It showed higher toxicity than rGel proteins and less than cGel (see chapter 7).

The cGel preparation was more potent to cells when applied together with FF103 polymer (in B16). At 10 µg/mL FF103, when mixed with cGel, decreased cell viability up to 20%. Since FF103 is likely to carry a net positive charge at neutral pH and it was assumed to be subject to endocytic capture by both non-specific adsorptive as well as the fluid phase mechanisms of endocytosis (Mellam, 1994) and may help in effective internalisation of gelonin along with the polymer (Richardson *et al.*, 2010).

Similar results were observed in Vero cells. FF91 showed 60% viability up to 3mg/mL concentration of polymer and adding cGel didn't resulted in increase in toxicity. But FF103 showed high cytotoxicity than FF91. When applied along with cGel, the IC₅₀ value of FF103 was decreased up to 445(±17.4) µg/mL from 625(±10.2) µg/mL (FF103 alone).

Molecular weights of ISA23 (M_n 10500) and ISA1 (M_n 5000) polymers analysed before (Patrick *et al*, 2001) were less than the polymers (FF103 M_n: 1800 and FF91 M_n: 12700) analysed during this study. As molecular weight has been shown to influence polymer cytotoxicity (FF91 and FF103), it may be possible to further enhance the toxicity (mediated through membrane disruption) and effective delivery (also mediated through membrane disruption) of gelonin by increasing the molecular weight of the PAAs used.

5.5 Conclusions

In this study, two recombinant gelonin constructs were successfully generated and sub-cloned into a bacterial expression cassette. The success of these sub-cloning efforts was confirmed by analysing the DNA sequence of the plasmids generated. One gelonin construct contained N-terminal 6His and V5 epitopes, and the other a C-terminal HA epitope, an additional cysteine residue and a 6His motif. Both proteins were successfully expressed, purified and characterised using SDS-PAGE and Western blotting.

The cytotoxicity of two rGel constructs described was evaluated and compared to recombinant mature (no additional C-terminal amino acids) and cGel. The cGel preparation showed cytotoxicity in both B16 and Vero cells (see chapter 7).

When cRTBC was mixed with cGel, an increase in cytotoxicity relative to the background toxicity of the cRTBC construct was not observed. This indicates that enhanced ER translocation did not promote the delivery of cGel into the cytosol. Re-association of cRTBC and cGel may enhance intracytoplasmic delivery of cGel though this experiment remains to be undertaken.

It was possible that the inclusion of C-terminal epitope may reduce the toxicity of recombinant gelonin constructs (see chapter 7 for further analysis), which might be expected relative to the proteolytic maturation of the wild type cGel protein. The incorporation of an extra C-terminal cysteine in rGel enhance the cytotoxicity of FF103. This might indicate that the FF103 polymers were interacting with intermolecular cysteine bonds within the gelonin molecule. The statistical analysis of these data is undertaken (Chapter 7).

The PAA-SSPy polymers ability to deliver rGel and cGel was evaluated. FF91 (similar to ISA23) did not enhance cytotoxicity when applied together with gelonin.

The PAA FF103 (similar to ISA1) contained an ethenyl dithiopyridine monomer capable of forming disulphide bonds with cystine residues within rGel constructs. Relative to published data, describing the effects of ISA1 (when mixed with cGel), FF013 appeared to enhance gelonin toxicity.

Chapter 6
**Evaluation of ISA1-FITC and ISA23-FITC Polymer Cytotoxicity
and Intracellular Trafficking by Fluorescent Microscopy**

6.1 Introduction

Biomaterials are substances used in therapeutic and diagnostic systems that are in contact with biological fluids or tissues. Polymers of both natural and synthetic origin are widely used as biomaterials in medicine and drug development (Nair and Laurencin, 2006). Polymers such as, alginates, used to coat tablets and capsules can be incorporated into a drug delivery systems. Similarly drug delivery systems may be composed of polymers conjugated to drugs or proteins. An example of a polymer conjugated drug delivery system is the HEMA copolymer-doxorubicin conjugate developed by Duncan and colleagues (Duncan, 2009) developed to treat cancer. Polymers can also be used in making extra corporal devices such as lenses (poly(methyl-methacrylate)) (Frazer *et al.*, 2005) or used in heart valves (poly(tetrafluoroethylene)) (Kidane *et al.*, 2008).

Before considering a polymer for biomedical application, its biocompatibility profile has to be evaluated. The assays for the evaluation biocompatibility of biomaterials are specific to the intended application. Many studies have been undertaken and *in vitro* systems have been established to describe the biocompatibility of soluble polymers in pre-clinical and pre-animal testing models (Sgouras and Duncan, 1990; Sgouras 1990).

In this study, the MTT assay (Sgouras, *et al.*, 1990) was used to assess the cytotoxicity of the poly(amidoamine) (PAA) polymers ISA1-FITC and ISA23-FITC. To standardise the assay, reference controls were also evaluated, serving as positive and negative controls respectively. These reference systems have been well characterised *in vitro* and have been used as standards against which any observed polymer toxicity was compared. Some of the reference polymers include poly(L-lysine), PEI, dextran and chitosan (Sgouras 1990; Richardson *et al.*, 1999). The values obtained from these *in vitro* studies help in choosing non-toxic polymer concentration ranges for microscopy and may not be extrapolated directly to *in vivo* studies.

Understanding endocytosis and the intracellular trafficking of macromolecular drugs (and delivery systems), is a prerequisite for developing effective novel drug delivery systems (Richardson *et al.*, 2008; Jones *et al.*, 2003). Several tools are available to evaluate the intracellular localisation of drug delivery systems or of macromolecules, such as, sub-cellular fractionation, epifluorescence microscopy, fluorescence laser scanning confocal microscopy and live cell imaging.

In this study, fluorescence microscopy has been used to detect fluorescently labelled PAA polymers inside the cell. Intracellular location of the polymers was confirmed using physiological markers such as BSA-TxR (Richardson *et al.*, 2004), WGA-TxR (Cresawn *et*

al., 2007) or immuno-labelling specific organelles using antibodies to define sub-cellular compartmentalisation. In this study, intracellular organelles were identified using specific antibodies. Early sorting endosome was immuno-labelled using an antibody specific for EEA1 (Mills *et al.*, 1999), the Golgi apparatus was identified using an antibody specific for GM130 (which decorates the *cis*- and *medial*- Golgi (Walker *et al.*, 2004)). Late endocytic structures were identified using an antibody specific for LAMP 1 (Luzio *et al.*, 2001). The internalisation and intracellular trafficking properties of BSA-TxR and WGA-TxR (Richardson *et al.*, 2008) were well characterised and were used as counter stains to identify the approximate intracellular location of the PAA polymer.

When compared to sub-cellular fractionation, fluorescence microscopy is quicker, less labour intensive and less expensive. However, even when optimal fixation and imaging protocols have been established, the data is at best, qualitative. After aldehyde or solvent fixation, permeabilising the cell membrane by detergent extraction, can result in the leakage of a polymer from one intracellular compartment to another. Another potential problem is, sometimes the fluorophore itself, which can demonstrate pH-dependent quenching. Further, free fluorophore released from the carrier molecule after its internalisation can also give rise to the misinterpretation of data.

In this study, the imaging of FITC-conjugated PAA polymers in live Vero cells was undertaken. During live cell imaging it was possible to visualise trafficking events between multiple compartments within an individual, living cell, over time. Using this method, it was not possible to utilise the immuno-labelling of the cellular organelles and the frequent use of intense light can result in either photo bleaching or cell damage. Despite these limitations, imaging using live cells relative to fixed cells, makes the documentation of fixation artefacts less likely. Further, the data sets acquired used polymer concentrations that were non-toxic, making it unlikely that polymer toxicity was responsible for false positive results *i.e.* artefacts.

The following questions were addressed in this chapter:

1. Are ISA1-FITC and ISA23-FITC polymers cytotoxic?
2. Is the ISA-FITC conjugate stable over time in cell culture media?
3. Is it possible to detect ISA-FITC polymers in the cytosol/nucleus over time in live cells?

6.2 Materials and methods

Cytotoxicity

Dextran and PEI were used as negative and positive controls during the MTT cell toxicity assays. Polymer solutions were made fresh every time before use. Prior to use, all polymer solutions were filter sterilised through a 0.2 μ m filter. Standard cell culture protocols were used to evaluate the cytotoxicity of the polymers ISA1-FITC and ISA23-FITC as described in section 2.2.10.

Evaluation of stability of ISA1-FITC in cell culture and RP media over time

ISA1-FITC stock solutions (2mg/mL) were prepared either in complete media or RP media. Then, 2.5mL of each ISA-FITC solution was placed into a 35mm dish and incubated at 37°C for 5h. During this time, PD10 columns (GE Healthcare, Buckinghamshire, UK) were prepared by discarding the column storage medium and equilibrating the columns using 35mL of 1xPBS (pH 7.2). To the each column, 2.5mL of ISA-FITC in either complete or RP media was allowed to enter the Sepharose matrix. The flow-through was discarded. Using 1xPBS as an eluent, 1mL fractions were collected using sterile Eppendorf tubes. The absorbance of the collected fractions were measured at 495nm. Using the Prism Graph Pad Software, graphs describing polymer-FITC stability (*i.e.* fraction number and FITC absorbance) were plotted. By calculating the area under the curve, the free FITC concentration was measured.

Epifluorescence microscopy

The intracellular trafficking of ISA1-FITC and ISA23-FITC PAA polymers were studied using Vero cells. Cell preparation was performed as described in section 2.2.14. When dosing the cells, BSA-TxR (10mg/mL), and ISA1-FITC or ISA23-FITC (2mg/mL) with leupeptin (final concentration: 200 μ M), were used in a 0.5mL final volume. Different time points were used (1h, 4h and 24h) for the analysis of the localisation of the polymer inside the cell. Two protocols were followed in the experiments (section 2.2.14). During first protocol, after the aldehyde fixation of the polymers, Vero cells were permeabilised using Triton extraction buffer. During second protocol, Vero cells were not permeabilised with detergent and after the blocking step, they were mounted on to the glass slide (section 2.2.14).

Live cell imaging

The preparation of cells in 35mm sterile dishes was performed as described in section 2.2.15. Polymer stock solutions were prepared as above and applied onto the cells with a final concentration of 2mg/mL, along with WGA-TxR (20 μ g/mL) and leupeptin (final concentration: 200 μ M) in 0.5mL total volume. Here WGA-TxR was used as a counter stain. After 1h incubation at standard culture conditions, cells were washed three times with 1xPBS and 2.5mL of sterile RP media applied. Live cell imaging was performed as described in section 2.2.15, over 4h using Nikon ECLIPSE Ti-U inverted microscope (Surry, UK).

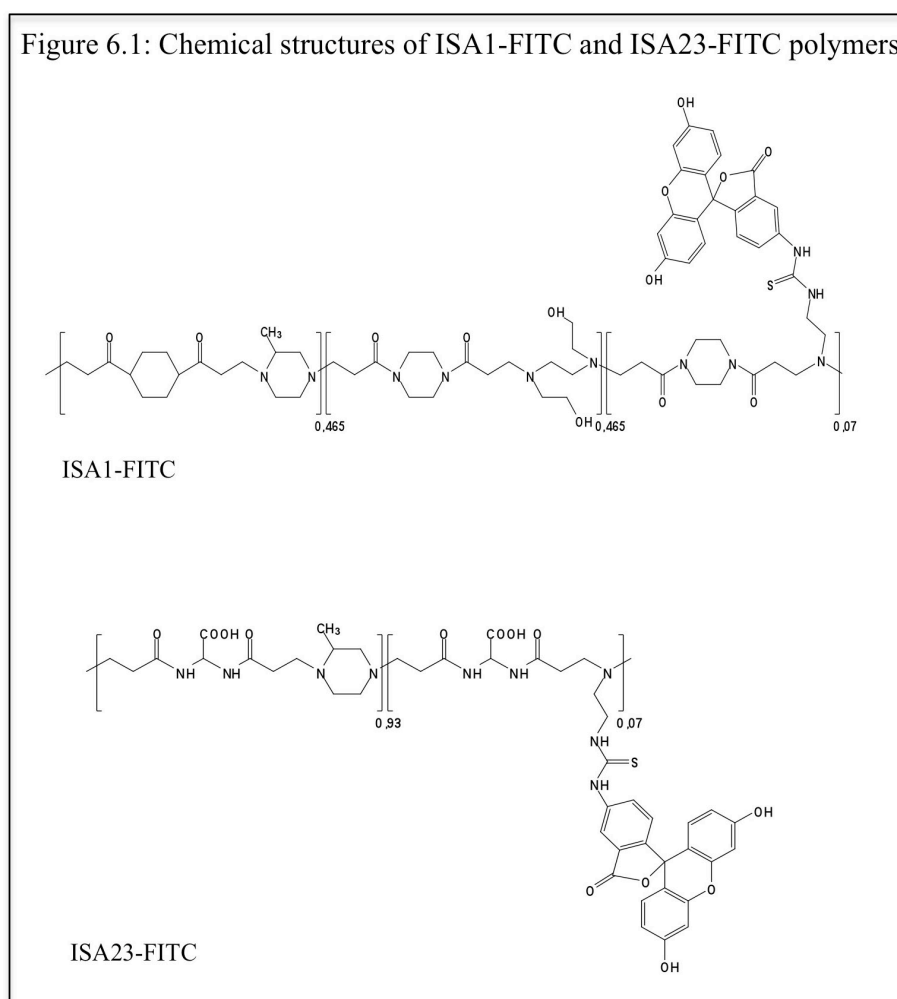
Synthesis and characterisation of ISA1-FITC and ISA23-FITC

The conjugation of ISA1 and ISA23 polymers to FITC was performed by Dr. Fabio Felini (University of Milan). The loading of FITC on ISA23- FITC sample was 6.95%, whereas the FITC loading of ISA1-FITC was 6.43% on a molar basis. Dr Felini also performed the characterisation of the polymers described here.

Table 6.1: ISA-FITC polymers evaluated in this study.

Polymer	M _n	M _w	PI
ISA1-FITC	12030	14070	1.17
ISA23-FITC	12100	23500	1.94

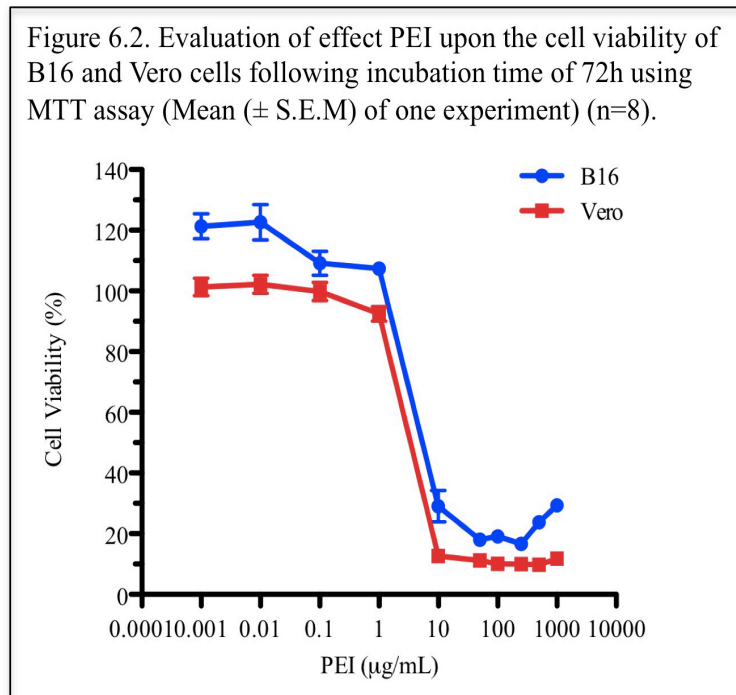
Figure 6.1: Chemical structures of ISA1-FITC and ISA23-FITC polymers



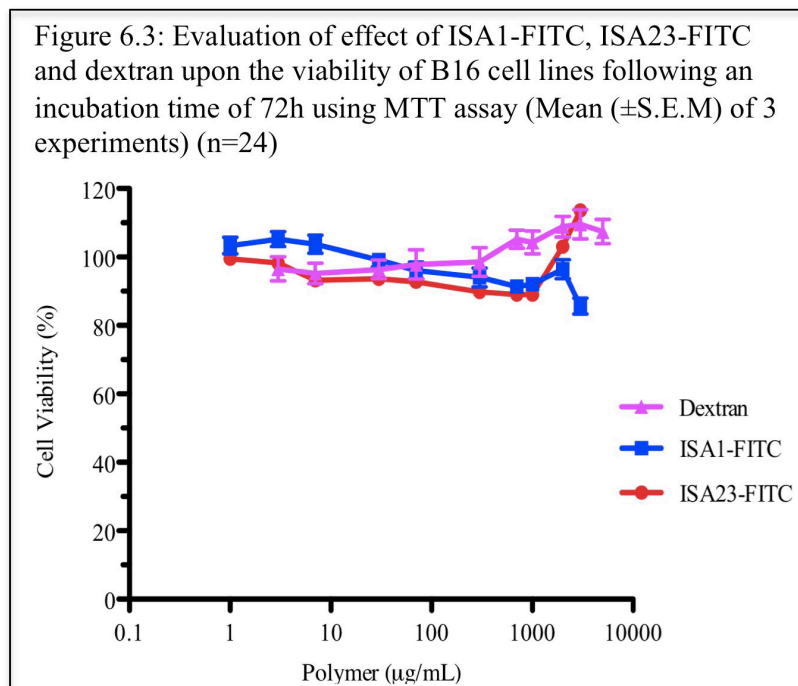
6.3 Results

6.3.1 Evaluation of FITC-conjugated PAA cytotoxicity

Before evaluating the cytotoxicity of the PAA-FITC conjugated polymers, control polymers (PEI and dextran) cytotoxicity was determined in Murine melanoma cell lines (B16) and African monkey kidney epithelial cell lines (Vero) using the MTT assay with a 72h incubation time. From figure 6.2 it was observed that in both B16 and Vero cells, PEI showed cytotoxicity. The IC_{50} of PEI in Vero cells was $6.35(\pm 0.41)\mu\text{g/mL}$ and in B16 it was $7.95(\pm 0.88)\mu\text{g/mL}$. As expected dextran, which was a negative control, was non-toxic to both the cell lines over the concentration range tested (figure 6.3 and 6.4).



ISA1-FITC and ISA23-FITC polymers toxicity was evaluated using MTT assay in both B16 and Vero cells with 72h incubation time. From figure 6.3, it was observed that, the ISA1-FITC and ISA23-FITC polymers were almost non-toxic (cell viability was above 80%) in B16 cells over the concentration ranges evaluated.



From figure 6.4, it was observed that, in Vero cells, both the polymers (ISA1-FITC and ISA23-FITC, at 3mg/mL concentration) had killed 50% of the population of cells they were tested against. When the concentration of the polymer increased to 10mg/mL, after a 24h incubation time, the cell population decreased to 10% (figure 6.5). The IC₅₀ values of PEI, ISA1-FITC and ISA23-FITC were also documented (table 6.2)

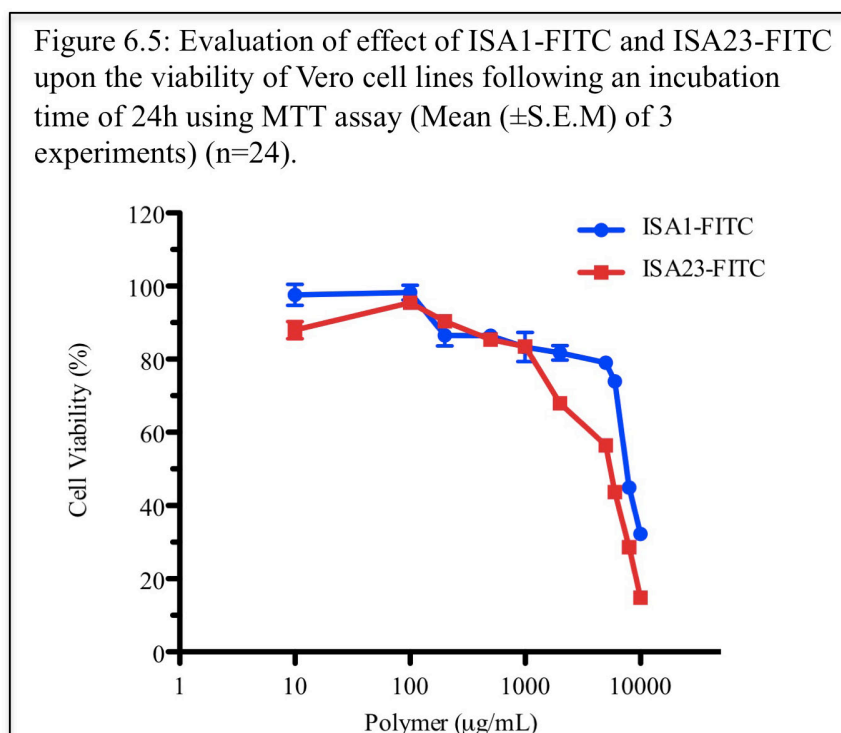
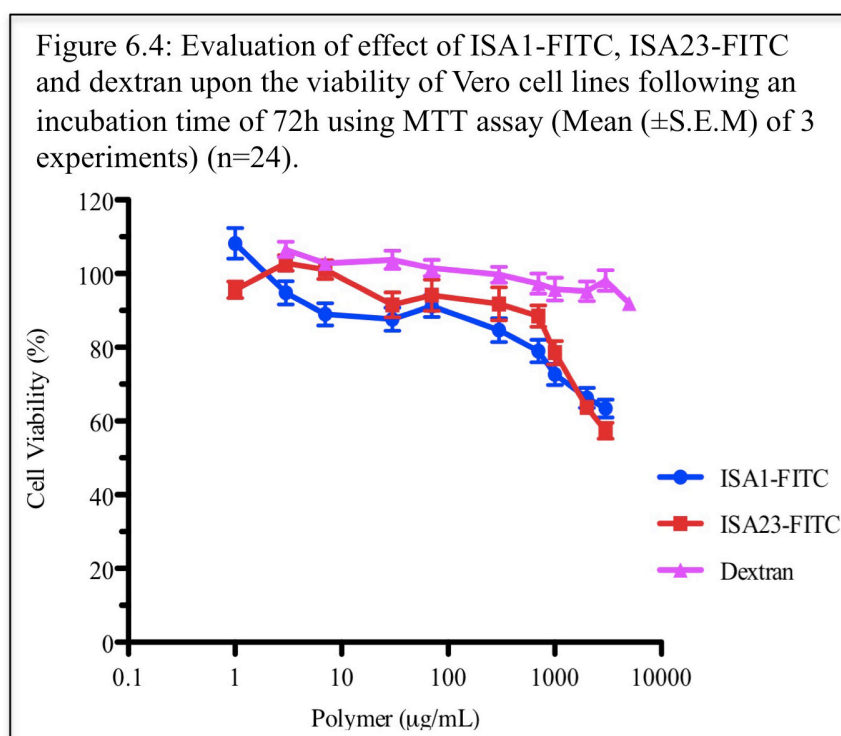
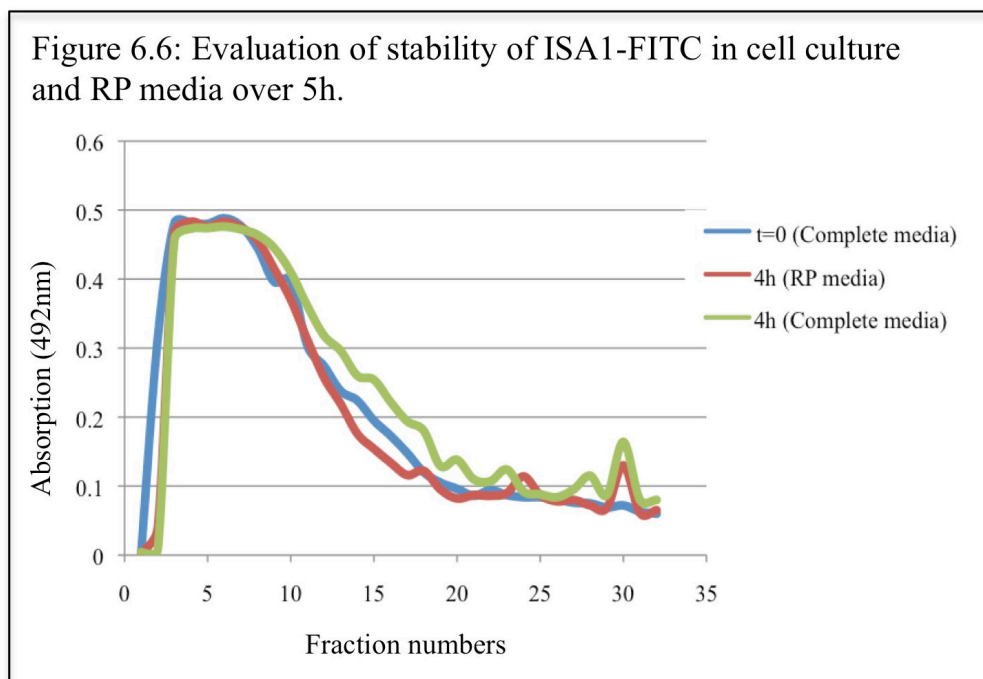


Table 6.2: Polymers (PEI, ISA1-FITC and ISA23-FITC) cytotoxicity in B16 and Vero cells.

Polymer	In B16 cells (IC ₅₀ : µg/mL, ± SEM)	In Vero cells (IC ₅₀ : µg/mL, ± SEM)
PEI (72h incubation)	7.95 (±0.88)	6.35 (±0.41)
ISA1-FITC (24h incubation)	Not determined	9222.5 (±171.67)
ISA23-FITC (24h incubation)	Not determined	8147 (±105.85)

6.3.2 Evaluation of stability of ISA1-FITC polymer in complete or RP media

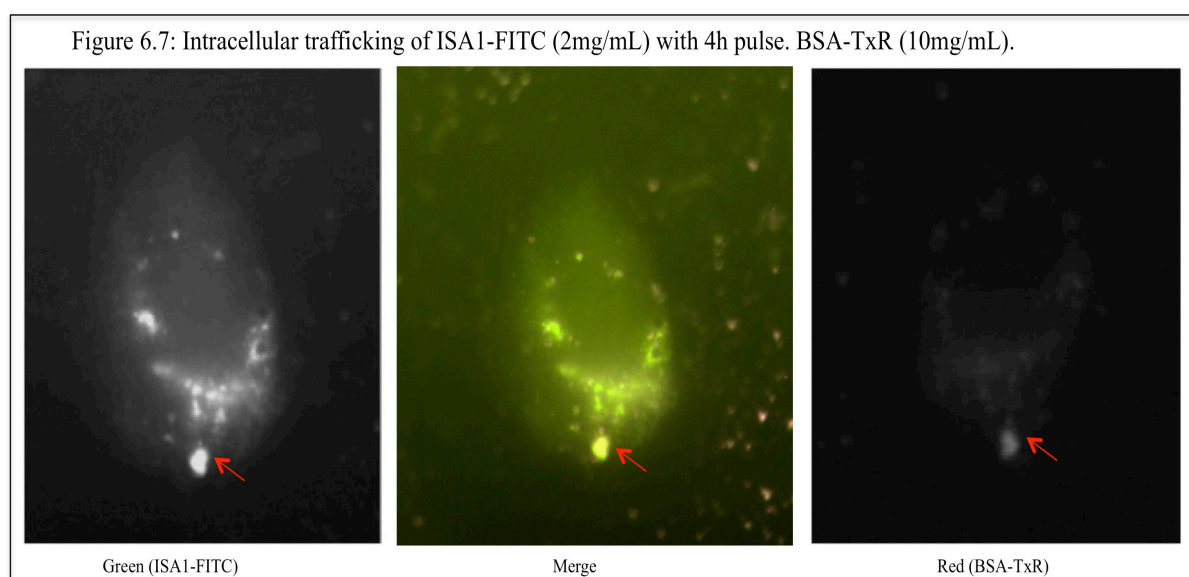
Figure 6.6, documents ISA1-FITC stability over 5h. Here 3.4% (w/v) of free FITC was released into RP media. Most of the FITC remained conjugated to the ISA1 polymer and was eluted in first 3-4 fractions. At t=0, there was no free FITC detected. In complete cell culture media there was a slight increase (0.06%) in the release of free FITC compared with in RP media.

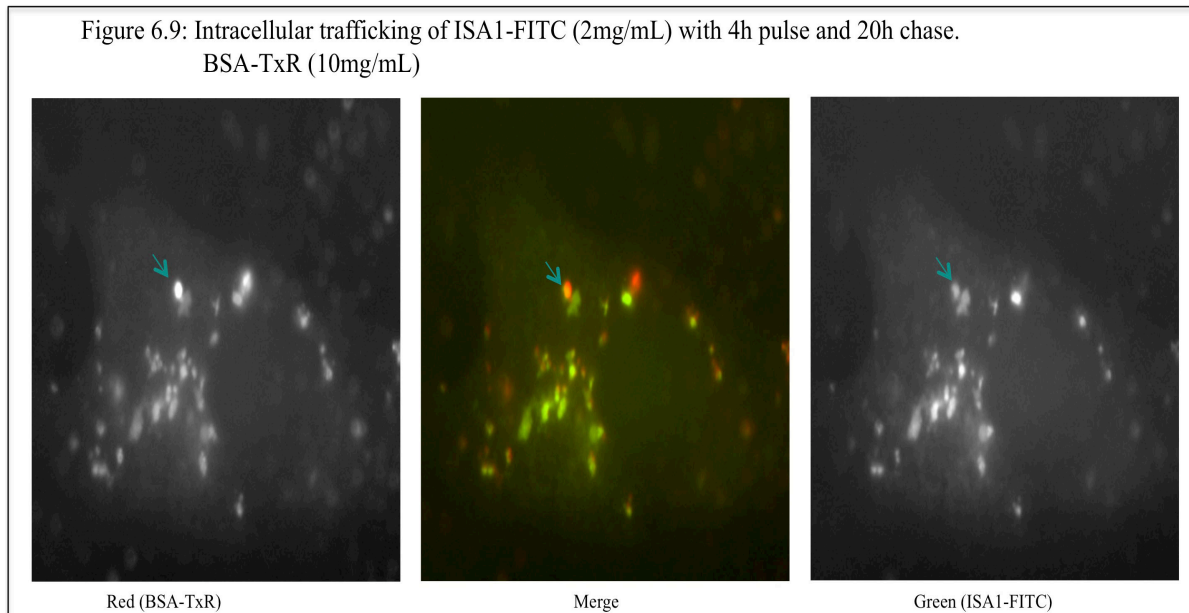
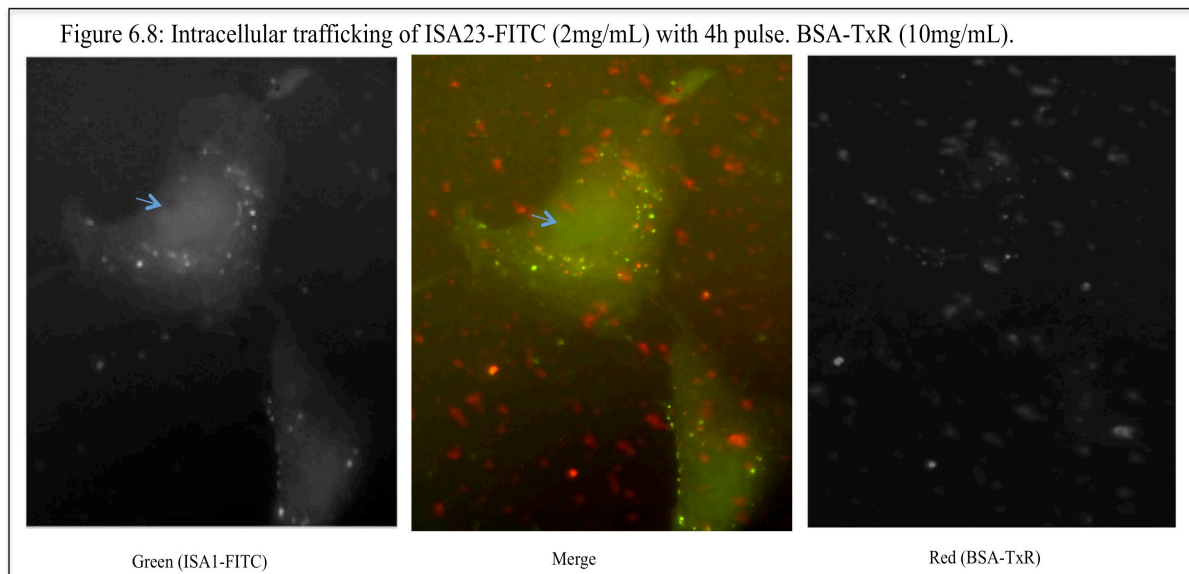


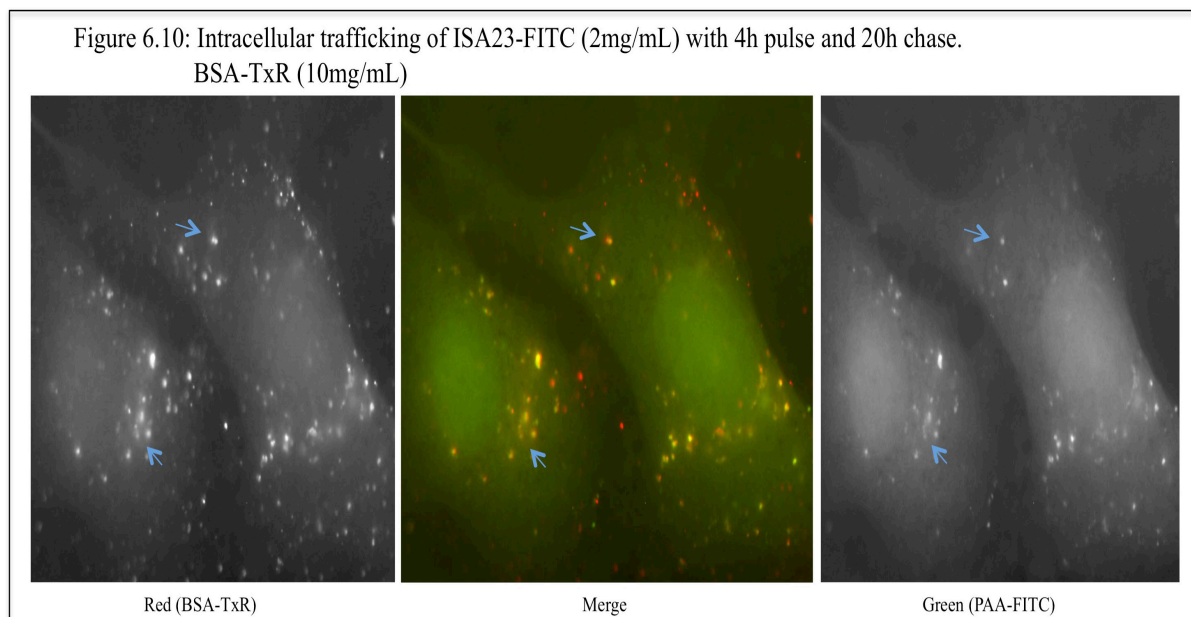
6.3.3 Investigation of polymer intracellular fate

Cell culture methodology and the addition of PAA polymers to cells was described in section 2.2.14. After aldehyde fixation, cells were subject to detergent extraction to facilitate immuno-labelling. Equivalently solvent extraction was used to fix the cells. Polymers were documented diffusing out of what were membrane delineated structures giving rise to false apparent cytosolic or nuclear polymer distribution. To circumvent this problem, the permeabilisation step was removed and non-immunological counterstaining techniques were deployed.

For both ISA1-FITC and ISA23-FITC, a 1h pulse was not sufficient to detect the polymer inside the cell (data not showed). After a 4h pulse (figure 6.7 and 6.8), both of the polymers were documented displaying a punctate intracellular distribution that would support the notion that they were localised within the lumen of endocytic organelles, such as endosomes. Data documenting ISA1-FITC and ISA23-FITC co-localising with BSA-TxR over a time course where BSA-TxR was known to be inside LAMP positive structure further supports this hypothesis (figure 6.7 and 6.8). Surprisingly ISA23-FITC can also be seen in the nucleus (figure 6.8), where as ISA1-FITC cannot be observed. At third time point, a 4h pulse with a 20h chase, clearly shows that (figure 6.9 and 6.10) both ISA1-FITC and ISA23-FITC can be seen in the cytosol as a green haze. There is also co-localisation of both ISA1-FITC and ISA23-FITC with BSA-TxR.



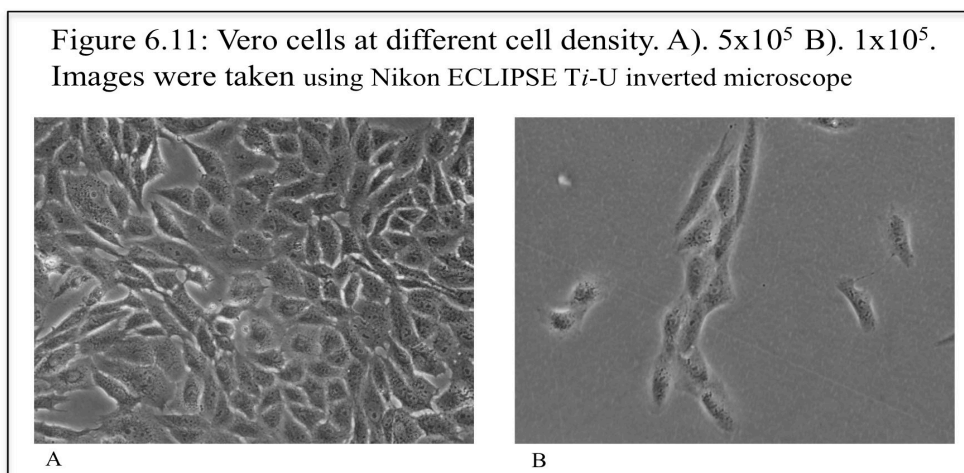




6.3.4 Live cell imaging

To document the internalisation of ISA1-FITC and ISA23-FITC in live cells, several parameters were optimised, such as cell density (1×10^5 or 5×10^5), polymer concentration (0.2mg/mL, 2mg/mL and 3mg/mL) and incubation time (1h, 4h and 24h). While determining the optimal time, cells were aldehyde fixed without permeabilisation *i.e.* omitting the Triton X-100 detergent extraction step. WGA-TxR was used as a counter stain. When optimising polymer concentration, WGA-TxR concentration was kept constant ($10 \mu\text{g/mL}$) and was administered with leupeptin (final concentration: $200 \mu\text{M}$).

At 5×10^5 cells/well, it was difficult to image individual cells. When the seeding density was decreased to 1×10^5 cells/well, cells were observed individually. In further experiments, this optimised cell density was used (figure 6.11).



At 0.2mg/mL ISA1-FITC or ISA23-FITC, there was not enough fluorescent signals to detect the polymer at all three time points (data not showed). When the polymer concentration was increased to 2mg/mL and with a 4h and 24h pulsing time, both ISA1-FITC and ISA23-FITC polymers were observed, first in *puncta*, then in the cytosol and in the nucleus. (figures 6.12, 6.13, 6.14 and 6.15)

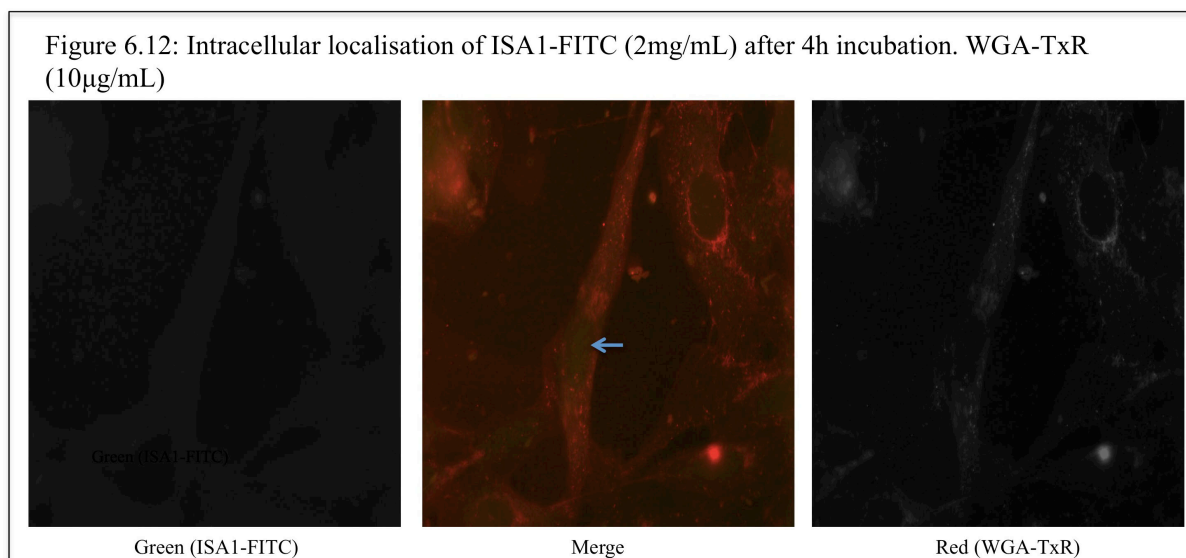


Figure 6.13: Intracellular localisation of ISA23-FITC (2mg/mL) after 4h incubation. WGA-TxR (10 μ g/mL)

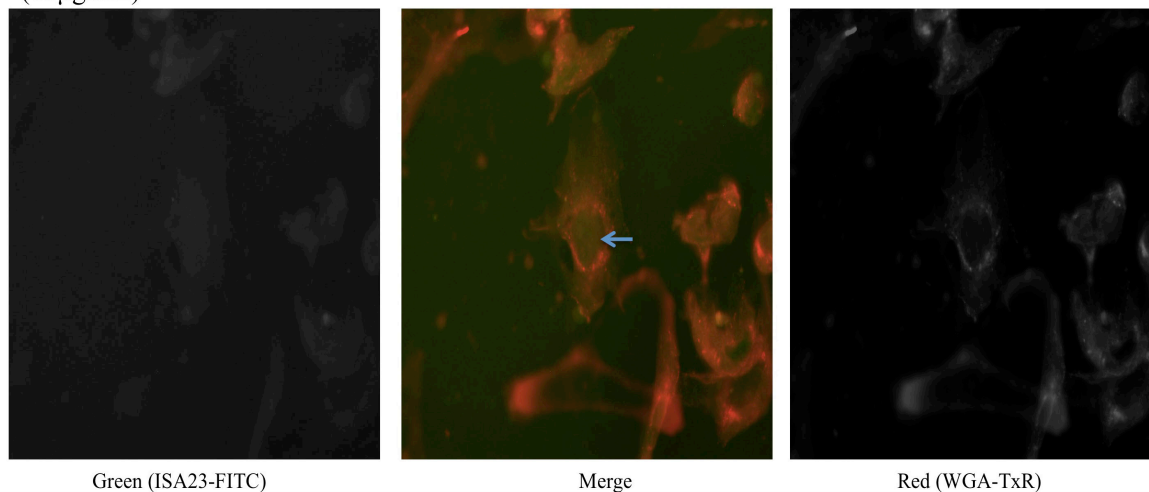
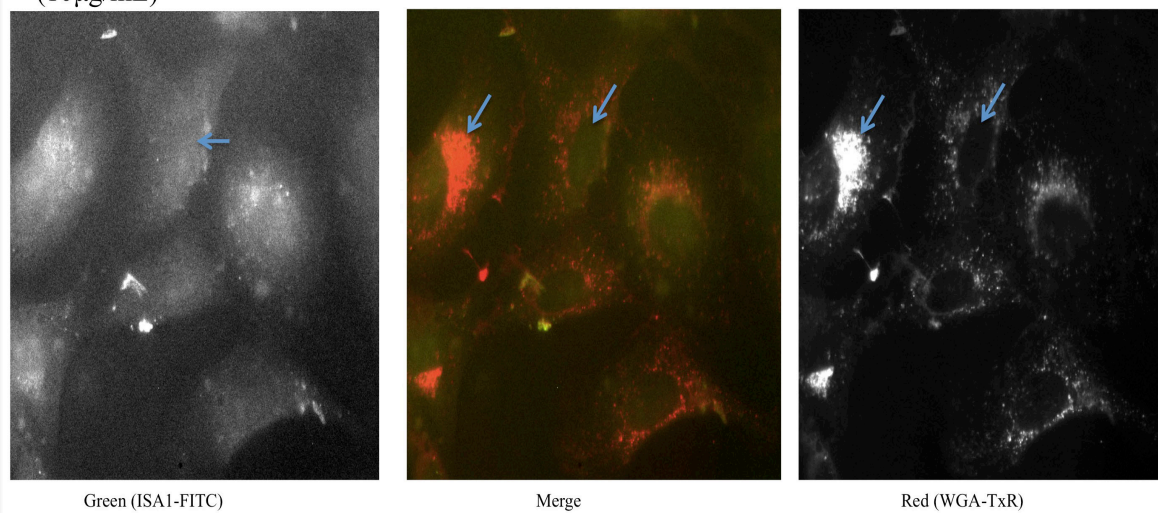
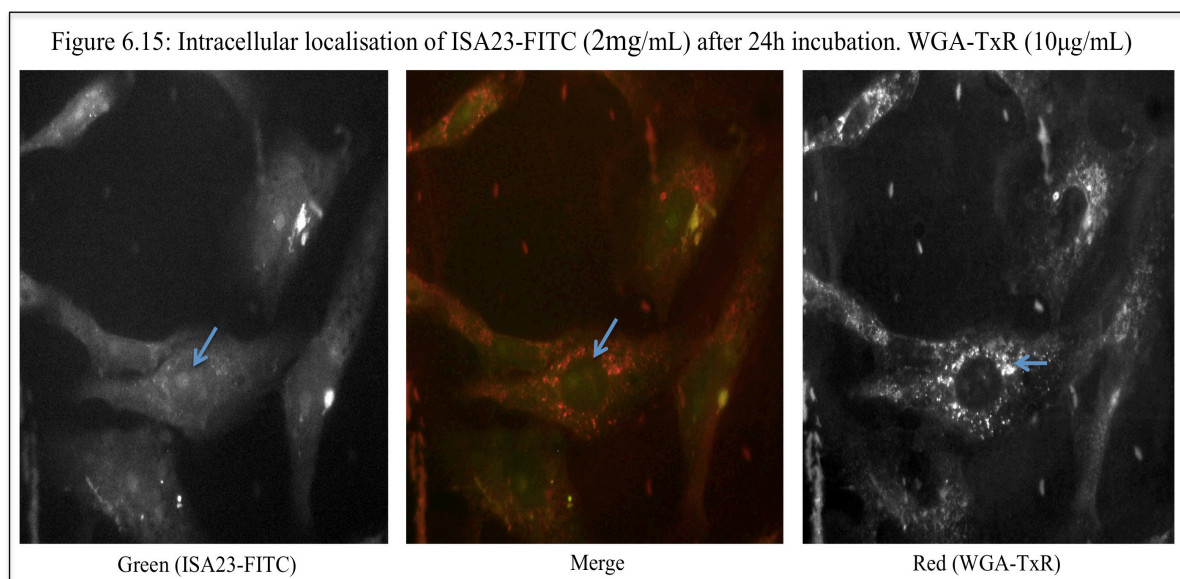


Figure 6.14: Intracellular localisation of ISA1-FITC (2mg/mL) after 24h incubation. WGA-TxR (10 μ g/mL)





This data (figure 6.12–6.15) reinforces the conclusions drawn from the previous experiments using BSA-TxR as a counter stain (figure 6.9, 6.10 and 6.11). ISA23-FITC showed strong nuclear localisation compared to ISA1-FITC (figure 6.13 and 6.15). WGA-TxR can be observed in late endocytic structures (Richardson, 2004). When polymer concentrations were increased to 3mg/mL, high background fluorescence was observed making it difficult to differentiate signal from noise.

The optimum concentration of WGA-TxR was evaluated directly via live cell imaging. Three concentrations of WGA-TxR were analysed (10µg/mL, 20µg/mL and 25µg/mL) (Richardson *et al.*, 2008). Among these concentrations, 20µg/mL proved optimum, which showed high fluorescence with minimum background (data not shown).

Live cell imaging was performed (described in section 2.2.15), by applying the optimised conditions which were obtained from fluorescence microscopy experiments (section 6.3.3). ISA1-FITC (2mg/mL), WGA-TxR (20µg/mL) and leupeptin (final concentration: 200µM) were applied to cells in 0.5mL volume. From movie 1 (Appendix I), it was clearly observed that with increasing time, ISA1-FITC was localised to the cytosol, whereas the counter stain WGA-TxR was only seen in lysosomes, not in the nucleus.

When the experiment was repeated using ISA23-FITC, no fluorescence was detected in the cytosol. Control experiment was performed using WGA-TxR (20µg/mL) and free FITC (4.8µg/mL) with same experimental conditions as with polymers. Free FITC concentration

was calculated as described in section (6.3.2). It was observed that free FITC was appearing as greenback ground.

6.4 Discussion

ISA1-FITC and ISA23-FITC polymers were approximately 400 times less cytotoxic than PEI in both Vero and B16 cells. In Vero cells, 60% cell viability was observed at 3mg/mL polymer concentration (ISA1-FITC and ISA23-FITC). These data were comparable with previous experiments characterising ISA1 and ISA23 polymers (Richardson *et al.*, 1999).

B16 and Vero cells displayed differential sensitivity to both polymers. Vero cells seem to be more sensitive to ISA1-FITC and ISA23-FITC polymers than B16 cells. PEI toxicity data was comparable with literature (Sgouras, 1990) and at a concentration of 10 μ g/mL, in both cell lines, viability diminished to approximately 10% of the control. This result is thought to be due to the cationic charge associated with PEI relative to the PAAs tested herein (Richardson *et al.*, 2010).

Dextran did not show any cytotoxicity in both B16 and Vero cell lines. After internalisation, up to 50% of the endocytosed dextran has been reported to be recycled back into plasma membrane. The remaining dextran degrades in the lysosomes. Previous reports would suggest that the net endosomal half-life of the dextran makes it useful as a marker for fluorescence work (Richardson *et al.*, 2008).

When the concentration of ISA1-FITC and ISA23-FITC polymers was increased to 10mg/mL, there was a clear increase in cytotoxicity for both polymers in Vero cells (table 6.2). This experiment was undertaken to evaluate the maximum concentration of the polymer that could be applied on to the cells during the fluorescence studies. Here the MTT assay was performed after 24h after exposing the cells to the polymers. Surprisingly ISA23-FITC showed high toxicity (IC₅₀: 8.14(\pm 0.10)mg/mL) compared to ISA1-FITC (IC₅₀: 9.22(\pm 0.17)mg/mL). At neutral pH, ISA1 posses slight net cationic charge, where as ISA23 carries a slight net negative charge (Griffiths *et al.*, 2004). In general cationic polymers tend to show high toxicity relative to amphiphilic and anionic polymers. It was concluded that a 3mg/mL concentration of PAA was appropriate for fluorescence microscopy experiments in Vero cell lines as little toxicity was observed at this concentration. This particular experiment was not performed with B16 cell lines despite these cells providing a useful comparison with previous published work from Professor Duncan's laboratory (Richardson *et al.*, 2010). However the presence of melanosomes and the non-standard trafficking pathways associated

with B16 cells make them hard to interpret regarding sub-cellular trafficking studies (Wade *et al.*, 2001).

During the fluorescent microscopic examination of PAA containing cells, it was observed that after fixing the cells with either aldehyde or solvent, permeabilising cell membrane could result in the diffusion of the soluble polymer out of the cell and cellular organelles (data not shown). Even though membrane permeabilisation with detergent buffer is essential for the immuno-labelling of the specific organelles, it resulted in the displacement of polymer signal (a fixation artifact). To overcome this problem, immuno-labelling of organelles was avoided and instead physiological markers like BSA-TxR and WGA-TxR were used to evaluate the localisation of the PAAs inside the cell (Richardson *et al.*, 2008). Albumin is widely used to characterise the endocytic pathway (Richardson *et al.*, 2004). BSA enters cells by fluid phase, adsorptive and receptor-mediated endocytosis mechanisms (John *et al.*, 2003). By observing its trafficking at different time points, it was possible to identify the endocytic sub-compartments occupied. WGA can bind to most cell types and is a more sensitive probe than BSA as a greater proportion enters the cell through membrane association (Weissenboeck *et al.*, 2004). This point is dramatically emphasised when the quantities of WGA and BSA necessary for fluorescent imaging are considered. BSA needs to be applied to cells at a minimum concentration of 5mg for a minimum of 1h. WGA can be documented in late endocytic structures after it is applied to cells at 20 μ g/mL concentration, approximately 100 fold less than BSA.

At the 4h time point, at a 2mg/mL polymer concentration both ISA1-FITC and ISA23-FITC polymers were seen to display a nebulous (cytosolic) distribution. Interestingly ISA23-FITC also showed nuclear localisation. Previously it was shown that ISA1 has high cell binding and internalisation (~60 times) than ISA23, due to ISA1's cationic charge at pH 7.4 (Richardson *et al.*, 2010). Here it was observed that at both 4h and 24h time points ISA23-FITC showed greater cytosolic and nuclear presence compare to ISA1-FITC (figure 6.7-6.10). It was already known that ISA1 has the ability to deliver non-permeant protein toxins (gelonin and RTAC (Patrick *et al.*, 2001)), where as ISA23 did not.

Here for the first time, the cytosolic accumulation of ISA1-FITC and ISA23-FITC polymers has been documented microscopically. Live cell imaging also revealed ISA1-FITC nuclear localisation after 5h.

Upon examination using fluorescence microscopy both ISA1-FITC and ISA23-FITC showed nuclear localisation however during live cell imaging, only ISA1-FITC showed clear nuclear

localisation. These data raise the question of fixation artefacts, which remains to be resolved. Previously it has been documented that ISA1 has a higher capacity to enter mammalian cells than ISA23 (Richardson *et al.*, 2010). However this observation is juxtaposed by the observation that ISA23 has previously displayed higher transfection efficiency than ISA1, PEI and lipofectamine under the conditions previously documented (Richardson *et al.*, 2001). This difference between ISA1 and ISA23 remains to be explained.

The effect of free FITC upon (PAA-) FITC distribution inside cells was controlled for by monitoring PAA-FITC stability and calculating the release of free FITC into cell culture media. The effect and distribution of free FITC was manifest as none-specific, light green background. Free FITC was not localised into the cytosol or nucleus. This nonspecific distribution of FITC would support both the literature describing the effects of the PAA ISA4 on cell endomembrane (Richardson *et al.*, 2001; Patrick *et al.*, 2001 and Richardson *et al.*, 2010).

6.5 Conclusions

ISA1-FITC and ISA23-FITC polymers exhibited little toxicity above or beyond that of the parent polymers (Richardson *et al.*, 1999).

It was shown that the FITC released from ISA-FITC conjugates in cell culture media did not localise to either the cytosol or nucleus (at detectable levels) in the cell culture system utilised herein.

It was possible to detect FITC in both the cytosol and the nucleus of live ISA1-FITC treated Vero cells over a 5h time course. This chapter supports the hypothesis that PAAs offer a viable alternative to a ricin based cytosolic drug delivery system.

Chapter 7
General Discussion

7 General Discussion and Conclusions

Project Aims

Clostridium botulinum serotoxin A, marketed as Botox[®] (Allergan, CA, USA) has been shown to selectively prevent the release of acetylcholine (a neurotransmitter) at the neuromuscular junction (Dressler *et al.*, 2005). Within the context of this study, the cosmetic application of a virulent bacterial toxin sets precedence, potentially paving the way for the use of attenuated toxins as therapeutic nucleic acid delivery vehicles. Herein a new generation of novel mutant RT constructs were produced, expressed and evaluated as potential “cytosolic shuttle” for therapeutic entities like siRNA and antisense agents. The mutations introduced to RTAC were intended to ablate RT toxicity.

RT is a heterodimeric protein, which contains a lectinic B chain and an enzymatically active A chain, linked together by a disulphide bond (Lord and Spooner, 2011). Ricin can enter mammalian cells by more than one endocytic pathway and the molecular regulation of its intracellular trafficking is starting to be well defined (Spooner *et al.*, 2010). RT intracellular trafficking has been described in some detail (section 1.4.2.1) and results in the translocation of a macromolecule (protein) of approximately 30kDa into the cytosol. Once in the cytosol, in the instance of the wild type RT holotoxin, RTAC can assimilate its target (the ribosomes) to mediate intoxication through the inhibition of protein synthesis (Lord *et al.*, 2003).

Toxin mutation and sub-cloning into a bacterial expression cassette

Attenuation of RT was attempted herein using recombinant DNA technology, mutating the putative active site responsible for ribosome depuration. This region was selected as it has been already showed that the substitution of an Arg¹⁸⁰ residue with histidine reduces *N*-glycosidase activity at least 1000 fold in a rabbit reticulocyte lysate assay (Frankel *et al.*, 1990) and 500 fold less against *Artemia salina* ribosomes (Day *et al.*, 1996). Conversion of Glu¹⁷⁷ (Glutamic acid) to Gln (Glutamine) also reduces activity 180-fold (Ready *et al.*, 1991). The mutation planned herein incorporated both of these critical residues within a well-conserved region thought of as the RTAC catalytic site.

As described in chapter 3, the first step required for the production of recombinant, attenuated RTAC was to introduce either mutations or deletions within in catalytic region of the lethal domain (RTAC amino acids 177-182 deleted, or mutated to Gly). Following this, either at N- or C- terminal epitope such as 6His, V5, KEDL and eGFP were fused in frame

with the RTAC coding sequence. These combinations of additions and alterations to the RTAC coding sequence are detailed in table 1.7. The 6His moiety helped not only during the enrichment of recombinant RTAC and RTBC proteins via IMAC (section 2.2.5.4), but also helped identify the protein during immuno-blotting using commercially available antibodies (Terpe, 2003). It had been previously shown that the introduction of an ER retrieval sequence (C-terminal amino acids (Lys-Asp-Glu-Leu) *i.e.* KEDL), could increase the cytotoxicity of RT (Wales *et al.*, 1992). Here it was hypothesised that the addition of a C-terminal KDEL sequence may help enhance the trafficking efficiency of RTAC from the Golgi to the ER.

Having successfully produced and sequenced the candidate plasmids, the next step was to characterise the selected plasmid constructs (table 1.7). Here, for the first time, plasmid maps were generated, graphically describing the selected, sequenced, constructs *in silico* using the SeqMan software module, part of the LaserGene DNA analysis suite (DNASar, Madison WI, USA) (figures 3.1-3.7). Plasmids were further characterised by agarose gel electrophoresis (figure 3.8) and their concentration determined both spectrophotometrically as well as by gel analysis and densitometry.

Making recombinant RT constructs

The plasmid constructs were used to generate rRTAC and rRTBC proteins produced in *E.coli* BL21*DE3, which carries the T7 *lac* promoter system. Consequently protein expression could be induced using IPTG (Donovan *et al.*, 1996). The recombinant proteins were produced in *E.coli*, as this organism can grow rapidly to high cell density using inexpensive media (Sorensen and Mortensen, 2005). After protein expression and the lysis of the induced *E.coli* (containing the designated plasmid), lysis was performed using a French press rather than by using detergents. During French pressing, mechanical forces break the bacterial cell membrane whilst cytosolic proteins remain intact. Mechanical lysis in this instance is preferable to cell lysis using detergent, as detergents can cause protein conformational relaxation. Recombinant proteins were enriched using affinity chromatography and further characterised by SDS-PAGE and immuno-blotting. After SDS-PAGE, protein bands were detected at the predicted molecular weight (figure 3.11) using Coomassie staining.

Western blotting and immuno-detection was used to detect specific proteins at levels of 1ng of protein/well and above using the ECL detection system (Amersham, GE Healthcare, Buckinghamshire, UK) (section 3.20). Immuno-blotting was optimised using X-ray film rather than the EpiChemi BioImaging system (UVP) (Cambridge, UK) (section 3.3.4) as X-

ray film proved to be several thousand times more sensitive than the equivalent charge-coupled device (CCD) based digital systems. Recombinant RTAC and RTBC proteins were detected using anti-6His, anti-RTAC and anti-RTBC specific antibodies (figures 3.19, 3.20 3.21 and 3.23). Detection of an epitope at the C-terminal of an enriched protein indicated that protein translation yielded full-length transcripts.

Optimisation of primary (anti-6His, anti-RTAC and anti-RTBC) and secondary antibody (HRP- conjugated anti-mouse and HRP- conjugated anti-rabbit secondary antibodies) hybridisation conditions were performed using RTAC. Here instead of enriched RTAC proteins, bacterial lysate from cultures expressing mutant RTAC (clone 189) or wild type RTAC (clone175) were used, minimizing the possibility of protein degradation. After affinity purification, protein concentration was calculated by densitometry *i.e.* by comparing the pixel density of immuno-blots against the signal from known quantities of a similar protein. This was deemed necessary as often protein yields were low or the protein was not purified to homogeneity after affinity purification limiting the usefulness of biochemical colorimetric protein detection. The yield of the recombinant RTAC was approximately 0.3 to 0.5mg/1000mL.

Protein expression was optimised using mini-induction experiments. Even though the conditions established using the mini-induction experiments (1.5mL), they may not extrapolate directly to large culture volumes, they were deemed useful as they could indicate whether obtaining high protein yield was going to be easily attainable. During the protein optimisation protocol, four parameters were identified: i) IPTG concentration (Donovan *et al.*, 1996) ii) temperature (O'Hare, *et al.*, 1987), iii) pre-induction culture time (Zhan *et al.*, 2004) and iv) post-induction culture times (Liu *et al.*, 2006) (section 3.3.5). For rRTAC (clone 189) the optimal IPTG concentration was found to be 0.25mM, the optimal temperature was 37°C, the optimal pre-induction time was 2h and the optimal post induction time was 4h.

Table 7.1: Protein yields of rRTBC and rRTAC constructs

Clone number	Construct	Typical Yield
204	RTBC	0.4mg/mL
216	RTAC-Mut-nt-HA	0.3mg/mL
217	RTAC-Del-nt-HA	0.34mg/mL
189	RTAC-Mut-ct-HA-6His-KDEL	0.38mg/mL
192	RTAC-Del-ct-3eGFP-KDEL	0.56mg/mL
224	RTAC-Mut-nt-eGFP-KDEL	0.41mg/mL
175	WT RTAC-ct-6His	0.56mg/mL

Recombinant protein toxicity

Having produced and characterised the desired recombinant proteins, the hypothesis that the mutations and deletions introduced (AA177-182) into recombinant RATC, reduced RTAC toxicity was tested. This required two things: (i) a means of assaying toxicity and (ii) a way of knowing that any reduction in toxicity was not due to the protein being unable to traffic to the cytosol.

Assaying toxicity using MTT

After the expression, purification and characterisation of both wild type and mutant RTAC proteins, their cytotoxicity was assessed using the MTT assay (section 4.3.4). When evaluated individually, all the constructs were found to be non-toxic to Vero cells over the concentration range tested (10 μ g/mL) after 72h incubation. This result was repeated after mixing specific RTAC constructs with an equal mass of recombinant (non-glycosylated) RTBC (clone 204) (concentrations quoted refer to RTAC equivalent) in both B16 and Vero cells. Previous studies showed that the IC₅₀ of RTAC in isolation was approximately 1.4 μ g/mL using B16 cells (Pattirck *et al.*, 2001), 0.9 μ g/mL in HeLa cells and 30 μ g/mL in human ovarian cancer line (SKOV-3 cells) (Zhan *et al.*, 2004). The rRTAC was shown to be relatively non-toxic, relative to RT holotoxin, which was toxic in B16 cells (IC₅₀ of 0.3 μ g/mL) (Pattirck *et al.*, 2001). Here studies had shown that after 72h, re-associated RT holotoxin had an IC₅₀ of 0.79(\pm 0.01) μ g/mL in B16 and in Vero cells it was more potent. At 0.1ng/mL there was only 20% cell viability recorded. This was comparable to commercial RT (Sigma), which had been previously shown to have an IC₅₀ of 0.82 μ g/mL in B16 cells and only 25% cell viability was observed at 0.7ng/mL over 72h (table 7.2).

Re-association of heterodimeric recombinant ricin

In order to extend this preliminary study comparing the toxicity of the inefficiently trafficked RTAC mutants with wild type RT holotoxin, it was necessary to not only generate recombinant RTBC but also be able to re-associate RTAC with RTBC in an approximately stoichiometric ratio creating an enriched population of RT heterodimers (Smith *et al.*, 2003). Recombinant RTBC (clone 204) was evaluated herein and was found to be immuno-reactive with a commercial RTBC specific antibody (abcam, Cambridge UK), approximately the correct molecular weight, but lacked lectinic activity, which might result from a lack of glycosylation attributable to the bacterial expression systems. Recombinant RTBC (clone 204) lectinic activity was evaluated by comparing the binding of cRTBC (positive control) with rRTBC (clone 204) by evaluating the proteins ability to bind to lactose-conjugated agarose beads. Wild type RTBC contains three galactose-binding sites (Frankel *et al.*, 1996), which play a key role in the endocytocytic uptake and intracellular trafficking of the holotoxin (Fu *et al.*, 1996). RTBC binds to galactose receptors on the surface of mammalian cells. Due to lack of measurable lectinic activities attributable to rRTBC (clone 204), this clone was not used in further toxicity, re-association and trafficking experiments.

Re-association of RTAC-RTBC was optimised by associating cRTAC and cRTBC using a protocol adapted from the Lord laboratory (Smith *et al.*, 2003) (section 2.2.11). Re-association of proteins was thought to be an important parameter, as homodimer formation would limit the specific activity of the preparation. The optimised conditions were then applied to re-associate rRTAC (clone 189)-cRTBC. However before these studies could be undertaken the cytotoxicity profile of cRTBC was established.

Surprisingly, cRTBC displayed measurable cytotoxicity. In the human ovarian cancer line (SKOV3), a 40% inhibition of protein synthesis was reported at a cRTBC concentration of 20 $\mu\text{g/mL}$ (Vector labs, Peterborough, UK). When tested herein Vero cells displayed marked cytotoxicity at concentrations above 0.7 $\mu\text{g/mL}$. RTBC does not contain the catalytic domain found in RTAC but, due to its lectinic activity, may interfere with the function of galactose containing molecules on cell surface. Galactose containing molecules at the cell surface have been reported to be necessary for the control of ion balance and nutrient transport (Fulton *et al.*, 1986).

Commercial RTAC was toxic to Vero cells and displayed an IC_{50} of 1.7 $\mu\text{g/mL}$ (48h incubation). No measurable IC_{50} was recorded after B16 cells were exposed to cRTBC over an identical concentration range and time. It was previously shown that the IC_{50} of RTAC in

B16 was 1.4 μ g/mL over a 72h incubation period (Patrick *et al.*, 2001). When cRTAC was re-associated with cRTBC, it was highly toxic to both B16 (IC₅₀ of 0.79 μ g/mL) and Vero cells (20% viability at 0.1ng/mL) (table 7.2 and 7.3).

Table 7.2: Cytotoxicity (IC₅₀) of RTAC and RTBC in Vero cells. (ND: Not determined)

Protein	IC ₅₀ (\pm SEM), 24h	IC ₅₀ , (\pm SEM), 48h	IC ₅₀ , (\pm SEM), 72h
cRTAC	ND	1.7(\pm 1.16) μ g/mL	1.81(\pm 0.15)ng/mL
rRTAC	ND	ND	Non-toxic (up to 10 μ g/mL)
rRTBC	ND	Non-toxic (up to 10 μ g/mL)	ND
rRTAC + rRTAC	ND	Non-toxic (up to 10 μ g/mL)	ND
cRTBC	ND	2.8(\pm 1.32) μ g/mL	0.7(\pm 0.04) μ g/mL
cRTAC + cRTBC	ND	Below 1ng/mL	ND
Re-associated cRTAC-cRTBC	ND	ND	Cell viability below 50% at 0.1ng/mL
Re-associated 189-cRTBC	ND	ND	0.39(\pm 0.04) μ g/mL
Commercial holotoxin (Sigma)	2.25ng/mL	Cell viability below 35% at 0.7ng/mL	Cell viability below 25% at 0.7ng/mL

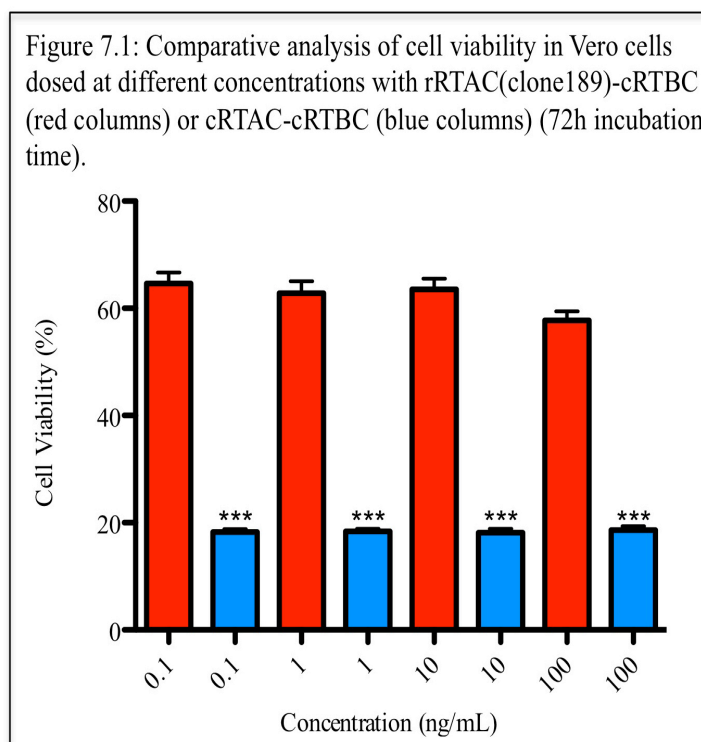
Re-associated rRTAC (clone 189)-cRTBC was non-toxic in B16 cells (up to 1 μ g/mL) and showed toxicity in Vero cells (IC₅₀ 0.39 μ g/mL). The measured toxicity may have been due to intrinsic cRTBC toxicity (IC₅₀ 0.7 μ g/mL in Vero cells).

Table 7.3: Cytotoxicity (IC₅₀) of RTAC and RTBC in B16 cells (ND: Not determined).

Protein	IC ₅₀ (±SEM), 24h	IC ₅₀ (±SEM), 48h	IC ₅₀ (±SEM), 72h
cRTAC	ND	8.55(±0.35)µg/mL	
rRTAC	ND	ND	ND
rRTBC	ND	Non-toxic (up to 10µg/mL)	ND
rRTAC + rRTBC	ND	Non-toxic (up to 10µg/mL)	ND
cRTBC	ND	Non-toxic up to 10µg/mL	
cRTAC + cRTBC		4.15(±0.12)µg/mL	
Re-associated cRTAC-cRTBC	ND	ND	0.79(±1.22)µg/mL
Re-associated 189-cRTBC	ND	ND	Non toxic up to 1µg/mL
Commercial holotoxin		0.825µg/mL	ND

Statistical evaluation of toxicity

Statistical evaluation of cell viability at different concentrations of either re-folded cRTBC and cRTAC or cRTBC and clone 189 (rRTAC), was evaluated using Prism (Graph Pad, version 5). Here paired t-test was performed using cell viability at different concentrations of re-associated protein. *P*- values were designated as follows: *P*>0.05 not significant; **P*=0.01-0.05 significant; ***P*=0.001-0.01 very significant; ****P*<0.001 extremely significant.



Here a statistical difference between re-folded cRTBC-cRTAC and cRTBC-rRTAC (clone 189) was clearly seen at concentrations up to 100ng/mL RTAC equivalent. Having ascertained that there was a dramatic reduction on toxicity that appeared to be attributable to the mutation introduced herein, it was deemed necessary to evaluate the sub-cellular distribution of RTAC. If the recombinant RTAC could not reach the cytosol a) the lack of observed toxicity could not be attributed to the mutation and b) the mutant RTAC would not be useful as a cytosolic drug delivery system.

Subcellular distribution of rRTAC

Sub-cellular fractionation experiments documented detectable quantities of mutant, rRTAC (clone 189) in a cytosolic fraction of Vero cells. This data was preliminary and more work is needed to confirm the conclusions drawn, however it indicated that the drop in toxicity observed (see above) was not due to the aberrant intracellular trafficking of the mutant ricin A chain. Further characterisation needs to be undertaken to confirm this conclusion, utilising both positive and negative controls such as the use of brefeldin A (to block the translocation of the toxin between the Golgi and the ER (Hunziker *et al.*, 1992)) as well as temperature (0°C inhibiting membrane trafficking) and adding EDTA to the cells (chelating divalent cations, arresting vesicle fusion (Garty and Asher, 1985)). Brefeldin A has been used

previously to protect cells from ricin intoxication by preventing the cytosolic translocation of the RTAC to the ER and cytosol (Yoshida *et al.*, 1991).

The trafficking properties of cRTBC with rRTBC (clone 204) were also evaluated using fluorescent microscopy in conjunction with antibodies specific for the cis- and medial- Golgi marker protein GM130 and trans- Golgi network marker protein TGN46. After 20minutes, co-localisation of immuno-labelled cRTBC with TGN46 markers indicate that cRTBC was translocating to the Golgi, as would be predicted from the literature (Sandvig *et al.*, 2004). Previously it was showed that after 30minutes, immuno-labelled holotoxin co-localised with GM130 (Richardson *et al.*, 2008). Under similar experimental conditions, rRTBC (clone 204) did not co-localise with either of the Golgi markers, and this maybe due rRTBC (clone 204) aforementioned lack of lectinic activity.

To conclude this first study, preliminary data indicated that the toxicity of the mutant RTAC constructs was decreased relative to the cRTAC once it has been allowed to re-associate into AB heterodimers with cRTBC. This result was supported statistically. This would support the rejection of the null hypothesis that the mutations introduced into rRTAC (clone 189) would not alter RT toxicity. From this point it was pertinent to evaluate how effective this recombinant delivery system was relative to synthetic polymers such as PAAs. This data is entirely novel as no one has made these mutant RTAC clones prior to this work.

Synthetic polymers mediating cytosolic delivery – efficiency relative to recombinant ricin based constructs

Given the application of recombinant toxins as cytosolic shuttles, it was decided to test the efficiency of these cytosolic shuttles relative to a set of synthetic polymers that had been previously documented to mediate cytosolic delivery. PAAs (FF91 and FF103) were chosen for this comparison due to their similarity to the PAA polymers ISA1 and ISA23, which have been documented to be considerably less toxic than other membrane destabilising polymers such as PEI (section 6.3.1). In addition, PAAs can deliver proteins such as gelonin and RTAC to the cytosol (Richardson *et al.*, 2010; Patrick *et al.*, 2001).

It was originally speculated that the thiol group(s) pendant to the FF91 and FF103 polymer main-chain, would foster an interaction between a “cargo protein” (rGel) and the polymer, and this possibility was encouraged through the use of recombinant technology to introduce an additional C-terminal cysteine residue into the rGel protein.

It was documented that non-covalent “mixtures” of PAA and either RTAC or Gel, when co-incubated with PAAs, could increase the toxicity of a sub-lethal concentration of either

RTAC or Gel to B16 cells (Patrick *et al.*, 2001). This study also recorded that, in order to increase protein toxicity, a huge excess of polymer was required. Consequently, it was hypothesised herein that it may be possible to increase the efficiency of cytosolic access by introducing thiol group's pendant to the polymer chain to foster polymer/protein interactions. This may serve two ends: 1) ensuring the protein toxin and the polymer are in the same spatially and temporally constrained compartment and 2) increase the efficiency of the uptake of the protein. The former may be important especially if intracellular trafficking of the protein (Gel or RTAC) is via fluid phase and polymer uptake is via absorptive endocytosis, potentially separating the toxin and polymer. The latter is interesting as it may serve to increase the amount of protein entering the cell, which also has the potential to increase toxin lethality. This conjecture remains to be tested.

In order to compare the efficiencies of both an “RT like” delivery system and a PAA based delivery system, several tools were required: (1) PAAs with thiol groups pendant to the main chain (FF91 and FF103, figure 5.1) (kindly supplied by Prof. Paolo Ferruti, University of Milano) and (2) A recombinant RTAC or Gel construct with and without an additional C-terminal cysteine residue (section 5.3.5). Following the generation and characterisation of these materials, a study evaluating their separate and combined toxicity was undertaken.

Cloning and sub-cloning of an appropriate “Cargo protein” (gelonin (Gel))

Here rGel with an additional C-terminal cysteine or without an additional C-terminal cysteine, were successfully sub-cloned into a bacterial expression cassette (pET151/D-TOPO) down stream from a V5 epitope and these constructs sequenced and mapped (section 5.3.5). Two recombinant proteins were produced from the aforementioned plasmid constructs and these were both characterised by SDS-PAGE and immuno-blotting. After SDS-PAGE and Coomassie staining, protein bands were documented above 34kDa and to evaluate whether these were immuno-equivalent to the predicted proteins, immuno-blotting was undertaken. After immuno-blotting using an anti-V5 primary antibody and also anti-6His primary antibody, protein bands were detected approximately at predicted molecular weight (34kDa) (figure 5.11).

The cytotoxicity of enriched: rGel, mGel and cGel constructs were evaluated in relation to protein concentration determined by immuno-blotting and densitometry. Both rGel proteins had IC_{50} above 10 μ g/mL (table 7.4) (figure 5.12), mGel had an IC_{60} of 10 μ g/mL. The cGel preparation was similar to that reported in the literature (Patrick *et al.*, 2001). The cGel

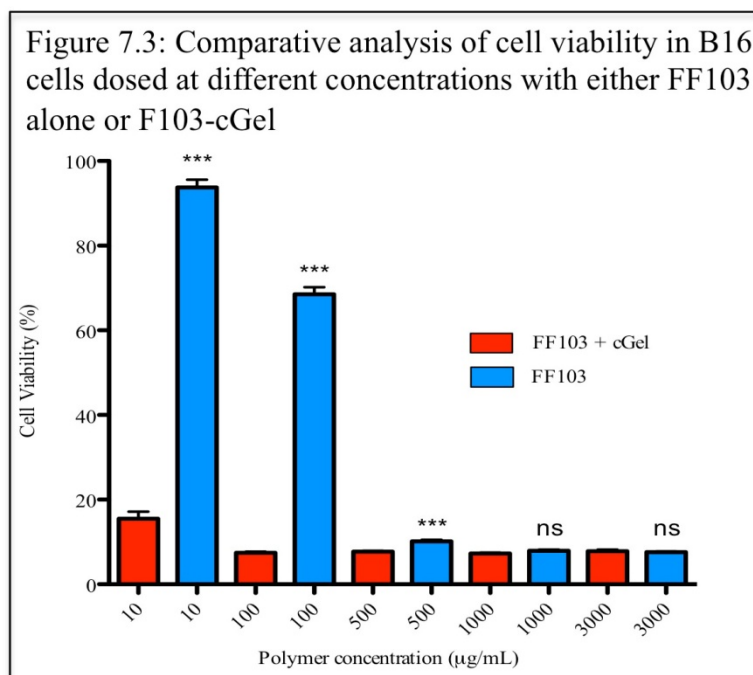
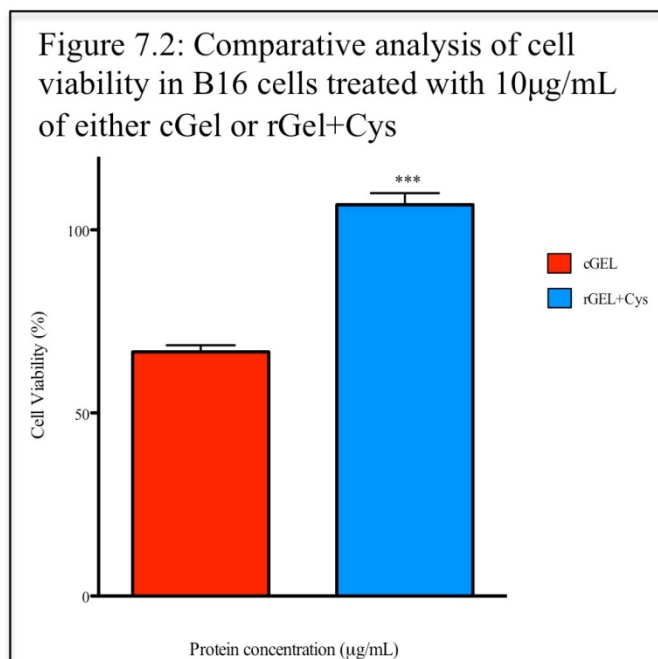
cytotoxicity was higher (10 folds) relative to rGel without cystine residue, and even higher (100 folds) than rGel with the C-terminal cystine residue.

Table 7.4: Cytotoxicity (IC_{50} (\pm SEM)) of rGel, mGel, cRTBC and cRTBC with cGel

Protein	In B16 cells	Vero cells
rGel (+Cys)	155.62(\pm 39.37) μ g/mL	ND
rGel (-Cys)	36.62(\pm 6.64) μ g/mL	ND
mGel	10 μ g/mL (IC_{60})	
cGel	19.75(\pm 0.12) μ g/mL	
cRTBC	8.657(\pm 0.15) μ g/mL	0.324(\pm 0.01) μ g/mL
cRTBC+cGel	8.875(\pm 0.58) μ g/mL	0.29(\pm 0.02) μ g/mL

PAAs similar to ISA1 (FF103) and ISA23 (FF91) were assayed for toxicity in B16 cells and found to have IC_{50} of more than 2mg/mL for FF91 and less than 2mg/mL for FF103 (figure 5.14 and 5.15). It was hypothesised that introduction of cysteine residue may help mediate an interaction between rGel and the PAA polymers containing thiol pendant to the polymer main chain (*i.e.* containing ethenyldithio pyridine (SSPy) monomers) and this interaction may enhance the delivery of rGel into cytosol. When FF103 was applied to B16 cells together with rGel (with and without cystine) IC_{50} values were equivocal (90 μ g/mL). This indicated that the additional C-terminal cysteine was not fostering a stronger interaction between the protein and the PAA. It is possible that the C-terminal cysteine was redundant as the polymers were interacting with other intermolecular cystine residues. When FF103 was administered alone (IC_{50} 890(\pm 53.34) μ g/mL) or with rGel, mGel or cGel, the addition of sub-lethal concentrations of protein toxin resulted in an increase in toxicity.

The statistical difference between the rGel with and without the C-terminal cysteine was unsurprising given the maturation of pre-gelonin to the proteins mature form, and it was for this reason that an additional mGel construct was made and evaluated. However, more poignant statistical differences were also documented showing differences in the toxicity profiles between FF103 with and without cGel (figure 7.3).



PAA FF91 (based on the same monomers as ISA23) and dextran did not foster an increase in cytotoxicity when applied together with rGel or cGel. This result was predictable, given the previously published data, which documented ISA23 being unable to enhance the toxicity of cGel or cRTAC. Preliminary experiments were performed to evaluate the ability of cRTBC

to deliver cGel. In this instance mixtures rather than re-associated mixtures of protein :: protein or protein :: polymer combinations were used to ensure an even comparison. It would have been beyond the scope of this thesis to reproducibly generate polymer :: protein heterooligomers and characterise the polymer :: protein interactions. This problem was compounded by a lack of antibodies specific for cGel in the lab as well as the similarity in molecular weight of cRTBC (32kDa) and cGel (30kDa) making their differentiation by SDS-PAGE and Coomassie staining also difficult. When applied together as a mixture, cRTBC did not enhance the cytotoxicity of cGel in B16 cells relative to FF103 (figure 5.13). If re-associated, cRTBC and cGel may show increased cytotoxicity.

In order to further substantiate the role of the PAAs during the delivery of macromolecules such as Gel, fluorescent microscopy following the intracellular distribution of FITC-conjugated PAAs was undertaken. ISA-FITC polymers were non-toxic up to 3mg/mL (section 6.3.1). This value was similar to the values previously published for the ISA series of PAAs (Richardson *et al* 1999). The intracellular trafficking properties of FITC conjugated-PAAs (section 6.3.3) were evaluated by fluorescence microscopy in both fixed and live cells. Both polymers (ISA1-FITC and ISA23-FITC (table 6.1)), showed nuclear localisation after fixation however, in live cells only ISA-FITC was shown to demonstrate nuclear localisation over 5h time period. By evaluating trafficking properties of polymers can result in understanding and developing effective drug delivery systems.

Control experiments conducted using an equivalent quantity of “free FITC”, indicate that the FITC signal in the nucleus denoted the presence of the polymer-FITC conjugate. This supports the notion that the delivery of Gel is mediated by PAAs destabilising the limiting membranes of endocytic vesicles as previously published (Richardson *et al.*, 2010).

The notion that PAAs can specifically release Gel into the cytosol is also supported by published data. Previously, ISA-OG when applied together with Gel-TxR enhanced the release of Gel-TxR into the cytosol, whereas ISA23-OG failed to show the similar effect (Richardson *et al.*, 2010). Here for the first time, localisation of PAA-FITC polymers in the nucleus was detected by fluorescence microscopy and live cell imaging in Vero cell lines.

Table 7.5: Cytotoxicity (IC_{50} (\pm SEM)) of FF103 alone or along with cGel, mGel or rGel

Polymer/Protein concentration	In B16 cells	In Vero cells
FF103	890(\pm 53.44) μ g/mL	
FF103+1.4 μ g rGel (+Cys)	88.25(\pm 3.17) μ g/mL	ND
FF103+14 μ g rGel (+Cys)	13.8(\pm 1.79) μ g/mL	ND
FF103+1.4 μ g rGel (-Cys)	89(\pm 5.20) μ g/mL	ND
FF103	310(\pm 30.26) μ g/mL	
FF103+1.4 μ g mGel	40(\pm 0.8) μ g/mL	ND
FF103+1.4 μ g cGel	Cell viability below 20%	
FF103		625(\pm 10.2) μ g/mL
FF103+cGel		445(\pm 17.4) μ g/mL

Conclusions

In this study, rRTAC, rRTBC and rGel proteins were produced from their respective plasmids, and these proteins were characterised by SDS-PAGE and immuno-blotting. Even though rRTBC was recognised by a commercial RTBC specific antibody, further investigation revealed rRTBC lacked lectinic activity. This construct (rRTBC) was not useful within the context of a drug delivery system. The rRTAC proteins produced were non-toxic over the concentration range tested (up to 10 μ g/mL) in Vero and B16 cell lines, alone or when mixed with rRTBC in equal amounts. Given the lectinic properties of RTBC, these experiments served as useful negative controls, providing context for positive controls utilising cRTBC and cRTAC. Re-associated rRTAC (clone 189)-cRTBC was non-toxic in B16 cells (up to 1 μ g/mL) but showed some toxicity in Vero cells (IC₅₀: 0.39(\pm 0.04) μ g/mL), which can be attributed largely to cRTBC (0.7(\pm 0.04) μ g/mL) toxicity. PAA FF103 when applied with sub-lethal concentrations of cGel was more shown to be toxic than at an equal concentration of FF103 alone (P value <0.001). FF103 appeared more effective at increasing Gel toxicity than the published data describing the PAA ISA1. This might indicate that intermolecular complex formation between the Gel and the PAA also increased the efficiency of delivery.

It can be concluded that the PAA systems evaluated herein were equally good at delivering a model protein (Gel) to the cytosol than those based upon RT (cRTBC). Further, the reason for cRTBC toxicity needs to be evaluated. If cRTBC toxicity is not due to the contamination of the RTBC preparation with RTAC, then this RT based study will stop immediately as there will be little possibility of using this system to deliver material to the cytosol without vector mediated toxicity. Further, the effect of the re-association of Gel with cRTBC needs to be established. Given that there is conservation between the active site of RTAC and Gel, it is likely they both use a retrograde transport step over the *Sec61p* translocon to access the cytosol. As Gel is a type I RIP it is also possible that translocation to the ER (containing the *Sec61p* translocon) is rate limiting. If this rate limit is removed then: (i) it may be possible to identify sequence contained in both Gel and RTAC that facilitates ER exit and (ii) evaluate whether translocation from the ER is as efficient as PAA mediated vesicle destabilisation when mediating cytosolic delivery. The data presented thus far indicates that there is no benefit to using a cRTBC based ER translocating system for cytosolic access, relative to the PAA systems described. This observation is brought into sharper focus when the immunogenicity of the PAAs is compared with that of RT.

Future work

- 1). Evaluation of cRTBC for the presence of RTAC using SDS-PAGE and immuno-blotting.

- 2). Finishing of sub-cellular fractionation using rRTAC (clone189)-cRTBC. Undertaking the optimisation of rRTAC (clone 189)-cRTBC concentration and exposure time in relation to cytosolic RTAC trafficking as well as the inclusion of appropriate positive and negative controls.

- 3). Evaluating the effect of the re-association of cRTBC with cGel upon cytotoxicity.

- 4). Evaluating intracellular membrane the trafficking properties using re-associated mutant RTAC-cRTBC by fluorescence live cell imaging.

- 5). Evaluating delivering ability of mutant RTAC constructs to deliver therapeutic molecules like siRNA or antisense.

References

- Aagaard, L. and Rossi, J. J. (2007) 'RNAi therapeutics: Principles, prospects and challenges', *Adv Drug Deliv Rev*, 59(2-3), 75-86.
- Agrawal, A. K. and Gupta, C. M. (2000) 'Tuftsin-bearing liposomes in treatment of macrophage-based infections', *Adv Drug Deliv Rev*, 41(2), 135-46.
- Agrawal, N., Dasaradhi, P. V., Mohammed, A., Malhotra, P., Bhatnagar, R. K. and Mukherjee, S. K. (2003) 'RNA interference: biology, mechanism, and applications', *Microbiol Mol Biol Rev*, 67(4), 657-85.
- Aigner, A., Fischer, D., Merdan, T., Brus, C., Kissel, T. and Czubayko, F. (2002) 'Delivery of unmodified bioactive ribozymes by an RNA-stabilizing polyethylenimine (LMW-PEI) efficiently down-regulates gene expression', *Gene Ther*, 9(24), 1700-7
- Aiuti, A., Bachoud-Levi, A. C., Blesch, A., Brenner, M. K., Cattaneo, F., Chiocca, E. A., Gao, G., High, K. A., Leen, A. M., Lemoine, N. R., McNeish, I. A., Meneguzzi, G., Peschanski, M., Roncarolo, M. G., Strayer, D. S., Tuszynski, M. H., Waxman, D. J. and Wilson, J. M. (2007) 'Progress and prospects: gene therapy clinical trials (part 2)', *Gene Ther*, 14(22), 1555-63.
- Aiuti, A., Brigida, I., Ferrua, F., Cappelli, B., Chiesa, R., Markt, S. and Roncarolo, M. G. (2009) 'Hematopoietic stem cell gene therapy for adenosine deaminase deficient-SCID', *Immunol Res*, 44(1-3), 150-9.
- Akhtar, S., Hughes, M. D., Khan, A., Bibby, M., Hussain, M., Nawaz, Q., Double, J. and Sayyed, P. (2000) 'The delivery of antisense therapeutics', *Adv Drug Deliv Rev*, 44(1), 3-21
- Akhtar, S., Kole, R. and Juliano, R. L. (1991) 'Stability of antisense DNA oligodeoxynucleotide analogs in cellular extracts and sera', *Life Sci*, 49(24), 1793-1801
- Aktories, K. and Barth, H. (2004) 'Clostridium botulinum C2 toxin--new insights into the cellular up-take of the actin-ADP-ribosylating toxin', *Int J Med Microbiol*, 293(7-8), 557-64.
- Alexander, B. L., Ali, R. R., Alton, E. W., Bainbridge, J. W., Braun, S., Cheng, S. H., Flotte, T. R., Gaspar, H. B., Grez, M., Griesenbach, U., Kaplitt, M. G., Ott, M. G., Seger, R., Simons, M., Thrasher, A. J., Thrasher, A. Z. and Yla-Herttuala, S. (2007) 'Progress and prospects: gene therapy clinical trials (part 1)', *Gene Ther*, 14(20), 1439-47
- Alexandrov, K., Horiuchi, H., Steele-Mortimer, O., Seabra, M. C. and Zerial, M. (1994) 'Rab escort protein-1 is a multifunctional protein that accompanies newly prenylated rab proteins to their target membranes', *EMBO J*, 13(22), 5262-73
- Allen, C., Han, J., Yu, Y., Maysinger, D. and Eisenberg, A. (2000) 'Polycaprolactone-b-poly(ethylene oxide) copolymer micelles as a delivery vehicle for dihydrotestosterone', *J Control Release*, 63(3), 275-86
- Almofiti, M. R., Harashima, H., Shinohara, Y., Almofiti, A., Li, W. and Kiwada, H. (2003) 'Lipoplex size determines lipofection efficiency with or without serum', *Mol Membr Biol*, 20(1), 35-43
- Altmann, K. H., Fabbro, D., Dean, N. M., Geiger, T., Monia, B. P., Muller, M. and Nicklin, P. (1996) 'Second-generation antisense oligonucleotides: structure-activity relationships and the design of improved signal-transduction inhibitors', *Biochem Soc Trans*, 24(3), 630-7
- Amlot, P. L., Stone, M. J., Cunningham, D., Fay, J., Newman, J., Collins, R., May, R., McCarthy, M., Richardson, J., Ghetie, V. and et al. (1993) 'A phase I study of an anti-CD22-deglycosylated ricin A chain immunotoxin in the treatment of B-cell lymphomas resistant to conventional therapy', *Blood*, 82(9), 2624-33
- Anant, J. S., Desnoyers, L., Machius, M., Demeler, B., Hansen, J. C., Westover, K. D., Deisenhofer, J. and Seabra, M. C. (1998) 'Mechanism of Rab geranylgeranylation: formation of the catalytic ternary complex', *Biochemistry*, 12559-68
- Appenzeller-Herzog, C. and Hauri, H. P. (2006) 'The ER-Golgi intermediate compartment (ERGIC): in search of its identity and function', *J Cell Sci*, 119(Pt 11), 2173-83

- Argent, R. H., Parrott, A. M., Day, P. J., Roberts, L. M., Stockley, P. G., Lord, J. M. and Radford, S. E. (2000) 'Ribosome-mediated folding of partially unfolded ricin A-chain', *J Biol Chem*, 275(13), 9263-9
- Argent, R. H., Roberts, L. M., Wales, R., Robertus, J. D. and Lord, J. M. (1994) 'Introduction of a disulfide bond into ricin A chain decreases the cytotoxicity of the ricin holotoxin', *J Biol Chem*, 269(43), 26705-10
- Audi, J., Belson, M., Patel, M., Schier, J. and Osterloh, J. (2005) 'Ricin poisoning: a comprehensive review', *JAMA*, 2342-51
- Bala, I., Hariharan, S. and Kumar, M. N. (2004) 'PLGA nanoparticles in drug delivery: the state of the art', *Crit Rev Ther Drug Carrier Syst*, 21(5), 387-422
- Ballabio, A. and Gieselmann, V. (2009) 'Lysosomal disorders: From storage to cellular damage', *Biochim Biophys Acta*, 1793(4), 684-696
- Ballard, J. D., Collier, R. J. and Starnbach, M. N. (1996) 'Anthrax toxin-mediated delivery of a cytotoxic T-cell epitope in vivo', *Proc Natl Acad Sci U S A*, 93(22), 12531-4
- Banerjee, R. (2001) 'Liposomes: applications in medicine', *J Biomater Appl*, 16(1), 3-21
- Baneyx, F. (1999) 'Recombinant protein expression in Escherichia coli', *Curr Opin Biotechnol*, 411-21
- Barbieri, L., Battelli, M. G. and Stirpe, F. (1993) 'Ribosome-inactivating proteins from plants', *Biochim Biophys Acta*, 1154(3-4), 237-82
- Barrett, P. N., Mundt, W., Kistner, O. and Howard, M. K. (2009) 'Vero cell platform in vaccine production: moving towards cell culture-based viral vaccines', *Expert Rev Vaccines*, 8(5), 607-18
- Bartosch, B. and Cosset, F. L. (2004) 'Strategies for retargeted gene delivery using vectors derived from lentiviruses', *Curr Gene Ther*, 4(4), 427-43
- Barzon, L., Stefani, A. L., Pacenti, M. and Palu, G. (2005) 'Versatility of gene therapy vectors through viruses', *Expert Opin Biol Ther*, 5(5), 639-62
- Basu, M. K. and Lala, S. (2004) 'Macrophage specific drug delivery in experimental leishmaniasis', *Curr Mol Med*, 4(6), 681-9
- Bennett, C. F. and Swayze, E. E. (2010) 'RNA targeting therapeutics: molecular mechanisms of antisense oligonucleotides as a therapeutic platform', *Annu Rev Pharmacol Toxicol*, 50, 259-93
- Bergamaschi, G., Perfetti, V., Tonon, L., Novella, A., Lucotti, C., Danova, M., Glennie, M. J., Merlini, G. and Cazzola, M. (1996) 'Saporin, a ribosome-inactivating protein used to prepare immunotoxins, induces cell death via apoptosis', *Br J Haematol*, 93(4), 789-94
- Bernardi, K. M., Forster, M. L., Lencer, W. I. and Tsai, B. (2008) 'Derlin-1 facilitates the retro-translocation of cholera toxin', *Mol Biol Cell*, 877-84
- Berridge, M. V. and Tan, A. S. (1993) 'Characterization of the cellular reduction of 3-(4,5-dimethylthiazol-2-yl)-2,5-diphenyltetrazolium bromide (MTT): subcellular localization, substrate dependence, and involvement of mitochondrial electron transport in MTT reduction', *Arch Biochem Biophys*, 474-82
- Bertrand, J. R., Pottier, M., Vekris, A., Opolon, P., Maksimenko, A. and Malvy, C. (2002) 'Comparison of antisense oligonucleotides and siRNAs in cell culture and in vivo', *Biochem Biophys Res Commun*, 296(4), 1000-4
- Bielinska, A. U., Kukowska-Latallo, J. F. and Baker, J. R. (1997) 'The interaction of plasmid DNA with polyamidoamine dendrimers: mechanism of complex formation and analysis of alterations induced in nuclease sensitivity and transcriptional activity of the complexed DNA', *Biochim Biophys Acta*, 1353(2), 180-190

- Bies, C., Lehr, C. M. and Woodley, J. F. (2004) 'Lectin-mediated drug targeting: history and applications', *Adv Drug Deliv Rev*, 425-35
- Binz, T. and Rummel, A. (2009) 'Cell entry strategy of clostridial neurotoxins', *J Neurochem*, 109(6), 1584-95
- Birikh, K. R., Heaton, P. A. and Eckstein, F. (1997) 'The structure, function and application of the hammerhead ribozyme', *Eur J Biochem*, 245(1), 1-16
- Birnboim, H. C. and Doly, J. (1979) 'A rapid alkaline extraction procedure for screening recombinant plasmid DNA', *Nucleic Acids Res*, 7(6), 1513-23
- Bishop, N. E. (2003) 'Dynamics of endosomal sorting', *Int Rev Cytol*, 232, 1-57
- Bloomfield, V. A. (1996) 'DNA condensation', *Curr. Opin. Struct. Biol*, 6(3), 334-341
- Blume, G. and Cevc, G. (1993) 'Molecular mechanism of the lipid vesicle longevity in vivo', *Biochim Biophys Acta*, 1146(2), 157-68
- Bramlage, B., Luzi, E. and Eckstein, F. (1998) 'Designing ribozymes for the inhibition of gene expression', *Trends Biotechnol*, 16(10), 434-438.
- Branco, M. C. and Schneider, J. P. (2009) 'Self-assembling materials for therapeutic delivery', *Acta Biomaterialia*, 5(3), 817-831
- Breunig, M., Lungwitz, U., Liebl, R., Fontanari, C., Klar, J., Kurtz, A., Blunk, T. and Goepferich, A. (2005) 'Gene delivery with low molecular weight linear polyethylenimines', *J Gene Med*, 7(10), 1287-98
- Brown, M. D., Schätzlein, A. G. and Uchegbu, I. F. (2001) 'Gene delivery with synthetic (non viral) carriers', *Int J Pharm*, 229(1-2), 1-21
- Brunger, A. T. (2005) 'Structure and function of SNARE and SNARE-interacting proteins', *Q Rev Biophys*, England: 1-47
- Bucci, C., Thomsen, P., Nicoziani, P., McCarthy, J. and van Deurs, B. (2000) 'Rab7: a key to lysosome biogenesis', *Mol Biol Cell*, 11(2), 467-80
- Buchschacher, G. L., Jr. (2001) 'Introduction to retroviruses and retroviral vectors', *Somat Cell Mol Genet*, 26(1-6), 1-11
- Burgdorf, S. and Kurts, C. (2008) 'Endocytosis mechanisms and the cell biology of antigen presentation', *Curr Opin Immunol*, 20(1), 89-95
- Cao, S., Cripps, A. and Wei, M. Q. (2010) 'New strategies for cancer gene therapy: progress and opportunities', *Clin Exp Pharmacol Physiol*, 37(1), 108-14
- Caplen, N. J., Kinrade, E., Sorgi, F., Gao, X., Gruenert, D., Geddes, D., Coutelle, C., Huang, L., Alton, E. W. and Williamson, R. (1995) 'In vitro liposome-mediated DNA transfection of epithelial cell lines using the cationic liposome DC-Chol/DOPE', *Gene Ther*, 2(9), 603-13
- Cavazzana-Calvo, M. and Fischer, A. (2007) 'Gene therapy for severe combined immunodeficiency: are we there yet?', *J Clin Invest*, 117(6), 1456-65
- Cavazzana-Calvo, M., Lagresle, C., Hacein-Bey-Abina, S. and Fischer, A. (2005) 'Gene therapy for severe combined immunodeficiency', *Annu Rev Med*, 56, 585-602
- Chalfie, M. (1995) 'Green fluorescent protein', *Photochem Photobiol*, 62(4), 651-6
- Cheng, K. W., Lahad, J. P., Gray, J. W. and Mills, G. B. (2005) 'Emerging role of RAB GTPases in cancer and human disease', *Cancer Res*, 2516-9

- Chinnapen, D. J., Chinnapen, H., Saslowsky, D. and Lencer, W. I. (2007) 'Rafting with cholera toxin: endocytosis and trafficking from plasma membrane to ER', *FEMS Microbiol Lett*, 129-37
- Chiu, Y. L. and Rana, T. M. (2002) 'RNAi in human cells: basic structural and functional features of small interfering RNA', *Mol Cell*, 10(3), 549-61
- Cho, W. and Stahelin, R. V. (2005) 'Membrane-protein interactions in cell signaling and membrane trafficking', *Annu Rev Biophys Biomol Struct*, 34, 119-51
- Choi, M. R., Stanton-Maxey, K. J., Stanley, J. K., Levin, C. S., Bardhan, R., Akin, D., Badve, S., Sturgis, J., Robinson, J. P., Bashir, R., Halas, N. J. and Clare, S. E. (2007) 'A cellular Trojan Horse for delivery of therapeutic nanoparticles into tumors', *Nano Lett*, 7(12), 3759-65
- Chudakov, D. M., Matz, M. V., Lukyanov, S. and Lukyanov, K. A. (2010) 'Fluorescent proteins and their applications in imaging living cells and tissues', *Physiol Rev*, 1103-63
- Citti, L. and Rainaldi, G. (2005) 'Synthetic hammerhead ribozymes as therapeutic tools to control disease genes', *Curr Gene Ther*, 5(1), 11-24
- Collier, R. J. (2001) 'Understanding the mode of action of diphtheria toxin: a perspective on progress during the 20th century', *Toxicon*, 39(11), 1793-1803
- Collier, R. J. (2009) 'Membrane translocation by anthrax toxin', *Mol Aspects Med*, 413-22
- Conner, S. D. and Schmid, S. L. (2003) 'Regulated portals of entry into the cell', *Nature*, 422(6927), 37-44
- Corbeel, L. and Freson, K. (2008) 'Rab proteins and Rab-associated proteins: major actors in the mechanism of protein-trafficking disorders', *Eur J Pediatr*, 167(7), 723-9
- Cortes, J. and Saura, C. (2010) 'Nanoparticle albumin-bound (nab(TM))-paclitaxel: improving efficacy and tolerability by targeted drug delivery in metastatic breast cancer', *European Journal of Cancer Supplements*, 8(1), 1-10
- Cotrim, A. P. and Baum, B. J. (2008) 'Gene therapy: some history, applications, problems, and prospects', *Toxicol Pathol*, 36(1), 97-103
- Coura Rdos, S. and Nardi, N. B. (2007) 'The state of the art of adeno-associated virus-based vectors in gene therapy', *Virol J*, 4, 99
- Cresawn, K. O., Potter, B. A., Oztan, A., Guerriero, C. J., Ihrke, G., Goldenring, J. R., Apodaca, G. and Weisz, O. A. (2007) 'Differential involvement of endocytic compartments in the biosynthetic traffic of apical proteins', *EMBO J*, 3737-48
- Cristalli, G., Costanzi, S., Lambertucci, C., Lupidi, G., Vittori, S., Volpini, R. and Camaioni, E. (2001) 'Adenosine deaminase: Functional implications and different classes of inhibitors', *Med Res Rev*, 21(2), 105-128
- Crooke, S. T. (1998) 'Vitravene--another piece in the mosaic', *Antisense Nucleic Acid Drug Dev*, 8(4), vii-viii
- Crooke, S. T. (1999) 'Molecular mechanisms of action of antisense drugs', *Biochim Biophys Acta*, 1489(1), 31-44
- Crooke, S. T. (2004a) 'Antisense strategies', *Curr Mol Med*, 4(5), 465-87
- Crooke, S. T. (2004b) 'Progress in antisense technology', *Annu Rev Med*, 55, 61-95
- Croy, S. R. and Kwon, G. S. (2006) 'Polymeric micelles for drug delivery', *Curr Pharm Des*, 12(36), 4669-84
- Daemen, T., Hoedemakers, R., Storm, G. and Scherphof, G. L. (1995) 'Opportunities in targeted drug delivery to Kupffer cells: delivery of immunomodulators to Kupffer cells-activation of tumoricidal properties', *Adv Drug Deliv Rev*, 17(1), 21-30

- Danis, R. P., Henry, S. P. and Ciulla, T. A. (2001) 'Potential therapeutic application of antisense oligonucleotides in the treatment of ocular diseases', *Expert Opin Pharmacother*, 2(2), 277-91
- Davis, M. E., Zuckerman, J. E., Choi, C. H., Seligson, D., Tolcher, A., Alabi, C. A., Yen, Y., Heidel, J. D., Ribas, A. (2010) 'Evidence of RNAi in humans from systemically administered siRNA via targeted nanoparticles', *Nature*, 464(7291), 1067-70
- Day, P. J., Ernst, S. R., Frankel, A. E., Monzingo, A. F., Pascal, J. M., Molina-Svinth, M. C. and Robertus, J. D. (1996) 'Structure and activity of an active site substitution of ricin A chain', *Biochemistry*, 11098-103
- Day, P. J., Owens, S. R., Wesche, J., Olsnes, S., Roberts, L. M. and Lord, J. M. (2001a) 'An interaction between ricin and calreticulin that may have implications for toxin trafficking', *J Biol Chem*, 276(10), 7202-8
- De Jong, W. H. and Borm, P. J. (2008) 'Drug delivery and nanoparticles: applications and hazards', *Int J Nanomedicine*, 3(2), 133-49
- De Smedt, S. C., Demeester, J. and Hennink, W. E. (2000) 'Cationic polymer based gene delivery systems', *Pharm Res*, 17(2), 113-26
- de Virgilio, M., Lombardi, A., Caliandro, R. and Fabbrini, M. S. (2010) 'Ribosome-inactivating proteins: from plant defense to tumor attack', *Toxins (Basel)*, 2699-737
- Deeks, E. D., Cook, J. P., Day, P. J., Smith, D. C., Roberts, L. M. and Lord, J. M. (2002) 'The low lysine content of ricin A chain reduces the risk of proteolytic degradation after translocation from the endoplasmic reticulum to the cytosol', *Biochemistry*, 3405-13
- Del Nery, E., Miserey-Lenkei, S., Falguieres, T., Nizak, C., Johannes, L., Perez, F. and Goud, B. (2006) 'Rab6A and Rab6A' GTPases play non-overlapping roles in membrane trafficking', *Traffic*, 394-407
- Delprino, L., Giacomotti, M., Dosio, F., Brusa, P., Ceruti, M., Grosa, G. and Cattell, L. (1993) 'Toxin-targeted design for anticancer therapy. II: Preparation and biological comparison of different chemically linked gelonin-antibody conjugates', *J Pharm Sci*, 82(7), 699-704
- Demidov, V., Frank-Kamenetskii, M. D., Egholm, M., Buchardt, O. and Nielsen, P. E. (1993) 'Sequence selective double strand DNA cleavage by peptide nucleic acid (PNA) targeting using nuclease S1', *Nucleic Acids Res*, 21(9), 2103-7
- Demidov, V. V., Potaman, V. N., Frank-Kamenetskii, M. D., Egholm, M., Buchard, O., Sönnichsen, S. H. and Nielsen, P. E. (1994) 'Stability of peptide nucleic acids in human serum and cellular extracts', *Biochem Pharmacol*, 48(6), 1310-1313
- Deneka, M., Neeft, M. and van der Sluijs, P. (2003) 'Regulation of membrane transport by rab GTPases', *Crit Rev Biochem Mol Biol*, 38(2), 121-42
- Dennig, J. and Duncan, E. (2002) 'Gene transfer into eukaryotic cells using activated polyamidoamine dendrimers', *J Biotechnol*, 339-47
- Derossi, D., Calvet, S., Trembleau, A., Brunissen, A., Chassaing, G. and Prochiantz, A. (1996) 'Cell internalization of the third helix of the Antennapedia homeodomain is receptor-independent', *J Biol Chem*, 271(30), 18188-93
- Di Cola, A., Frigerio, L., Lord, J. M., Ceriotti, A. and Roberts, L. M. (2001) 'Ricin A chain without its partner B chain is degraded after retrotranslocation from the endoplasmic reticulum to the cytosol in plant cells' *Proc Natl Acad Sci U S A*, 14726-31
- Di Gioia, S. and Conese, M. (2009) 'Polyethylenimine-mediated gene delivery to the lung and therapeutic applications', *Drug Des Devel Ther*, 2, 163-88
- Dixit, G., Mikoryak, C., Hayslett, T., Bhat, A. and Draper, R. K. (2008) 'Cholera toxin up-regulates endoplasmic reticulum proteins that correlate with sensitivity to the toxin', *Exp Biol Med (Maywood)*, 163-75

- Donovan, R. S., Robinson, C. W. and Glick, B. R. (1996) 'Review: optimizing inducer and culture conditions for expression of foreign proteins under the control of the lac promoter', *J Ind Microbiol*, 16(3), 145-54
- Dreborg, S. and Akerblom, E. B. (1990) 'Immunotherapy with monomethoxypolyethylene glycol modified allergens', *Crit Rev Ther Drug Carrier Syst*, 6(4), 315-65
- Dressler, D., Saberi, F. A. and Barbosa, E. R. (2005) 'Botulinum toxin: mechanisms of action' *Arq Neuropsiquiatr*, 180-5
- Drin, G., Mazel, M., Clair, P., Mathieu, D., Kaczorek, M. and Tamsamani, J. (2001) 'Physico-chemical requirements for cellular uptake of pAntp peptide. Role of lipid-binding affinity', *Eur J Biochem*, 268(5), 1304-14
- Duan, D. (2006) 'Challenges and opportunities in dystrophin-deficient cardiomyopathy gene therapy', *Hum Mol Genet*, 15 Spec No 2, R253-61
- Dube, D. H. and Bertozzi, C. R. (2005) 'Glycans in cancer and inflammation. Potential for therapeutics and diagnostics', *Nat Rev Drug Discov*, 4(6), 477-488
- Dufès, C., Uchegbu, I. F. and Schätzlein, A. G. (2005) 'Dendrimers in gene delivery', *Adv Drug Deliv Rev*, 57(15), 2177-2202
- Duman, J. G. and Forte, J. G. (2003) 'What is the role of SNARE proteins in membrane fusion?', *Am J Physiol Cell Physiol*, C237-49
- Duncan, R. (2009) 'Development of HPMA copolymer-anticancer conjugates: clinical experience and lessons learnt', *Adv Drug Deliv Rev*, 1131-48
- Dunne, M., Corrigan, O. I. and Ramtoola, Z. (2000) 'Influence of particle size and dissolution conditions on the degradation properties of polylactide-co-glycolide particles', *Biomaterials*, 21(16), 1659-1668
- Dyer, P. D. and Richardson, S. C. (2011) 'Delivery of biologics to select organelles--the role of biologically active polymers', *Expert Opin Drug Deliv*, 8(4), 403-7
- Elbashir, S. M., Harborth, J., Weber, K. and Tuschl, T. (2002) 'Analysis of gene function in somatic mammalian cells using small interfering RNAs', *Methods*, 26(2), 199-213
- Ellgaard, L. and Helenius, A. (2003) 'Quality control in the endoplasmic reticulum', *Nat Rev Mol Cell Biol*, 4(3), 181-91
- Endo, Y. and Tsurugi, K. (1986) 'Mechanism of action of ricin and related toxic lectins on eukaryotic ribosomes', *Nucleic Acids Symp Ser*, (17), 187-90
- Endo, Y. and Tsurugi, K. (1987) 'RNA N-glycosidase activity of ricin A-chain. Mechanism of action of the toxic lectin ricin on eukaryotic ribosomes', *J Biol Chem*, 262(17), 8128-30
- Escors, D. and Breckpot, K. (2010) 'Lentiviral vectors in gene therapy: their current status and future potential', *Arch Immunol Ther Exp (Warsz)*, 58(2), 107-19
- Fahr, A., Hoogevest, P. v., May, S., Bergstrand, N. and S. Leigh, M. L. (2005) 'Transfer of lipophilic drugs between liposomal membranes and biological interfaces: Consequences for drug delivery', *Eur J Pharm Sci*, 26(3-4), 251-265
- Falguieres, T. and Johannes, L. (2006) 'Shiga toxin B-subunit binds to the chaperone BiP and the nucleolar protein B23', *Biol Cell*, 125-34
- Falnes, P. O. and Sandvig, K. (2000) 'Penetration of protein toxins into cells' *Curr Opin Cell Biol*, 407-13
- Fang, N., Chan, V., Mao, H. Q. and Leong, K. W. (2001) 'Interactions of phospholipid bilayer with chitosan: effect of molecular weight and pH', *Biomacromolecules*, 1161-8

- Faraji, A. H. and Wipf, P. (2009) 'Nanoparticles in cellular drug delivery', *Bioorg Med Chem*, 17(8), 2950-2962
- Farhood, H., Serbina, N. and Huang, L. (1995) 'The role of dioleoyl phosphatidylethanolamine in cationic liposome mediated gene transfer', *Biochim Biophys Acta*, 1235(2), 289-95
- Fasshauer, D. (2003) 'Structural insights into the SNARE mechanism', *Biochim Biophys Acta*, 87-97
- Fasshauer, D., Sutton, R. B., Brunger, A. T. and Jahn, R. (1998) 'Conserved structural features of the synaptic fusion complex: SNARE proteins reclassified as Q- and R-SNAREs', *Proc Natl Acad Sci U S A*, 95(26), 15781-6
- Feelders, R. A., Kuiper-Kramer, E. P. and van Eijk, H. G. (1999) 'Structure, function and clinical significance of transferrin receptors', *Clin Chem Lab Med*, 37(1), 1-10
- Feng, S. S., Mu, L., Win, K. Y. and Huang, G. (2004) 'Nanoparticles of biodegradable polymers for clinical administration of paclitaxel', *Curr Med Chem*, 11(4), 413-24
- Feng, Y., Jadhav, A. P., Rodighiero, C., Fujinaga, Y., Kirchhausen, T. and Lencer, W. I. (2004) 'Retrograde transport of cholera toxin from the plasma membrane to the endoplasmic reticulum requires the trans-Golgi network but not the Golgi apparatus in Exo2-treated cells', *EMBO Rep*, 596-601
- Ferruti, P., Manzoni, S., Richardson, S.C., Duncan, R., Patrick, N.G., Mendichi, R and Casolaro, M (2000) 'Amphoteric Linear Poly(amido-amine)s as endosomolytic polymers: correlation between physicochemical and biological properties' *Macromolecules*, 2000, 33 (21), pp 7793–7800
- Fewell, J. G., MacLaughlin, F., Mehta, V., Gondo, M., Nicol, F., Wilson, E. and Smith, L. C. (2001) 'Gene therapy for the treatment of hemophilia B using PINC-formulated plasmid delivered to muscle with electroporation', *Mol Ther*, 3(4), 574-83
- Fire, A., Xu, S., Montgomery, M. K., Kostas, S. A., Driver, S. E. and Mello, C. C. (1998) 'Potent and specific genetic interference by double-stranded RNA in *Caenorhabditis elegans*', *Nature*, 391(6669), 806-11
- Fisher, T. L., Terhorst, T., Cao, X. and Wagner, R. W. (1993) 'Intracellular disposition and metabolism of fluorescently-labeled unmodified and modified oligonucleotides microinjected into mammalian cells', *Nucleic Acids Res*, 21(16), 3857-65
- Flotte, T. R., Ng, P., Dylla, D. E., McCray, P. B., Jr., Wang, G., Kolls, J. K. and Hu, J. (2007) 'Viral vector-mediated and cell-based therapies for treatment of cystic fibrosis', *Mol Ther*, 15(2), 229-41
- Frankel, A., Welsh, P., Richardson, J. and Robertus, J. D. (1990) 'Role of arginine 180 and glutamic acid 177 of ricin toxin A chain in enzymatic inactivation of ribosomes', *Mol Cell Biol*, 10(12), 6257-63
- Frankel, A. E. (2004) 'Reducing the immune response to immunotoxin', *Clin Cancer Res*, 10(1 Pt 1), 13-5
- Frankel, A. E., Burbage, C., Fu, T., Tagge, E., Chandler, J. and Willingham, M. C. (1996) 'Ricin toxin contains at least three galactose-binding sites located in B chain subdomains 1 alpha, 1 beta, and 2 gamma', *Biochemistry*, 14749-56
- Frankel, A. E., Laver, J. H., Willingham, M. C., Burns, L. J., Kersey, J. H. and Vallera, D. A. (1997) 'Therapy of patients with T-cell lymphomas and leukemias using an anti-CD7 monoclonal antibody-ricin A chain immunotoxin', *Leuk Lymphoma*, 26(3-4), 287-98
- Frazer, R. Q., Byron, R. T., Osborne, P. B. and West, K. P. (2005) 'PMMA: an essential material in medicine and dentistry' in *J Long Term Eff Med Implants*, United States: 629-39.
- Fulton, R. J., Blakey, D. C., Knowles, P. P., Uhr, J. W., Thorpe, P. E. and Vitetta, E. S. (1986) 'Purification of ricin A1, A2, and B chains and characterization of their toxicity', *J Biol Chem*, 261(12), 5314-9

- Futter, C. E., Pearse, A., Hewlett, L. J. and Hopkins, C. R. (1996) 'Multivesicular endosomes containing internalized EGF-EGF receptor complexes mature and then fuse directly with lysosomes', *J Cell Biol*, 132(6), 1011-23
- Ganley, I. G., Espinosa, E. and Pfeffer, S. R. (2008) 'A syntaxin 10-SNARE complex distinguishes two distinct transport routes from endosomes to the trans-Golgi in human cells', *J Cell Biol*, 180(1), 159-72
- Garred, O., van Deurs, B. and Sandvig, K. (1995) 'Furin-induced cleavage and activation of Shiga toxin', *J Biol Chem*, 270(18), 10817-21
- Garty, H. and Asher, C. (1985) 'Ca²⁺-dependent, temperature-sensitive regulation of Na⁺ channels in tight epithelia. A study using membrane vesicles', *J Biol Chem*, 260(14), 8330-5
- Gebhart, C. L. and Kabanov, A. V. (2001) 'Evaluation of polyplexes as gene transfer agents', *J Control Release*, 73(2-3), 401-16
- Geoffroy, M. C. and Salvetti, A. (2005) 'Helper functions required for wild type and recombinant adeno-associated virus growth', *Curr Gene Ther*, 5(3), 265-71
- Gething, M. J. (1999) 'Role and regulation of the ER chaperone BiP', *Semin Cell Dev Biol*, 10(5), 465-472
- Ghetie, V. and Vitetta, E. S. (2001) 'Chemical construction of immunotoxins', *Mol Biotechnol*, 18(3), 251-68
- Ghosh, Y. K., Visweswariah, S. S. and Bhattacharya, S. (2002) 'Advantage of the ether linkage between the positive charge and the cholesteryl skeleton in cholesterol-based amphiphiles as vectors for gene delivery', *Bioconjug Chem*, 13(2), 378-84
- Gil, J. and Esteban, M. (2000) 'Induction of apoptosis by the dsRNA-dependent protein kinase (PKR): mechanism of action', *Apoptosis*, 5(2), 107-14
- Girod, A., Storrie, B., Simpson, J. C., Johannes, L., Goud, B., Roberts, L. M., Lord, J. M., Nilsson, T. and Pepperkok, R. (1999) 'Evidence for a COP-I-independent transport route from the Golgi complex to the endoplasmic reticulum', *Nat Cell Biol*, 1(7), 423-30
- Gluck, R. (1995) 'Liposomal presentation of antigens for human vaccines', *Pharm Biotechnol*, 6, 325-45
- Grabowski, G. A. (2008) 'Phenotype, diagnosis, and treatment of Gaucher's disease', *The Lancet*, 372(9645), 1263-1271
- Grassi, G., Dawson, P., Guarnieri, G., Kandolf, R. and Grassi, M. (2004) 'Therapeutic potential of hammerhead ribozymes in the treatment of hyper-proliferative diseases', *Curr Pharm Biotechnol*, 5(4), 369-86
- Griesenbach, U., Geddes, D. M., Alton, E. and Co, U. K. C. F. G. T. (2006) 'Gene therapy progress and prospects: cystic fibrosis', *Gene Ther*, 13(14), 1061-1067
- Grimaldi, E., Claassen, E. A. W., Michael Lord, J., Smith, D. C. and Easton, A. J. (2007) 'Stimulation of pneumovirus-specific CD8⁺ T-cells using a non-toxic recombinant ricin delivery system', *Mol Immunol*, 44(5), 993-998
- Grosshans, B. L., Ortiz, D. and Novick, P. (2006) 'Rabs and their effectors: achieving specificity in membrane traffic', *Proc Natl Acad Sci U S A*, 11821-7
- Gruenberg, J. (2001) 'The endocytic pathway: a mosaic of domains', *Nat Rev Mol Cell Biol*, 2(10), 721-30
- Gruenberg, J. and Maxfield, F. R. (1995) 'Membrane transport in the endocytic pathway', *Curr Opin Cell Biol*, 7(4), 552-563
- Gruenberg, J. and van der Goot, F. G. (2006) 'Mechanisms of pathogen entry through the endosomal compartments', *Nat Rev Mol Cell Biol*, 7(7), 495-504

- Gu, F. and Gruenberg, J. (1999) 'Biogenesis of transport intermediates in the endocytic pathway', *FEBS Lett*, 61-6
- Haasnoot, J. and Berkhout, B. (2006) 'RNA interference: its use as antiviral therapy', *Handb Exp Pharmacol*, (173), 117-50
- Hadaschik, B. A., Jackson, J., Fazli, L., Zoubeidi, A., Burt, H. M., Gleave, M. E. and So, A. I. (2008) 'Intravesically administered antisense oligonucleotides targeting heat-shock protein-27 inhibit the growth of non-muscle-invasive bladder cancer', *BJU Int*, 102(5), 610-6
- Hall, W. A. and Fodstad, O. (1992) 'Immunotoxins and central nervous system neoplasia', *J Neurosurg*, 76(1), 1-12
- Hannon, G. J. (2002) 'RNA interference', *Nature*, 418(6894), 244-51
- Hans, M. L. and Lowman, A. M. (2002) 'Biodegradable nanoparticles for drug delivery and targeting', *Curr. Opin. Solid State Mater. Sci*, 6(4), 319-327
- Harrington, K. J., Rowlinson-Busza, G., Syrigos, K. N., Uster, P. S., Vile, R. G. and Stewart, J. S. (2000) 'Pegylated liposomes have potential as vehicles for intratumoral and subcutaneous drug delivery', *Clin Cancer Res*, 6(6), 2528-37
- Hartley, M. R. and Lord, J. M. (2004) 'Cytotoxic ribosome-inactivating lectins from plants', *Biochim Biophys Acta*, 1701(1-2), 1-14
- Hassan, I., Wunderlich, A., Burchert, A., Hoffmann, S. and Zielke, A. (2006) 'Antisense p53 oligonucleotides inhibit proliferation and induce chemosensitivity in follicular thyroid cancer cells', *Anticancer Res*, 26(2A), 1171-6
- Heese, B. A. (2008) 'Current Strategies in the Management of Lysosomal Storage Diseases', *Semin Pediatr Neurol*, 15(3), 119-126
- Heinze, M., Brezesinski, G., Dobner, B. and Langner, A. (2010) 'Novel cationic lipids based on malonic acid amides backbone: transfection efficacy and cell toxicity properties', *Bioconjug Chem*, 21(4), 696-708
- Hengen, P. (1995) 'Purification of His-Tag fusion proteins from Escherichia coli', *Trends Biochem Sci*, England: 285-6
- Herzenberg, L. A. (1959) 'Studies on the induction of beta-galactosidase in a cryptic strain of Escherichia coli', *Biochim Biophys Acta*, 31(2), 525-38
- Hinners, I. and Tooze, S. A. (2003) 'Changing directions: clathrin-mediated transport between the Golgi and endosomes', *J Cell Sci*, 116(Pt 5), 763-71
- Hirling, H. (2009) 'Endosomal trafficking of AMPA-type glutamate receptors', *Neuroscience*, 158(1), 36-44
- Hong, W. (2005) 'SNAREs and traffic', *Biochim Biophys Acta*, 120-44
- Hosur MV, Nair B, Satyamurthy P, Misquith S, Surolia A, Kannan KK (1995) 'X-ray structure of gelonin at 1.8 Å resolution', *J Mol Biol*, 250(3), 368-80
- Hui, Z., He, Z. G., Zheng, L., Li, G. Y., Shen, S. R. and Li, X. L. (2008) 'Studies on polyamidoamine dendrimers as efficient gene delivery vector', *J Biomater Appl*, 22(6), 527-44
- Hunziker, W., Whitney, J. A. and Mellman, I. (1992) 'Brefeldin A and the endocytic pathway. Possible implications for membrane traffic and sorting', *FEBS Lett*, 93-6
- Huwylar, J., Cerletti, A., Fricker, G., Eberle, A. N. and Drewe, J. (2002) 'By-passing of P-glycoprotein using immunoliposomes', *J Drug Target*, 10(1), 73-9

- Hélène, C. and Toulmé, J.-J. (1990) 'Specific regulation of gene expression by antisense, sense and antigenic nucleic acids', *Biochimica et Biophysica Acta (BBA) - Biochim Biophys Acta*, 1049(2), 99-125
- Ideue, T., Hino, K., Kitao, S., Yokoi, T. and Hirose, T. (2009) 'Efficient oligonucleotide-mediated degradation of nuclear noncoding RNAs in mammalian cultured cells', *RNA*, 15(8), 1578-87
- Immordino, M. L., Brusa, P., Arpicco, S., Stella, B., Dosio, F. and Cattel, L. (2003) 'Preparation, characterization, cytotoxicity and pharmacokinetics of liposomes containing docetaxel', *J Control Release*, 91(3), 417-29
- Immordino, M. L., Dosio, F. and Cattel, L. (2006) 'Stealth liposomes: review of the basic science, rationale, and clinical applications, existing and potential', *Int J Nanomedicine*, 1(3), 297-315
- Ispas, C., Andreescu, D., Patel, A., Goia, D. V., Andreescu, S. and Wallace, K. N. (2009) 'Toxicity and developmental defects of different sizes and shape nickel nanoparticles in zebrafish', *Environ Sci Technol*, 43(16), 6349-56
- Iversen, T. G., Skretting, G., Llorente, A., Nicoziani, P., van Deurs, B. and Sandvig, K. (2001) 'Endosome to Golgi transport of ricin is independent of clathrin and of the Rab9- and Rab11-GTPases', *Mol Biol Cell*, 12(7), 2099-107
- Jahn, R. and Scheller, R. H. (2006) 'SNAREs--engines for membrane fusion', *Nat Rev Mol Cell Biol*, 631-43
- Jain, T. K., Morales, M. A., Sahoo, S. K., Leslie-Pelecky, D. L. and Labhasetwar, V. (2005) 'Iron oxide nanoparticles for sustained delivery of anticancer agents', *Mol Pharm*, 2(3), 194-205
- Jiao, Y. H., Li, Y., Wang, S., Zhang, K., Jia, Y. G. and Fu, Y. (2010) 'Layer-by-layer assembly of poly(lactic acid) nanoparticles: a facile way to fabricate films for model drug delivery', *Langmuir*, 26(11), 8270-3
- Johannes, L. and Decaudin, D. (2005) 'Protein toxins: intracellular trafficking for targeted therapy', *Gene Ther*, 12(18), 1360-8
- Johannes, L. and Romer, W. (2010) 'Shiga toxins--from cell biology to biomedical applications', *Nat Rev Microbiol*, England: 105-16
- John, T. A., Vogel, S. M., Tiruppathi, C., Malik, A. B. and Minshall, R. D. (2003) 'Quantitative analysis of albumin uptake and transport in the rat microvessel endothelial monolayer', *Am J Physiol Lung Cell Mol Physiol*, 284(1), L187-96
- Johnson, L. G., Olsen, J. C., Sarkadi, B., Moore, K. L., Swanstrom, R. and Boucher, R. C. (1992) 'Efficiency of gene transfer for restoration of normal airway epithelial function in cystic fibrosis', *Nat Genet*, 2(1), 21-25
- Johnston, H. D., Foote, C., Santeford, A. and Nothwehr, S. F. (2005) 'Golgi-to-late endosome trafficking of the yeast pheromone processing enzyme Ste13p is regulated by a phosphorylation site in its cytosolic domain', *Mol Biol Cell*, 16(3), 1456-68
- Jones, A. T., Gumbleton, M. and Duncan, R. (2003) 'Understanding endocytic pathways and intracellular trafficking: a prerequisite for effective design of advanced drug delivery systems', *Adv Drug Deliv Rev*, 1353-7
- Jones, M. C. and Leroux, J.-C. (1999) 'Polymeric micelles - a new generation of colloidal drug carriers', *Eur J Pharm Biopharm*, 48(2), 101-111
- Juliano, R., Alam, M. R., Dixit, V. and Kang, H. (2008) 'Mechanisms and strategies for effective delivery of antisense and siRNA oligonucleotides', *Nucleic Acids Res*, 36(12), 4158-71
- Kabanov, A. V., Astafyeva, I. V., Chikindas, M. L., Rosenblat, G. F., Kiselev, V. I., Severin, E. S. and Kabanov, V. A. (1991) 'DNA interpolyelectrolyte complexes as a tool for efficient cell transformation', *Biopolymers*, 31(12), 1437-43
- Kabanov, A. V. and Kabanov, V. A. (1995) 'DNA complexes with polycations for the delivery of genetic material into cells', *Bioconjug Chem*, 6(1), 7-20

- Kagedal, K., Zhao, M., Svensson, I. and Brunk, U. T. (2001) 'Sphingosine-induced apoptosis is dependent on lysosomal proteases', *Biochem J*, 359(Pt 2), 335-43
- Karmali, P. P. and Chaudhuri, A. (2007) 'Cationic liposomes as non-viral carriers of gene medicines: Resolved issues, open questions, and future promises', *Med Res Rev*, 27(5), 696-722
- Karmali, P. P., Majeti, B. K., Sreedhar, B. and Chaudhuri, A. (2006) 'In vitro gene transfer efficacies and serum compatibility profiles of novel mono-, di-, and tri-histidinylated cationic transfection lipids: a structure-activity investigation', *Bioconjug Chem*, 17(1), 159-71
- Kashani-Sabet, M. (2004) 'Non-viral delivery of ribozymes for cancer gene therapy', *Expert Opin Biol Ther*, 4(11), 1749-55
- Kastan, M. B. (2007) 'Wild-type p53: Tumors can't stand it', *Cell*, 128(5), 837-840
- Kataoka, K., Harada, A. and Nagasaki, Y. (2001) 'Block copolymer micelles for drug delivery: design, characterization and biological significance', *Adv Drug Deliv Rev*, 47(1), 113-31
- Katayose, S. and Kataoka, K. (1997) 'Water-soluble polyion complex associates of DNA and poly(ethylene glycol)-poly(L-lysine) block copolymer', *Bioconjug Chem*, 8(5), 702-7
- Katayose, S. and Kataoka, K. (1998) 'Remarkable increase in nuclease resistance of plasmid DNA through supramolecular assembly with poly(ethylene glycol)-poly(L-lysine) block copolymer', *J Pharm Sci*, 87(2), 160-3
- Kazunori, K., Glenn S, K., Masayuki, Y., Teruo, O. and Yasuhisa, S. (1993) 'Block copolymer micelles as vehicles for drug delivery', *J Control Release*, 24(1-3), 119-132
- Keller, P. and Simons, K. (1997) 'Post-Golgi biosynthetic trafficking', *J Cell Sci*, 110 (Pt 24), 3001-9
- Kerkis, A., Hayashi, M. A., Yamane, T. and Kerkis, I. (2006) 'Properties of cell penetrating peptides (CPPs)', *IUBMB Life*, 58(1), 7-13
- Khan, A. U. (2006) 'Ribozyme: A clinical tool', *Clinica Chimica Acta*, 367(1-2), 20-27.
- Kidane, A. G., Burriesci, G., Cornejo, P., Dooley, A., Sarkar, S., Bonhoeffer, P., Edirisinghe, M. and Seifalian, A. M. (2009) 'Current developments and future prospects for heart valve replacement therapy', *J Biomed Mater Res B Appl Biomater*, 88(1), 290-303
- Killion, J. J. and Fidler, I. J. (1994) 'Systemic Targeting of Liposome-Encapsulated Immunomodulators to Macrophages for Treatment of Cancer Metastasis', *ImmunoMethods*, 4(3), 273-279
- Kim, I.-S. and Kim, S.-H. (2003) 'Development of polymeric nanoparticulate drug delivery systems: evaluation of nanoparticles based on biotinylated poly(ethylene glycol) with sugar moiety', *Int J Pharm*, 257(1-2), 195-203
- Kirchels, R., Schuller, S., Brunner, S., Ogris, M., Heider, K. H., Zauner, W. and Wagner, E. (1999) 'Polycation-based DNA complexes for tumor-targeted gene delivery in vivo', *J Gene Med*, 1(2), 111-20
- Kohn, D. B. (2010) 'Update on gene therapy for immunodeficiencies', *Clin Immunol*, 135(2), 247-254
- Kopitz, J., Holz, F. G., Kaemmerer, E. and Schutt, F. (2004) 'Lipids and lipid peroxidation products in the pathogenesis of age-related macular degeneration', *Biochimie*, 86(11), 825-831
- Kreitman, R. J. (2006) 'Immunotoxins for targeted cancer therapy', *AAPS J*, 8(3), E532-51
- Kreitman, R. J. (2009) 'Recombinant immunotoxins for the treatment of chemoresistant hematologic malignancies', *Curr Pharm Des*, 15(23), 2652-64

- Kreitman, R. J., Wilson, W. H., Bergeron, K., Raggio, M., Stetler-Stevenson, M., FitzGerald, D. J. and Pastan, I. (2001) 'Efficacy of the anti-CD22 recombinant immunotoxin BL22 in chemotherapy-resistant hairy-cell leukemia', *N Engl J Med*, 345(4), 241-7
- Kreuter, J. (2001) 'Nanoparticulate systems for brain delivery of drugs', *Adv Drug Deliv Rev*, 47(1), 65-81
- Kreuter, J., Ramge, P., Petrov, V., Hamm, S., Gelperina, S. E., Engelhardt, B., Alyautdin, R., von Briesen, H. and Begley, D. J. (2003) 'Direct evidence that polysorbate-80-coated poly(butylcyanoacrylate) nanoparticles deliver drugs to the CNS via specific mechanisms requiring prior binding of drug to the nanoparticles', *Pharm Res*, 20(3), 409-16
- Kroll, R. A., Pagel, M. A., Muldoon, L. L., Roman-Goldstein, S., Fiamengo, S. A. and Neuwelt, E. A. (1998) 'Improving drug delivery to intracerebral tumor and surrounding brain in a rodent model: a comparison of osmotic versus bradykinin modification of the blood-brain and/or blood-tumor barriers', *Neurosurgery*, 43(4), 879-86; discussion 886-9
- Kukowska-Latallo, J. F., Bielinska, A. U., Johnson, J., Spindler, R., Tomalia, D. A. and Baker, J. R., Jr. (1996) 'Efficient transfer of genetic material into mammalian cells using Starburst polyamidoamine dendrimers', *Proc Natl Acad Sci U S A*, 93(10), 4897-902
- Kumari, A., Yadav, S. K. and Yadav, S. C. (2010) 'Biodegradable polymeric nanoparticles based drug delivery systems', *Colloids Surf B Biointerfaces*, 75(1), 1-18
- Kunath, K., von Harpe, A., Fischer, D., Petersen, H., Bickel, U., Voigt, K. and Kissel, T. (2003) 'Low-molecular-weight polyethylenimine as a non-viral vector for DNA delivery: comparison of physicochemical properties, transfection efficiency and in vivo distribution with high-molecular-weight polyethylenimine', *J Control Release*, 89(1), 113-125
- Kundu, P.P Sharma, V. (2008) 'Synthetic polymeric vectors in gene therapy', *Curr Opin Solid State Mater Sci*, 12(5-6), 89-102
- Kurien, B. T. and Scofield, R. H. (2003) 'Protein blotting: a review', *J Immunol Methods*, 1-15
- Kurreck, J. (2003) 'Antisense technologies. Improvement through novel chemical modifications', *Eur J Biochem*, 270(8), 1628-44
- Kwoh, D. Y., Coffin, C. C., Lollo, C. P., Jovenal, J., Banaszczyk, M. G., Mullen, P., Phillips, A., Amini, A., Fabrycki, J., Bartholomew, R. M., Brostoff, S. W. and Carlo, D. J. (1999) 'Stabilization of poly-L-lysine/DNA polyplexes for in vivo gene delivery to the liver', *Biochim Biophys Acta*, 171-90
- Kwon, G., Suwa, S., Yokoyama, M., Okano, T., Sakurai, Y. and Kataoka, K. (1994) 'Enhanced tumor accumulation and prolonged circulation times of micelle-forming poly (ethylene oxide-aspartate) block copolymer-adriamycin conjugates', *J Control Release*, 29(1-2), 17-23
- Laemmli, U. K., Molbert, E., Showe, M. and Kellenberger, E. (1970) 'Form-determining function of the genes required for the assembly of the head of bacteriophage T4', *J Mol Biol*, 49(1), 99-113
- Laginha, K. M., Moase, E. H., Yu, N., Huang, A. and Allen, T. M. (2008) 'Bioavailability and therapeutic efficacy of HER2 scFv-targeted liposomal doxorubicin in a murine model of HER2-overexpressing breast cancer', *J Drug Target*, 16(7), 605-10
- Lambert, J. M., Blattler, W. A., McIntyre, G. D., Goldmacher, V. S. and Scott, C. F., Jr. (1988) 'Immunotoxins containing single-chain ribosome-inactivating proteins', *Cancer Treat Res*, 37, 175-209
- Laske, D. W., Youle, R. J. and Oldfield, E. H. (1997) 'Tumor regression with regional distribution of the targeted toxin TF-CRM107 in patients with malignant brain tumors', *Nat Med*, 3(12), 1362-8
- Lavasanifar, A., Samuel, J. and Kwon, G. S. (2002a) 'Poly(ethylene oxide)-block-poly(-amino acid) micelles for drug delivery', *Adv Drug Deliv Rev*, 54(2), 169-190

- Lavasanifar, A., Samuel, J., Sattari, S. and Kwon, G. S. (2002b) 'Block copolymer micelles for the encapsulation and delivery of amphotericin B', *Pharm Res*, 19(4), 418-22
- Lech, P. and Somia, N. V. (2008) 'Retrovirus vectors', *Contrib Nephrol*, 159, 30-46
- Lee, M. T., Mishra, A. and Lambright, D. G. (2009) 'Structural mechanisms for regulation of membrane traffic by rab GTPases', *Traffic*, 1377-89
- Lencer, W. I., Constable, C., Moe, S., Jobling, M. G., Webb, H. M., Ruston, S., Madara, J. L., Hirst, T. R. and Holmes, R. K. (1995) 'Targeting of cholera toxin and Escherichia coli heat labile toxin in polarized epithelia: role of COOH-terminal KDEL', *J Cell Biol*, 131(4), 951-62
- Lencer, W. I. and Tsai, B. (2003) 'The intracellular voyage of cholera toxin: going retro' in *Trends Biochem Sci*, 639-45
- Leonard, J. N. and Schaffer, D. V. (2006) 'Antiviral RNAi therapy: emerging approaches for hitting a moving target', *Gene Ther*, 13(6), 532-40
- Leung, R. K. M. and Whittaker, P. A. (2005) 'RNA interference: From gene silencing to gene-specific therapeutics', *Pharmacol Ther*, 107(2), 222-239
- Levine, B. L., Humeau, L. M., Boyer, J., MacGregor, R. R., Rebello, T., Lu, X., Binder, G. K., Slepishkin, V., Lemiale, F., Mascola, J. R., Bushman, F. D., Dropulic, B., June, C. H. (2006) 'Gene transfer in humans using a conditionally replicating lentiviral vector', *Proc Natl Acad Sci*, 103(46), 17372-7
- Lilley, D. M. J. (2005) 'Structure, folding and mechanisms of ribozymes', *Curr Opin Struct Biol*, 15(3), 313-323
- Limberis, M. P. (2008) 'Cystic fibrosis: recent advances in lung-directed therapies', *Drug Discov Today Ther Strat*, 5(4), 243-248
- Lin, Z. H., Fukuda, N., Suzuki, R., Takagi, H., Ikeda, Y., Saito, S., Matsumoto, K., Kanmatsuse, K. and Mugishima, H. (2004) 'Adenovirus-encoded hammerhead ribozyme to PDGF A-chain mRNA inhibits neointima formation after arterial injury', *J Vasc Res*, 41(4), 305-13
- Lindgren, M., Hällbrink, M., Prochiantz, A. and Langel, Ü. (2000) 'Cell-penetrating peptides', *Trends Pharm. Sci*, 21(3), 99-103
- Lingel, A. and Izaurralde, E. (2004) 'RNAi: finding the elusive endonuclease', *RNA*, 10(11), 1675-9
- Liu, Q., Zhan, J., Chen, X. and Zheng, S. (2006) 'Ricin A chain reaches the endoplasmic reticulum after endocytosis', *Biochem Biophys Res Commun*, 857-63
- Lollo, C. P., Banaszczyk, M. G., Mullen, P. M., Coffin, C. C., Wu, D., Carlo, A. T., Bassett, D. L., Gouveia, E. K. and Carlo, D. J. (2002) 'Poly-L-lysine-based gene delivery systems. Synthesis, purification, and application', *Methods Mol Med*, 69, 1-13
- Lopez-Gigosos, R. M., Plaza, E., Diez-Diaz, R. M. and Calvo, M. J. (2011) 'Vaccination strategies to combat an infectious globe: oral cholera vaccines', *J Glob Infect Dis*, 56-62
- Lord, J. M., Deeks, E., Marsden, C. J., Moore, K., Pateman, C., Smith, D. C., Spooner, R. A., Watson, P. and Roberts, L. M. (2003) 'Retrograde transport of toxins across the endoplasmic reticulum membrane', *Biochem Soc Trans*, 31(Pt 6), 1260-2
- Lord, J. M. and Roberts, L. M. (1998) 'Toxin entry: retrograde transport through the secretory pathway', *J Cell Biol*, 140(4), 733-6
- Lord, J. M., Roberts, L. M. and Robertus, J. D. (1994) 'Ricin: structure, mode of action, and some current applications', *FASEB J*, 8(2), 201-8
- Lord, J. M. and Spooner, R. A. (2011) 'Ricin trafficking in plant and Mammalian cells' *Toxins* (Basel), 787-801

- Lord, M. J., Jolliffe, N. A., Marsden, C. J., Pateman, C. S., Smith, D. C., Spooner, R. A., Watson, P. D. and Roberts, L. M. (2003) 'Ricin. Mechanisms of cytotoxicity', *Toxicol Rev*, 22(1), 53-64
- Lu, Y., Friedman, R., Kushner, N., Doling, A., Thomas, L., Touzjian, N., Starnbach, M. and Lieberman, J. (2000) 'Genetically modified anthrax lethal toxin safely delivers whole HIV protein antigens into the cytosol to induce T cell immunity', *Proc Natl Acad Sci*, 97(14), 8027-32
- Lu, X., Yu, Q., Binder, G. K., Chen, Z., Slepushkina, T., Rossi, J., Dropulic, B. (2004) 'Antisense-mediated inhibition of human immunodeficiency virus (HIV) replication by use of an HIV type 1-based vector results in severely attenuated mutants incapable of developing resistance', *J Virol*, 78(13), 7079-88
- Lukyanov, A. N., Elbayoumi, T. A., Chakilam, A. R. and Torchilin, V. P. (2004) 'Tumor-targeted liposomes: doxorubicin-loaded long-circulating liposomes modified with anti-cancer antibody', *J Control Release*, 100(1), 135-44
- Lundqvist, M., Stigler, J., Elia, G., Lynch, I., Cedervall, T. and Dawson, K. A. (2008) 'Nanoparticle size and surface properties determine the protein corona with possible implications for biological impacts', *Proc Natl Acad Sci U S A*, 105(38), 14265-70
- Lundstrom, K. (2003) 'Latest development in viral vectors for gene therapy', *Trends Biotechnol*, 21(3), 117-22
- Lungwitz, U., Breunig, M., Blunk, T. and Göpferich, A. (2005) 'Polyethylenimine-based non-viral gene delivery systems', *Eur J Pharm Biopharm*, 60(2), 247-266
- Luten, J., van Nostrum, C. F., De Smedt, S. C. and Hennink, W. E. (2008) 'Biodegradable polymers as non-viral carriers for plasmid DNA delivery', *J Control Release*, 126(2), 97-110.
- Luton, D., Oudrhiri, N., de Lagausie, P., Aissaoui, A., Hauchecorne, M., Julia, S., Oury, J. F., Aigrain, Y., Peuchmaur, M., Vigneron, J. P., Lehn, J. M. and Lehn, P. (2004) 'Gene transfection into fetal sheep airways in utero using guanidinium-cholesterol cationic lipids', *J Gene Med*, 6(3), 328-36
- Luzio, J. P., Mullock, B. M., Pryor, P. R., Lindsay, M. R., James, D. E. and Piper, R. C. (2001) 'Relationship between endosomes and lysosomes', *Biochem Soc Trans*, 29(Pt 4), 476-80
- Luzio, J. P., Parkinson, M. D., Gray, S. R. and Bright, N. A. (2009) 'The delivery of endocytosed cargo to lysosomes', *Biochem Soc Trans*, 37(Pt 5), 1019-21
- Luzio, J. P., Poupon, V., Lindsay, M. R., Mullock, B. M., Piper, R. C. and Pryor, P. R. (2003) 'Membrane dynamics and the biogenesis of lysosomes', *Mol Membr Biol*, 20(2), 141-154
- Macedo, M. F. and de Sousa, M. (2008) 'Transferrin and the transferrin receptor: of magic bullets and other concerns', *Inflamm Allergy Drug Targets*, 7(1), 41-52
- Madan, S. and Ghosh, P. C. (1992) 'Interaction of gelonin with macrophages: effect of lysosomotropic amines', *Exp Cell Res*, 52-8
- Maeda, H., Bharate, G. Y. and Daruwalla, J. (2009) 'Polymeric drugs for efficient tumor-targeted drug delivery based on EPR-effect', *Eur J Pharm Biopharm*, 71(3), 409-19
- Maeda, H., Sawa, T. and Konno, T. (2001) 'Mechanism of tumor-targeted delivery of macromolecular drugs, including the EPR effect in solid tumor and clinical overview of the prototype polymeric drug SMANCS', *J Control Release*, 74(1-3), 47-61
- Mainardes, R. M. and Evangelista, R. C. (2005) 'PLGA nanoparticles containing praziquantel: effect of formulation variables on size distribution', *Int J Pharm*, 290(1-2), 137-144
- Majoul, I., Sohn, K., Wieland, F. T., Pepperkok, R., Pizza, M., Hillemann, J. and Soling, H. D. (1998) 'KDEL receptor (Erd2p)-mediated retrograde transport of the cholera toxin A subunit from the Golgi involves COPI, p23, and the COOH terminus of Erd2p', *J Cell Biol*, 143(3), 601-12

- Mallard, F., Antony, C., Tenza, D., Salamero, J., Goud, B. and Johannes, L. (1998) 'Direct pathway from early/recycling endosomes to the Golgi apparatus revealed through the study of shiga toxin B-fragment transport', *J Cell Biol*, 143(4), 973-90
- Mallard, F., Tang, B. L., Galli, T., Tenza, D., Saint-Pol, A., Yue, X., Antony, C., Hong, W., Goud, B. and Johannes, L. (2002) 'Early/recycling endosomes-to-TGN transport involves two SNARE complexes and a Rab6 isoform', *J Cell Biol*, 653-64
- Mamot, C., Drummond, D. C., Noble, C. O., Kallab, V., Guo, Z., Hong, K., Kirpotin, D. B. and Park, J. W. (2005) 'Epidermal growth factor receptor-targeted immunoliposomes significantly enhance the efficacy of multiple anticancer drugs in vivo', *Cancer Res*, 65(24), 11631-8
- Marchisio, M. A., Longo, T. and Ferruti, P. (1973) 'A selective de-heparinizer filter made of new cross-linked polymers of a poly-amido-amine structure', *Experientia*, 29(1), 93-5
- Markert, C. D., Atala, A., Cann, J. K., Christ, G., Furth, M., Ambrosio, F. and Childers, M. K. (2009) 'Mesenchymal stem cells: emerging therapy for Duchenne muscular dystrophy', *PM R*, 1(6), 547-59
- Massignani, M., LoPresti, C., Blanz, A., Madsen, J., Armes, S. P., Lewis, A. L. and Battaglia, G. (2009) 'Controlling cellular uptake by surface chemistry, size, and surface topology at the nanoscale', *Small*, 5(21), 2424-32
- Massol, R. H., Larsen, J. E., Fujinaga, Y., Lencer, W. I. and Kirchhausen, T. (2004) 'Cholera toxin toxicity does not require functional Arf6- and dynamin-dependent endocytic pathways', *Mol Biol Cell*, 3631-41
- Mastrobattista, E., Bravo, S. A., van der Aa, M. and Crommelin, D. J. A. (2005) 'Nonviral gene delivery systems: From simple transfection agents to artificial viruses', *Drug Discovery Today: Technologies*, 2(1), 103-109
- Mastrobattista, E., Koning, G. A., van Bloois, L., Filipe, A. C., Jiskoot, W. and Storm, G. (2002) 'Functional characterization of an endosome-disruptive peptide and its application in cytosolic delivery of immunoliposome-entrapped proteins', *J Biol Chem*, 277(30), 27135-43
- Matlack, K. E., Mothes, W. and Rapoport, T. A. (1998) 'Protein translocation: tunnel vision', *Cell*, 92(3), 381-90
- Mellman, I. (1996) 'Endocytosis and molecular sorting', *Annu Rev Cell Dev Biol*, 12, 575-625
- Mellman, I. (1994) 'Membranes and sorting', *Curr Opin Cell Biol*, 497-8
- Messmer, D. and Kipps, T. J. (2005) 'Treatment of solid tumors with immunotoxins', *Breast Cancer Res*, 7(5), 184-6
- Miaczynska, M. and Stenmark, H. (2008) 'Mechanisms and functions of endocytosis', *J Cell Biol*, 180(1), 7-11
- Miesenbock, G. and Rothman, J. E. (1995) 'The capacity to retrieve escaped ER proteins extends to the trans-most cisterna of the Golgi stack', *J Cell Biol*, 129(2), 309-19
- Mills, I. G., Urbe, S. and Clague, M. J. (2001) 'Relationships between EEA1 binding partners and their role in endosome fusion', *J Cell Sci*, 114(Pt 10), 1959-65
- Mishra, B., Patel, B. B. and Tiwari, S. (2010) 'Colloidal nanocarriers: a review on formulation technology, types and applications toward targeted drug delivery', *Nanomedicine*, 6(1), 9-24
- Miwa, A., Ishibe, A., Nakano, M., Yamahira, T., Itai, S., Jinno, S. and Kawahara, H. (1998) 'Development of novel chitosan derivatives as micellar carriers of taxol', *Pharm Res*, 15(12), 1844-50
- Moghimi, S. M., Hunter, A. C. and Murray, J. C. (2001) 'Long-circulating and target-specific nanoparticles: theory to practice', *Pharmacol Rev*, 53(2), 283-318

- Moolten, F. L. and Cooperband, S. R. (1970) 'Selective destruction of target cells by diphtheria toxin conjugated to antibody directed against antigens on the cells', *Science*, 169(940), 68-70
- Morille, M., Passirani, C., Vonarbourg, A., Clavreul, A. and Benoit, J. P. (2008) 'Progress in developing cationic vectors for non-viral systemic gene therapy against cancer', *Biomaterials*, 29(24-25), 3477-96
- Mosmann, T. (1983) 'Rapid colorimetric assay for cellular growth and survival: application to proliferation and cytotoxicity assays', *J Immunol Methods*, 65(1-2), 55-63
- Mu, F. T., Callaghan, J. M., Steele-Mortimer, O., Stenmark, H., Parton, R. G., Campbell, P. L., McCluskey, J., Yeo, J. P., Tock, E. P. and Toh, B. H. (1995) 'EEA1, an early endosome-associated protein. EEA1 is a conserved alpha-helical peripheral membrane protein flanked by cysteine "fingers" and contains a calmodulin-binding IQ motif', *J Biol Chem*, 270(22), 13503-11
- Mulligan, R. C. (1993) 'The basic science of gene therapy', *Science*, 260(5110), 926-32
- Mullock, B. M., Bright, N. A., Fearon, C. W., Gray, S. R. and Luzio, J. P. (1998) 'Fusion of lysosomes with late endosomes produces a hybrid organelle of intermediate density and is NSF dependent', *J Cell Biol*, 140(3), 591-601
- Mumper, R. J. and Rolland, A. P. (1998) 'Plasmid delivery to muscle: Recent advances in polymer delivery systems', *Adv Drug Deliv Rev*, 30(1-3), 151-172
- Mumper, R. J., Wang, J., L. Klakamp, S., Nitta, H., Anwer, K., Tagliaferri, F. and Rolland, A. P. (1998) 'Protective interactive noncondensing (PINC) polymers for enhanced plasmid distribution and expression in rat skeletal muscle', *J Control Release*, 52(1-2), 191-203
- Myers, D. E., Irvin, J. D., Smith, R. S., Kuebelbeck, V. M. and Uckun, F. M. (1991) 'Production of a pokeweed antiviral protein (PAP)-containing immunotoxin, B43-PAP, directed against the CD19 human B lineage lymphoid differentiation antigen in highly purified form for human clinical trials', *J Immunol Methods*, 136(2), 221-37
- Nagarajan, R. and Ruckenstein, E. (1977) 'Critical micelle concentration: A transition point for micellar size distribution : A statistical thermodynamical approach', *J. Colloid Interface Sci*, 60(2), 221-231
- Nair, L. S. and Laurencin, C. T. (2006) 'Polymers as biomaterials for tissue engineering and controlled drug delivery', *Adv Biochem Eng Biotechnol*, 102, 47-90
- Nakanishi, T., Fukushima, S., Okamoto, K., Suzuki, M., Matsumura, Y., Yokoyama, M., Okano, T., Sakurai, Y. and Kataoka, K. (2001) 'Development of the polymer micelle carrier system for doxorubicin', *J Control Release*, 74(1-3), 295-302
- Nakatsukasa, K. and Brodsky, J. L. (2008) 'The recognition and retrotranslocation of misfolded proteins from the endoplasmic reticulum', *Traffic*, 861-70
- Namgung, R., Kim, J., Singha, K., Kim, C. H. and Kim, W. J. (2009) 'Synergistic effect of low cytotoxic linear polyethylenimine and multiarm polyethylene glycol: study of physicochemical properties and in vitro gene transfection', *Mol Pharm*, 6(6), 1826-35
- Newton, D. L., Wales, R., Richardson, P. T., Walbridge, S., Saxena, S. K., Ackerman, E. J., Roberts, L. M., Lord, J. M. and Youle, R. J. (1992) 'Cell surface and intracellular functions for ricin galactose binding', *J. Biol. Chem*, 267(17), 11917-11922
- Nicolas, E., Beggs, J. M. and Taraschi, T. F. (2000) 'Gelonin is an unusual DNA glycosylase that removes adenine from single-stranded DNA, normal base pairs and mismatches', *J Biol Chem, United States*, 31399-406
- Nilsson, T. and Warren, G. (1994) 'Retention and retrieval in the endoplasmic reticulum and the Golgi apparatus', *Curr Opin Cell Biol*, 6(4), 517-21

- Nishino, I., Fu, J., Tanji, K., Yamada, T., Shimojo, S., Koori, T., Mora, M., Riggs, J. E., Oh, S. J., Koga, Y., Sue, C. M., Yamamoto, A., Murakami, N., Shanske, S., Byrne, E., Bonilla, E., Nonaka, I., DiMauro, S. and Hirano, M. (2000) 'Primary LAMP-2 deficiency causes X-linked vacuolar cardiomyopathy and myopathy (Danon disease)', *Nature*, 406(6798), 906-10
- Nishiyama, N. and Kataoka, K. (2003) 'Polymeric micelle drug carrier systems: PEG-PAsp (Dox) and second generation of micellar drugs', *Adv Exp Med Biol*, 519, 155-77
- Noguchi, M., Yi, H., Rosenblatt, H. M., Filipovich, A. H., Adelstein, S., Modi, W. S., McBride, O. W. and Leonard, W. J. (1993) 'Interleukin-2 receptor gamma chain mutation results in X-linked severe combined immunodeficiency in humans', *Cell*, 73(1), 147-157
- Nykanen, A., Haley, B. and Zamore, P. D. (2001) 'ATP requirements and small interfering RNA structure in the RNA interference pathway', *Cell*, 107(3), 309-21
- Nystrom, T. (2004) 'Stationary-phase physiology', *Annu Rev Microbiol*, 58, 161-81
- O'Brien, A. D., Tesh, V. L., Donohue-Rolfe, A., Jackson, M. P., Olsnes, S., Sandvig, K., Lindberg, A. A. and Keusch, G. T. (1992) 'Shiga toxin: biochemistry, genetics, mode of action, and role in pathogenesis', *Curr Top Microbiol Immunol*, 180, 65-94
- O'Hara, J. M., Neal, L. M., McCarthy, E. A., Kasten-Jolly, J. A., Brey, R. N., 3rd and Mantis, N. J. (2010) 'Folding domains within the ricin toxin A subunit as targets of protective antibodies', *Vaccine*, 7035-86
- O'Hare, M., Roberts, L. M., Thorpe, P. E., Watson, G. J., Prior, B. and Lord, J. M. (1987) 'Expression of ricin A chain in Escherichia coli', *FEBS Lett*, 73-8
- O'Loughlin, E. V. and Robins-Browne, R. M. (2001) 'Effect of Shiga toxin and Shiga-like toxins on eukaryotic cells', *Microbes Infect*, 493-507
- Odumosu, O., Nicholas, D., Yano, H. and Langridge, W. (2010) 'AB Toxins: A Paradigm Switch from Deadly to Desirable', *Toxins (Basel)*, 1612-45
- Ogris, M. and Wagner, E. (2002) 'Targeting tumors with non-viral gene delivery systems', *Drug Discovery Today*, 7(8), 479-485
- Olsnes, S. (2004) 'The history of ricin, abrin and related toxins' in *Toxicon*, 361-70.
- Olsnes, S. and Kozlov, J. V. (2001) 'Ricin', *Toxicon*, 1723-8
- Olsnes, S. and Pihl, A. (1973) 'Different biological properties of the two constituent peptide chains of ricin, a toxic protein inhibiting protein synthesis', *Biochemistry*, 12(16), 3121-6
- Onishi, Y., Eshita, Y., Murashita, A., Mizuno, M. and Yoshida, J. (2007) 'Characteristics of DEAE-dextran-MMA graft copolymer as a nonviral gene carrier', *Nanomedicine*, 3(3), 184-191
- Pai, L. H., Wittes, R., Setser, A., Willingham, M. C. and Pastan, I. (1996) 'Treatment of advanced solid tumors with immunotoxin LMB-1: an antibody linked to Pseudomonas exotoxin', *Nat Med*, 2(3), 350-3
- Pai-Scherf, L. H., Villa, J., Pearson, D., Watson, T., Liu, E., Willingham, M. C. and Pastan, I. (1999) 'Hepatotoxicity in cancer patients receiving erb-38, a recombinant immunotoxin that targets the erbB2 receptor', *Clin Cancer Res*, 5(9), 2311-5
- Panyam, J. and Labhasetwar, V. (2003) 'Biodegradable nanoparticles for drug and gene delivery to cells and tissue', *Adv Drug Deliv Rev*, 55(3), 329-347
- Papahadjopoulos, D., Allen, T. M., Gabizon, A., Mayhew, E., Matthey, K., Huang, S. K., Lee, K. D., Woodle, M. C., Lasic, D. D., Redemann, C. and et al. (1991) 'Sterically stabilized liposomes: improvements in pharmacokinetics and antitumor therapeutic efficacy', *Proc Natl Acad Sci U S A*, 88(24), 11460-4

- Park, I. Y., Kim, I. Y., Yoo, M. K., Choi, Y. J., Cho, M.-H. and Cho, C. S. (2008) 'Mannosylated polyethylenimine coupled mesoporous silica nanoparticles for receptor-mediated gene delivery', *Int J Pharm*, 359(1-2), 280-287
- Park, J. W., Hong, K., Kirpotin, D. B., Colbern, G., Shalaby, R., Baselga, J., Shao, Y., Nielsen, U. B., Marks, J. D., Moore, D., Papahadjopoulos, D. and Benz, C. C. (2002) 'Anti-HER2 immunoliposomes: enhanced efficacy attributable to targeted delivery', *Clin Cancer Res*, 8(4), 1172-81
- Pastan, I. (2003) 'Immunotoxins containing Pseudomonas exotoxin A: a short history', *Cancer Immunol Immunother*, 52(5), 338-41
- Pastan, I., Hassan, R., FitzGerald, D. J. and Kreitman, R. J. (2007) 'Immunotoxin treatment of cancer', *Annu Rev Med*, 58, 221-37
- Pastores, G. M. (2009) 'Lysosomal System', Larry, R. S., ed. Encyclopedia of Neuroscience [doi: DOI: 10.1016/B978-008045046-9.01512-6], Oxford: Academic Press, 571-580
- Patil, S. D., Rhodes, D. G. and Burgess, D. J. (2005) 'DNA-based therapeutics and DNA delivery systems: a comprehensive review', *AAPS J*, 7(1), E61-77
- Patrick, N. G., Richardson, S. C., Casolaro, M., Ferruti, P. and Duncan, R. (2001a) 'Poly(amidoamine)-mediated intracytoplasmic delivery of ricin A-chain and gelonin', *J Control Release*, 225-32
- Pelham, H. R. (1990) 'The retention signal for soluble proteins of the endoplasmic reticulum', *Trends Biochem Sci*, 15(12), 483-6
- Penz, Z. (2005) 'Current status of gendicine in China: Recombinant Ad-p53 agent for treatment of cancers', *Hum. Gene Ther*, 16, 1016-1027
- Pereira-Leal, J. B. and Seabra, M. C. (2000) 'The mammalian Rab family of small GTPases: definition of family and subfamily sequence motifs suggests a mechanism for functional specificity in the Ras superfamily', *J Mol Biol, England, Academic Press*, 1077-87
- Petersen, H., Fechner, P. M., Martin, A. L., Kunath, K., Stolnik, S., Roberts, C. J., Fischer, D., Davies, M. C. and Kissel, T. (2002) 'Polyethylenimine-graft-poly(ethylene glycol) copolymers: influence of copolymer block structure on DNA complexation and biological activities as gene delivery system', *Bioconjug Chem*, 13(4), 845-54
- Pfeffer, S. R. (2007) 'Unsolved mysteries in membrane traffic', *Annu Rev Biochem*, 76, 629-45
- Piasecki, P. (1999) 'FDA approves fusion protein for treatment of lymphoma', *J Am Pharm Assoc (Wash)*, 39(4), 571-2
- Piper, R. C. and Luzio, J. P. (2004) 'CUPpling calcium to lysosomal biogenesis', *Trends Cell Biol*, 14(9), 471-473
- Pitard, B. (2002) 'Supramolecular assemblies of DNA delivery systems', *Somat Cell Mol Genet*, 27(1-6), 5-15
- Podesta, J. E. and Kostarelos, K. (2009) 'Chapter 17 Engineering Cationic Liposome: siRNA Complexes for In Vitro and In Vivo Delivery', Nejat, D., ed. *Methods Enzymol*, [doi: DOI: 10.1016/S0076-6879(09)64017-9], Academic Press, 343-354
- Poli, M.A., Roy, C., Huebner, K.D., Franz, D.R., Nancy, K., and Jaax, N.K. (2007). 'Ricin. In: Medical Aspects of Biological Warfare', (Z.F. Dembek, Ed). Falls Church, VA: Office of the Surgeon General United States Army and Washington, DC: Borden Institute, Walter Reed Medical Center, pp. 323-335.
- Potala, S., Sahoo, S. K. and Verma, R. S. (2008) 'Targeted therapy of cancer using diphtheria toxin-derived immunotoxins', *Drug Discov Today*, 13(17-18), 807-815

- Praseuth, D., Guieysse, A. L. and Hélène, C. (1999) 'Triple helix formation and the antigene strategy for sequence-specific control of gene expression', *Biochim Biophys Acta*, 1489(1), 181-206
- Prescott, A. R., Lucocq, J. M., James, J., Lister, J. M. and Ponnambalam, S. (1997) 'Distinct compartmentalization of TGN46 and beta 1,4-galactosyltransferase in HeLa cells', *Eur J Cell Biol*, 72(3), 238-46
- Press, O. W., Vitetta, E. S. and Martin, P. J. (1986) 'A simplified microassay for inhibition of protein synthesis in reticulocyte lysates by immunotoxins', *Immunol Lett, Netherlands*, 37-41
- Qasim, W., Gaspar, H. B. and Thrasher, A. J. (2009) 'Progress and prospects: gene therapy for inherited immunodeficiencies', *Gene Ther*, 16(11), 1285-91
- Ramos-Vara, J. A. (2005) 'Technical aspects of immunohistochemistry', *Vet Pathol, United States*, 405-26
- Rao, P. V. L., Jayaraj, R., Bhaskar, A. S. B., Kumar, O., Bhattacharya, R., Saxena, P., Dash, P. K. and Vijayaraghavan, R. (2005) 'Mechanism of ricin-induced apoptosis in human cervical cancer cells', *Biochem Pharmacol*, 69(5), 855-865
- Rapak, A., Falnes, P. O. and Olsnes, S. (1997) 'Retrograde transport of mutant ricin to the endoplasmic reticulum with subsequent translocation to cytosol', *Proc Natl Acad Sci U S A*, 94(8), 3783-8
- Ready, M. P., Kim, Y. and Robertus, J. D. (1991) 'Site-directed mutagenesis of ricin A-chain and implications for the mechanism of action', *Proteins*, 10(3), 270-8
- Redhead, H. M., Davis, S. S. and Illum, L. (2001) 'Drug delivery in poly(lactide-co-glycolide) nanoparticles surface modified with poloxamer 407 and poloxamine 908: in vitro characterisation and in vivo evaluation', *J Control Release*, 70(3), 353-63
- Reidy, J. M., (2006) 'Engineering of the RTB Lectin as a Carrier Platform for Proteins and Antigens', PhD thesis, Virginia Polytechnic Institute and State University, USA
- Reiter, Y. (2001) 'Recombinant immunotoxins in targeted cancer cell therapy', *Adv Cancer Res*, 81, 93-124
- Richards, A. A., Stang, E., Pepperkok, R. and Parton, R. G. (2002) 'Inhibitors of COP-mediated transport and cholera toxin action inhibit simian virus 40 infection', *Mol Biol Cell*, 13(5), 1750-64
- Richardson, S., Ferruti, P. and Duncan, R. (1999) 'Poly(amidoamine)s as potential endosomolytic polymers: evaluation in vitro and body distribution in normal and tumour-bearing animals', *J Drug Target*, 6(6), 391-404
- Richardson, S. C., Patrick, N. G., Lavignac, N., Ferruti, P. and Duncan, R. (2010) 'Intracellular fate of bioresponsive poly(amidoamine)s in vitro and in vivo', *J Control Release*, 142(1), 78-88
- Richardson, S. C., Patrick, N. G., Man, Y. K., Ferruti, P. and Duncan, R. (2001) 'Poly(amidoamine)s as potential nonviral vectors: ability to form interpolyelectrolyte complexes and to mediate transfection in vitro', *Biomacromolecules*, 2(3), 1023-8
- Richardson, S. C., Wallom, K. L., Ferguson, E. L., Deacon, S. P., Davies, M. W., Powell, A. J., Piper, R. C. and Duncan, R. (2008) 'The use of fluorescence microscopy to define polymer localisation to the late endocytic compartments in cells that are targets for drug delivery', *J Control Release*, 1-11
- Richardson, S. C., Winistorfer, S. C., Poupon, V., Luzio, J. P. and Piper, R. C. (2004) 'Mammalian late vacuole protein sorting orthologues participate in early endosomal fusion and interact with the cytoskeleton', *Mol Biol Cell*, 1197-210
- Richardson, S. C. W., Patrick, N. G., Lavignac, N., Ferruti, P. and Duncan, R. (2010) 'Intracellular fate of bioresponsive poly(amidoamine)s in vitro and in vivo', *J Control Release*, 142(1), 78-88
- Richardson, S. C. W., Wallom, K. L., Ferguson, E. L., Deacon, S. P. E., Davies, M. W., Powell, A. J., Piper, R. C. and Duncan, R. (2008) 'The use of fluorescence microscopy to define polymer localisation to the late endocytic compartments in cells that are targets for drug delivery', *J Control Release*, 127(1), 1-11

- Riess, G. (2003) 'Micellization of block copolymers', *Prog. Polym. Sci*, 28(7), 1107-1170
- Rimessi, P., Sabatelli, P., Fabris, M., Braghetta, P., Bassi, E., Spitali, P., Vattei, G., Tomelleri, G., Mari, L., Perrone, D., Medici, A., Neri, M., Bovolenta, M., Martoni, E., Maraldi, N. M., Gualandi, F., Merlini, L., Ballestri, M., Tondelli, L., Sparnacci, K., Bonaldo, P., Caputo, A., Laus, M. and Ferlini, A. (2009) 'Cationic PMMA nanoparticles bind and deliver antisense oligoribonucleotides allowing restoration of dystrophin expression in the mdx mouse', *Mol Ther*, 17(5), 820-7
- Rink, J., Ghigo, E., Kalaidzidis, Y. and Zerial, M. (2005) 'Rab conversion as a mechanism of progression from early to late endosomes', *Cell*, 122(5), 735-49
- Roberts, L. M. and Smith, D. C. (2004) 'Ricin: the endoplasmic reticulum connection', *Toxicon*, 469-72
- Roberts, R. L., Barbieri, M. A., Pryse, K. M., Chua, M., Morisaki, J. H. and Stahl, P. D. (1999) 'Endosome fusion in living cells overexpressing GFP-rab5', *J Cell Sci*, 112 (Pt 21), 3667-75
- Roday, S., Sturm, M. B., Blakaj, D. and Schramm, V. L. (2008) 'Detection of an abasic site in RNA with stem-loop DNA beacons: Application to an activity assay for Ricin Toxin A-Chain', *J Biochem Biophys Methods*, 70(6), 945-953
- Rodighiero, C., Tsai, B., Rapoport, T. A. and Lencer, W. I. (2002) 'Role of ubiquitination in retro-translocation of cholera toxin and escape of cytosolic degradation', *EMBO Rep, England*, 1222-7
- Roizen, N. J. and Patterson, D. (2003) 'Down's syndrome', *The Lancet*, 361(9365), 1281-1289
- Rosenberg, A. H., Lade, B. N., Chui, D. S., Lin, S. W., Dunn, J. J. and Studier, F. W. (1987) 'Vectors for selective expression of cloned DNAs by T7 RNA polymerase', *Gene*, 56(1), 125-35
- Rosenblum, M. G., Kohr, W. A., Beattie, K. L., Beattie, W. G., Marks, W., Toman, P. D. and Cheung, L. (1995) 'Amino acid sequence analysis, gene construction, cloning, and expression of gelonin, a toxin derived from *Gelonium multiflorum*', *J Interferon Cytokine Res*, 15(6), 547-55
- Rossi, J. J., Elkins, D., Zaia, J. A. and Sullivan, S. (1992) 'Ribozymes as anti-HIV-1 therapeutic agents: principles, applications, and problems', *AIDS Res Hum Retroviruses*, 8(2), 183-9
- Roth, J., Yam, G. H., Fan, J., Hirano, K., Gaplovska-Kysela, K., Le Fourn, V., Guhl, B., Santimaria, R., Torossi, T., Ziak, M. and Zuber, C. (2008) 'Protein quality control: the who's who, the where's and therapeutic escapes', *Histochem Cell Biol*, 129(2), 163-77
- Russell, W. C. (2009) 'Adenoviruses: update on structure and function', *J Gen Virol*, 90(Pt 1), 1-20
- Rytting, E., Nguyen, J., Wang, X. and Kissel, T. (2008) 'Biodegradable polymeric nanocarriers for pulmonary drug delivery', *Expert Opin Drug Deliv*, 5(6), 629-39
- Safinya, C. R., Ewert, K., Ahmad, A., Evans, H. M., Raviv, U., Needleman, D. J., Lin, A. J., Slack, N. L., George, C. and Samuel, C. E. (2006) 'Cationic liposome-DNA complexes: from liquid crystal science to gene delivery applications', *Philos Transact A Math Phys Eng Sci*, 364(1847), 2573-96
- Saftig, P. and Klumperman, J. (2009) 'Lysosome biogenesis and lysosomal membrane proteins: trafficking meets function', *Nat Rev Mol Cell Biol*, 10(9), 623-35
- Sahay, G., Alakhova, D. Y. and Kabanov, A. V. (2010) 'Endocytosis of nanomedicines', *J Control Release*, 145(3): 182-95
- Sambrook, J., Fritsch, E. F., and Maniatis, T. (1989) Molecular cloning: a laboratory manual. [ISBN 0-87969-309-6] 2nd ed. N.Y., Cold spring Harbor Laboratory, Cold Spring Harbor Laboratory Press, p 6.5
- Sanchez, J. and Holmgren, J. (2011) 'Cholera toxin - a foe & a friend', *Indian J Med Res, India*, 153-63

- Sands, M. S. and Haskins, M. E. (2008) 'CNS-directed gene therapy for lysosomal storage diseases', *Acta Paediatr Suppl*, 97(457), 22-7
- Sandvig, K. (2001) 'Shiga toxins', *Toxicon, England*, 1629-35
- Sandvig, K., Spilsberg, B., Lauvrak, S. U., Torgersen, M. L., Iversen, T. G. and van Deurs, B. (2004) 'Pathways followed by protein toxins into cells', *Int J Med Microbiol*, 293(7-8), 483-90
- Sandvig K, Bergan J, Dyve AB, Skotland T, Torgersen ML (2010) 'Endocytosis and retrograde transport of Shiga toxin', *Toxicon*, 15; 56(7): 1181-5
- Sandvig, K. and van Deurs, B. (2000) 'Entry of ricin and Shiga toxin into cells: molecular mechanisms and medical perspectives', *EMBO J*, 19(22), 5943-50
- Sandvig, K. and van Deurs, B. (2002) 'Transport of protein toxins into cells: pathways used by ricin, cholera toxin and Shiga toxin', *FEBS Lett*, 49-53
- Sandvig, K. and van Deurs, B. (2005) 'Delivery into cells: lessons learned from plant and bacterial toxins', *Gene Ther*, 12(11), 865-72
- Sannerud, R., Saraste, J. and Goud, B. (2003) 'Retrograde traffic in the biosynthetic-secretory route: pathways and machinery', *Curr Opin Cell Biol*, 15(4), 438-445
- Sauer, A. V. and Aiuti, A. (2009) 'New insights into the pathogenesis of adenosine deaminase-severe combined immunodeficiency and progress in gene therapy', *Curr Opin Allergy Clin Immunol*, 9(6), 496-502
- Scanlon, K. J. (2004) 'Anti-genes: siRNA, ribozymes and antisense', *Curr Pharm Biotechnol*, 5(5), 415-20
- Schatzlein, A. G. (2003) 'Targeting of Synthetic Gene Delivery Systems', *J Biomed Biotechnol*, 2003(2), 149-158
- Scherphof, G. L., Dijkstra, J., Spanjer, H. H., Derksen, J. T. and Roerdink, F. H. (1985) 'Uptake and intracellular processing of targeted and nontargeted liposomes by rat Kupffer cells in vivo and in vitro', *Ann N Y Acad Sci*, 446, 368-84
- Scherr, M., Morgan, M. A. and Eder, M. (2003) 'Gene silencing mediated by small interfering RNAs in mammalian cells', *Curr Med Chem*, 10(3), 245-56
- Scherrmann, J.-M. and Tamsamani, J. (2005) 'The use of Pep: Trans vectors for the delivery of drugs into the central nervous system', *International Congress Series*, 1277, 199-211
- Schlossman, D., Withers, D., Welsh, P., Alexander, A., Robertus, J. and Frankel, A. (1989) 'Role of glutamic acid 177 of the ricin toxin A chain in enzymatic inactivation of ribosomes', *Mol Cell Biol*, 9(11), 5012-21
- Schmidt-Wolf, G. D. and Schmidt-Wolf, I. G. H. (2003) 'Non-viral and hybrid vectors in human gene therapy: an update', *Trends Mol Med*, 9(2), 67-72
- Schmitz, A., Herrgen, H., Winkeler, A. and Herzog, V. (2000) 'Cholera toxin is exported from microsomes by the Sec61p complex', *J Cell Biol*, 148(6), 1203-12
- Schnell, R., Vitetta, E., Schindler, J., Borchmann, P., Barth, S., Ghetie, V., Hell, K., Drillich, S., Diehl, V. and Engert, A. (2000) 'Treatment of refractory Hodgkin's lymphoma patients with an anti-CD25 ricin A-chain immunotoxin', *Leukemia*, 14(1), 129-35
- Schubert, S. and Kurreck, J. (2004) 'Ribozyme- and deoxyribozyme-strategies for medical applications', *Curr Drug Targets*, 5(8), 667-81
- Schultz, R. M., Papamatheakis, J. D. and Chirigos, M. A. (1977) 'Interferon: an inducer of macrophage activation by polyanions', *Science*, 197(4304), 674-6

- Seabra, M. C., Mules, E. H. and Hume, A. N. (2002) 'Rab GTPases, intracellular traffic and disease', *Trends Mol Med*, 23-30
- Seedorf, U., Leberer, E., Kirschbaum, B. J. and Pette, D. (1986) 'Neural control of gene expression in skeletal muscle. Effects of chronic stimulation on lactate dehydrogenase isoenzymes and citrate synthase', *Biochem J*, 239(1), 115-20
- Sgouras, D. (1990) 'The evaluation of biocompatibility of soluble polymers and assessment of their potential as specific drug delivery systems, PhD thesis, University of Keele
- Sgouras, D. and Duncan, R. (1990) 'Methods for the evaluation of biocompatibility of soluble synthetic polymers which have potential for biomedical use: 1-Use of the tetrazolium-based colorimetric assay (MTT) as a preliminary screen for the evaluation of in vitro cytotoxicity', *J. Mater. Sci. - Mater. Med.*, 1, 61-68
- Shapira, A. and Benhar, I. (2010) 'Toxin-based therapeutic approaches', *Toxins (Basel)*, 2519-83
- Sharma, A. and Sharma, U. S. (1997) 'Liposomes in drug delivery: Progress and limitations', *Int J Pharm*, 154(2), 123-140
- Shi, F. and Hoekstra, D. (2004) 'Effective intracellular delivery of oligonucleotides in order to make sense of antisense', *J Control Release*, 97(2), 189-209
- Simons, R. W. and Kleckner, N. (1988) 'Biological regulation by antisense RNA in prokaryotes', *Annu Rev Genet*, 22, 567-600
- Simpson, J. C., Lord, J. M. and Roberts, L. M. (1995a) 'Point mutations in the hydrophobic C-terminal region of ricin A chain indicate that Pro250 plays a key role in membrane translocation', *Eur J Biochem*, 232(2), 458-63
- Simpson, J. C., Roberts, L. M. and Lord, J. M. (1995b) 'Catalytic and cytotoxic activities of recombinant ricin A chain mutants with charged residues added at the carboxyl terminus', *Protein Expr Purif, United States*, 665-70
- Sims, R. J., 3rd, Mandal, S. S. and Reinberg, D. (2004) 'Recent highlights of RNA-polymerase-II-mediated transcription', *Curr Opin Cell Biol, United States*: 263-71
- Singh, R. and Lillard Jr, J. W. (2009) 'Nanoparticle-based targeted drug delivery', *Exp Mol Pathol*, 86(3), 215-223
- Smith, D. C., Lord, J. M., Roberts, L. M., Tartour, E. and Johannes, L. (2002) '1st class ticket to class I: protein toxins as pathfinders for antigen presentation', *Traffic*, 3(10), 697-704
- Smith, D. C., Marsden, C. J., Lord, J. M. and Roberts, L. M. (2003) 'Expression, Purification and Characterization of Ricin vectors used for exogenous antigen delivery into the MHC Class I presentation pathway', *Biol Proced Online*, 5, 13-19
- Sollner, T., Bennett, M. K., Whiteheart, S. W., Scheller, R. H. and Rothman, J. E. (1993) 'A protein assembly-disassembly pathway in vitro that may correspond to sequential steps of synaptic vesicle docking, activation, and fusion', *Cell*, 409-18
- Soltyk, A. M., MacKenzie, C. R., Wolski, V. M., Hiramata, T., Kitov, P. I., Bundle, D. R. and Brunton, J. L. (2002) 'A mutational analysis of the globotriaosylceramide-binding sites of verotoxin VT1', *J Biol Chem*, 5351-9
- Song, J. J., Smith, S. K., Hannon, G. J. and Joshua-Tor, L. (2004) 'Crystal structure of Argonaute and its implications for RISC slicer activity', *Science*, 305(5689), 1434-7
- Sorensen, H. P. and Mortensen, K. K. (2005) 'Advanced genetic strategies for recombinant protein expression in Escherichia coli', *J Biotechnol*, 113-28

- Southern, J. A., Young, D. F., Heaney, F., Baumgartner, W. K. and Randall, R. E. (1991) 'Identification of an epitope on the P and V proteins of simian virus 5 that distinguishes between two isolates with different biological characteristics', *J Gen Virol*, 72 (Pt 7), 1551-7
- Sperti, S., Brigotti, M., Zamboni, M., Carnicelli, D. and Montanaro, L. (1991) 'Requirements for the inactivation of ribosomes by gelonin', *Biochem J*, 277 (Pt 1), 281-4
- Spooner, R. A. and Lord, J. M. (2011) 'How Ricin and Shiga Toxin Reach the Cytosol of Target Cells: Retrotranslocation from the Endoplasmic Reticulum', *Curr Top Microbiol Immunol*.
- Spooner, R. A., Watson, P. D., Marsden, C. J., Smith, D. C., Moore, K. A., Cook, J. P., Lord, J. M. and Roberts, L. M. (2004) 'Protein disulphide-isomerase reduces ricin to its A and B chains in the endoplasmic reticulum', *Biochem J*, 285-93
- Stanislawska, J. and Olszewski, W. L. (2005) 'RNA interference--significance and applications', *Arch Immunol Ther Exp (Warsz)*, 53(1), 39-46
- Stenmark, H. and Olkkonen, V. M. (2001) 'The Rab GTPase family', *Genome Biol*, 2(5), REVIEWS3007
- Stephenson, M. L. and Zamecnik, P. C. (1978) 'Inhibition of Rous sarcoma viral RNA translation by a specific oligodeoxyribonucleotide', *Proc Natl Acad Sci U S A*, 75(1), 285-8
- Stirpe, F., Olsnes, S. and Pihl, A. (1980) 'Gelonin, a new inhibitor of protein synthesis, nontoxic to intact cells. Isolation, characterization, and preparation of cytotoxic complexes with concanavalin A', *J Biol Chem*, 255(14), 6947-53
- Stirpe, F., Sandvig, K., Olsnes, S. and Pihl, A. (1982) 'Action of viscumin, a toxic lectin from mistletoe, on cells in culture', *J Biol Chem*, 257(22), 13271-7
- Stolnik, S., Illum, L. and Davis, S. S. (1995) 'Long circulating microparticulate drug carriers', *Adv Drug Deliv Rev*, 16(2-3), 195-214
- Stolz, A. and Wolf, D. H. (2010) 'Endoplasmic reticulum associated protein degradation: A chaperone assisted journey to hell', *Biochim Biophys Acta*, 1803(6), 694-705
- Stone, M. J., Sausville, E. A., Fay, J. W., Headlee, D., Collins, R. H., Figg, W. D., Stetler-Stevenson, M., Jain, V., Jaffe, E. S., Solomon, D., Lush, R. M., Senderowicz, A., Ghetie, V., Schindler, J., Uhr, J. W. and Vitetta, E. S. (1996) 'A phase I study of bolus versus continuous infusion of the anti-CD19 immunotoxin, IgG-HD37-dgA, in patients with B-cell lymphoma', *Blood*, 88(4), 1188-97
- Storm, G. and Crommelin, D. J. A. (1998) 'Liposomes: quo vadis?', *PSTT*, 1(1), 19-31
- Strebhardt, K. and Ullrich, A. (2008) 'Paul Ehrlich's magic bullet concept: 100 years of progress', *Nat. Rev. Cancer*, 8(6), 473-480
- Stuart, L. M. and Ezekowitz, R. A. (2008) 'Phagocytosis and comparative innate immunity: learning on the fly', *Nat Rev Immunol*, 8(2), 131-41
- Studier, F. W. and Moffatt, B. A. (1986) 'Use of bacteriophage T7 RNA polymerase to direct selective high-level expression of cloned genes', *J Mol Biol*, 113-30
- Studier, F. W., Rosenberg, A. H., Dunn, J. J. and Dubendorff, J. W. (1990) 'Use of T7 RNA polymerase to direct expression of cloned genes', *Methods Enzymol*, 185, 60-89
- Subramaniam, V. N., Summerville, L. and Wallace, D. F. (2002) 'Molecular and cellular characterization of transferrin receptor 2', *Cell Biochem Biophys*, 36(2-3), 235-9
- Suhan, M. L. and Hovde, C. J. (1998) 'Disruption of an internal membrane-spanning region in Shiga toxin 1 reduces cytotoxicity', *Infect Immun*, 66(11), 5252-9

- Sulkowski, W. W., Pentak, D., Nowak, K. and Sulkowska, A. (2005) 'The influence of temperature, cholesterol content and pH on liposome stability', *Journal of Molecular Structure*, 744-747
- Symons, R. H. (1992) 'Small catalytic RNAs', *Annu Rev Biochem*, 61, 641-71
- Szewczak, A. A., Moore, P. B., Chang, Y. L. and Wool, I. G. (1993) 'The conformation of the sarcin/ricin loop from 28S ribosomal RNA', *Proc Natl Acad Sci U S A*, 90(20), 9581-5
- Tang, M. X. and Szoka, F. C. (1997) 'The influence of polymer structure on the interactions of cationic polymers with DNA and morphology of the resulting complexes', *Gene Ther*, 4(8), 823-32
- Tarragó-Trani, M. T. and Storrie, B. (2007) 'Alternate routes for drug delivery to the cell interior: Pathways to the Golgi apparatus and endoplasmic reticulum', *Adv Drug Deliv Rev*, 59(8), 782-797
- Tegel, H., Ottosson, J. and Hober, S. (2011) 'Enhancing the protein production levels in Escherichia coli with a strong promoter', *FEBS J*, 278(5), 729-39
- Terman, A. and Brunk, U. T. (2004) 'Lipofuscin', *Int J Biochem Cell Biol*, 36(8), 1400-1404
- Terpe, K. (2003) 'Overview of tag protein fusions: from molecular and biochemical fundamentals to commercial systems', *Appl Microbiol Biotechnol*, 60(5), 523-33
- Thompson, J. D., Ayers, D. F., Malmstrom, T. A., McKenzie, T. L., Ganousis, L., Chowrira, B. M., Couture, L. and Stinchcomb, D. T. (1995) 'Improved accumulation and activity of ribozymes expressed from a tRNA-based RNA polymerase III promoter', *Nucleic Acids Res*, 23(12), 2259-68
- Tong, H., Qin, S., Fernandes, J. C., Li, L., Dai, K. and Zhang, X. (2009a) 'Progress and prospects of chitosan and its derivatives as non-viral gene vectors in gene therapy', *Curr Gene Ther*, 9(6), 495-502
- Tong, H., Qin, S., Fernandes, J. C., Li, L., Dai, K. and Zhang, X. (2009b) 'Progress and prospects of chitosan and its derivatives as non-viral gene vectors in gene therapy', *Curr Gene Ther*, 495-502
- Torchilin, V. P. (2004) 'Targeted polymeric micelles for delivery of poorly soluble drugs', *Cell Mol Life Sci*, 61(19-20), 2549-59
- Torchilin, V. P. (2005) 'Lipid-core micelles for targeted drug delivery', *Curr Drug Deliv*, 2(4), 319-27
- Torgersen, M. L., Skretting, G., van Deurs, B. and Sandvig, K. (2001) 'Internalization of cholera toxin by different endocytic mechanisms', *J Cell Sci*, 114(Pt 20), 3737-47
- Towbin, H., Staehelin, T. and Gordon, J. (1979) 'Electrophoretic transfer of proteins from polyacrylamide gels to nitrocellulose sheets: procedure and some applications', *Proc Natl Acad Sci U S A*, 76(9), 4350-4
- Tsai, B. and Rapoport, T. A. (2002) 'Unfolded cholera toxin is transferred to the ER membrane and released from protein disulfide isomerase upon oxidation by Ero1', *J Cell Biol*, 207-16
- Tsai, B., Rodighiero, C., Lencer, W. I. and Rapoport, T. A. (2001) 'Protein disulfide isomerase acts as a redox-dependent chaperone to unfold cholera toxin', *Cell*, 937-48
- Uckun, F. M. (1993) 'Immunotoxins for the treatment of leukaemia', *Br J Haematol*, 85(3), 435-8
- Ullrich, O., Reinsch, S., Urbe, S., Zerial, M. and Parton, R. G. (1996) 'Rab11 regulates recycling through the pericentriolar recycling endosome', *J Cell Biol*, 135(4), 913-24
- Ullrich, O., Stenmark, H., Alexandrov, K., Huber, L. A., Kaibuchi, K., Sasaki, T., Takai, Y. and Zerial, M. (1993) 'Rab GDP dissociation inhibitor as a general regulator for the membrane association of rab proteins', *J Biol Chem*, 268(24), 18143-50
- Urban, E. and Noe, C. R. (2003) 'Structural modifications of antisense oligonucleotides', *Il Farmaco*, 58(3), 243-258

- Van den Hout, J. M., Reuser, A. J., de Klerk, J. B., Arts, W. F., Smeitink, J. A. and Van der Ploeg, A. T. (2001) 'Enzyme therapy for pompe disease with recombinant human alpha-glucosidase from rabbit milk', *J Inherit Metab Dis*, 24(2), 266-74
- van der Aa, L. J., Vader, P., Storm, G., Schiffelers, R. M. and Engbersen, J. F. (2011) 'Optimization of poly(amido amine)s as vectors for siRNA delivery', *J Control Release*, 177-86
- van der Ploeg, A. T. and Reuser, A. J. (2008) 'Pompe's disease', *Lancet*, 372(9646), 1342-53
- van Deurs, B., Sandvig, K., Petersen, O. W., Olsnes, S., Simons, K. and Griffiths, G. (1988) 'Estimation of the amount of internalized ricin that reaches the trans-Golgi network', *J Cell Biol*, 106(2), 253-67
- van Ijzendoorn, S. C. (2006) 'Recycling endosomes', *J Cell Sci*, 119(Pt 9), 1679-81
- van Vliet, C., Thomas, E. C., Merino-Trigo, A., Teasdale, R. D. and Gleeson, P. A. (2003) 'Intracellular sorting and transport of proteins', *Prog Biophys Mol Biol*, 83(1), 1-45
- Vanden Broeck, D., Horvath, C. and De Wolf, M. J. (2007) 'Vibrio cholerae: cholera toxin', *Int J Biochem Cell Biol*, 1771-5
- Varol, B., Bektas, M., Nurten, R. and Bermek, E. (2011) 'The cytotoxic effect of diphtheria toxin on the actin cytoskeleton', *Cell Mol Biol Lett*
- Verbaan, F. J., Klein Klouwenberg, P., van Steenis, J. H., Snel, C. J., Boerman, O., Hennink, W. E. and Storm, G. (2005) 'Application of poly(2-(dimethylamino)ethyl methacrylate)-based polyplexes for gene transfer into human ovarian carcinoma cells', *Int J Pharm*, 185-92
- Verbaan, F. J., Klouwenberg, P. K., Steenis, J. H. v., Snel, C. J., Boerman, O., Hennink, W. E. and Storm, G. (2005) 'Application of poly(2-(dimethylamino)ethyl methacrylate)-based polyplexes for gene transfer into human ovarian carcinoma cells', *Int J Pharm*, 304(1-2), 185-192.
- Verma, I. M. and Somia, N. (1997) 'Gene therapy -- promises, problems and prospects', *Nature*, 389(6648), 239-42
- Verma, I. M. and Weitzman, M. D. (2005) 'Gene therapy: Twenty-first century medicine', *Annu Rev Biochem*, 74, 711-738
- Vigneron, J. P., Oudrhiri, N., Fauquet, M., Vergely, L., Bradley, J. C., Basseville, M., Lehn, P. and Lehn, J. M. (1996) 'Guanidinium-cholesterol cationic lipids: efficient vectors for the transfection of eukaryotic cells', *Proc Natl Acad Sci U S A*, 93(18), 9682-6
- Vilgelm, A. E., Chumakov, S. P. and Prassolov, V.S. (2006) 'RNA interference: Biology and prospects of application in biomedicine and biotechnology', *Mol Biol*, 40(3), 339-354
- Vitetta, E. S., Stone, M., Amlot, P., Fay, J., May, R., Till, M., Newman, J., Clark, P., Collins, R., Cunningham, D. and et al. (1991) 'Phase I immunotoxin trial in patients with B-cell lymphoma', *Cancer Res*, 51(15), 4052-8
- Voeltz, G. K., Rolls, M. M. and Rapoport, T. A. (2002) 'Structural organization of the endoplasmic reticulum', *EMBO Rep*, 3(10), 944-50
- von Zastrow, M. and Sorkin, A. (2007) 'Signaling on the endocytic pathway', *Curr Opin Cell Biol*, 436-45
- Wade, N., Bryant, N. J., Connolly, L. M., Simpson, R. J., Luzio, J. P., Piper, R. C. and James, D. E. (2001) 'Syntaxin 7 complexes with mouse Vps10p tail interactor 1b, syntaxin 6, vesicle-associated membrane protein (VAMP)8, and VAMP7 in b16 melanoma cells', *J Biol Chem*, 19820-7
- Wadia, J. S., Stan, R. V. and Dowdy, S. F. (2004) 'Transducible TAT-HA fusogenic peptide enhances escape of TAT-fusion proteins after lipid raft macropinocytosis', *Nat Med*, 10(3), 310-5

- Wahlund, P.-O., Izumrudov, V. A., Gustavsson, P.-E., Larsson, P.-O. and Galaev, I. Y. (2003) 'Phase Separations in Water-Salt Solutions of Polyelectrolyte Complexes Formed by RNA and Polycations: Comparison with DNA Complexes', *Macromol. Biosci*, 3(8), 404-411
- Wales, R., Chaddock, J. A., Roberts, L. M. and Lord, J. M. (1992) 'Addition of an ER retention signal to the ricin A chain increases the cytotoxicity of the holotoxin', *Exp Cell Res*, 1-4
- Wales, R., Roberts, L. M. and Lord, J. M. (1993) 'Addition of an endoplasmic reticulum retrieval sequence to ricin A chain significantly increases its cytotoxicity to mammalian cells', *J Biol Chem*, 268(32), 23986-90
- Walker, A., Ward, C., Sheldrake, T. A., Dransfield, I., Rossi, A. G., Pryde, J. G. and Haslett, C. (2004) 'Golgi fragmentation during Fas-mediated apoptosis is associated with the rapid loss of GM130', *Biochem Biophys Res Commun*, 6-11
- Walker, F. O. (2007) 'Huntington's disease', *The Lancet*, 369(9557), 218-228
- Walther, W. and Stein, U. (2000) 'Viral vectors for gene transfer: a review of their use in the treatment of human diseases', *Drugs*, 60(2), 249-71
- Wang, S. and Kool, E. T. (1994) 'Circular RNA oligonucleotides. Synthesis, nucleic acid binding properties, and a comparison with circular DNAs', *Nucleic Acids Res*, 22(12), 2326-33
- Ward, C. M., Read, M. L. and Seymour, L. W. (2001) 'Systemic circulation of poly(L-lysine)/DNA vectors is influenced by polycation molecular weight and type of DNA: differential circulation in mice and rats and the implications for human gene therapy', *Blood*, 97(8), 2221-9
- Watson, P., Jones, A. T. and Stephens, D. J. (2005) 'Intracellular trafficking pathways and drug delivery: fluorescence imaging of living and fixed cells', *Adv Drug Deliv Rev*, 43-61
- Watson, P. and Spooner, R. A. (2006) 'Toxin entry and trafficking in mammalian cells', *Adv Drug Deliv Rev*, 58(15), 1581-1596
- Weissenboeck, A., Bogner, E., Wirth, M. and Gabor, F. (2004) 'Binding and uptake of wheat germ agglutinin-grafted PLGA-nanospheres by caco-2 monolayers', *Pharm Res*, 21(10), 1917-23
- Wennerberg, K., Rossman, K. L. and Der, C. J. (2005) 'The Ras superfamily at a glance', *J Cell Sci*, 843-6
- Werner, D., Brunar, H. and Noe, C. R. (1998) 'Investigations on the influence of 2'-O-alkyl modifications on the base pairing properties of oligonucleotides', *Pharm Acta Helv*, 73(1), 3-10
- Wernick, N. L., Chinnapen, D. J., Cho, J. A. and Lencer, W. I. (2010) 'Cholera toxin: an intracellular journey into the cytosol by way of the endoplasmic reticulum', *Toxins (Basel)*, 310-25
- Wesche, J. (2002) 'Retrograde transport of ricin', *Int J Med Microbiol*, 291(6-7), 517-21
- Wesche, J., Rapak, A. and Olsnes, S. (1999) 'Dependence of ricin toxicity on translocation of the toxin A-chain from the endoplasmic reticulum to the cytosol', *J Biol Chem*, 274(48), 34443-9
- Westra, D. F., Welling, G. W., Koedijk, D. G., Scheffer, A. J., The, T. H. and Welling-Wester, S. (2001) 'Immobilised metal-ion affinity chromatography purification of histidine-tagged recombinant proteins: a wash step with a low concentration of EDTA', *J Chromatogr B Biomed Sci Appl*, 760(1), 129-36
- White, J., Johannes, L., Mallard, F., Girod, A., Grill, S., Reinsch, S., Keller, P., Tzschaschel, B., Echard, A., Goud, B. and Stelzer, E. H. (1999) 'Rab6 coordinates a novel Golgi to ER retrograde transport pathway in live cells', *J Cell Biol*, 147(4), 743-60
- Wilcke, M., Johannes, L., Galli, T., Mayau, V., Goud, B. and Salamero, J. (2000) 'Rab11 regulates the compartmentalization of early endosomes required for efficient transport from early endosomes to the trans-golgi network', *J Cell Biol*, 151(6), 1207-20

- Wilkinson, B. and Gilbert, H. F. (2004) 'Protein disulfide isomerase', *Biochim Biophys Acta*, 1699(1-2), 35-44
- Williams, D. B. (2006) 'Beyond lectins: the calnexin/calreticulin chaperone system of the endoplasmic reticulum', *J Cell Sci*, 119(Pt 4), 615-23
- Wilson, J M. (2005) 'Gendicine: The first commercial gene therapy product', *Hum. Gene Ther*, 16,1014-1015
- Winchester, B., Vellodi, A. and Young, E. (2000) 'The molecular basis of lysosomal storage diseases and their treatment', *Biochem Soc Trans*, 28(2), 150-4
- Winkler, U., Barth, S., Schnell, R., Diehl, V. and Engert, A. (1997) 'The emerging role of immunotoxins in leukemia and lymphoma', *Ann Oncol*, 8 Suppl 1, 139-46
- Wolf, P. and Elsasser-Beile, U. (2009) 'Pseudomonas exotoxin A: from virulence factor to anti-cancer agent', *Int J Med Microbiol*, 161-76
- Wong, S. Y., Pelet, J. M. and Putnam, D. 'Polymer systems for gene delivery--Past, present, and future', *Prog. Polym. Sci*, 32(8-9), 799-837
- Wu, D. Q., Lu, B., Chang, C., Chen, C. S., Wang, T., Zhang, Y. Y., Cheng, S. X., Jiang, X. J., Zhang, X. Z. and Zhuo, R. X. (2009) 'Galactosylated fluorescent labeled micelles as a liver targeting drug carrier', *Biomaterials*, 30(7), 1363-71
- Xia, T., Kovochich, M., Brant, J., Hotze, M., Sempf, J., Oberley, T., Sioutas, C., Yeh, J. I., Wiesner, M. R. and Nel, A. E. (2006) 'Comparison of the abilities of ambient and manufactured nanoparticles to induce cellular toxicity according to an oxidative stress paradigm', *Nano Lett*, 6(8), 1794-807
- Xu, Y. and Szoka, F. C., Jr. (1996) 'Mechanism of DNA release from cationic liposome/DNA complexes used in cell transfection', *Biochemistry*, 35(18), 5616-23
- Yamamoto, K., Fujii, R., Toyofuku, Y., Saito, T., Koseki, H., Hsu, V. W. and Aoe, T. (2001) 'The KDEL receptor mediates a retrieval mechanism that contributes to quality control at the endoplasmic reticulum', *EMBO J*, 20(12), 3082-91
- Yang, Z., Yang, M., Xiahou, G., Peng, J. and Zhang, J. (2009) 'Targeted delivery of insulin-modified immunoliposomes in vivo', *J Liposome Res*, 19(2), 116-21
- Yoncheva, K., Lizarraga, E. and Irache, J. M. (2005) 'Pegylated nanoparticles based on poly(methyl vinyl ether-co-maleic anhydride): preparation and evaluation of their bioadhesive properties', *Eur J Pharm Sci*, 411-9
- Yoshida, T., Chen, C. C., Zhang, M. S. and Wu, H. C. (1991) 'Disruption of the Golgi apparatus by brefeldin A inhibits the cytotoxicity of ricin, modeccin, and Pseudomonas toxin', *Exp Cell Res*, 192(2), 389-95
- Yu, B. G., Okano, T., Kataoka, K. and Kwon, G. (1998) 'Polymeric micelles for drug delivery: solubilization and haemolytic activity of amphotericin B', *J Control Release*, 53(1-3), 131-6
- Yu, M. and Haslam, D. B. (2005) 'Shiga toxin is transported from the endoplasmic reticulum following interaction with the luminal chaperone HEDJ/ERdj3', *Infect Immun*, 2524-32
- Zabner, J., Fasbender, A. J., Moninger, T., Poellinger, K. A. and Welsh, M. J. (1995) 'Cellular and molecular barriers to gene transfer by a cationic lipid', *J Biol Chem*, 270(32), 18997-9007
- Zamboni, W. C. (2005) 'Liposomal, nanoparticle, and conjugated formulations of anticancer agents', *Clin Cancer Res*, 11(23), 8230-4
- Zhan, J., Chen, Y., Wang, K. and Zheng, S. (2004) 'Expression of ricin A chain and ricin A chain-KDEL in Escherichia coli', *Protein Expr Purif*, 34(2), 197-201

-
- Zhan, J., Stayton, P. and Press, O. W. (1998) 'Modification of ricin A chain, by addition of endoplasmic reticulum (KDEL) or Golgi (YQRL) retention sequences, enhances its cytotoxicity and translocation', *Cancer Immunol Immunother*, 46(1), 55-60
- Zhang, H., Ma, Y. and Sun, X. L. (2010) 'Recent developments in carbohydrate-decorated targeted drug/gene delivery', *Med Res Rev*, 30(2), 270-89
- Zhang, J. X., Yan, M. Q., Li, X. H., Qiu, L. Y., Li, X. D., Li, X. J., Jin, Y. and Zhu, K. J. (2007) 'Local delivery of indomethacin to arthritis-bearing rats through polymeric micelles based on amphiphilic polyphosphazenes', *Pharm Res*, 24(10), 1944-53
- Zhang, X., Pan, S. R., Hu, H. M., Wu, G. F., Feng, M., Zhang, W. and Luo, X. (2008) 'Poly(ethylene glycol)-block-polyethylenimine copolymers as carriers for gene delivery: effects of PEG molecular weight and PEGylation degree', *J Biomed Mater Res A*, 84(3), 795-804
- Zhi, D., Zhang, S., Wang, B., Zhao, Y., Yang, B. and Yu, S. (2010) 'Transfection efficiency of cationic lipids with different hydrophobic domains in gene delivery', *Bioconjug Chem*, 21(4), 563-77
- Zhu, S., Hong, M., Tang, G., Qian, L., Lin, J., Jiang, Y. and Pei, Y. (2010) 'Partly PEGylated polyamidoamine dendrimer for tumor-selective targeting of doxorubicin: The effects of PEGylation degree and drug conjugation style', *Biomaterials*, 31(6), 1360-1371
- Zielenski, J. and Tsui, L. C. (1995) 'Cystic fibrosis: genotypic and phenotypic variations', *Annu Rev Genet*, 29, 777-807

Appendix I

Compositions of commercial stock solutions

6x DNA loading dye (Fermentas)

10mM Tris-HCl (pH 7.6)

60mM EDTA

0.003% Bromophenol blue

0.003% Xylene Cyanol FF

60% Glycerol

SOC medium (Invitrogen)

2% Tryptone

0.5% Yeast extract

0.05% NaCl

2.5mM KCl

10mM MgCl₂

10mM MgSO₄

20mM Glucose

Composition of Buffers in Qiagen Miniprep Kit

Buffer P1 (Resuspension buffer)

50mM Tris-Cl, pH 8

10mM EDTA

100µg/mL RNase A

After addition of RNase A, buffer stored at 4°C.

Buffer P2 (Lysis buffer)

200mM NaOH, 1%SDS (w/v)

Buffer P3 (Neutralisation buffer)

Guanidine hydrochloride

Acetic acid

Buffer PB

Guanidine hydrochloride

Isopropanol

Epitopes and fluorescent “tags” used in the RTAC and RTBC constructs

6 Histidine moiety (6His): 6His consists of six consecutive histidine residues and was placed either at either the N- or C-terminus of the protein. This 6His motif enables the enrichment of the desired protein from a crude bacterial lysate by affinity chromatography (Hengen, 1995). Histidine coding codons are CAC and CAU and enrichment is achieved using immobilised metal ion chromatography (IMAC). This is a widely used method for the affinity purification of proteins. IMAC is based on the interaction between a metal ion, immobilised in a solid phase matrix and specific amino acid side chain (*i.e.* 6His). For this purpose various metal ions and matrices were used *e.g.* Ni⁺². Histidine readily coordinates with immobilised transition metal ions and consequently proteins with 6His moieties attached to the transition metal ions, as the electron donor groups on the histidine imidazole ring readily forms coordination bonds with the immobilised transition metals. Non-specifically bound proteins and weakly attached proteins may be eliminated by sequential washing steps. The 6His motif-containing protein may be eluted by using imidazole (~500mM). The relatively small size and charge of the 6His motif rarely affects the function and immunogenicity of the protein. Amino acids like cystine and naturally occurring histidine rich regions in host proteins may result in unwanted protein binding during the IMAC purification (Westra *et al.*, 2001).

HA (Hemagglutinin): HA is derived from human influenza hemagglutinin protein and corresponds to amino acids 98-106 (YPYDVPDYA). Human Influenza hemagglutinin is a surface glycoprotein required for the infectivity of the human virus. Widely used, an HA tag does not interfere with the bioactivity and bio-distribution of recombinant proteins and is used during detection of the recombinant proteins again by Western blotting using a commercially available antibody.

A **V5 epitope** is obtained from the C-terminal sequence of the P- and V- proteins of the Simian Virus 5 (SV5). It made up of with 14 amino acid sequences (GKPIP NPLLGLDST) (Southern *et al.*, 1991).

Green Fluorescent Protein (GFP) was first isolated from the jellyfish *Aequorea Victoria*, is composed of 238 amino acids (26.9kDa) and exhibits bright green fluorescence when exposed to blue light (Chalfie, 1995). In cell and molecular biology it is used as reporter of

gene expression. In fluorescence microscopy it can be used to locate the position of the protein inside the cell and it can also be used to study protein folding and targeting as well as protein-protein interactions by FRET (Fluorescent resonance energy transfer) (Chudakov *et al.*, 2010).

KDEL motif: KDEL is an endoplasmic retention signal. Many proteins resident in the ER lumen contain a C-terminal KDEL (Lys-Asp-Glu-Leu) sequence that facilitates the return of the protein to the ER from the Golgi. The KDEL sequence is recognised by a KDEL receptor located in the cis-Golgi network and in ER-to-Golgi transport vesicles (Yamamoto *et al.*, 2001). *Pseudomonas* exotoxin A and cholera toxin A chain contain KDEL like sequences, which facilitate retrograde transport of the toxins from Golgi to ER. It has been reported that inclusion of a KDEL sequence onto the CT- of RTAC increases the toxicity of the RT molecule (Wales *et al.*, 1993; Zhan *et al.*, 1998; Zhan *et al.*, 2004).

Movie 1

Live cell imaging of ISA1-FITC polymer was exported as a movie file onto DVD.

Appendix II

Publications

1. Structural and biological investigation of ferrocene-substituted 3-methylidene-1,3-dihydro-2H-indol-2-ones. Spencer J, Mendham AP, Kotha AK, Richardson SC, Hillard EA, Jaouen G, Male L, Hursthouse MB. *Dalton Trans.* 2009 Feb 14;(6): 918-21.
2. Synthesis of a 1,4-benzodiazepine containing palladacycle with in vitro anticancer and cathepsin B activity. Spencer J, Rathnam RP, Motukuri M, Kotha AK, Richardson SC, Hazrati A, Hartley JA, Male L, Hursthouse MB. *Dalton Trans.* 2009 Jun 14; (22): 4299-303.
3. Imaging Select Mammalian Organelles Using Fluorescent Microscopy: Applications to Drug Delivery. Paul D. R. Dyer, Arun K. Kotha, Marie W. Pettit, Simon C. W. Richardson. In "Cellular and Subcellular Nanotechnology: Methods and Protocols" 2011 Eds: Weissig V., Olsen M. and Elbayoumi T. Humana Press (USA) (*in press*).

Poster presentations

'Characterisation of a Recombinant Cytosolic Shuttle Based on Ricin Toxin' at 2nd International Symposium "Cellular Delivery of Therapeutic Macromolecules" which was held in Cardiff University, England, June 2008.

'Characterisation of a Recombinant Cytosolic Shuttle Based on Ricin Toxin' at 2nd European Summer School on Nanomedicine, Lisbon, Portugal, June 2009.

School seminar presentations:

On 29th April 2009, 16th June 2010 and 6th July 2011 presented seminar on **'Characterisation of a Recombinant Cytosolic Shuttle based on Ricin Toxin'**.

Prizes

Won 2nd prize for my poster in 2nd International Symposium "Cellular Delivery of Therapeutic Macromolecules" which was held in Cardiff University, June 2008.

Won the best student poster on "Spotlight on Science" day, which was held in the University of Greenwich, July 2008.